

**University of Alberta**

Identification and Characterization of Virulence Factors in the Principal  
Pathogenic Species of the *Burkholderia cepacia* Complex

by

Euan L.S. Thomson

A thesis submitted to the Faculty of Graduate Studies and Research

in partial fulfillment of the requirements for the degree of

Doctor of Philosophy

in

Microbiology and Biotechnology

Biological Sciences

©Euan L.S. Thomson

Fall 2013

Edmonton, Alberta

Permission is hereby granted to the University of Alberta Libraries to reproduce single copies of this thesis and to lend or sell such copies for private, scholarly or scientific research purposes only.

Where the thesis is converted to, or otherwise made available in digital form, the University of Alberta will advise potential users of the thesis of these terms.

The author reserves all other publication and other rights in association with the copyright in the thesis and, except as herein before provided, neither the thesis nor any substantial portion thereof may be printed or otherwise reproduced in any material form whatsoever without the author's prior written permission.

## **Dedication**

For my father, who has only ever left one job unfinished.

## Abstract

Cystic fibrosis (CF) is the most common heritable disease among Caucasian populations, with afflicted individuals experiencing a immune, respiratory and digestive system complications. Compromised mucus clearance from the CF airway provides a habitat for bacteria and generates oxygen gradients within the mucus. Members of the *Burkholderia cepacia* complex (Bcc) are devastating airway pathogens of CF patients, with innate antibiotic resistance and the propensity to establish invasive necrotic infections. Their mechanisms of infection remain largely uncharacterized, though a number of virulence factors have been identified using standard model hosts. Among these factors are gene products common in human pathogens, interlaced by a complex regulatory network comprising global regulators, communication networks and environmental sensors. The objective of this study is to identify and detail virulence elements of the most prevalent Bcc species in the CF community using established model systems and a novel high-throughput plant host, *Lemna minor* (Common duckweed). First, a strong correlation was found between the relative virulence of Bcc strains in duckweed and the established insect model, *Galleria mellonella* (Greater wax moth larva). A non-ribosomal peptide synthetase gene cluster was identified in *B. vietnamiensis* and shown to cause erythrocyte lysis and contribute to virulence in the larval model. To identify virulence factors in *B. cenocepacia*, 5,980 plasposon mutants were screened for attenuation against duckweed. Several novel virulence factors were found, including a regulator, a putative DNA binding protein, and metabolism-related proteins. Type VI

secretion was studied for its contribution to *B. cenocepacia* virulence, but showed only antibacterial activity against *Escherichia coli*, suggesting a role for Bcc type VI secretion in competitive colonization of the CF lung. Finally, the enigmatic *B. multivorans*, which demonstrates negligible virulence effects in most model hosts but accounts for nearly half of Bcc infections in CF, demonstrated virulence activation in both low oxygen and high temperature, indicating a regulatory effect of these CF-relevant environmental cues akin to the recently-identified *lxa* locus in *B. cenocepacia*. This finding indicates that standard infection models may be insufficient for characterizing this pathogen, and approaches that allow modified environmental conditions may be required to fully understand Bcc pathogenesis.

## Acknowledgements

This work was carried out through turbulent times and would have amounted to little more than a puddle of blood, sweat and tears without extensive support.

For providing oft-needed perspective and for their unwavering belief in me across thousands of kilometres, I thank my family: Jane, Callum, Dugald and Jimmy Thomson. I drew a lot of inspiration from the Goudie family and Phil Grace, who showed incredible resolve to live life to its fullest through their own turmoil. My friends Brett Ehlers, Ben Anderson, Dan Wowryk, Sam Clement, Sean Davey, Mike Lavender, Reid Tannahill, Andrew Bullied and others helped keep me active through the dark winter months and kept the laughter alive.

I was fortunate to have labmates and colleagues that positively influenced the quality of both this research and my enjoyment of the last five years, including Mandi Goudie, Gerardo Juarez-Lara, Ashraf Abdu, Karlene Lynch, Shannon Leblanc, Julia Wong and Stefanie Vogt. Thanks to all members of the Dennis lab present throughout my degree – it was an honour to work alongside such talented and self-motivated individuals.

My former professors throughout my undergraduate degree deserve recognition for maintaining an interest in my life and helping me through difficult periods. Dr. Lori Graham, Dr. Nikhil Thomas, Mr. Randy Lauff, and Dr. Russell Wyeth played important supportive roles. The idea for the duckweed project came from a class run by Dr. Barry Taylor, who, incidentally, first got me hooked on scientific research.

Steven Williams in the Biological Sciences greenhouse provided the initial duckweed samples and the knowledge to get the plants growing. The Raivio, Szymanski and Feldman labs provided materials and expertise that contributed to the work presented herein. Chesceri Mason was instrumental in ensuring the completeness of scholarship applications, and I was supported by the Natural Sciences and Engineering Research Council for much of my degree.

I thank my supervisor, Dr. Jonathan Dennis, who gave me a rare amount of freedom to pursue my ideas throughout this work, and provided important and relevant direction for the duckweed project at a critical moment. My thesis committee, Dr. Susan Jensen and Dr. Stefan Pukatzki, were instrumental in designing and executing the hemolysin and type VI secretion projects, respectively.

Finally, Karen Lithgow helped me through to the end of this degree in innumerable ways. As my best friend, intellectual advisor, athletic inspiration, artistic complement, co-adventurer, and compassionate partner, she has made many sacrifices and I cannot thank her enough.

I am indebted to these and many more people who got me to this point. Thank you.

## Table of contents

General Introduction: Virulence pathways of the <i>Burkholderia cepacia</i> complex	1
Opportunistic pathogenesis by the <i>Burkholderia cepacia</i> complex	2
Bcc ecology reflects metabolic and genetic versatility	4
Interactions with soil organisms	4
Genomic plasticity	8
Characteristics of the CF lung	10
Innate defence mechanisms of a healthy lung	10
Innate immune deficiencies in the CF lung and nutrient availability	14
Microbial and viral biodiversity in the CF lung	22
Localization of Bcc bacteria in the CF lung	25
Infection models for Bcc pathogenesis	27
Animal models	27
Plant models	33
Cell lines	36
Multihost analyses	40
General virulence pathways of the Bcc	42
Iron acquisition	43
Resistance to host defences	46
Inflammation and epithelial degradation	50
Cell and tissue invasion	54
Social behaviours	57
Quorum sensing	57
Swarming motility	60
Biofilm formation	61
Summary	65
References	67
Chapter 1 – <i>Lemna minor</i> (Common duckweed) as model host for the <i>Burkholderia cepacia</i> complex	90
Introduction	91
Common duckweed as a model host for the <i>Burkholderia cepacia</i> complex	91
Advantages and disadvantages of using a plant model host	93
Objectives	94

Materials and Methods.....	95
Strains, plasmids and culture conditions.....	95
Duckweed growth and sterilization.....	97
Duckweed infection .....	98
EPEC infections .....	99
Concentration of culture supernatants .....	99
Heat inactivation of bacteria .....	100
Bacteriophage rescue .....	100
Surface sterilization of infected plants.....	101
LD <sub>50</sub> calculations.....	101
Results.....	103
Development of duckweed as a model host for the <i>B. cepacia</i> complex....	103
Correlation between Bcc virulence in plant and insect models .....	107
Extension of the duckweed model to enteropathogenic <i>Escherichia coli</i> ..	109
Dynamics of bacteriophage rescue of plants from <i>B. cenocepacia</i> infection .....	111
Discussion.....	113
References.....	121
Chapter 2 – <i>Burkholderia vietnamiensis</i> produces a glycosylated hemolytic virulence factor <i>via</i> a non-ribosomal peptide synthetase .....	124
Introduction.....	125
<i>Burkholderia vietnamiensis</i> .....	125
<i>Bv</i> virulence pathways .....	126
Iron acquisition.....	126
Resistance to host defences.....	128
Inflammation and epithelial destruction.....	129
Cellular invasion.....	130
Social behaviours.....	131
Non-ribosomal peptide synthetases .....	132
Secondary metabolites in <i>Bv</i> and the Bcc.....	134
Objectives .....	137
Materials and Methods.....	137
Bacterial strains, plasmids, antibiotics and culture conditions .....	137
Random plasposon mutagenesis .....	140

Targeted mutagenesis.....	142
Genetic complementation .....	143
Liquid hemolysis assay .....	143
Wax moth larva killing assay.....	145
Prevalence of the hemolysin NRPS cluster in the Bcc .....	146
Results.....	146
Identification of an NRPS cluster through plasposon mutagenesis .....	146
Uniquely structured toxin is a broad-specificity hemolysin .....	149
Virulence in multiple model hosts .....	155
Prevalence of the NRPS gene cluster in the Bcc species .....	159
Discussion .....	165
References .....	172
Chapter 3 – Identification of <i>Burkholderia cenocepacia</i> virulence factors .....	178
Introduction.....	179
<i>Burkholderia cenocepacia</i> .....	179
<i>Bc</i> virulence pathways .....	180
Resistance to host defences.....	183
Objectives .....	191
Materials and Methods.....	192
Bacterial strains, plasmids, antibiotics and culture conditions .....	192
Random plasposon mutagenesis and virulence screening .....	193
Genetic complementation of mutant 46B2 .....	195
Duckweed infection .....	195
Wax moth larval infection.....	196
Phenotypic characterization of mutants .....	197
Overgrowth phenotype.....	197
Polymyxin B minimum inhibitory concentration.....	197
Swimming motility.....	198
Electron microscopy.....	198
Immunoblotting.....	198
Bioinformatics.....	199
Statistical analysis.....	200
Results.....	200

Identification of putative <i>Bc</i> virulence factors through plasposon mutagenesis .....	200
<i>In silico</i> characterization of putative virulence factors .....	202
Genetic complementation of mutant 46B2 .....	208
Additional phenotypic characterization of 16A11 and 46B2 .....	212
16A11 .....	212
46B2 .....	212
Discussion .....	216
References .....	231
Chapter 4: The <i>B. cenocepacia</i> antibacterial type VI secretion system .....	238
Introduction .....	239
The type VI secretion system .....	239
Functions of the <i>Bc</i> T6SS .....	240
Type VI secretion in <i>Bc</i> .....	243
Objectives .....	245
Materials and methods .....	246
Bacterial strains, plasmids, antibiotics and culture conditions .....	246
Insertional mutagenesis of <i>tssF</i> .....	248
Unmarked clean deletion of <i>tssF</i> .....	250
Genetic complementation .....	252
Interspecies competition experiment .....	253
Susceptibility of other human pathogens to <i>Bc</i> T6SS-mediated killing .....	254
Promoter prediction, protein localization and structural homology software .....	254
Results .....	255
The <i>B. cenocepacia</i> T6SS is homologous to T6SS-1 of <i>B. thailandensis</i> ..	255
Insertional mutagenesis of <i>tssF</i> disrupts T6SS activity in <i>B. cenocepacia</i> .	261
Clean deletion of <i>tssF</i> disrupts T6SS activity by <i>Bc</i> but is not restored by genetic complementation .....	263
Susceptibility of human pathogens to <i>Bc</i> T6SS-mediated killing .....	265
Type VI secretion does not contribute to duckweed or wax moth larval pathogenesis .....	268
Discussion .....	272
References .....	283

Chapter 5: <i>Burkholderia multivorans</i> virulence is activated by physiologically relevant temperature and oxygen levels.....	287
Introduction.....	288
<i>Burkholderia multivorans</i> .....	288
<i>Bm</i> virulence factors.....	289
Objectives .....	292
Materials and Methods.....	292
Bacterial strains, plasmids, antibiotics and culture conditions .....	292
Duckweed infection .....	292
Greater wax moth larval infections.....	293
Results.....	294
Manipulation of the duckweed model to mimic cystic fibrosis lung conditions.....	294
Discussion.....	297
Microaerophilic virulence activation (MVA) .....	297
Temperature-linked virulence activation .....	304
References.....	307
Conclusion .....	311
Research question .....	312
Project goals.....	314
Findings.....	315
Study limitations .....	316
Future directions .....	319
References.....	321

## List of Figures

Figure 1. Sample data for determination of <i>B. vietnamiensis</i> DBO1 LD <sub>50</sub> .....	102
Figure 2. <i>Lemna minor</i> provides both quantitative and qualitative assessments of bacterial strain lethality.....	104
Figure 3. The virulence of Bcc strains in duckweed correlates with their virulence in wax moth larvae.....	108
Figure 4. The virulence of enteropathogenic <i>Escherichia coli</i> (EPEC) strains in duckweed correlates with their virulence in wax moth larvae.....	110
Figure 5. <i>B. cenocepacia</i> infection of duckweed is alleviated by bacteriophage treatment up to 12 h but not after 18 h.....	112
Figure 6. Extension of a nonribosomal peptide, illustrated with the example of tyrocidine A synthesis in <i>Bacillus brevis</i> .....	133
Figure 7. The NRPS cluster responsible for toxic activity in <i>B. vietnamiensis</i> DBO1. ....	148
Figure 8. Bcc hemolytic activity on TSA 5% sheep blood agar.....	150
Figure 9. Development of a high-throughput liquid hemolysis assay.....	151
Figure 10. Lysis of human erythrocytes by <i>B. vietnamiensis</i> DBO1 requires the intact NRPS cluster, including biosynthetic genes and Lux regulators.....	154
Figure 11. <i>B. vietnamiensis</i> DBO1 requires intact NRPS cluster genes for full virulence against <i>Galleria mellonella</i> larvae.....	156
Figure 12. Genetic complementation of a putative NRPS cluster regulator in <i>B. vietnamiensis</i> DBO1 restores full virulence against <i>Galleria mellonella</i> larvae.....	157
Figure 13. <i>B. vietnamiensis</i> DBO1 may require a putative NRPS cluster regulator for full virulence against <i>Lemna minor</i> .....	159
Figure 14. Human erythrocyte lysis requires the presence of the NRPS cluster in <i>B. cepacia</i> complex isolates.....	164
Figure 15. Complementation of mutant 46B2 with <i>bcal1124</i> restores plant killing.....	209
Figure 16. Mutant 46B2 is attenuated in wax moth larval model.....	210
Figure 17. Western blots showing expression of Bcal1124 and Bcal1124” from whole cell lysates of strains 46B2/p1124 and 46B2/p1124”.....	211
Figure 18. Overgrowth phenotype of mutant 46B2 is partially relieved by constitutive expression of <i>bcal1124</i> in trans.....	214
Figure 19. Mutagenesis of <i>bcal1124</i> has no obvious morphological effects on <i>B. cenocepacia</i> K56-2.....	215
Figure 21. Mutagenesis, complementation and sequencing oligonucleotide locations in the <i>tssDEFG</i> locus.....	250
Figure 22. Inactivation of <i>B. cenocepacia</i> K56-2 type VI secretion through mutagenesis of <i>tssF</i> results in the abolishment of <i>E. coli</i> killing.....	262

Figure 23. Deletion of <i>tssF</i> abolishes the <i>E. coli</i> killing phenotype, but the phenotype is not restored by complementation <i>in trans</i> .....	264
Figure 24. Neural Network promoter analysis suggests the elimination of two putative promoters by the deletion of <i>tssF</i> .....	265
Figure 25. An intact T6SS has no effect on CF pathogens <i>P. aeruginosa</i> or <i>S. aureus</i> .....	266
Figure 26. Incubation with <i>B. cenocepacia</i> K56-2 reduces survivability of <i>K. aerogenes</i> , possibly through T6SS-mediated killing .....	267
Figure 27. The <i>Vibrio cholerae</i> V52 T6SS is active against <i>B. cenocepacia</i> K56-2 .....	268
Figure 28. The <i>B. cenocepacia</i> T6SS has no apparent role in virulence against <i>Galleria mellonella</i> (Greater wax moth larvae) or <i>Lemna minor</i> (Common duckweed) .....	270
Figure 29. Inactivation of <i>B. multivorans</i> ATCC 17616 type VI secretion through mutagenesis of <i>tssF</i> results in the abolishment of <i>E. coli</i> killing.....	271
Figure 30. Low oxygen increases the virulence of <i>B. multivorans</i> C5274 during <i>G. mellonella</i> infection. ....	296

## List of Tables

Table 1. Bacterial strains used in this study.....	95
Table 2. Strains and plasmids used in this study. ....	138
Table 3. Oligonucleotides used in this study. ....	140
Table 4. Bcc and related strains analyzed in this study .....	160
Table 5. Transcriptional changes of virulence-linked <i>B. cenocepacia</i> regulators and exported toxins under varying physiological conditions versus normal growth controls.....	190
Table 6. Strains and plasmids used in this study. ....	192
Table 7. Oligonucleotides used in this study. ....	194
Table 8. <i>B. cenocepacia</i> K56-2 plasposon mutants attenuated against duckweed plants. ....	200
Table 9. Genetic loci of virulence-attenuating plasposon insertions. ....	203
Table 10. Bioinformatical analysis of virulence genes. ....	205
Table 11. Strains and plasmids used in this study. ....	246
Table 12. Oligonucleotides used in this study. ....	249
Table 13. The <i>B. cenocepacia</i> J2315 genome encodes 10 putative VgrG proteins in 7 gene clusters.....	256
Table 14. <i>In silico</i> characterization of genes neighbouring <i>B. cenocepacia</i> J2315 VgrG homologs.....	259
Table 15. Effect of temperature and oxygen on the virulence of Bcc strains against duckweed. ....	295

## List of Abbreviations

CF: Cystic fibrosis

Bcc: *Burkholderia cepacia* complex

*Bv*: *Burkholderia vietnamiensis*

*Bc*: *Burkholderia cenocepacia*

*Bm*: *Burkholderia multivorans*

T6SS: Type VI secretion system

T6S: Type VI secretion

MVA: Microaerophilic virulence activation

PTVA: Physiological temperature virulence activation

NRPS: Nonribosomal peptide synthetase

EPEC: Enteropathogenic *Escherichia coli*

BCESM: *Burkholderia cepacia* epidemic strain marker

SHS: Schenk-Hildebrandt basal salt medium supplemented with 1% w/v sucrose

HR: hypersensitive response

---

# General Introduction: Virulence pathways of the *Burkholderia cepacia* complex

---

## **Opportunistic pathogenesis by the *Burkholderia cepacia* complex**

The *Burkholderia cepacia* complex (Bcc) is a group of Gram negative opportunistic pathogens with increasingly severe roles in hospitals, where they can infect a variety of immunocompromised individuals. Members of the Bcc were initially identified as opportunistic human pathogens over forty years ago (81), and became widespread among immunocompromised patients, particularly those suffering from the genetic diseases cystic fibrosis (CF) and chronic granulomatous disease (CGD; (52)). CF is caused by various mutations in the gene encoding the cystic fibrosis transmembrane conductance regulator (CFTR), a chloride ion channel that occurs in lung epithelial cells, resulting in the incapacitation of mucociliary clearance through the airway and particularly viscous saliva (230). Without proper mucus clearance, CF patients develop long-term bacterial colonization which is often associated with decreasing lung function. CGD results from a mutation in the gene encoding phagocyte oxidase, an enzyme responsible for the generation of reactive oxygen species (ROS) within phagocyte lysosomes. Without ROS, phagocytes cannot kill endocytosed microbes, which results in increased recruitment of phagocytes and prolonged, damaging inflammatory responses (2).

In North America, the prevalence of CF and CGD are approximately 1 in 3,000 and 1 in 200,000 live births, respectively (206). Among CF patients, the

infection rate is 5% in Canada (CF Canada, 2010), with mortality following Bcc acquisition as high as 20% (230). Particularly devastating impacts follow lung transplant because of the tendency of these bacteria to persist within sanitation products (41, 72, 153). Bcc infection is the second leading cause of death among CGD sufferers (165). Person-to-person Bcc transmission is known to occur, but the mechanisms and genetic markers of hypertransmissibility remain largely elusive (230), which confounds treatment regimens or limits them to a narrow range of antibiotics, to which Bcc are rapidly becoming resistant (102).

The first polyphasic metabolic and genetic profiling of the organisms initially classified as *Pseudomonas cepacia* and later *Burkholderia cepacia* divided *B. cepacia* into five genomovars (292), which were subsequently expanded into our current taxonomy comprising 17 species (293) encompassing the *Burkholderia cepacia* complex (Bcc). The large genomes of these bacteria are typically partitioned into several replicons, which likely give rise to the remarkable metabolic diversity of these organisms (202).

The primary CF pathogens of the Bcc are *B. cenocepacia* and *B. multivorans*, with *B. vietnamiensis* third in prevalence. Bcc species, and even strains, appear to employ different modes of pathogenesis. While *B. cenocepacia* strains usually demonstrate a high level of virulence in animal and plant infection models, *B. vietnamiensis* strains generally exhibit moderate virulence and *B. multivorans* strains exhibit comparative docility and in the same systems, underscoring a major gap in our understanding of these most important of Bcc species. Furthermore, *B. cenocepacia*-colonized patients undergoing lung

transplant tend to have poor prognosis compared with patients colonized with other members of the Bcc (300). *B. cenocepacia* and *B. multivorans* are among the most divergent of the Bcc based on whole-genome identity but are the most deadly within the CF lung, despite their contradictory behaviours in other eukaryotic hosts. *B. multivorans* and *B. vietnamiensis* are fairly close in phylogeny (291). The overarching objective of the projects that follow are to further delineate the pathological features of these bacteria and help to resolve the means by which they utilize their extensive rhizosphere adaptations to cause such devastating harm in CF patients.

## **Bcc ecology reflects metabolic and genetic versatility**

### **Interactions with soil organisms**

Most Bcc species have representative strains isolated from the rhizosphere of diverse plants, and in some cases identical strains have been isolated from clinical and environmental samples. The diversity of their interactions with abiotic and biotic factors within soil habitats is demonstrated by the widespread desire to use Bcc members as both biological control agents and plant growth promoters (44). In the former case, Bcc bacteria are useful in fending off root rot of pea plants (114) and damping-off in maize (112), both fungal infections. In terms of promoting plant growth, the bacteria typically stimulate root growth following colonization of the roots, which allows for greater soil nutrient absorption by the plant (45). Bcc bacteria invade the roots of several plants, including sugar cane (174), rice (248), and tobacco (61). Inside the roots, they normally exist as

symbionts, mobilizing limiting nutrients such as phosphate and nitrogen for plant use, and inhibiting infection by pathogenic fungi (61). Root invasion, at least in rice roots, appears to occur following bacterial alignment along the cleft between adjacent root epidermal cells, after which enzymes are required to degrade cell wall polymers for bacterial invasion through several layers of differentiated cells (248).

A symbiosis therefore develops in which bacteria fix nitrogen or mobilize phosphate in exchange for “payments” of nutrient-rich exudates from plant roots (15). There is currently great interest in the use of Bcc and other bacteria to help diminish the use of chemical fertilizers and pesticides. Bacteria representing such potential are referred to as plant growth-promoting bacteria (PGPB; (44)).

The potential of Bcc strains as PGPB, though contentious on account of the opportunistic pathogenicity displayed by some of these bacteria, is reflected in their metabolic diversity. Nitrogen and phosphorus are typical limiting growth factors for plants, and many Bcc strains contain the necessary genetic and cellular machinery to provide these elements in their usable forms. Nitrogen fixation occurs first by the energy-intensive reductive breakage of dinitrogen to generate ammonia, using a nitrogenase complex encoded by the *nif* genes (78). Ammonia is then oxidized by nitrifying bacteria to generate nitrate, which is a more commonly usable nitrogen source for plants (15).

In its insoluble form, phosphate is not absorbed by plant roots. Even following the application of phosphate-containing chemical fertilizer to soil, much

of the phosphate precipitates, forming insoluble tricalcium phosphate. Bcc bacteria are known to mobilize phosphate from this state to a soluble form available to plant roots (203), a process that relies on the oxidation of glucose to gluconic acid by GabY (10). Thus, one would expect that large densities of *gabY*<sup>+</sup> Bcc would colonize root surfaces as a result of the exchange between plants and bacteria of root exudates and a limiting plant growth factor, though studies on the frequency of this gene among root-colonizing Bcc have not been carried out.

An understated feature of Bcc ecology involves its interactions with bacteriophages. Lysogenic phages are believed to be a major factor promoting the genetic versatility of Bcc; of the nine Bcc genomovars known in 2003, seven were found to contain prophages within their genomes (150). This discovery, combined with the fact that Bcc-infecting phages are routinely isolated from soil samples (150, 245), indicates that Bcc habitats are rife with lytic and lysogenic phages with which the bacteria have coevolved.

The Bcc, like other soil bacteria, probably represent important prey for grazing protozoa (9), nematodes (121) and predatory fungi (277). Certain predatory fungi can even grow using bacterial cell envelopes as their sole carbon and nitrogen source (277). Accordingly, Bcc strains have developed modes of predator evasion, including the production of polyketide, nonribosomal peptide and fatty acid-based antifungal compounds (4, 107, 125, 130, 136, 154, 157, 176, 210, 241, 264, 272, 275). Interestingly, some of these compounds are positively regulated by quorum sensing (241), perhaps suggesting that Bcc bacteria produce antibiotics in defence of territory rather than invasion. An enzymatic antifungal

defence of the Bcc is  $\beta$ -1,3-glucanase, which degrades fungal cell walls (307). *Burkholderia* bacteria are also apparently able to defend against nematodes and protozoa (nematodes will be discussed at length in a later section). One study has shown that *B. pseudomallei* kills *Caenorhabditis elegans* by endotoxin-mediated paralysis that interferes with calcium signaling in the nematode (197). *B. multivorans* has been shown to kill another nematode, *Panagrellus redivivus*, by an uncharacterized mechanism that does not involve cellular invasion (152). Meanwhile, studies on interactions between the Bcc and amoebae have made particular use of *Dictyostelium discoideum* and *Acanthamoeba polyphaga*. *B. cenocepacia* and *B. vietnamiensis* invade *A. polyphaga* and may replicate within acidic vacuoles, averting the fusion of lysosomes and exposure to degradation factors (147). Bcc cells have also been observed replicating within the amoebal phagosome (149), though evidence to the contrary has also been presented (147). The former case suggests that Bcc parasitizes soil amoebae, while the latter case hints that Bcc utilizes amoebae for transport among soil microenvironments – a tactic known as phoretic transport. Another interesting possibility might be that since amoebae can form cysts that are highly resistant to harsh environmental conditions, Bcc (non-spore formers) invade these protozoa under conditions of extreme stress. Survival within cysts has been shown in *Legionella pneumophila* and *Mycobacterium avium* (50, 267), though the ability of Bcc bacteria to perform this task has not yet been studied. In terms of mechanism, Aubert *et al.* demonstrated cytotoxicity by Bcc type VI secretion system-mediated actin rearrangement in both *Dictyostelium* and macrophage models (9). The parallels

between these two models emphasize the possibility for concurrent adaptations enhancing Bcc survivability within their mammalian hosts and in soils.

### **Genomic plasticity**

It has long been realized among Bcc researchers that the Bcc genome can be quite dynamic, with rearrangements and transposition of insertion sequences (IS) fairly common (95). It is thought that ISs allow for genome reduction and rearrangement events following IS duplication, transposition to other regions of a given chromosome, and deletion of the region between the ISs by homologous recombination. For example, the emergence of *B. mallei* from its ancestral species *B. pseudomallei* likely occurred following the former species' acquisition of several IS elements, *IS407* being the predominant of these (260). The genome reduction and consequent host specialization of *B. mallei* from the opportunism of *B. pseudomallei* to an obligate mammalian pathogen is attributed to *IS407*-mediated deletions and rearrangements of the genome, ultimately guided by selection pressures within the host. Deleted genes in *B. mallei* generally relate to survival outside of mammalian hosts (191).

A recent study characterized the ISs of the Bcc, with particular emphasis on the prevalence of *IS407* and its implications for the genomes of epidemic *B. cenocepacia* lineages (105). *B. cenocepacia* J2315 is among the most well-characterized Bcc strains as a result of its membership in the ET12 clonal complex, which devastated the UK and Canada in the 1980s. The authors revealed a 1.34 Mb IS-mediated genome reduction in J2315 relative to another lineage.

This reduction was distributed among 58 separate events, demonstrating the dramatic impacts of IS propagation through a genome.

It is unclear what roles such genomic modifications play in CF infection. One piece of evidence in support of such roles is that the movement of *ISBcen20* in *B. cenocepacia* can be triggered by oxidative stress (79), while ISs in *B. multivorans* transpose in response to high temperature, but not oxidative stress or starvation (198). *B. vietnamiensis* was also found to have highly active ISs under normal growth conditions (177). *B. multivorans* undergoes substantial phenotypic changes during chronic colonization, including decreased mucoidy, motility, and virulence, as well as increased biofilm formation and antibiotic resistance, but most of these changes correlate with reduced transcription of phenotype-relevant genes. In addition, a clone isolated later during chronic infection grew better on minimal media, providing indirect evidence that it had not lost important metabolic genes through genetic rearrangement (253). A similar analysis in *B. cenocepacia* performed with a much greater number of isolates showed better growth under iron limitation by a later isolate as compared with the earliest one, a sharp decline in motility among isolates over time, and a general increase in unsaturated fatty acid content (60). Likewise, the increase in growth under iron limitation runs against the likelihood of gene loss. Most likely, a subset of the population undergoes genetic rearrangements and deletions that generally are not noticeable until one clone emerges with a strong competitive advantage; in studies such as those described above, analyzing single isolates is useful in defining

regulatory trends for sequential isolates in a given environment, but may not reveal large-scale genetic rearrangements.

## **Characteristics of the CF lung**

### **Innate defence mechanisms of a healthy lung**

During inhalation, many particles are introduced to the respiratory tract, including dust, moisture droplets, and spores. Bacteria are frequently carried on dust particles or within moisture droplets. As air velocity decreases sharply with increasing distance from the pharynx, most of these particles will settle and be trapped by the mucus lining the inner surfaces of the respiratory tract, to be phagocytosed by antigen-presenting cells (APC) of the immune system (2) or swept upward toward the pharynx to be expelled or swallowed (164). This sweeping motion is mediated by the cilia of ciliated epithelial cells that permeate the upper airway.

Ciliated epithelial cells arrange their microtubules such that slender membranous outgrowths appear on their apical surfaces. In the lower regions of the respiratory tract, simple squamous epithelia dominate, providing a thin barrier to allow for facilitated gas exchange between the blood and alveolar sacs (35). Below these epithelia is a dense extracellular matrix composed primarily of collagen, proteoglycans and glycoproteins that functions to embed and support the epithelium. Two forms of junction connect adjacent epithelial cells. Tight junctions serve as permeability barriers to selectively allow the passage of nutrients and signaling molecules, water, and immune cells between the apical

and basal epithelial surfaces. Three nanometre-wide hydrophobic gap junctions connect adjacent cells and allow for intercellular electrical or chemical communication (20).

Bronchial and alveolar epithelial cells dominate human airways. In the large airways, bronchial epithelial cells and goblet cells function in the regulation of ion exchange, production of mucin, inflammation, and repair responses. Goblet cells, in concert with submucosal glands, are the main players involved in mucin production and secretion, which occurs in response to physical and chemical cues (46). Small airways are lined with type I and II alveolar cells (83), Clara cells, and serous cells (46). Type I alveolar cells (or simple squamous alveolar cells) are flat cells that make up 95% of the epithelial surface area and consequently are important as a physical barrier in the lung, and allow for gas exchange. Contrastingly, type II alveolar cells are cuboidal in shape, and while they make up a small proportion of the surface area in the lung, they can act as progenitors to replace damaged type I alveolar cells (158). Type II alveolar cells are crucial for lung defense as they are able to secrete antimicrobial products, sense invasion from pathogens, and produce cytokines and chemokines to regulate inflammation in the lung (83). Additionally, they secrete surfactant and surfactant-associated proteins, which promote lower surface tension, effective gas exchange, and defense through antimicrobial and anti-inflammatory processes (2, 170).

Once bound to the epithelium, bacteria encounter several elements that select for suitably adapted cells. Among these pressures are antimicrobial compounds secreted by epithelial cells (2), phagocytes and competition for

nutrients with established commensal bacteria (164). Mucosal antibodies, secreted through the epithelium, can bind antigens found on the surfaces of invading bacteria to promote phagocytosis of these cells (2). The epithelium is also littered with a spectrum of toll-like receptors (TLRs) responsible for detecting pathogen specific molecules to initiate immune responses (8). There are currently 10 known TLRs in humans and they each detect one or more pathogen-associated molecular patterns (PAMPs), such as LPS, which signals through TLR4 and a co-receptor, and flagellin, which signals through TLR5 (196). Signal transduction passes information concerning the invader to an adapter protein (often MyD88) and an appropriate response is triggered in the cell and surrounding tissue to limit the invader's progress.

Defensins and cathelicidins are the most prevalent antimicrobial peptides produced in the lung (18, 145). Neutrophils and lung epithelial cells secrete  $\beta$ -defensins. While Human  $\beta$ -defensin-1 (HBD-1) is constitutively expressed and secreted into the lungs, HBD-2, -3, and -4 are stimulated when pathogens, inflammatory cytokines, or TLR ligands are present (109, 255). LL-37, a human cathelicidin, is also induced by the presence of pathogens (14). These antimicrobial peptides play immunomodulatory roles: LL37 can recruit neutrophils, monocytes, mast cells, and T-cells (192); HBD-2 can recruit mast cells; and HBD-3 and -4 can attract monocytes and macrophages (314).

Enveloping the alveolar sacs are blood capillaries with single-cell endothelial layers. These endothelia, in conjunction with type I pneumocytes, provide an ideal interface for the exchange of carbon dioxide and oxygen (35).

Immune cells may pass across the endothelium when recruited to the lungs by cytokine signaling (2), but macrophages are the first line of cellular defence before such triggered migration, regularly patrolling the alveolar sacs and ingesting particles that penetrate beyond the ciliated upper regions of the airway. Alveolar macrophages have at their disposal reactive oxygen species, lysozyme, proteases and antimicrobial peptides to eliminate invading microbes following phagocytosis. Upon encountering large numbers of microbes, alveolar macrophages release inflammatory cytokines to recruit neutrophils as additional reinforcements (227). However, macrophages are also responsible for clearing dead immune cells from the air spaces; depletion of the macrophages by chemical or biological elements exacerbates any existing problems by the build-up of purulent fluid in the alveoli (227).

Counteracting some of the deleterious effects of these defence mechanisms is glutathione (GSH). An antioxidant found in abundance in the lung, GSH detoxifies a number of different compounds, including carcinogens, reactive oxygen species, pollutants, xenobiotics, and peroxides. In healthy lungs, GSH is secreted at the apical surface of epithelial cells *via* CFTR (137).

These physical and chemical defences are buttressed by the presence of colonizing microbes. Until recently, the lung was considered to be relatively sterile. However, the emergence of metagenomics has revealed vast diversity that should not surprise microbiologists, considering the omnipresence of microbes on other mucosa (27). The authors suggested that, like in the gut, commensal

microbes may play a protective role in defending against invaders by competing for niche space.

The mammalian airway presents a unique combination of ecological factors that prevent the entry and colonization of microbial pathogens. Individuals such as CF sufferers lack a number of innate defences against microbial colonization.

### **Innate immune deficiencies in the CF lung and nutrient availability**

The success of an infection hinges on the invader's abilities to acquire nutrients and to respond appropriately to environmental factors and host signals. The CF lung represents an environment unique in the living world that has proven difficult to model accurately, but with our growing knowledge of the physicochemical conditions governing microbial activity within CF lungs, portrayals of the infection process are beginning to acknowledge the crucial interplay between immune system miscues and the physicochemical conditions permeating this environment.

Until recently, mucus clearance in the healthy human lung was represented by a gel-on-liquid mucus clearance model, in which an osmotically dense mucus layer is moved out of the lung toward the trachea by the beating action of cilia embedded within a periciliary layer of lower osmolarity. This represents a logical inversion whereby a layer of higher osmolarity is supported by a matrix of lower osmolarity. The shortcomings of this model have been mended by recent work

pinpointing high concentrations of membrane-tethered mucins as the mysterious source of density preventing the mucus layer from collapsing upon the periciliary layer (33); the tethered nature of these mucins prevented their prior identification in studies examining the osmolarity of extracted airway fluids (171). This gel-on-brush model provides an excellent starting point for understanding the physicochemical environment of the CF lung. Dehydration of the mucus layer due to lack of chloride secretion increases its osmolarity, causing it to collapse upon the periciliary layer. This collapse halts the cilia-mediated movement of the mucus out of the airway to generate the inviting microbial habitat of CF sputum. This section will describe some emerging stories in our understanding of CF lung conditions that may relate to pathogen activity.

The first major study showing hints of the true microbial diversity within healthy human lungs was seeking to develop a microbial signature for CF, comparing sequencing reads from sputum in a group of CF patients with a group of healthy individuals. CF lungs were characterized by lower diversity indices and greater numbers of uncultivated bacteria than healthy lungs. Principle component analysis suggested that bacterial phyla associated with healthy lungs included Bacteroidetes, Spirochetes and Fusobacteria, while phyla associated with CF included Firmicutes, Proteobacteria and Actinobacteria (27).

Recent efforts in deciphering the molecular signatures of the CF lung include the publication of several recipes for artificial CF sputum media. One of these (201) was based on the average results obtained from chromatographic analyses of CF sputum taken from twelve *P. aeruginosa*-carrying patients, and

provided estimates for free amino acid, lactate, glucose and various anion concentrations. A surprising result of this analysis was the abundance of aromatic amino acids within CF sputum. This abundance may be reflected in the selection of amino acid auxotrophs among Bcc isolates from CF sputum (17). However, this recipe lacked both DNA and mucin (discussed later), both of which are known contributing factors to the establishment of *P. aeruginosa* microcolonies in the CF lung, prompting Fung *et al.* (94) to develop a synthetic medium (ASMDM) for *P. aeruginosa* gene expression analysis. Their results showed down-regulation of virulence-related genes and up-regulation of nutrient acquisition machinery during static growth in ASMDM. The efforts of these and other groups (265) will no doubt underpin future work aimed at modelling behaviours of microbes in this complex environment.

Relating back to the collapse of the airway mucus layer and the consequent stasis of CF lung sputum, two early studies investigated oxygen levels within the mucus layer and their effect on *P. aeruginosa*. A steep oxygen gradient was observed between the oxic epithelial surface, the hypoxic mucus layer where the bacteria are known to reside, and the oxic lumen within the airway *in vivo* (311). This study went on to show that *P. aeruginosa* depends on motility to access the hypoxic zone, up-regulates alginate – an exopolysaccharide linked to cyanide production during mucoid growth (51) – in response to hypoxia, and grows to greatest density in the more hypoxic mucus. Yoon *et al.* (317) then showed that an outer membrane porin, OprF, is up-regulated during anaerobic growth, required for biofilm formation, and targeted by host antibodies. Further

work demonstrated the importance of this protein for virulence, linking it to both quorum sensing and type III secretion in *P. aeruginosa* (89). These results suggest that as the interplay unfolds between *P. aeruginosa* and its host during colonization and the subsequent development of chronic infection in the CF lung, lung microenvironments change dramatically in favour of organisms able to adapt to low oxygen levels. The recent update of the CF periciliary brush model by Button *et al.* (33), described above, supports this phenomenon by providing a feasible mechanism by which CF airway fluids dehydrate and collapse upon the mucociliary clearance cilia, thereby providing an ideal breeding ground for adapted bacteria.

This updated model implicates mucins – heavily glycosylated, sulfated or sialylated, polymeric proteins that exist in both secreted and tethered forms in the airway. They play a protective role in healthy lungs, helping to encapsulate microbes for clearance. Current techniques have been unable to resolve whether mucins are overproduced or underproduced in the CF lung (226, 278), so the adhesive nature of CF sputum and the mucociliary clearance deficiency of CF patients remain partially obscure. In a healthy lung, mucins occur largely in polymeric form; a study finding decreased levels of polymeric mucins in CF sputum relative to healthy controls (113) may be explained by mucin depolymerization as a consequence of the abundant proteases found in the CF lung (278). Regardless, mucin does appear to be degraded by microbial and host factors, and further mucin degradation may even occur *via* microbial

desulfurization, although the released sulfate is not a suspected nutrient source (220).

High protease levels in the CF lung also give rise to microbleeds that release hemoglobin into the lung. Hemoglobin is then degraded by the abundant proteases found in the CF lung, including *Pseudomonas* proteases and, primarily, neutrophil elastase (NE) (58). Once in the lung, heme can help to promote microbial growth, which in a healthy lung is hindered by ferritin, transferrin and lactoferrin-mediated iron sequestration (284). The Bcc are able to bind heme through poorly understood means (42, 256), and produce a number of hemolytic products that could potentially yield iron bonanzas for the bacteria through the release of hemoglobin from erythrocytes (4, 26, 86, 118, 190, 276, 294). Unique among human pathogens, *B. cenocepacia* can acquire iron directly from ferritin through its proteolysis (308); since ferritin is found at 70 to 700-fold higher levels in the CF lung than in a healthy lung (218, 268), likely as a result of its up-regulation in lung tissues (96), this could represent a major factor in Bcc infection.

The release of heme into the lungs promotes further inflammation *via* the induction of cytokines IL-8 and IL-10 (58). The primary inflammatory cells migrating to the lungs are neutrophils, whose contribution to CF lung disease cannot be overstated. In healthy lung epithelial lining fluid, neutrophils make up only about 1% of inflammatory cells, but in a CF lung, neutrophils represent up to 90% of immune cells, even in young infants (306). The most damaging of their exported proteases appears to be NE, which at the low levels found in a healthy lung acts to kill internalized bacteria and combine with chromatin to form

neutrophil extracellular traps (NETs), important antibacterial agents (135). In the CF lung, however, NE contributes to a number of adverse side effects, including proinflammatory cytokine up-regulation, degradation of many extracellular matrix proteins, induction of mucin production by epithelial cells, and cleavage of cell surface proteins (135). In an ironic twist, NE has been shown to cleave receptor CXCR1, which receives the IL-8 neutrophil activation signal, thereby disabling the killing mechanisms of these phagocytes in a protease concentration-dependent manner (110). Cleaved CXCR1 fragments then trigger additional release of IL-8 at the epithelium *via* TLR2. These discoveries help explain the perpetuation of inflammatory pathways in CF.

The antibacterial role of proteases is supplemented in healthy lungs by additional compounds, including nitric oxide (NO). NO is produced by phagocytes and epithelial cells particularly during inflammation, when inducible nitric oxide synthase (iNOS) is stimulated. Despite the inflammatory nature of the CF lung, CF bronchial epithelial cells exhibit decreased iNOS expression (175), which causes an increase in epithelial adherence of *P. aeruginosa* (66). This trend has not yet been studied in the Bcc. Since NO and hydrogen peroxide (H<sub>2</sub>O<sub>2</sub>) can combine to kill *B. cenocepacia* (257), the NO production deficiency in CF patients may partly explain the efficacy of these organisms in colonizing CF lung tissues.

Autophagy is the controlled degradation of unnecessary or excessive cellular components and foreign microbes. In CF macrophages, this process has been shown to be defective through the mislocalization of protein BECN1 away

from the endoplasmic reticulum, which occurs with the absence of activation of protein TG by CFTR. The consequence of BECN1 mislocalization is that important proteins related to vacuolar sorting and autophagosome formation are not activated. These events coincide with the overproduction of ROS in the cytoplasm by defective mitochondria, which would otherwise be degraded in the autophagosome (299).

Although there is evidence that TLRs and their cognate ligands are expressed and functional in the CF airway epithelium (53), a reduction in apical surface expression of TLR4, poor response to stimulation with LPS, and decreased signaling *via* adaptor proteins MyD88 and TRIF has been observed in CF epithelial cells (126, 127).

Another compromised defence that helps explain the bacterial colonization of the CF lung epithelium is the peroxidase system. Lactoperoxidase (LPO) works by catalyzing the oxidation of thiocyanate (SCN<sup>-</sup>) to OSCN<sup>-</sup>, an antimicrobial compound, using H<sub>2</sub>O<sub>2</sub>. A recent study has shown that defective SCN<sup>-</sup> transport in CF lung epithelia, which normally occurs *via* CFTR, results in decreased activity against *P. aeruginosa* (55). A structural relative of LPO is myeloperoxidase (MPO), which is produced by neutrophils and through the use of H<sub>2</sub>O<sub>2</sub> yields hypochlorous acid (HOCl), also an antimicrobial compound (208). MPO and LPO have been shown to co-localize in the lung, and the interaction between HOCl and LPO causes spontaneous release of free iron through the breakdown of heme (263). Heme degradation was then shown to be inhibited by

SCN<sup>-</sup>, which as noted above is not transported properly to the CF lung epithelial surface.

Similarly, decreased levels of GSH are observed in the CF lung because CFTR is normally responsible for its efflux (69). Airway treatment with a glutathione prodrug caused decreased neutrophil burden and elastase activity in the lungs of CF patients, supporting the anti-inflammatory role of this molecule in healthy lungs (280).

Finally, the role of pH is gaining increasing attention. Recent experiments in which immobilized *Staphylococcus aureus* and *E. coli* were placed in CF and non-CF porcine airways showed that killing of the bacteria correlated with the higher pH found in the non-CF pigs (205). This killing appeared to depend on the efflux of HCO<sub>3</sub><sup>-</sup> into the lungs by CFTR, and was proposed to occur through an antimicrobial peptide mechanism. Other recent findings suggest that *Burkholderia glumae* and other species outside of the Bcc are susceptible to alkaline pH, and, as will be discussed further, produce oxalic acid in response. Therefore, regardless of whether or not the innate resistance of the Bcc is enough to survive exposure to antimicrobial peptides in the lungs, the bacteria likely have a growth advantage in the slightly acidic CF lung. Hopanoid production, widespread in *Burkholderia* (65) but not known in other pathogens, has been shown to contribute to acid tolerance in the Bcc (239). Although the authors showed a decrease in growth at pH 4.5 in a hopanoid-deficient mutant versus the wild type *B. cenocepacia* strain, the data suggest other possible means by which the Bcc gain a competitive advantage in the CF lung.

The literature describes the CF lung as an environment dominated by host microbes, particularly concerning neutrophil activity, and characterized by low oxygen levels, highly disruptive and inflammatory protease activity, a high degree of iron and amino acid availability, and high osmolarity that should be taken into account when designing experiments seeking to mimic CF lung conditions.

### **Microbial and viral biodiversity in the CF lung**

While characterizing the interactions between host and Bcc cells clearly presents a vast challenge for researchers, the importance of competitive and cooperative microbial interactions should not be overlooked. Recent studies have begun to identify the vast diversity of bacteria present in CF sputum using both culture-dependent and -independent approaches, and are summarized in three excellent reviews (161, 211, 318). Several emerging trends are apparent from the literature. The first is that microbial diversity appears to negatively correlate with patient age, with the usual CF pathogens tending to dominate later in life, suggesting an undesirable form of ecological succession. Second, a number of organisms previously unknown to the CF research community are commonly found in sputum samples, including a variety of obligate anaerobes that seem to co-occur with *P. aeruginosa* (74). Although the presence of these obligate anaerobes was explained by suggesting contamination of sputum samples with oropharyngeal microbes during extraction (101), an alternative explanation is that the submucosal layer of the CF lung becomes anoxic as a result of microbial activity in relatively static mucus (311). There is currently little evidence linking these anaerobes, which include *Prevotella*, with decreasing lung function.

However, other previously overlooked bacteria, most notably of the *Streptococcus milleri* group (SMG), may play substantial roles in guiding disease states among patients. Sibley *et al.* (251) showed correlations between pulmonary exacerbations in CF patients and population blooms of *S. milleri*. Follow-up on this work applied pulsed-field gel electrophoresis to show patient specificity of SMG isolates, concluding that patient-to-patient transmission is unlikely (252). Another emerging trend suggests that increasing patient age and decreasing lung function correlate inversely with microbial diversity (measured by both species number and evenness), with *P. aeruginosa* often coming to dominate the habitat. This may indicate that the classical CF pathogens are initially kept at bay by a high diversity, only to squeeze out their competitors in the later stages of infection. Decreasing microbial diversity could be a result of differential microbial resistance to host immune factors or to microbial competition. If the latter holds true, interspecies interactions in the CF lung may play a substantial role in disease progression. For example, pyocin production by *P. aeruginosa* PAO1 was shown to cause large shifts in population dynamics when grown with a pyocin-sensitive *P. aeruginosa* strain in an anaerobic biofilm (302). Another study has shown bacteriocin-mediated growth inhibition of *P. aeruginosa* and Bcc strains by CF isolates of both groups (12); that is, strains of these pathogens antagonize both related and unrelated bacteria. This finding was recently reaffirmed in a study showing that *P. aeruginosa* antagonistic factors are most effective against relatives of intermediate genetic distance (242). The proposed rationale behind this strategy is that closely related organisms are likely to maintain similar

immunity systems, while more distantly related organisms are unlikely to compete within the same niches. Further research should investigate the antagonistic interactions among other co-isolated strains of CF pathogens.

An often overlooked aspect of CF pathology is fungal infection; it is not surprising that with the prolonged antibacterial therapy that many CF patients undergo, research has begun to show high incidence of fungal pathogens including *Aspergillus fumigatus* and *Candida albicans* in patients' lungs (11). A review by Nagano *et al.* (188) highlights the predominant fungal colonizers of the CF lung and points out the main findings in that field: fungal colonization tends to follow on the heels of heavy antibacterial therapy as well as lung transplants, when opportunistic infections often occur as a result of patient immunosuppression; fungal colonization tends to occur in older patients; and culture-independent approaches are unveiling the high prevalence of fungal infection in CF patients. The pathological relevance of fungal infections remains unclear, with conflicting reports on the benefits of antifungal treatment of *Aspergillus* (1, 250). With continuing research, such as that carried out by Delhaes *et al.* (74), the major fungal colonizers can be assessed in terms of their relationship with patient disease state.

The spatial heterogeneity of bacteria and their accompanying bacteriophages has been investigated in two studies using explant and post-mortem infected lungs of CF patients (309, 310). Together, the studies show significant taxonomic variation among the different regions of lung. Interestingly, bacteriophages were largely absent from the upper lobes of the explant lung,

which are typically the site of greatest inflammation and infection in the CF lung. Although the authors suggest that the upper lobes may represent a safe haven from bacteriophages, the presence of bacteriophages in the upper lobes of the deceased patient's lungs contradicts this hypothesis. Identified bacteriophages included predators of *Burkholderia*, *Pseudomonas*, *Staphylococcus* and *Haemophilus*. Interestingly, recent work demonstrated that phage-to-bacteria ratios are on average 4.4-fold higher on mucosal surfaces than in surrounding environments in a diverse panel of metazoans. Phage T4 was then shown to adhere to mucins *via* an immunoglobulin-like capsid domain (16), suggesting a possible mutualistic interaction between metazoans and phages. In addition to implying a novel facet of innate immunity in animals, this finding may relate to the heterogeneous distribution of phage in the lobes of the CF lung and mucin production therein.

The recent advances in CF lung biodiversity are helping to produce a more complete landscape of the CF lung. With improved 'omics methods, the metabolic significance of this biodiversity will help researchers identify the real microbial contributions – positive and negative – to the progressive deterioration in lung function experienced by CF sufferers.

### **Localization of Bcc bacteria in the CF lung**

Now that we have a more vivid description of CF lung environment, it is worth mentioning where Bcc bacteria reside within it. Sajjan *et al.* (232) used antibodies raised against two surface adhesins of *B. cenocepacia* epidemic strains to immunolocalize bacteria within lungs acquired from nine deceased and post-

transplant CF patients. Their findings demonstrate an idiosyncrasy of Bcc infection in the CF lung: disseminating into most lung sections, the bacteria were able to invade multiple layers of tissue down to the alveolar capillary lumen and even into alveolar macrophages. Widespread dissemination within the lung is known from postmortem analyses (254, 258) and supporting evidence has been provided that several Bcc species invade both lung tissues and phagocytes from *in vitro* invasion studies using *CFTR*-mutated (*CFTR*-) cells, as will be discussed later. To our knowledge, there is no published evidence describing CF lung tissue or phagocyte invasion by other common CF lung pathogens, including *Staphylococcus aureus*, *Pseudomonas aeruginosa*, *Haemophilus influenzae*, *Stenotrophomonas maltophilia*, and *Streptococcus* spp.

The emergence of metagenomics has provided another powerful avenue by which we can localize pathogens within the CF lung. In particular, a metagenomics analysis of postmortem and explanted CF lung sections show some regional distribution of microbial communities within the samples but very different overall community structures between the two patients, with the post-mortem lung dominated by *P. aeruginosa*, and the explanted lung showing greater diversity (310). Not surprisingly, the infrequency of Bcc infections (<5% of CF patients) reduces the usefulness of such studies in identifying key pulmonary loci in Bcc infection; in this case, the explanted lung showed traces of *Burkholderia* bacteria in several regions of the lung, while the postmortem lung had no hits. Future studies could use this approach in lungs of transplant or deceased patients

known to have suffered from Bcc infection to establish further support for the invasive nature of the Bcc.

In short, Bcc bacteria are able to disseminate to most regions of the lung and even beyond it by invading the underlying tissues. This characteristic is unique among CF pathogens and its mechanism is multi-factorial, as later sections will expose.

## **Infection models for Bcc pathogenesis**

The unique characteristics of the CF lung make modeling infection quite troublesome. A number of models have been developed for the Bcc that have contributed to the identification and characterization of virulence pathways, host responses, potential therapies and even effects of polymicrobial infection. However, it is only recently that true CF models have emerged, enabling the possibility of sifting out the important elements of Bcc pathogenesis.

### **Animal models**

An early study using mice compared the persistence and virulence of *P. aeruginosa* and *B. cepacia* in a burn wound model, since *P. aeruginosa* was considered an important pathogen of burn wounds and *B. cepacia* had not yet been identified as a CF pathogen. The study found that although *B. cepacia* was highly persistent, its lethality in this system was much lower than that of *P. aeruginosa* (271). Since then, most studies using mice and rats have focused on pulmonary Bcc infections. Because acute infections tend to be cleared within several days unless immunosuppressive agents are used, bacteria are typically

embedded within an agar matrix to establish chronic infection. Embedding bacteria in agar is thought to have the added advantage of providing the microaerophilic conditions in which bacteria thrive in the CF lung (31). These models have been used to assess: the importance of virulence factors such as proteases, exopolysaccharides, siderophores and others, (49, 56, 90, 139, 301); the efficacy of potential therapies including bacteriophage therapy, quorum sensing inhibition, immunization, and innate immunity stimulation (3, 25, 30, 39, 319); the invasive nature of different Bcc isolates (47); the requirements for and effects of chronic infection (117, 266); and communication in polymicrobial infection (219).

While the rodent models are reliable because of the presence of innate and adaptive immunity, roaming defender cells and similar lung cells and structures to humans, they are hindered by cost and time. A number of cheaper and faster animal models have emerged in the past decade to address those concerns, and the first among these was *Caenorhabditis elegans* (nematode) (141, 197). It was found that *C. elegans* underwent either fast or slow killing after feeding on *B. cenocepacia* depending on osmolarity of the growth medium, both of which were abolished by inactivation of *cep* quorum sensing. However, only slow killing was abolished by inactivation of a quorum sensing-regulated gene, *aidA*. Although *P. aeruginosa* is known to use cyanide in the killing of *C. elegans*, the authors concluded that *B. cenocepacia* was not using cyanide because it was not detected in culture media following growth (141). However, as will be discussed in a section to follow, it was later shown that cyanide is only produced by the Bcc

during biofilm growth (228). The mechanism by which AidA influences slow killing could well be through cyanide production following the establishment of biofilms in the *C. elegans* gut. No role for AidA has yet been established. Nonetheless, a number of studies have used *C. elegans* to identify or assess the importance of other virulence factors in the Bcc. Such virulence factors include a type II secretion pseudopilin (259), an acyl carrier protein potentially involved in secondary metabolite production or fatty acid synthesis (261), an apparent regulator of stress resistance (215), carbon metabolism (151), and the regulatory RNA chaperone Hfq (262). Two studies compared *C. elegans* slow killing among Bcc species, and in both cases *B. multivorans* exhibited low relative virulence while *B. cenocepacia*, *B. ambifaria* and *B. pyrrocinia* showed high but somewhat strain-variable virulence (38, 57). A useful element of this infection model was the possibility for large-scale high-throughput screening of randomly generated mutants, as initially performed in *P. aeruginosa* by Tan *et al.* (274) and later repeated in *Staphylococcus aureus* by Begun *et al.* (21). This approach was taken to identify Bcc virulence factors in a 3,000 mutant screen for virulence attenuation (259).

The next invertebrate model established for use in the Bcc was the *Galleria mellonella* larva. This model was the first to introduce a 50% lethal dose (LD<sub>50</sub>) format to compare virulence among strains. As in *C. elegans*, *B. multivorans* was consistently found to be the least virulent among the species tested. Meanwhile, *B. cepacia*, *B. pyrrocinia* and *B. cenocepacia* were the most virulent (246). This model was then harnessed to investigate the therapeutic

potential of bacteriophage therapy in the Bcc, which had to this point not yet been demonstrated *in vivo*. Seed and Dennis (247) showed that larval survival hinged in large part on the timing of treatment, with larvae treated immediately showing greater survival than larvae treated at 12 hours post-infection. This work was followed by a study demonstrating the elimination of a lysogenic phenotype in a phage through the inactivation of its putative repressor gene. The authors went on to show that the phage required lower doses to rescue larvae during *B. cenocepacia* infection (160). Novel Bcc virulence factors characterized using the *G. mellonella* model include a nonribosomally-synthesized glycopeptide produced in several Bcc species (276), an adhesin limited to ET-12 epidemic *B. cenocepacia* strains (179, 180), and a tyrosine kinase with a role in biosynthesis of the exopolysaccharide cepacian (88). A clear advantage of this model host is its ability to withstand a wide range of temperatures, including 37 °C.

The most recent invertebrate model that has been developed for the Bcc is the fruit fly *Drosophila melanogaster* (40). Unlike with *C. elegans*, Bcc bacteria were not able to cause deleterious effects when delivered to the gut of the insects by feeding, but through a pricking method the authors were able to establish infections. Once again, *B. multivorans* ranked among the least virulent species in this model, with strains of *B. cepacia*, *B. cenocepacia*, *B. pyrrocinia*, *B. stabilis* and *B. ubonensis* killing the flies most efficiently. The authors showed the importance to *B. cenocepacia* virulence of the genes *zmpA*, a zinc metalloprotease, and *hldA*, involved with LPS core oligosaccharide biosynthesis. The decreased virulence of these mutants implicate bacterial tolerance of host

antimicrobial peptides in the infection process, since ZmpA can cleave antimicrobial peptides and the LPS core oligosaccharide is involved with antimicrobial peptide resistance. This study also introduced the competitive index to Bcc invertebrate studies by co-infecting *B. cenocepacia* mutants with their parent strain. In this case, the *hldA* mutant showed greatly reduced competitiveness relative to the wild type strain, while the abilities of the other mutants to compete in the host were less clear-cut.

*Danio rerio* (zebrafish) embryos have recently been established as a useful model (75, 297). This model, while maintaining the low-cost and high-throughput benefits that make the invertebrate models attractive, presents at least one clear advantage that is absent from the invertebrate models: the presence of roaming phagocytes similar to the neutrophils and macrophages the Bcc would encounter in the CF lung. By real-time fluorescence microscopy, the authors showed that *B. cenocepacia* could invade and replicate within zebrafish macrophages and thus disseminate throughout the embryos (296) – the same tactic proposed in the context of migration through soil environments within amoebae. Through a limited comparison of several Bcc strains representing four species of the complex, it was determined that *B. cepacia* and *B. cenocepacia* were the most virulent against the embryos, while *B. stabilis* and *B. vietnamiensis* were unable to induce mortality or establish proliferating infections at the tested dose. Finally, the authors showed a role for quorum sensing in *B. cenocepacia* virulence within the embryos.

To approximate CF lung conditions, mice have been produced either with point mutations in *CFTR* of the type that are common in the human form of CF or with *CFTR* knocked out completely. The phenotypes that emerge from such manipulations demonstrate CF gastrointestinal symptoms but not the pulmonary symptoms including neutrophil buildup, mucus plugging and bronchiectasis (31). These phenotypes have been attributed to the possibility of redundant ion channels in mice that account for missing CFTR. In addition, the cellular distribution of CFTR is biased toward submucosal glands, and these penetrate much deeper in the human lung than in the mouse lung; as these glands are expected to play an important role in human CF, any deleterious effects on the glands in mice would not appear in deep lung tissue. Nonetheless, *CFTR*-mutated mice are less able to clear Bcc infection after repeated infection than healthy mice (68, 234).

A mutation in mice that more closely approximates the human CF condition targets the sodium channel gene *Scnn1b* and causes the up-regulation of sodium absorption from the lungs. Relevant phenotypes included depleted airway fluid volume and increased mucus concentration and adherence to airway surfaces. These mice exhibit spontaneous lung infection and so were thought to demonstrate the sought-after characteristics of a good CF model (31). Thus far, Bcc studies have not been carried out using this model.

Although these mouse models have been useful for the general characterization of CF infection, their use was likely limited because their cost was not perceived to reflect their benefits in resembling the human CF lung. A

recently developed *CFTR*-deficient pig model has been shown to produce disease symptoms that closely resemble those seen in humans (200, 221). Likely as a result of cost, no studies have yet examined Bcc infection using these animals.

## **Plant models**

Since the Bcc were initially identified as plant pathogens, several groups have studied Bcc virulence from this perspective. Although the animal models described above intuitively represent a more accurate model to depict the human infection process, with similarities in cell and tissue types, innate immune systems, and metabolism, plants are gaining recognition for their usefulness in modeling bacterial pathogenesis in animal hosts, in some cases revealing conserved infection mechanisms (24, 155, 207, 238). The groundwork for these advances were made during investigations of *P. aeruginosa* infection of *Arabidopsis thaliana* showing that these bacteria make use of the same type III secretion effector proteins to manipulate host cell pathways in plants and animals (212, 213). Plants have innate immune systems that respond to invading bacteria, viruses and fungi (222) with the production of oxidative bursts, secondary metabolites and antimicrobial peptides (36, 122, 270), offering parallels to some of the most important stresses that pathogens encounter in animal hosts. For pathogens that are able to infect a wide range of hosts, including many Bcc species, plants could offer an inexpensive and easily manipulated model for the exploration of virulence factors, the infection process, and the evolutionary processes by which these bacteria emerged as pathogens of humans. However, even *Salmonella enterica*, a pathogen with highly specialized adaptations for

mammalian gut infection, has been shown to apply its type III secretion effectors to plant infection (238) and is able to invade lettuce tissues *via* the stomata (142).

For the study of Bcc phytopathogenesis and its relationship to animal pathogenesis, three plant models have been developed, the first being the onion model (316). This study was carried out prior to the division of the Bcc genomovars or species, but found that onion maceration by Bcc strains generally occurred in the strains showing pectolytic activity. A more recent study showed that the vast majority of a large sample of soil-isolated Bcc strains from *B. cepacia*, *B. cenocepacia*, *B. ambifaria* were able to cause maceration, necrosis or water-soaking in wounded onion tissue, while *B. pyrrocinia* isolates were generally avirulent (124). Dose dependence of the infections was not determined. Interestingly, growth of *B. cenocepacia* for 1,000 generations in macerated onion tissue caused a loss of virulence against *C. elegans* (84), suggesting a reduction in host range following adaptation to a particular host. Modified phenotypes of these adaptive mutants included motility and biofilm formation. Another study identified a type IV secretion system as the basis for a water-soaking phenotype that remains when pectolytic activity is knocked out (85).

Another useful plant model adapted for the Bcc is alfalfa (24). Like the larval, fruit fly and zebrafish embryo models, alfalfa infection was performed through a piercing method. The authors demonstrated, consistent with the above-described animal models, that *B. multivorans* strains are the least virulent of the species tested, while *B. cepacia*, *B. cenocepacia* and *B. ambifaria* were the most virulent. In general, there was some level of consistency between ability to cause

disease in alfalfa and in the rat agar bead model, although strain variability within each species was very high in the rat model. The authors next examined plant pathology by several *B. cenocepacia* strains with mutations in previously characterized virulence factors. They found that mutation of an ornibactin biosynthesis gene but not the receptor gene caused a large decline in virulence against the plants, suggesting that iron sequestration from the host plays a role in *B. cenocepacia* virulence against alfalfa. In general, dose dependence of the different Bcc strains was not analyzed in alfalfa, except for *B. cenocepacia* K56-2, which was also shown to cause increasing pathogenesis in response to higher temperatures.

The next published plant model was the lettuce midrib, which relies on stabbing a bacterial strain into the plant tissue and watching for signs of pathology (184). Manifestations of Bcc infection in the midribs included water soaking and chlorosis in the first few days followed by blackened, soft rotting after 4-5 days (120). Using transmission electron microscopy, the authors showed Bcc bacteria invading and replicating within lettuce cells. In qualitative virulence analysis, *B. cenocepacia* strains were highly virulent, while *B. cepacia*, *B. multivorans*, *B. vietnamiensis* and *B. seminalis* show weak to no virulence. *B. multivorans* demonstrated greatly reduced tissue invasion relative to the other tested species, *B. cepacia*, *B. cenocepacia* and *B. contaminans*. These results correlated extremely well with both alfalfa and larval infections performed using these strains in the same study. Interestingly, clinical isolates of both *B. cepacia* and *B.*

*cenoepectacia* were significantly more virulent than their agricultural counterparts, a trend not yet seen in the literature.

## **Cell lines**

While the whole-organism approach to infection is useful for assigning broad functions to gene products and for identifying virulence patterns, a more reductionist approach for mechanistic studies is to use cell lines derived from the tissue of interest. Several pulmonary and immune cell lines have been used in Bcc studies, and they have provided the means by which to identify a range of important bacterial phenotypes, including both intracellular and paracellular invasion, activation of inflammatory pathways, and differences in these activities between CF and non-CF cells.

The most widely used among these cell lines is the A549 alveolar epithelial cell derived from a tumour (97). The cells grow as a squamous epithelial monolayer, and represent a good starting point for cell interaction studies because the Bcc are often found in the deep lungs. Studies making use of A549 cells have shown the importance of pili for adherence to and clumping on the epithelium as well as cytotoxicity and apoptosis of the cells (43, 48, 143); facets of the Bcc invasive phenotypes include the role of flagella (282), invasion dynamics and intracellular survival (32, 132, 169), strain and species dependence of invasion (80, 133), and the demonstration of lactoferrin as an invasion inhibitor for *B. cenoepectacia* (23).

BEAS-2B cells are immortalized bronchial epithelial cells that also form simple monolayers. These cells have been used to study the cytotoxicity of clinical *B. cenocepacia* isolates as well as to demonstrate protection of Bcc-infected airway cells by a cationic antimicrobial peptide (63, 279). The latter study showed that while the peptide could protect BEAS-2B cells from *B. cenocepacia*, *B. multivorans*, *B. stabilis* and *B. vietnamiensis*, *B. cenocepacia* still caused a high level of cytotoxicity despite its *in vitro* sensitivity to the peptide.

Progressing from these more basic cell lines are the immortalized bronchial epithelial cell 16HBE14o- and the bronchial submucosal cancer-derived cell Calu-3 (304, 320). Although they are not derived from alveolar cells, both form polarized monolayers, meaning there are apical and basolateral faces. The different faces and their accompanying plasma membrane composition are defined by tight junctions, which promote adhesion between adjacent cells and provide an extracellular barrier between the apical and basal faces of the cell. 16HBE14o- cells consistently produce cilia (62), while Calu-3 cells produce few (106); although ciliary function is known to be hindered in the CF lung, cilia provide additional realism through fluid motion and attachment sites. Therefore, the use of such cell types more closely reflects the obstacles and heterogeneities encountered by pathogens in the lung than does a simple monolayer such as that formed by A549 or BEAS-2B cells. A comparison of the invasion efficiency of several *B. multivorans* and *B. cenocepacia* strains into A549, 16HBE14o- and Calu-3 cells showed that while all strains invaded A549 cells with high efficiency, their invasive abilities dropped considerably in the other cell lines (45). The

authors showed large strain variability in crossing the monolayer, and demonstrated that transmigration may be due in part to extracellular factors. In general, *B. cenocepacia* was the only species unable to transmigrate. Another study showed differences in proinflammatory cytokine production from the different cell lines, with A549 and Calu-3 cells releasing 3-fold greater amounts of IL-8 than 16HBE14o- or a CFTR-deficient derivative (described next) in response to exposure to *B. cenocepacia* and *B. multivorans* (131). Studies focusing on 16HBE14o- cells have shown reduced adherence to the cells by *B. multivorans* pre-treated with a variety of sugars (312), activation of matrix metalloproteinases by *B. cenocepacia* to reduce wound repair (313), and the requirement of unidentified glycolipid receptors for Bcc invasion (186).

A final epithelial cell line that has been used for Bcc investigations is CFBE41o-, which was immortalized from tracheo-bronchial cells of a CF patient and carries a homozygous  $\Delta F508$  mutation in *CFTR* (82), which is responsible for 70-90% of CF cases in North America and Northern Europe and prevents CFTR from leaving the endoplasmic reticulum (28). Like Calu-3 and 16HBE14o- cells, CFBE41o- cells form tight monolayers, allowing for more detailed explorations of bacterial pathogenesis. The first Bcc study carried out using these cells was published in 2010, and as described above revealed the glycolipid requirement for Bcc invasion into both 16HBE14o- and CFBE41o- cells. Specifically, *B. multivorans* and *B. cenocepacia* strains were shown to lose invasion ability when CFBE41o- cells were treated with glycolipid biosynthesis inhibitors (186). The next study using this cell line was also described above, and it was found that,

similar to 16HBE14o-, CFBE41o- released 3 times less IL-8 in response to Bcc exposure. Furthermore, the study showed IL-8 concentration-dependent increases in intracellular growth and survival of Bcc cells in both cell lines (131). Another study using this cell line (previously mentioned and to be described in greater detail) showed similar activation of matrix metalloproteinases in 16HBE14o- and CFBE41o- cells in response to Bcc exposure and the negative effect of this activation on epithelial wound repair (313). A potential role for lipase production in *B. multivorans* invasion of epithelia was also demonstrated using these two cell lines, as pretreatment of the epithelia with lipase yielded significantly greater invasion by both tested strains (187).

A newer strategy for generating lung epithelia that differentiate to form more structures and cell types is to harvest stem cells from a patient's lung and allow them to grow under conditions promoting proliferation and differentiation. This method has been adapted to produce well-differentiated CF airway epithelia and results from studies employing such cell lines can be expected to strongly reflect many of the epithelial structures and responses present during infection. This approach was used in studies showing invasion incongruities among Bcc species that point to their divergent strategies (243), actin-independent intracellular and paracellular invasion by *B. multivorans* (244), and different susceptibilities of CF and non-CF derived epithelia to Bcc exposure (233).

To mimic the deficiencies presented by *CFTR*-mutated phagocytes, researchers have studied Bcc-phagocyte interactions using both  $\Delta F508$  mouse macrophages and, more recently, human-derived CF macrophages. The  $\Delta F508$

mouse macrophages were employed in a recent study demonstrating that, adding to the dysfunctional autophagy exhibited by *CFTR*-deficient macrophages, the Bcc may actively down-regulate autophagy in host phagocytes (3). Using human-derived CF macrophages, Kopp *et al.* (140) demonstrated increases in the release of a range of cytokines from CF-derived macrophages compared with healthy macrophages in response to *B. cenocepacia* exposure, then used confocal microscopy and cell counts to demonstrate that the bacteria were able to avoid lysosomal degradation only within the CF macrophages. Cytotoxicity to the CF macrophages by the bacteria was also increased. Studies using RAW264.7 macrophages from healthy mice have demonstrated *B. cenocepacia* persistence within macrophages and the type VI secretion system, LPS, magnesium and stress response- dependence of this phenomenon (91, 119, 134, 146, 148, 166, 199, 223, 225), differences in Bcc species macrophage invasion and intracellular persistence (240). The relevance of these findings lies within the suspicion held among researchers that Bcc bacteria might use phagocyte invasion as a means of establishing the dreaded systemic infections that escalate to cepacia syndrome (169, 296).

### **Multihost analyses**

Several studies have used a combination of infection models to characterize virulence pathways. In doing so, the studies purport to more completely address the likelihood that such virulence factors occupy central roles in human pathogenesis. One such study investigated the specificity versus universality of a range of suspected and partially characterized *B. cenocepacia*

virulence factors by comparing lethality of mutants in these genes to the wild type strain in four model hosts, including alfalfa, *C. elegans*, *G. mellonella*, and rodents (287). The results revealed several genes required for full virulence in multiple models, including the ornibactin biosynthesis gene *orbA* and its cognate receptor gene *pvdA*, which are largely responsible for the iron scavenging abilities of *B. cenocepacia* and may play a role in the CF lung if iron is under tight competition by co-inhabiting bacteria. Mutation of *shvR* (a widely active regulator) completely attenuates *B. cenocepacia* K56-2 in the alfalfa model and causes decreased inflammation in the rat agar bead model, but had no apparent effect in either invertebrate model. Later studies showing overlap among infection models include the previously-mentioned 3,000 member mutant library screen for *B. cenocepacia* attenuation against *C. elegans*, where it was found that a pseudopilin gene *gspJ* caused defects in virulence against *C. elegans* and onion, implying a role for type II secretion in these hosts (259). Recently, a sweeping study demonstrated that the third chromosome found in many Bcc species is not required for growth under most circumstances when it was replaced with an incompatible plasmid. Rather, this megaplasmid was proposed to carry virulence genes, and its elimination caused loss of EPS production in *B. ambifaria* and *B. pyrrocinia*, loss of antifungal activity in almost all strains tested, decreased proteolytic activity in some strains and large virulence decreases by most strains tested in *C. elegans*, *G.mellonella*, zebrafish and the rat agar bead model (5).

A therapeutic investigation into the use of rapamycin to ameliorate macrophage autophagy showed the efficacy of this intervention in both healthy

and CF macrophage cell lines and then in CF mice, demonstrating the usefulness of following a reductionist approach with a more complex one (3). Overall, the literature demonstrates that there is some overlap among virulence factor specificity among the model hosts, but to show a true relevance in CF infection, these genes and therapeutic approaches should be further characterized using more CF-relevant means such as the newly developed CF pig model, where cost permits. Where studies are limited to simpler models, methods should be adapted to better reflect the conditions found in the CF lung, such as the low oxygen concentrations mimicked by the rodent agar bead models.

### **General virulence pathways of the Bcc**

Considerable attention has been directed over the last two decades to identifying and characterizing Bcc virulence factors using an array of model systems. This work has revealed a variety of adhesins, secretion systems and their exported products, motility systems, immunomodulatory elements, nutrient harvesting machinery and communication infrastructure. The anticipated application of such studies is to develop alternative means to counter the progression of bacterial disease by disabling or down-regulating key pathogenesis pathways at crucial moments in the infection. Identifying these pathways provides a starting point from which to design alternative therapeutic strategies based on attenuating virulence enough for the immune system to clear the infection.

Members of the Bcc produce a range of virulence factors that, based on studies in model hosts and recent *in vivo* transcriptomic data, are thought to

contribute to their survival, growth and pathology in the CF lung. For growth and survival, the bacteria must access limiting nutrients while evading host defences. Bcc pathology results from lung structure degradation, inflammation, and tissue invasion. Certain virulence pathways, such as secondary metabolite production, tend to be species- and even strain-specific, and will be discussed in more detail in later chapters. The sections that follow will primarily focus on the pathways that are shared by multiple Bcc species. In the following chapters, this framework will be used to define the major virulence factors found in each of the organisms being dissected in this thesis: *B. vietnamiensis*, *B. cenocepacia* and *B. multivorans*.

### **Iron acquisition**

Earlier, we explored the metabolic versatility of the Bcc and the bacteria's propensity to mobilize nutrients from recalcitrant compounds such as dinitrogen and insoluble phosphate. The metabolic versatility of the Bcc can have growth-promoting effects within the rhizosphere but may also help explain the ability of the Bcc to survive and proliferate within the CF lung.

As previously discussed, in a healthy lung iron availability is stringently controlled by the presence of iron-chelating molecules, which maintain free iron levels at roughly  $10^{-20}$  M. The CF lung may contain available iron concentrations as high as  $10^{-6}$  M as a result of protease damage, microbleeds, heme release and oxygen limitation, which serves to solubilize iron to its usable form. Despite this apparent availability of iron, transcriptomic and proteomic data has shown that expression of siderophores in clonal isolates of *B. cenocepacia* sampled three years apart increased during this period of chronic colonization (163, 181). A

plausible explanation for this upregulation under circumstances that would seem to void additional efforts to acquire iron is the presence of competing microbes, each producing its own host of siderophores which substitute the human host's faulty iron sequestration network for a microbial version. Siderophores produced by Bcc include salicylic acid, ornibactin, pyochelin, and cepabactin (67). Mutating the genes encoding either the ornibactin- or salicylic acid-synthesizing enzymes causes reduced virulence in the rat agar bead model (Sokol *et al.* 1999; Sokol *et al.* 2000).

The confusion generated by this debate has been alleviated somewhat by recent data presented by Ghio *et al.* (96) which confirms the earlier suspicions concerning elevated iron levels in the CF lung; this group showed increases in total iron, ferritin, and transferrin, as well as the more bioavailable heme and hemoglobin relative to healthy individuals. These findings are especially important given the earlier discovery that *B. cenocepacia* is able to use ferritin as an iron source through degradation by a serine protease (308). Until recently, it was thought that *B. cenocepacia* was unique among CF pathogens in its ability to glean iron from ferritin; however, it is now known that both *P. aeruginosa* and *Candida albicans* are able to perform this feat, the former through both siderophores and protease-mediated ferritin degradation (73) and the latter through a multipurpose adhesin expressed during hyphal growth (6). With up to 4,500 bound iron atoms per molecule of ferritin, this molecule represents a singularly rich iron source for invading microbes that would make an attractive target by which to compete for niche space within the CF lung. Although the *B.*

*cenoepeacia* serine protease was never identified, the authors pointed to 4 serine proteases in the *B. cenoepeacia* J2315 genome. Of these, a brief analysis indicates that 3 of these (*bcam0922*, *bcam0957*, and *bcam1744*) have homologs in most other CF-prevalent Bcc strains, while the fourth (*bcas0405*) is present in most Bcc representatives but not in *B. multivorans*.

A final tactic, to be discussed in detail in Chapter 2, is the production of extracellular hemolysins to lyse erythrocytes for the acquisition of hemoglobin. The previously-discussed microbleeds in the CF lung offer easy access to erythrocytes as well as released hemoglobin. It is interesting to note that hemolysins are more often found in environmental isolates than in clinical isolates (298), suggesting that extracellular products may play important roles in defending Bcc root niches and in combating grazers and competitors. More specifically, this finding implies that so-called hemolysins likely emerged in Bcc for general destruction of eukaryotic cells, and were adapted for use in human hosts at some point in the emergence of Bcc pathogens. In short, the importance of these gene products appears to extend well beyond their clinical relevance.

The differences in iron availability between lungs of healthy and CF-afflicted individuals is symptomatic of other chemical changes that may affect the behaviour of CF-colonizing bacteria upon entry into the lung and during long-term growth. Several recent studies have begun to resolve the complex chemical mixture of CF sputum; their results were described previously and suggest that CF sputum is rich in amino acids (particularly those with aromatic side chains), salts, DNA, and mucins. The nitrogen richness of this environment was demonstrated as

a possible cause of the loss of N<sub>2</sub>-fixation phenotype among *B. vietnamiensis* isolates, suggesting that the bacteria adapt to their environment during long-term colonization (173).

## **Resistance to host defences**

While accessing nutrients is crucial for proliferation within their hosts, bacteria must also contend with patrolling immune cells. Healthy humans maintain a population of alveolar macrophages that phagocytose and destroy invading microbes within the phagosome. However, CFTR-deficient macrophages have partially defective phagosomal maturation when processing live *B. cenocepacia* cells. This result was not observed when processing the non-CF pathogen *Salmonella enterica* (148). This phenotype appears to rely on the type VI secretion system, which is present throughout the Bcc in a single conserved operon, and though similar phenotypes have not been explored in other species of the Bcc, it seems likely that the T6SS-dependent intracellular survival phenotype of *B. cenocepacia* operates similarly in the other Bcc members. However, the mechanism of *B. multivorans* survival within macrophages unfolds along a different pathway than that of *B. cenocepacia*, which remains uncharacterized (240).

Details of the *B. cenocepacia* intracellular persistence timeline are still blurry, but several important findings have emerged. First, T6S disrupts the actin cytoskeleton of macrophages through interference with several cytosolic GTPases and disrupts reactive oxygen species delivery into *B. cenocepacia*-containing vacuoles (BcCV) through interference with cytosolic NADPH oxidase complex

proteins (225) – an interesting parallel to the propensity of the Bcc to infect chronic granulomatous disease patients, whose phagocytes are unable to form this complex. Second, T6S disrupts the BcCV membrane, causing leakage of type II secreted proteins, including ZmpA and ZmpB, into the macrophage cytosol, which cause recruitment of the inflammasome and subsequent cell pyroptosis (223). Finally, an azurin homologue produced by the Bcc and normally used for denitrification was shown to cause macrophage apoptosis following its localization to the nucleus (209). The authors briefly discussed the idea that since mitochondrial proteins are so intimately tied to the apoptotic pathway in mammalian cells, it comes as no surprise that proteins involved with energetic processes might have been retained in prokaryotes for induction of apoptosis. This study also correlated the production of the azurin homologue to patient morbidity, which indicates a potential role for the protein in Bcc pathogenicity. These results suggest that Bcc bacteria may be adapted for invasion of and survival within macrophages through the complex manipulation of host cell processes.

Although the manipulation of macrophages may indicate host-specific adaptations of the Bcc, neutrophils are the primary immune cells present in the CF lung, occupying 70% of the total share versus only 1% in a healthy lung. Migrating in vast numbers to the lung in response to TNF $\alpha$  release from respiratory epithelial cells (54), neutrophils degranulate upon contact with foreign organisms, releasing toxic products to the surrounding medium. These include hydrogen peroxide, lysozyme (164), and massive amounts of elastase, which damages lung tissue and causes microbleeds, as previously outlined. Activated

neutrophils harm not only the target invaders but also the surrounding host cells (236), contributing to the dismantling of the epithelial barrier. A recent review article summarized the major Bcc gene products involved with neutrophil evasion (206). These include catalases, a melanin-like pigment, superoxide dismutase and the exopolysaccharide cepacian to resist oxidative killing; and ZmpA, ZmpB, LPS modifications and the alternative sigma factor RpoE to resist antimicrobial peptides. Other factors have been shown to be important for survival in macrophages, including type IV and VI secretion systems, but their importance in neutrophils has not been established.

Members of the Bcc are thought to resist cationic antimicrobial peptides such as  $\beta$ -defensin through the positive charges conferred by 4-amino-4-deoxy-L-arabinose (Ara4N) residues present in the LPS inner core. By balancing cell surface charge in such a way, it was suggested that Bcc cells repel cAMPs and thus avoid cell membrane disruption (71). However, it has also been shown that despite the resistance of *B. cepacia* to polymyxin B, the affinity of its LPS for the cAMP is as high as *E. coli* LPS (300). A later study produced evidence that factors within the *B. cenocepacia* core oligosaccharide provide protection against antimicrobial peptides of varying structures and charges in addition to Ara4N-mediated cAMP resistance (159). Following this work, the group showed that progressive truncations to the inner core cause increasing affinity of the cAMP polymyxin B for the cell surface (199). Finally, it was shown that ZmpA is able to cleave  $\beta$ -defensin-1 and ZmpB is able to cleave cathelicidin LL-37 (138),

demonstrating apparent redundancy of active and passive systems in these bacteria to combat host immune tactics.

Previously, the CFTR-mediated pH maintenance within healthy lungs through  $\text{HCO}_3^-$  flux was discussed. This strategy may achieve antimicrobial activity through the activation of antimicrobial peptides. Other recent findings suggest that *Burkholderia* bacteria are particularly susceptible to alkaline pH, and release oxalate to neutralize their surroundings in stationary phase to promote survival (103, 189). The biosynthetic enzymes ObcA and ObcB responsible for this phenotype were the first such bacterial enzymes described and are present throughout the Bcc with ~25% (Bcam2294) and ~60% (Bcal2175) homology, respectively, but have yet to be characterized. Interestingly, Bcal2175 was predicted to be part of the Burkholderiales core genome by *in silico* analysis (129), while Bcam2294 expression was shown to be down-regulated in CF sputum versus soil conditions (315). Therefore, the production of oxalate in the slightly acidic CF lung may not be required, but this acidity may represent an ideal habitat for these alkaline-sensitive bacteria. Hopanoids, as discussed earlier, were also shown to contribute to acid tolerance in the Bcc (239), likely through the lowering of membrane permeability.

While the acid resistance of the Bcc plays a role in phagocyte evasion (289), the slightly acidic fluids in the CF lung may also have implications for phosphate availability. A pair of studies linked the accumulation of polyphosphate in the Bcc to lower pH (182, 185), suggesting yet another possible adaptation to the CF lung. In *P. aeruginosa*, polyphosphate promotes biofilm formation and

virulence in mice (217), while *E. coli* polyphosphate accumulation was shown to promote late-stage growth (144).

Finally, biofilm formation by the Bcc appears to support the bacteria's long-term colonization strategy through added defence against the host immune system and antibiotic therapy as well as conferring a social lifestyle that promotes alternative behaviours. A later section will detail this and other social behaviours of the Bcc.

### **Inflammation and epithelial degradation**

While approximately 20% of CF carriers of Bcc bacteria succumb to “cepacia syndrome”, characterized by necrotizing pneumonia and septic shock (123), the two most frequent Bcc colonizers, *B. cenocepacia* and *B. multivorans*, are both associated with this unfortunate progression (128). The presence of Bcc bacteria can trigger copious release of pro-inflammatory cytokines from immune cells, with the subsequent inflammatory response necrotizing cells lining the airway tissue. This occurs in addition to the chronic inflammation which causes extensive neutrophil-mediated tissue damage even in the absence of microbes early in a CF patient's life (216). Prolonged damage to the lungs results in reduced lung function, eventually leading to lung failure. Damage to airway tissues can allow bacterial access to blood capillaries underlying the alveolar air sacs (230).

Partially driving this vast release of cytokines is the Bcc lipopolysaccharide (LPS). An early study investigating the unusual tendency of

the Bcc to trigger powerful immune reactions found that each strain of a panel of *B. cepacia*, *B. multivorans*, *B. cenocepacia* and Bcc relative *B. gladioli* effected considerably greater immunostimulatory TNF $\alpha$  cytokine release from mouse fibroblasts and had much stronger endotoxic activity than *P. aeruginosa* LPS (249). During infection, the Bcc LPS is also thought to play an important protective role from cAMPs. The innate resistance of the Bcc to antimicrobial peptides is complemented by the secretion of zinc-dependent metalloproteases ZmpA and ZmpB. Both enzymes cleave elafin and secretory leukocyte inhibitor, which act as both neutrophil elastase inhibitors and antimicrobial peptides. The importance of ZmpA and ZmpB effects on the neutrophil elastase inhibitors is underscored by the devastating effects that elastase has within the CF lung, as previously discussed. ZmpA was determined to be present in the genomes of *B. cepacia*, *B. cenocepacia*, *B. stabilis*, *B. ambifaria* and *B. pyrrocinia* but absent in *B. multivorans*, *B. vietnamiensis*, *B. dolosa* and *B. anthina* (99).

Supplementing the damaging effects of ZmpA and ZmpB, Bcc members may release cyanide into their surroundings. Cyanide production by *P. aeruginosa* was originally shown to correlate with declining lung function (228). This group went on to show that cyanide production is widespread among the Bcc and only occurs during growth on solid media; planktonic growth in liquid culture did not give rise to cyanide production (229). Based on this study, it is likely that *P. aeruginosa* and Bcc bacteria are the only cyanide-producing CF pathogens – the highly variable cyanide levels reported in Bcc-containing sputum indicate that, contrary to the authors' conclusions, Bcc-generated cyanide is detectable in some

Bcc infections. It is interesting to consider that cyanide production likely plays an additional role in interspecific competition within mixed biofilms – those bacteria able to withstand cyanide can produce it to the detriment of susceptible species (229). Cyanide has been detected in moderate concentrations in CF sputum with probable microbial origin (237). The process by which cyanide damages host cells is the disruption of aerobic respiration in the mitochondria, causing the cell to undergo anaerobic respiration and produce lactic acid at toxic levels (7). While cyanide production by *P. aeruginosa* has been confirmed, its production by the Bcc remains contentious. Recent work on a panel of CF isolates using a novel detection technique was unable to show cyanide production linked to any of the strains beyond background levels by planktonic or biofilm cultures or from patient exhalation (98).

Typically, a wounded epithelial cell layer can repair itself. Matrix metalloproteinases (MMPs) are membrane-anchored epithelial proteins with modulatory roles in inflammation and repair. They are up-regulated in the CF versus healthy lungs. *P. aeruginosa* is known to induce the expression of MMPs by its flagellin and possibly elastase, and this induction has negative consequences for the formation of tight junctions along the epithelium. *B. cenocepacia* was shown to activate MMPs in both CFTR-positive 16HBE14o- and CFTR-negative CFBE41o- lung epithelial cells more strongly than *B. multivorans*, causing delayed wound repair (313). The effect of MMP activation was not related to the disruption of tight junctions by the Bcc, discussed later.

Epithelial cell death can occur through apoptosis, pyroptosis or necrosis. The effective difference between these processes is in the inflammatory response; while apoptosis and pyroptosis are a mechanism by which cells can quietly self-destruct, necrosis triggers cytokine release and subsequent migration of phagocytes to the site of infection (43). Such phagocyte migration through the endothelium and epithelium disrupts tight junctions between the epithelial cells, potentially creating spaces through which bacteria may pass.

Cheung *et al.* (43) showed that *B. cenocepacia* cable pili may be responsible for activating both an apoptotic cascade and cell necrosis in A549 cells. Interactions between dendritic cells and *B. cenocepacia* or *B. multivorans* were later investigated, and the authors found that while both species triggered similar release of proinflammatory cytokines, only *B. cenocepacia* could cause necrosis of dendritic cells (162). Diffuse cell death along the epithelium might generate lesions that bacteria could exploit for dissemination into the bloodstream. Furthermore, the subsequent migration of phagocytes through the endothelium and epithelium could further exacerbate the problem by opening up more portals for bacterial dispersal.

Finally, studies using *C. elegans* (168) and mice (281) have shown attenuating effects of mutagenizing the *B. cenocepacia* type III secretion system. Beyond this, no studies have investigated the mechanistic details of the T3SS, but it appears throughout the Bcc except in *B. cepacia* (100). T3SS genes are not up-regulated during infection in the rat agar bead model versus broth culture (194), which may indicate that the T3SS is dispensable for infection under these

conditions, given that pathogens often respond to host cues with the up-regulation of this machinery (93). T3SS effector proteins can have varying roles, but most relevant to the Bcc might be their necrotic (269) and apoptotic (111) effects in macrophages and epithelial cells by other airway pathogens.

## **Cell and tissue invasion**

It has been suggested by *in vitro* and *in vivo* studies that Bcc invades respiratory epithelial cells. The first step to invasion is adherence, and early studies on the Bcc demonstrated the existence of *B. cenocepacia* adhesins that may play a role in this. A cable pilus biosynthesis operon is induced at high osmolarity, physiological temperature (37 °C) and pH (6.8) – all conditions representative of the CF lung – as well as low iron, which casts some additional controversy into the previously outlined debate over pulmonary iron availability in CF (283). Cable pilus derives its name from its intertwined morphology and is known to play an important role in the establishment of infection by certain Bcc strains as a result of its mucin and respiratory epithelial cell binding. Mucins are congenial binding substrates for Bcc since these mucosal proteins are poorly cleared from CF airways. Furthermore, the lowered hydration of CF mucus increases mucin adhesion (235), which is likely exploited by a cable-pilus-associated 22 kDa adhesin that increases binding not only to mucin but also to buccal epithelial cells (231).

High iron concentrations were shown to induce aggregation, biofilm formation and loss of motility in *P. aeruginosa* and *B. cenocepacia* (22). Though the iron levels investigated in this study may not be representative of the CF lung

(“low iron” was represented by 1  $\mu\text{M}$ , while “high iron” meant 10-100  $\mu\text{M}$ ; in this study, the “low iron” condition is within the expected range for the CF lung), the findings may suggest local phenotypic differences among microcolonies in the lung. Furthermore, biofilm formation was shown to correlate with invasion of human alveolar epithelial cells. The extremely high percentage (94%) of intracellular bacteria compared with those adhered to the A549 cells during biofilm growth certainly seems significant as a demonstrated behaviour, at least *in vitro*. Meanwhile, invasion by *B. multivorans* into both 16HBE14o- and CFBE41o- cells was shown to be significantly higher following pretreatment of the host cells with Bcc lipase (187). This effect was independent of lipase-mediated tight junction disruption and plasma membrane disruption, and could also occur independently of actin rearrangement, as shown by Schwab *et al.* (244), who found similar patterns of intracellular and paracellular invasion by *B. multivorans* when well-differentiated airway epithelial cells were untreated or pretreated with an actin polymerization inhibitor. These cells had been previously used by the same group to demonstrate invasion differences among Bcc species, where it was found that *B. multivorans* had the most diverse assortment of invasive strategies compared with *B. cepacia* and *B. cenocepacia* (243). Finally, exposure of well-differentiated airway epithelia derived from healthy and CF individuals to *B. cenocepacia* showed greater susceptibility in the CF cells to invasion, cell damage and bacterial growth, indicating that the cellular effects of CFTR deficiency have ramifications for defence against infection that are independent of the previously-described collapsing of mucus layers and

mucociliary clearance defects, phagocytic activity, microbial commensals, and inflammation, none of which would be present in this model. Rather, the increased bacterial growth on CF epithelia suggests deficiencies in innate immunity specific to the epithelial cells.

Although intracellular invasion appears to be one component of the Bcc lifestyle within the CF lung mucosa, paracellular invasion of the epithelium has also been demonstrated using Calu-3 and 16HBE14o- cells (80). In this study, four Bcc species, *B. cepacia*, *B. multivorans*, *B. cenocepacia*, and *B. stabilis* were compared in their abilities to invade polarized or unpolarized monolayers of both cell types and to disrupt transepithelial resistance (a measure of tight junction integrity). All species disrupted tight junctions. Notably, the two *B. cenocepacia* strains did not exhibit transepithelial migration, as did the other five strains. Invasion by *B. multivorans* appeared to depend partly on the presence of basolateral receptors (which would not normally be accessible on the lung epithelium), since the bacteria were more invasive against the unpolarized cells. Later work demonstrated that while nine Bcc species induced similar IL-8 release from BEAS-2B cells, *B. multivorans* strains exhibited the greatest adherence and invasion of the cells (183). Both *B. multivorans* and *B. cenocepacia* may use the neutrophil chemotactic signal IL-8 as a growth stimulus, perhaps through an uncharacterized signaling pathway, and when uptake and clearance of Bcc bacteria are compared between CFTR-positive 16HBE14o- cells and CFTR-negative CFBE41o- cells, 16HBE14o- cells permit less intracellular bacterial growth (131). Invasion of both 16HBE14o- and CFBE41o- cells by the Bcc was

later determined to occur through binding of glycolipid receptors, though different Bcc strains appear to bind different glycolipids (186).

Transmigration across squamous epithelium, which is often produced for repair in the lower lung epithelium, was found to be dependent on both cable pili and the 22-kDa adhesin in *B. cenocepacia* (288). While the 22-kDa adhesin is found in other Bcc species, the cable pilus on which it is thought to reside is not, indicating that adhesion relies on different factors among different Bcc species. In *B. multivorans*, adhesion using exopolysaccharides (typically probed in the Bcc by growth on mannitol) was shown to play a strain-specific role, but the authors then identified novel fimbrial and filamentous hemagglutinin-like adhesins that also contribute to mucin adherence and biofilm formation. These gene clusters appear so far to be limited within the Bcc to *B. multivorans* and *B. ambifaria* (77).

## **Social behaviours**

### *Quorum sensing*

With the discovery of quorum sensing from the late 1960s through to the 1990s, it became apparent that multicellular organisms are not alone in their use of communications to control social behaviour. For pathogenic bacteria, overcoming a large host requires a large number of bacterial cells acting in concert. However, bacteria can communicate for other purposes, such as taking a census of self versus nonself cells. Within the Bcc are several distinct communication systems with apparently diverse functions that appear to play a role in CF pathology.

The first communication system characterized in the Bcc was the CepIR system, with homology to the LuxIR system first identified in *Vibrio harveyi*. This system is found in all Bcc species (104) and operates through the intracellular production and export of *N*-octanoyl-homoserine lactone (C8-HSL) plus small quantities of *N*-hexanoyl-homoserine lactone (156). The CepIR system controls diverse processes within the cell, including motility, biofilm formation, and siderophore and toxin production (273). Acting against the CepIR system in epidemic *B. cenocepacia* strains is the CciIR system, which produces C6-HSL plus C8-HSL in small quantities (13). The *cciIR* operon is activated by CepR and in turn negatively regulates both the *cepIR* operon and its regulon (195), allowing for fine-tuning of important virulence genes through negative feedback. No system has yet been found to counter the CepIR system in this way among other Bcc species, although CepR was found to activate *bviIR* in *B. vietnamiensis*, a system that gives rise to *N*-decanoyl-homoserine lactone (C10-HSL) (167). AHLs have been found in Bcc and *P. aeruginosa*-containing CF sputum samples (178), demonstrating their probable importance in virulence regulation or microbial signaling *in vivo*. This is underscored by the ability of *B. cenocepacia* to perceive *P. aeruginosa* AHL signals during mouse lung infection, as measured by protease activity in a AHL biosynthesis-deficient *B. cenocepacia* mutant exposed to *P. aeruginosa* AHLs (219).

Another quorum sensing system was later identified that may play a role in interspecies signaling in the Bcc. *Burkholderia* diffusible signal factor (BDSF), or *cis*-2-dodecenoic acid, is a fatty acid that accumulates in late-stationary phase

but is not subject to the positive feedback mechanism normally exhibited by Lux-homologous systems (75). Mutants defective in BDSF synthesis or signal reception are defective in mucin adherence, motility, exopolysaccharide production, defence against antimicrobial compounds, protease activity, and biofilm formation (273). Furthermore, BDSF was shown to act as a surrogate for the *Xanthomonas campestris* signaling compound, DSF (29), and inhibit germ tube formation in the CF pathogenic yeast *Candida albicans* (108), demonstrating that *B. cenocepacia* is capable not only of inter-species but also inter-kingdom signaling. Like AHLs, BDSF has been found in CF sputum (285). BDSF is widespread among the Bcc, having been shown to be produced by representatives from at least nine species. *B. multivorans*, *B. pyrrocinia*, *B. anthina* and *B. stabilis* produce additional uncharacterized variants of BDSF (76).

The interplay between the Lux-based and BDSF systems in *B. cenocepacia* has been explored in several studies. The first showed that while deletion of the BDSF synthase *bcam0581* had no impact on the expression of *cciI* or *cepI*, BDSF could restore phenotypes lost in a *cepR* mutant, suggesting that the systems act in parallel (75). Next, McCarthy *et al.* (172) used microarrays for mutants in the synthesis of each signaling molecule (C6-HSL, C8-HSL, or BDSF) to explore the regulons of each system and found minimal overlap between the BDSF and Lux-based systems. The most recent analysis of potential cross-talk among the systems has been carried out using single, double and triple deletion strains in the synthase genes for each system, and it was found that the BDSF synthase knockout strain produced substantially less C6-HSL and C8-HSL than

the wild type strain (286), suggesting that the BDSF system may occupy a higher place in the cellular regulatory hierarchy, though the authors did not measure BDSF production in the *cep* and *cci* mutants. Since Deng *et al.* (75) found no change in *cci* or *cepI* expression as a result of a *bcam0581* deletion, further work will no doubt investigate whether BDSF has a role in the synthesis of the HSL molecules.

Diketopiperazines (DKP) are cyclic dipeptides produced either by cyclopeptide synthetases or by nonribosomal peptide synthetase complexes (70) and are known to play a role in signalling in Gram negative bacteria (305). *B. vietnamiensis* produces and exports at least five different DKPs. While the authors claimed that the DKPs had an effect on production of an antifungal molecule by the bacteria, their data suggest that, in fact, the DKPs may interfere with the antifungal activity of Bcc cell-free supernatants. These molecules have not been explored in other Bcc species, nor have their biosynthetic pathways been characterized. However, based on the finding that other organisms, including *Pseudomonas*, *Enterobacter*, *Serratia* and *Citrobacter*, both produce and respond to the molecules through positive and antagonistic interactions of DKPs with their Lux-based quorum sensing systems (115), it stands to reason that the Bcc may also use these molecules for signalling.

### *Swarming motility*

It makes intuitive sense that bacteria would respond to lowered nutrient levels with phenotypic changes that enable outward spread to new microenvironments. High cell density, which limits the nutrient availability of

individual cells, triggers such phenotypic changes in the Bcc, as surfactant production is controlled by quorum sensing in the Bcc for the purpose of swarming. It was shown that mutating the *cep* quorum sensing system in one Bcc strain abolished that strain's ability to swarm on agar plates, but by adding surfactants to the plate, the bacteria regained their swarming phenotype (116). Lending support to the idea that high cell density regardless of the population can contribute to the urge to spread outward is a study showing cooperative swarming behaviour between *P. aeruginosa* and *B. cepacia* when the *P. aeruginosa* QS systems are intact (295). Co-swarming did not occur when *E. coli* or *Chromobacterium violaceum* were mixed with *P. aeruginosa*, indicating that the cross-talk between QS systems described above has real-world implications for the behaviour of these bacteria in the CF lung, whether for good or bad. An *in vivo* study examining transcripts and phenotypic changes from two clonal isolates of *B. cenocepacia* taken from a CF patient several years apart revealed an overall decrease in swarming in the later isolate (59).

### *Biofilm formation*

By controlling the behaviour of individual cells using such communication networks, bacteria act as multicellular organisms. A prime example of this multicellular lifestyle is the biofilm, a 3-dimensional structure comprising a dense matrix of polysaccharides, DNA, and bacterial cells. By adopting this community format, Bcc bacteria withstand higher concentrations of antibiotics, evade the onslaught of neutrophils and share resources. Converting to a sessile biofilm lifestyle under certain conditions may highlight limiting growth factors for Bcc

bacteria in their natural habitats, as they seek to exploit environments containing such factors. The formation of biofilms at higher iron concentrations, outlined in a previous section, likely reflects this strategy.

The mechanism of antibiotic resistance conferred by the Bcc biofilm involves several factors, including differential growth rates of cells, limited diffusion of antibiotics into the biofilm, and the formation of persister cells. One study compared the antibiotic susceptibility of six Bcc strains grown planktonically and in biofilms and found that meropenem, piperacillin-tazobactam and, to lesser extents, ceftazidime and aztreonam required higher dosages to inhibit biofilms, while no difference was observed for a range of other antibiotics (37). The authors did not mention that the antibiotics requiring higher inhibitory doses for biofilms were exclusively  $\beta$ -lactams, while those showing no difference in inhibitory dose for biofilms or planktonic cells were macrolides, fluoroquinolones, or aminoglycosides. This trend could point to a mechanism of biofilm resistance. One possibility is that persister cells, which show greatly reduced growth rates, are impervious to the effects of  $\beta$ -lactams, which generally require cell growth to lyse target cells. Meanwhile, the other classes of antibiotics are still somewhat effective against persisters, since they target protein synthesis (macrolides and aminoglycosides) or disrupt the cell membrane (aminoglycosides). The blocking of DNA replication by fluoroquinolones could likely not be explained by persisters, since they are relatively dormant (290, 303). It was recently determined that the mechanism by which Bcc persister cells growing in biofilms survive antibiotics could be a down-regulation of electron

transport and up-regulation of alternative pathways to the TCA cycle, thereby reducing reactive oxygen species production in the cell (290). This was shown by the addition of two different alternative pathway inhibitors – one to inhibit the glyoxylate shunt *via* isocitrate lyase (ICL), the other to inhibit succinate dehydrogenase. However, a similar reduction in surviving persister cells was not seen in a double-knockout of *B. cenocepacia* ICL genes, suggesting that the inhibitor has targets beyond ICL that were not disrupted by the mutations but are targeted by the inhibitor, or that the inhibitor has additional deleterious effects for which the authors did not account.

In any case, biofilm formation has additional effects on the pathogenic behaviour of Bcc cells. As previously discussed, Bcc bacteria produce cyanide during biofilm but not planktonic growth (229). Of further interest for CF pathogenesis is that in *P. aeruginosa*, cyanide production is up-regulated under microaerophilic conditions (204), such as those seen under the mucus layer along the CF lung epithelium. The gene responsible for cyanide insensitivity in *P. aeruginosa* is found throughout the Bcc with high homology (55-58% amino acid identity). Cyanide has been shown to inhibit neutrophil chemotaxis (92) – an effect aggravated by the production of the exopolysaccharide cepacian, which is produced throughout the Bcc (87). In addition to chemotaxis (34), cepacian was also shown to inhibit neutrophil phagocytosis (56). Cepacian is not required for the initiation of biofilm synthesis in the Bcc, but plays a role in its structural development (64).

This destructive phenotype might be followed by an invasive one in some strains – *in vitro* invasion into a lung epithelial layer was shown to be biofilm-dependent in *B. cenocepacia* and, to a lesser extent, *B. multivorans*, while invasion by *B. dolosa* was not linked to biofilm formation but rather actin rearrangement in the host cells (243), suggesting a tantalizing link to type VI secretion.

Biofilms are activated in the Bcc by the QS regulators described above as well as other pathways. A LysR-like regulator, ShvR, which will be discussed in more detail in Chapter 3, influences a number of phenotypes in *B. cenocepacia* K56-2, including biofilm formation. This influence appears to occur through the activation of the antifungal agent gene cluster (encoded by *afc* genes, among others). A recent study found that the product of this gene cluster is involved with membrane morphology, permeability, and lipid composition, suggesting that the product has a potential effect on multiple metabolic pathways (272). This regulator also negatively regulates AHL synthesis, adding another layer of complexity to the communication network (193). Interestingly, RND-type efflux transporter knockout mutations have been shown to reduce antibiotic resistance in *B. cenocepacia* while promoting biofilm production (19). This effect was not consistently linked to differential regulation of particular genes during a microarray analysis; however, the authors implicated the regulation of flagella, fimbriae and cellulose biosynthesis. Since there are 14 additional RND pumps that this study did not explore, there is clearly much to be done to elucidate the regulatory and phenotypic effects of efflux deficiencies. Full biofilm formation in

*B. cenocepacia* also relies on the presence of the putative inositol phosphatase SuhB (224) and the small noncoding RNA MtvR (214) through uncharacterized but likely regulatory means.

## **Summary**

There is clearly much to be discovered about Bcc virulence mechanisms and their roles in the pathological process of CF infection. Of the pathways that are understood, among the most important are those permitting Bcc bacteria to penetrate the epithelium and gain access to the underlying tissues and the bloodstream. This process appears to involve a combination of adhesins, biofilm factors, flagella, extracellular toxins, and uncharacterized host modulation factors, in addition to the possibility of phoretic transport within migrating phagocytes, which involves secretion systems, stress responses and nutrient acquisition machinery. As discussed, the adaptations required for root invasion may be even more involved than those required for the invasion of epithelia in humans. The fact that Bcc bacteria can perform both tasks is remarkable, though it would be interesting to compare the specific enzymes required for each.

Throughout the deployment of such tactics, Bcc cells tolerate a terrific onslaught of innate immune defences such as antimicrobial peptides by using its host of proteases and its own form of innate defence – a cell envelope designed perfectly for the repulsion of the animal kingdom's first lines of defence. Meanwhile, the bacteria encounter changing nutritional and physicochemical circumstances including oxygen levels and iron availability, to which they are

able to respond appropriately with incredibly diverse metabolic capabilities. The multipurpose nature of these Bcc adaptations provides insight into possible mechanisms by which Bcc emerged as a human pathogen.

The chapters that follow will explore the relationship between Bcc pathogenesis in plants and animals, and build on this foundation for further investigations into specific virulence tactics employed by these bacteria. First, the broad bioactivity of a nonribosomal peptide will be described in *B. vietnamiensis*, providing some additional insight into potential modes of iron acquisition by the Bcc that may have evolved for predator defence in their native soil habitats. Next, novel *B. cenocepacia* virulence factors will be described and discussed in the context of their potential functions. The final chapter will help alleviate the staggering incongruence between the importance of *B. multivorans* in CF and what is understood about its infection by unveiling a potential trigger for its virulence in two model hosts.

## References

1. Aaron SD, Vandemheen KL, Freitag A, Pedder L, Cameron W, Lavoie A, et al. Treatment of *Aspergillus fumigatus* in patients with cystic fibrosis: a randomized, placebo-controlled pilot study. PLOS One. 2012;7(4):e36077.
2. Abbas AK, Lichtman, A.H. Basic immunology: functions and disorders of the immune system. 3 ed. Philadelphia, PA: Saunders Elsevier; 2010.
3. Abdulrahman BA, Khweek AA, Akhter A, Caution K, Kotrange S, Abdelaziz DH, et al. Autophagy stimulation by rapamycin suppresses lung inflammation and infection by *Burkholderia cenocepacia* in a model of cystic fibrosis. Autophagy. 2011;7(11):1359-70.
4. Abe M, Nakazawa T. Characterization of hemolytic and antifungal substance, cepalydin, from *Pseudomonas cepacia*. Microbiol Immunol. 1994;38(1):1-9.
5. Agnoli K, Schwager S, Uehlinger S, Vergunst A, Viteri DF, Nguyen DT, et al. Exposing the third chromosome of *Burkholderia cepacia* complex strains as a virulence plasmid. Mol Microbiol. 2012;83(2):362-78.
6. Almeida RS, Brunke S, Albrecht A, Thewes S, Laue M, Edwards JE, et al. The hyphal-associated adhesin and invasin Als3 of *Candida albicans* mediates iron acquisition from host ferritin. PLoS Pathog. 2008;4(11):e1000217.
7. Anderson RD, Roddam LF, Bettioli S, Sanderson K, Reid DW. Biosignificance of bacterial cyanogenesis in the CF lung. J Cyst Fibros. 2010;9(3):158-64.
8. Armstrong L, Medford AR, Uppington KM, Robertson J, Witherden IR, Tetley TD, et al. Expression of functional Toll-like receptor-2 and -4 on alveolar epithelial cells. Am J Respir Cell Mol Biol. 2004;31(2):241-5.
9. Aubert DF, Flannagan RS, Valvano MA. A novel sensor kinase-response regulator hybrid controls biofilm formation and type VI secretion system activity in *Burkholderia cenocepacia*. Infect Immun. 2008;76(5):1979-91.
10. Babu-Khan S, Yeo TC, Martin WL, Duron MR, Rogers RD, Goldstein AH. Cloning of a mineral phosphate-solubilizing gene from *Pseudomonas cepacia*. Appl Environ Microbiol. 1995;61(3):972-8.
11. Bakare N, Rickerts V, Bargon J, Just-Nubling G. Prevalence of *Aspergillus fumigatus* and other fungal species in the sputum of adult patients with cystic fibrosis. Mycoses. 2003;46(1-2):19-23.
12. Bakkal S, Robinson SM, Ordonez CL, Waltz DA, Riley MA. Role of bacteriocins in mediating interactions of bacterial isolates taken from cystic fibrosis patients. Microbiology. 2010;156(Pt 7):2058-67.
13. Baldwin A, Sokol PA, Parkhill J, Mahenthalingam E. The *Burkholderia cepacia* epidemic strain marker is part of a novel genomic island encoding both virulence and metabolism-associated genes in *Burkholderia cenocepacia*. Infect Immun. 2004;72(3):1537-47.

14. Bals R, Wang X, Zasloff M, Wilson JM. The peptide antibiotic LL-37/hCAP-18 is expressed in epithelia of the human lung where it has broad antimicrobial activity at the airway surface. *Proc Natl Acad Sci U S A*. 1998;95(16):9541-6.
15. Bardgett R. *The Biology of Soils: A Community and Ecosystem Approach*. New York, NY: Oxford University Press Inc.; 2005. 254 p.
16. Barr JJ, Auro R, Furlan M, Whiteson KL, Erb ML, Pogliano J, et al. Bacteriophage adhering to mucus provide a non-host-derived immunity. *Proc Natl Acad Sci U S A*. 2013.
17. Barth AL, Pitt TL. Auxotrophy of *Burkholderia (Pseudomonas) cenocepacia* from cystic fibrosis patients. *J Clin Microbiol*. 1995;33(8):2192-4.
18. Bartlett JA, Fischer AJ, McCray PB, Jr. Innate immune functions of the airway epithelium. *Contrib Microbiol*. 2008;15:147-63.
19. Bazzini S, Udine C, Sass A, Pasca MR, Longo F, Emiliani G, et al. Deciphering the role of RND efflux transporters in *Burkholderia cenocepacia*. *PLOS One*. 2011;6(4):e18902.
20. Becker WM, Kleinsmith, L.J., Hardin, J. *The World of the Cell*. 6 ed. San Francisco, CA: Pearson - Benjamin Cummings; 2005. 944 p.
21. Begun J, Sifri CD, Goldman S, Calderwood SB, Ausubel FM. *Staphylococcus aureus* virulence factors identified by using a high-throughput *Caenorhabditis elegans*-killing model. *Infect Immun*. 2005;73(2):872-7.
22. Berlutti F, Morea C, Battistoni A, Sarli S, Cipriani P, Superti F, et al. Iron availability influences aggregation, biofilm, adhesion and invasion of *Pseudomonas aeruginosa* and *Burkholderia cenocepacia*. *Int J Immunopathol Pharmacol*. 2005;18(4):661-70.
23. Berlutti F, Superti F, Nicoletti M, Morea C, Frioni A, Ammendolia MG, et al. Bovine lactoferrin inhibits the efficiency of invasion of respiratory A549 cells of different iron-regulated morphological forms of *Pseudomonas aeruginosa* and *Burkholderia cenocepacia*. *Int J Immunopathol Pharmacol*. 2008;21(1):51-9.
24. Bernier SP, Silo-Suh L, Woods DE, Ohman DE, Sokol PA. Comparative analysis of plant and animal models for characterization of *Burkholderia cepacia* virulence. *Infect Immun*. 2003;71(9):5306-13.
25. Bertot GM, Restelli MA, Galanternik L, Aranibar Urey RC, Valvano MA, Grinstein S. Nasal immunization with *Burkholderia multivorans* outer membrane proteins and the mucosal adjuvant adamantylamide dipeptide confers efficient protection against experimental lung infections with *B. multivorans* and *B. cenocepacia*. *Infect Immun*. 2007;75(6):2740-52.
26. Bevivino A, Dalmastri C, Tabacchioni S, Chiarini L, Belli ML, Piana S, et al. *Burkholderia cepacia* complex bacteria from clinical and environmental sources in Italy: genomovar status and distribution of traits related to virulence and transmissibility. *J Clin Microbiol*. 2002;40(3):846-51.
27. Blainey PC, Milla CE, Cornfield DN, Quake SR. Quantitative analysis of the human airway microbial ecology reveals a pervasive signature for cystic fibrosis. *Sci Transl Med*. 2012;4(153):153ra30.

28. Bobadilla JL, Macek M, Jr., Fine JP, Farrell PM. Cystic fibrosis: a worldwide analysis of CFTR mutations--correlation with incidence data and application to screening. *Hum Mutat.* 2002;19(6):575-606.
29. Boon C, Deng Y, Wang LH, He Y, Xu JL, Fan Y, et al. A novel DSF-like signal from *Burkholderia cenocepacia* interferes with *Candida albicans* morphological transition. *ISME J.* 2008;2(1):27-36.
30. Brackman G, Cos P, Maes L, Nelis HJ, Coenye T. Quorum sensing inhibitors increase the susceptibility of bacterial biofilms to antibiotics *in vitro* and *in vivo*. *Antimicrob Agents Chemother.* 2011;55(6):2655-61.
31. Bragonzi A. Murine models of acute and chronic lung infection with cystic fibrosis pathogens. *Int J Med Microbiol.* 2010;300(8):584-93.
32. Burns JL, Jonas M, Chi EY, Clark DK, Berger A, Griffith A. Invasion of respiratory epithelial cells by *Burkholderia (Pseudomonas) cepacia*. *Infect Immun.* 1996;64(10):4054-9.
33. Button B, Cai LH, Ehre C, Kesimer M, Hill DB, Sheehan JK, et al. A periciliary brush promotes the lung health by separating the mucus layer from airway epithelia. *Science.* 2012;337(6097):937-41.
34. Bylund J, Burgess LA, Cescutti P, Ernst RK, Speert DP. Exopolysaccharides from *Burkholderia cenocepacia* inhibit neutrophil chemotaxis and scavenge reactive oxygen species. *J Biol Chem.* 2006;281(5):2526-32.
35. Campbell NA, Reece, J.B. *Biology.* San Francisco, CA: Pearson - Benjamin Cummings; 2008.
36. Cao H, Baldini RL, Rahme LG. Common mechanisms for pathogens of plants and animals. *Annu Rev Phytopathol.* 2001;39:259-84.
37. Caraher E, Reynolds G, Murphy P, McClean S, Callaghan M. Comparison of antibiotic susceptibility of *Burkholderia cepacia* complex organisms when grown planktonically or as biofilm *in vitro*. *Eur J Clin Microbiol Infect Dis.* 2007;26(3):213-6.
38. Cardona ST, Wopperer J, Eberl L, Valvano MA. Diverse pathogenicity of *Burkholderia cepacia* complex strains in the *Caenorhabditis elegans* host model. *FEMS Microbiol Lett.* 2005;250(1):97-104.
39. Carmody LA, Gill JJ, Summer EJ, Sajjan US, Gonzalez CF, Young RF, et al. Efficacy of bacteriophage therapy in a model of *Burkholderia cenocepacia* pulmonary infection. *J Infect Dis.* 2010;201(2):264-71.
40. Castonguay-Vanier J, Vial L, Tremblay J, Deziel E. *Drosophila melanogaster* as a model host for the *Burkholderia cepacia* complex. *PLOS One.* 2010;5(7):e11467.
41. Chaparro C, Maurer J, Gutierrez C, Krajden M, Chan C, Winton T, et al. Infection with *Burkholderia cepacia* in cystic fibrosis: outcome following lung transplantation. *Am J Respir Crit Care Med.* 2001;163(1):43-8.
42. Charalabous P, Risk JM, Jenkins R, Birss AJ, Hart CA, Smalley JW. Characterization of a bifunctional catalase-peroxidase of *Burkholderia cenocepacia*. *FEMS Immunol Med Microbiol.* 2007;50(1):37-44.

43. Cheung KJ, Jr., Li G, Urban TA, Goldberg JB, Griffith A, Lu F, et al. Pilus-mediated epithelial cell death in response to infection with *Burkholderia cenocepacia*. *Microbes Infect.* 2007;9(7):829-37.
44. Chiarini L, Bevivino A, Dalmastrì C, Tabacchioni S, Visca P. *Burkholderia cepacia* complex species: health hazards and biotechnological potential. *Trends Microbiol.* 2006;14(6):277-86.
45. Chiarini L, Bevivino A., Tabacchioni, S., Dalmastrì, C. . Inoculation of *Burkholderia cepacia*, *Pseudomonas fluorescens* and *Enterobacter* sp. on *Sorghum bicolor*: root colonization and plant growth promotion of dual strain inocula. *Soil Biol Biochem* 1998;30:81-7.
46. Chilvers MA, O'Callaghan C. Local mucociliary defence mechanisms. *Paediatr Respir Rev.* 2000;1(1):27-34.
47. Chiu CH, Ostry A, Speert DP. Invasion of murine respiratory epithelial cells in vivo by *Burkholderia cepacia*. *J Med Microbiol.* 2001;50(7):594-601.
48. Chiu CH, Wong S, Hancock RE, Speert DP. Adherence of *Burkholderia cepacia* to respiratory tract epithelial cells and inhibition with dextrans. *Microbiology.* 2001;147(Pt 10):2651-8.
49. Chung JW, Speert DP. Proteomic identification and characterization of bacterial factors associated with *Burkholderia cenocepacia* survival in a murine host. *Microbiology.* 2007;153(Pt 1):206-14.
50. Cirillo JD, Falkow S, Tompkins LS. Growth of *Legionella pneumophila* in *Acanthamoeba castellanii* enhances invasion. *Infect Immun.* 1994;62(8):3254-61.
51. Cody WL, Pritchett CL, Jones AK, Carterson AJ, Jackson D, Frisk A, et al. *Pseudomonas aeruginosa* AlgR controls cyanide production in an AlgZ-dependent manner. *J Bacteriol.* 2009;191(9):2993-3002.
52. Coenye T, Vandamme P, Govan JR, LiPuma JJ. Taxonomy and identification of the *Burkholderia cepacia* complex. *J Clin Microbiol.* 2001;39(10):3427-36.
53. Cohen TS, Prince A. Cystic fibrosis: a mucosal immunodeficiency syndrome. *Nat Med.* 2012;18(4):509-19.
54. Conese M, Copreni E, Di Gioia S, De Rinaldis P, Fumarulo R. Neutrophil recruitment and airway epithelial cell involvement in chronic cystic fibrosis lung disease. *J Cyst Fibros.* 2003;2(3):129-35.
55. Conner GE, Wijkstrom-Frei C, Randell SH, Fernandez VE, Salathe M. The lactoperoxidase system links anion transport to host defense in cystic fibrosis. *FEBS Lett.* 2007;581(2):271-8.
56. Conway BA, Chu KK, Bylund J, Altman E, Speert DP. Production of exopolysaccharide by *Burkholderia cenocepacia* results in altered cell-surface interactions and altered bacterial clearance in mice. *J Infect Dis.* 2004;190(5):957-66.
57. Cooper VS, Carlson WA, Lipuma JJ. Susceptibility of *Caenorhabditis elegans* to *Burkholderia* infection depends on prior diet and secreted bacterial attractants. *PLOS One.* 2009;4(11):e7961.
58. Cosgrove S, Chotirmall SH, Greene CM, McElvaney NG. Pulmonary proteases in the cystic fibrosis lung induce interleukin 8 expression from

- bronchial epithelial cells via a heme/meprin/epidermal growth factor receptor/Toll-like receptor pathway. *J Biol Chem.* 2011;286(9):7692-704.
59. Coutinho CP, de Carvalho CC, Madeira A, Pinto-de-Oliveira A, Sa-Correia I. *Burkholderia cenocepacia* phenotypic clonal variation during a 3.5-year colonization in the lungs of a cystic fibrosis patient. *Infect Immun.* 2011;79(7):2950-60.
  60. Coutinho CP, Dos Santos SC, Madeira A, Mira NP, Moreira AS, Sa-Correia I. Long-term colonization of the cystic fibrosis lung by *Burkholderia cepacia* complex bacteria: epidemiology, clonal variation, and genome-wide expression alterations. *Front Cell Infect Microbiol.* 2011;1:12.
  61. Coventry HS, Dubery, I.A. Lipopolysaccharides from *Burkholderia cepacia* contribute to an enhanced defensive capacity and the induction of pathogenesis-related proteins in *Nicotiana tabacum*. *Physiol Mol Plant Pathol.* 2001;48:149-58.
  62. Cozens AL, Yezzi MJ, Kunzelmann K, Ohrui T, Chin L, Eng K, et al. CFTR expression and chloride secretion in polarized immortal human bronchial epithelial cells. *Am J Respir Cell Mol Biol.* 1994;10(1):38-47.
  63. Cunha LG, Jr., Assis MC, Machado GB, Assef AP, Marques EA, Leao RS, et al. Potential mechanisms underlying the acute lung dysfunction and bacterial extrapulmonary dissemination during *Burkholderia cenocepacia* respiratory infection. *Respir Res.* 2010;11:4.
  64. Cunha MV, Sousa SA, Leitao JH, Moreira LM, Videira PA, Sa-Correia I. Studies on the involvement of the exopolysaccharide produced by cystic fibrosis-associated isolates of the *Burkholderia cepacia* complex in biofilm formation and in persistence of respiratory infections. *J Clin Microbiol.* 2004;42(7):3052-8.
  65. Cvejic JH, Putra SR, El-Beltagy A, Hattori R, Hattori T, Rohmer M. Bacterial triterpenoids of the hopane series as biomarkers for the chemotaxonomy of *Burkholderia*, *Pseudomonas* and *Ralstonia* spp. *FEMS Microbiol Lett.* 2000;183(2):295-9.
  66. Darling KE, Evans TJ. Effects of nitric oxide on *Pseudomonas aeruginosa* infection of epithelial cells from a human respiratory cell line derived from a patient with cystic fibrosis. *Infect Immun.* 2003;71(5):2341-9.
  67. Darling P, Chan M, Cox AD, Sokol PA. Siderophore production by cystic fibrosis isolates of *Burkholderia cepacia*. *Infect Immun.* 1998;66(2):874-7.
  68. Davidson DJ, Dorin JR, McLachlan G, Ranaldi V, Lamb D, Doherty C, et al. Lung disease in the cystic fibrosis mouse exposed to bacterial pathogens. *Nat Genet.* 1995;9(4):351-7.
  69. Day BJ. Glutathione: a radical treatment for cystic fibrosis lung disease? *Chest.* 2005;127(1):12-4.
  70. de Carvalho MP, Abraham WR. Antimicrobial and biofilm inhibiting diketopiperazines. *Curr Med Chem.* 2012;19(21):3564-77.
  71. De Soyza A, Ellis CD, Khan CM, Corris PA, Demarco de Hormaeche R. *Burkholderia cenocepacia* lipopolysaccharide, lipid A, and proinflammatory activity. *Am J Respir Crit Care Med.* 2004;170(1):70-7.
  72. De Soyza A, McDowell A, Archer L, Dark JH, Elborn SJ, Mahenthiralingam E, et al. *Burkholderia cepacia* complex genomovars and

- pulmonary transplantation outcomes in patients with cystic fibrosis. *Lancet*. 2001;358(9295):1780-1.
73. Dehner C, Morales-Soto N, Behera RK, Shrout J, Theil EC, Maurice PA, et al. Ferritin and ferrihydrite nanoparticles as iron sources for *Pseudomonas aeruginosa*. *J Biol Inorg Chem*. 2013;18(3):371-81.
  74. Delhaes L, Monchy S, Frealle E, Hubans C, Salleron J, Leroy S, et al. The airway microbiota in cystic fibrosis: a complex fungal and bacterial community--implications for therapeutic management. *PLOS One*. 2012;7(4):e36313.
  75. Deng Y, Boon C, Eberl L, Zhang LH. Differential modulation of *Burkholderia cenocepacia* virulence and energy metabolism by the quorum-sensing signal BDSF and its synthase. *J Bacteriol*. 2009;191(23):7270-8.
  76. Deng Y, Wu J, Eberl L, Zhang LH. Structural and functional characterization of diffusible signal factor family quorum-sensing signals produced by members of the *Burkholderia cepacia* complex. *Appl Environ Microbiol*. 2010;76(14):4675-83.
  77. Denman CC, Brown AR. Mannitol promotes adherence of an outbreak strain of *Burkholderia multivorans* via an exopolysaccharide-independent mechanism that is associated with upregulation of newly identified fimbrial and afimbrial adhesins. *Microbiology*. 2013;159(Pt 4):771-81.
  78. Dixon R, Kahn D. Genetic regulation of biological nitrogen fixation. *Nat Rev Microbiol*. 2004;2(8):621-31.
  79. Drevinek P, Baldwin A, Lindenburg L, Joshi LT, Marchbank A, Vosahlikova S, et al. Oxidative stress of *Burkholderia cenocepacia* induces insertion sequence-mediated genomic rearrangements that interfere with macrorestriction-based genotyping. *J Clin Microbiol*. 2010;48(1):34-40.
  80. Duff C, Murphy PG, Callaghan M, McClean S. Differences in invasion and translocation of *Burkholderia cepacia* complex species in polarised lung epithelial cells in vitro. *Microb Pathog*. 2006;41(4-5):183-92.
  81. Ederer GM, Matsen JM. Colonization and infection with *Pseudomonas cepacia*. *J Infect Dis*. 1972;125(6):613-8.
  82. Ehrhardt C, Collnot EM, Baldes C, Becker U, Laue M, Kim KJ, et al. Towards an *in vitro* model of cystic fibrosis small airway epithelium: characterisation of the human bronchial epithelial cell line CFBE41o. *Cell Tissue Res*. 2006;323(3):405-15.
  83. Eisele NA, Anderson DM. Host defense and the airway epithelium: frontline responses that protect against bacterial invasion and pneumonia. *J Pathog*. 2011;2011:249802.
  84. Ellis CN, Cooper VS. Experimental adaptation of *Burkholderia cenocepacia* to onion medium reduces host range. *Appl Environ Microbiol*. 2010;76(8):2387-96.
  85. Engledow AS, Medrano EG, Mahenthalingam E, LiPuma JJ, Gonzalez CF. Involvement of a plasmid-encoded type IV secretion system in the plant tissue watersoaking phenotype of *Burkholderia cenocepacia*. *J Bacteriol*. 2004;186(18):6015-24.
  86. Fehlner-Gardiner CC, Hopkins TM, Valvano MA. Identification of a general secretory pathway in a human isolate of *Burkholderia vietnamiensis*

- (formerly *B. cepacia* complex genomovar V) that is required for the secretion of hemolysin and phospholipase C activities. *Microb Path.* 2002;32(5):249-54.
87. Ferreira AS, Leitao JH, Silva IN, Pinheiro PF, Sousa SA, Ramos CG, et al. Distribution of cepacian biosynthesis genes among environmental and clinical *Burkholderia* strains and role of cepacian exopolysaccharide in resistance to stress conditions. *Appl Environ Microbiol.* 2010;76(2):441-50.
  88. Ferreira AS, Silva IN, Oliveira VH, Becker JD, Givskov M, Ryan RP, et al. Comparative transcriptomic analysis of the *Burkholderia cepacia* tyrosine kinase *bceF* mutant reveals a role in tolerance to stress, biofilm formation, and virulence. *Appl Environ Microbiol.* 2013;79(9):3009-20.
  89. Fito-Boncompte L, Chapalain A, Bouffartigues E, Chaker H, Lesouhaitier O, Gicquel G, et al. Full virulence of *Pseudomonas aeruginosa* requires OprF. *Infect Immun.* 2011;79(3):1176-86.
  90. Flannagan RS, Aubert D, Kooi C, Sokol PA, Valvano MA. *Burkholderia cenocepacia* requires a periplasmic HtrA protease for growth under thermal and osmotic stress and for survival *in vivo*. *Infect Immun.* 2007;75(4):1679-89.
  91. Flannagan RS, Valvano MA. *Burkholderia cenocepacia* requires RpoE for growth under stress conditions and delay of phagolysosomal fusion in macrophages. *Microbiology.* 2008;154(Pt 2):643-53.
  92. Fossati G, Moulding DA, Spiller DG, Moots RJ, White MR, Edwards SW. The mitochondrial network of human neutrophils: role in chemotaxis, phagocytosis, respiratory burst activation, and commitment to apoptosis. *J Immunol.* 2003;170(4):1964-72.
  93. Francis MS, Wolf-Watz H, Forsberg A. Regulation of type III secretion systems. *Curr Opin Microbiol.* 2002;5(2):166-72.
  94. Fung C, Naughton S, Turnbull L, Tingpej P, Rose B, Arthur J, et al. Gene expression of *Pseudomonas aeruginosa* in a mucin-containing synthetic growth medium mimicking cystic fibrosis lung sputum. *J Med Microbiol.* 2010;59(Pt 9):1089-100.
  95. Gaffney TD, Lessie TG. Insertion sequence-dependent rearrangements of *Pseudomonas cepacia* plasmid pTGL1. *J Bacteriol.* 1987;169(1):224-30.
  96. Ghio AJ, Roggli VL, Soukup JM, Richards JH, Randell SH, Muhlebach MS. Iron accumulates in the lavage and explanted lungs of cystic fibrosis patients. *J Cyst Fibros.* 2013;12(4):390-8.
  97. Giard DJ, Aaronson SA, Todaro GJ, Arnstein P, Kersey JH, Dosik H, et al. In vitro cultivation of human tumors: establishment of cell lines derived from a series of solid tumors. *J Natl Cancer Inst.* 1973;51(5):1417-23.
  98. Gilchrist FJ SH, Alcock A, Jones AM, Bright-Thomas RJ, Smith D, Spanel P, Webb AK, Lenney W. Is hydrogen cyanide a marker of *Burkholderia cepacia* complex? *J Clin Microbiol* 2013;Epub ahead of print.
  99. Gingués S, Kooi C, Visser MB, Subsin B, Sokol PA. Distribution and expression of the ZmpA metalloprotease in the *Burkholderia cepacia* complex. *J Bacteriol.* 2005;187(24):8247-55.
  100. Glendinning KJ, Parsons YN, Duangsonk K, Hales BA, Humphreys D, Hart CA, et al. Sequence divergence in type III secretion gene clusters of the *Burkholderia cepacia* complex. *FEMS Microbiol Lett.* 2004;235(2):229-35.

101. Goddard AF, Staudinger BJ, Dowd SE, Joshi-Datar A, Wolcott RD, Aitken ML, et al. Direct sampling of cystic fibrosis lungs indicates that DNA-based analyses of upper-airway specimens can misrepresent lung microbiota. *Proc Natl Acad Sci U S A*. 2012;109(34):13769-74.
102. Golshahi L, Seed KD, Dennis JJ, Finlay WH. Toward modern inhalational bacteriophage therapy: nebulization of bacteriophages of *Burkholderia cepacia* complex. *J Aerosol Med Pulm Drug Deliv*. 2008;21(4):351-60.
103. Goo E, Majerczyk CD, An JH, Chandler JR, Seo YS, Ham H, et al. Bacterial quorum sensing, cooperativity, and anticipation of stationary-phase stress. *Proc Natl Acad Sci U S A*. 2012;109(48):19775-80.
104. Gotschlich A, Huber B, Geisenberger O, Togl A, Steidle A, Riedel K, et al. Synthesis of multiple N-acylhomoserine lactones is wide-spread among the members of the *Burkholderia cepacia* complex. *Syst Appl Microbiol*. 2001;24(1):1-14.
105. Graindorge A, Menard A, Monnez C, Cournoyer B. Insertion sequence evolutionary patterns highlight convergent genetic inactivations and recent genomic island acquisitions among epidemic *Burkholderia cenocepacia*. *J Med Microbiol*. 2012;61(Pt 3):394-409.
106. Grainger CI, Greenwell LL, Lockley DJ, Martin GP, Forbes B. Culture of Calu-3 cells at the air interface provides a representative model of the airway epithelial barrier. *Pharm Res*. 2006;23(7):1482-90.
107. Gu G, Smith L, Wang N, Wang H, Lu SE. Biosynthesis of an antifungal oligopeptide in *Burkholderia contaminans* strain MS14. *Biochem Biophys Res Commun*. 2009;380(2):328-32.
108. Hall RA, Turner KJ, Chaloupka J, Cottier F, De Sordi L, Sanglard D, et al. The quorum-sensing molecules farnesol/homoserine lactone and dodecanol operate via distinct modes of action in *Candida albicans*. *Eukaryot Cell*. 2011;10(8):1034-42.
109. Harder J, Meyer-Hoffert U, Teran LM, Schwichtenberg L, Bartels J, Maune S, et al. Mucoid *Pseudomonas aeruginosa*, TNF-alpha, and IL-1beta, but not IL-6, induce human beta-defensin-2 in respiratory epithelia. *Am J Respir Cell Mol Biol*. 2000;22(6):714-21.
110. Hartl D, Latzin P, Hordijk P, Marcos V, Rudolph C, Woischnik M, et al. Cleavage of CXCR1 on neutrophils disables bacterial killing in cystic fibrosis lung disease. *Nat Med*. 2007;13(12):1423-30.
111. Hauser AR, Engel JN. *Pseudomonas aeruginosa* induces type-III-secretion-mediated apoptosis of macrophages and epithelial cells. *Infect Immun*. 1999;67(10):5530-7.
112. Hebbbar KP, Martel, M.H., Heulin, T. Suppression of pre- and postemergence damping-off in corn by *Burkholderia cepacia*. *Eur J Plant Path*. 1998;104(1):29-36.
113. Henke MO, Renner A, Huber RM, Seeds MC, Rubin BK. MUC5AC and MUC5B mucins are decreased in cystic fibrosis airway secretions. *Am J Respir Cell Mol Biol*. 2004;31(1):86-91.

114. Heungens K, Parke JL. Postinfection biological control of oomycete pathogens of pea by *Burkholderia cepacia* AMMDR1. *Phytopathology*. 2001;91(4):383-91.
115. Holden MT, Ram Chhabra S, de Nys R, Stead P, Bainton NJ, Hill PJ, et al. Quorum-sensing cross talk: isolation and chemical characterization of cyclic dipeptides from *Pseudomonas aeruginosa* and other gram-negative bacteria. *Mol Microbiol*. 1999;33(6):1254-66.
116. Huber B, Riedel K, Hentzer M, Heydorn A, Gotschlich A, Givskov M, et al. The cep quorum-sensing system of *Burkholderia cepacia* H111 controls biofilm formation and swarming motility. *Microbiology*. 2001;147(Pt 9):2517-28.
117. Hunt TA, Kooi C, Sokol PA, Valvano MA. Identification of *Burkholderia cenocepacia* genes required for bacterial survival *in vivo*. *Infect Immun*. 2004;72(7):4010-22.
118. Hutchison ML, Poxton IR, Govan JR. *Burkholderia cepacia* produces a hemolysin that is capable of inducing apoptosis and degranulation of mammalian phagocytes. *Infect Immun*. 1998;66(5):2033-9.
119. Huynh KK, Plumb JD, Downey GP, Valvano MA, Grinstein S. Inactivation of macrophage Rab7 by *Burkholderia cenocepacia*. *J Innate Immun*. 2010;2(6):522-33.
120. Ibrahim M, Tang Q, Shi Y, Almoneafy A, Fang Y, Xu L, et al. Diversity of potential pathogenicity and biofilm formation among *Burkholderia cepacia* complex water, clinical, and agricultural isolates in China. *World J Microbiol Biotechnol*. 2012;28(5):2113-23.
121. Ikonen EK. Life history studies of the hermaphrodite nematode *Acrobeloides* sp. with *Pseudomonas cepacia* as a food source on agar. *Nematol*. 2001;3:759-66.
122. Iriti M, Faoro F. Review of innate and specific immunity in plants and animals. *Mycopathologia*. 2007;164(2):57-64.
123. Isles A, Maclusky I, Corey M, Gold R, Prober C, Fleming P, et al. *Pseudomonas cepacia* infection in cystic fibrosis: an emerging problem. *J Paed*. 1984;104(2):206-10.
124. Jacobs JL, Fasi AC, Ramette A, Smith JJ, Hammerschmidt R, Sundin GW. Identification and onion pathogenicity of *Burkholderia cepacia* complex isolates from the onion rhizosphere and onion field soil. *Appl Environ Microbiol*. 2008;74(10):3121-9.
125. Ji X, Lu G, Gai Y, Gao H, Lu B, Kong L, et al. Colonization of *Morus alba* L. by the plant-growth-promoting and antagonistic bacterium *Burkholderia cepacia* strain Lu10-1. *BMC Microbiol*. 2010;10:243.
126. John G, Chillappagari S, Rubin BK, Gruenert DC, Henke MO. Reduced surface toll-like receptor-4 expression and absent interferon-gamma-inducible protein-10 induction in cystic fibrosis airway cells. *Exp Lung Res*. 2011;37(6):319-26.
127. John G, Yildirim AO, Rubin BK, Gruenert DC, Henke MO. TLR-4-mediated innate immunity is reduced in cystic fibrosis airway cells. *Am J Respir Cell Mol Biol*. 2010;42(4):424-31.

128. Jones AM, Dodd ME, Govan JR, Barcus V, Doherty CJ, Morris J, et al. *Burkholderia cenocepacia* and *Burkholderia multivorans*: influence on survival in cystic fibrosis. *Thorax*. 2004;59(11):948-51.
129. Juhas M, Stark M, von Mering C, Lumjiaktase P, Crook DW, Valvano MA, et al. High confidence prediction of essential genes in *Burkholderia cenocepacia*. *PLOS One*. 2012;7(6):e40064.
130. Kang Y, Carlson R, Tharpe W, Schell MA. Characterization of genes involved in biosynthesis of a novel antibiotic from *Burkholderia cepacia* BC11 and their role in biological control of *Rhizoctonia solani*. *Appl Env Microbiol*. 1998;64(10):3939-47.
131. Kaza SK, McClean S, Callaghan M. IL-8 released from human lung epithelial cells induced by cystic fibrosis pathogens *Burkholderia cepacia* complex affects the growth and intracellular survival of bacteria. *Int J Med Microbiol*. 2011;301(1):26-33.
132. Keig PM, Ingham E, Kerr KG. Invasion of human type II pneumocytes by *Burkholderia cepacia*. *Microb Pathog*. 2001;30(3):167-70.
133. Keig PM, Ingham E, Vandamme PA, Kerr KG. Differential invasion of respiratory epithelial cells by members of the *Burkholderia cepacia* complex. *Clin Microbiol Infect*. 2002;8(1):47-9.
134. Keith KE, Hynes DW, Sholdice JE, Valvano MA. Delayed association of the NADPH oxidase complex with macrophage vacuoles containing the opportunistic pathogen *Burkholderia cenocepacia*. *Microbiology*. 2009;155(Pt 4):1004-15.
135. Kelly E, Greene CM, McElvaney NG. Targeting neutrophil elastase in cystic fibrosis. *Expert Opin Ther Targets*. 2008;12(2):145-57.
136. Kerr J. Inhibition of fungal growth by *Pseudomonas aeruginosa* and *Pseudomonas cepacia* isolated from patients with cystic fibrosis. *J Infect*. 1994;28(3):305-10.
137. Kogan I, Ramjeesingh M, Li C, Kidd JF, Wang Y, Leslie EM, et al. CFTR directly mediates nucleotide-regulated glutathione flux. *EMBO J*. 2003;22(9):1981-9.
138. Kooi C, Sokol PA. *Burkholderia cenocepacia* zinc metalloproteases influence resistance to antimicrobial peptides. *Microbiology*. 2009;155(Pt 9):2818-25.
139. Kooi C, Subsin B, Chen R, Pohorelic B, Sokol PA. *Burkholderia cenocepacia* ZmpB is a broad-specificity zinc metalloprotease involved in virulence. *Infect Immun*. 2006;74(7):4083-93.
140. Kopp BT, Abdulrahman BA, Khweek AA, Kumar SB, Akhter A, Montione R, et al. Exaggerated inflammatory responses mediated by *Burkholderia cenocepacia* in human macrophages derived from cystic fibrosis patients. *Biochem Biophys Res Commun*. 2012;424(2):221-7.
141. Kothe M, Antl M, Huber B, Stoecker K, Ebrecht D, Steinmetz I, et al. Killing of *Caenorhabditis elegans* by *Burkholderia cepacia* is controlled by the cep quorum-sensing system. *Cell Microbiol*. 2003;5(5):343-51.
142. Kroupitski Y, Golberg D, Belausov E, Pinto R, Swartzberg D, Granot D, et al. Internalization of *Salmonella enterica* in leaves is induced by light and

- involves chemotaxis and penetration through open stomata. *Appl Env Microbiol.* 2009;75(19):6076-86.
143. Kuehn M, Lent K, Haas J, Hagenzieker J, Cervin M, Smith AL. Fimbriation of *Pseudomonas cepacia*. *Infect Immun.* 1992;60(5):2002-7.
144. Kuroda A, Nomura K, Ohtomo R, Kato J, Ikeda T, Takiguchi N, et al. Role of inorganic polyphosphate in promoting ribosomal protein degradation by the Lon protease in *E. coli*. *Science.* 2001;293(5530):705-8.
145. Lai Y, Gallo RL. AMPed up immunity: how antimicrobial peptides have multiple roles in immune defense. *Trends Immunol.* 2009;30(3):131-41.
146. Lamothe J, Huynh KK, Grinstein S, Valvano MA. Intracellular survival of *Burkholderia cenocepacia* in macrophages is associated with a delay in the maturation of bacteria-containing vacuoles. *Cell Microbiol.* 2007;9(1):40-53.
147. Lamothe J, Thyssen S, Valvano MA. *Burkholderia cepacia* complex isolates survive intracellularly without replication within acidic vacuoles of *Acanthamoeba polyphaga*. *Cell Microbiol.* 2004;6(12):1127-38.
148. Lamothe J, Valvano MA. *Burkholderia cenocepacia*-induced delay of acidification and phagolysosomal fusion in cystic fibrosis transmembrane conductance regulator (CFTR)-defective macrophages. *Microbiology.* 2008;154(Pt 12):3825-34.
149. Landers P, Kerr KG, Rowbotham TJ, Tipper JL, Keig PM, Ingham E, et al. Survival and growth of *Burkholderia cepacia* within the free-living amoeba *Acanthamoeba polyphaga*. *Eur J Clin Microbiol Infect Dis.* 2000;19(2):121-3.
150. Langley R. Lysogeny and bacteriophage host range within the *Burkholderia cepacia* complex. *J Med Microbiol.* 2003;52(6):483-90.
151. Law RJ, Hamlin JN, Sivro A, McCorrister SJ, Cardama GA, Cardona ST. A functional phenylacetic acid catabolic pathway is required for full pathogenicity of *Burkholderia cenocepacia* in the *Caenorhabditis elegans* host model. *J Bacteriol.* 2008;190(21):7209-18.
152. Laws TR, Smith SA, Smith MP, Harding SV, Atkins TP, Titball RW. The nematode *Panagrellus redivivus* is susceptible to killing by human pathogens at 37 degrees C. *FEMS Microbiol Lett.* 2005;250(1):77-83.
153. Ledson MJ, Gallagher MJ, Jackson M, Hart CA, Walshaw MJ. Outcome of *Burkholderia cepacia* colonisation in an adult cystic fibrosis centre. *Thorax.* 2002;57(2):142-5.
154. Lee CH, Kim S, Hyun B, Suh JW, Yon C, Kim C, et al. Cepacidine A, a novel antifungal antibiotic produced by *Pseudomonas cepacia*. I. Taxonomy, production, isolation and biological activity. *J Antibiot (Tokyo).* 1994;47(12):1402-5.
155. Lee YH, Chen Y, Ouyang X, Gan YH. Identification of tomato plant as a novel host model for *Burkholderia pseudomallei*. *BMC Microbiol.* 2010;10:28-2180-10-28.
156. Lewenza S, Conway B, Greenberg EP, Sokol PA. Quorum sensing in *Burkholderia cepacia*: identification of the LuxRI homologs CepRI. *J Bacteriol.* 1999;181(3):748-56.

157. Li X, Quan CS, Fan SD. Antifungal activity of a novel compound from *Burkholderia cepacia* against plant pathogenic fungi. *Lett Appl Microbiol*. 2007;45(5):508-14.
158. Liu Y, Sadikot RT, Adami GR, Kalinichenko VV, Pendyala S, Natarajan V, et al. FoxM1 mediates the progenitor function of type II epithelial cells in repairing alveolar injury induced by *Pseudomonas aeruginosa*. *J Exp Med*. 2011;208(7):1473-84.
159. Loutet SA, Flannagan RS, Kooi C, Sokol PA, Valvano MA. A complete lipopolysaccharide inner core oligosaccharide is required for resistance of *Burkholderia cenocepacia* to antimicrobial peptides and bacterial survival *in vivo*. *J Bacteriol*. 2006;188(6):2073-80.
160. Lynch KH, Seed KD, Stothard P, Dennis JJ. Inactivation of *Burkholderia cepacia* complex phage KS9 gp41 identifies the phage repressor and generates lytic virions. *J Virol*. 2010;84(3):1276-88.
161. Lynch SV, Bruce KD. The cystic fibrosis airway microbiome. *Cold Spring Harb Perspect Med*. 2013;3(3):a009738.
162. MacDonald KL, Speert DP. Differential modulation of innate immune cell functions by the *Burkholderia cepacia* complex: *Burkholderia cenocepacia* but not *Burkholderia multivorans* disrupts maturation and induces necrosis in human dendritic cells. *Cell Microbiol*. 2008;10(10):2138-49.
163. Madeira A, Santos PM, Coutinho CP, Pinto-de-Oliveira A, Sa-Correia I. Quantitative proteomics (2-D DIGE) reveals molecular strategies employed by *Burkholderia cenocepacia* to adapt to the airways of cystic fibrosis patients under antimicrobial therapy. *Proteomics*. 2011;11(7):1313-28.
164. Madigan MT, Martinko, J.M. Brock Biology of Microorganisms. 11 ed. Upper Saddle River, NJ: Pearson Prentice Hall; 2006.
165. Mahenthiralingam E, Urban TA, Goldberg JB. The multifarious, multireplicon *Burkholderia cepacia* complex. *Nat Rev Microbiol*. 2005;3(2):144-56.
166. Maloney KE, Valvano MA. The *mgtC* gene of *Burkholderia cenocepacia* is required for growth under magnesium limitation conditions and intracellular survival in macrophages. *Infect Immun*. 2006;74(10):5477-86.
167. Malott RJ, Sokol PA. Expression of the *bviIR* and *cepIR* quorum-sensing systems of *Burkholderia vietnamiensis*. *J Bacteriol*. 2007;189(8):3006-16.
168. Markey KM, Glendinning KJ, Morgan JA, Hart CA, Winstanley C. *Caenorhabditis elegans* killing assay as an infection model to study the role of type III secretion in *Burkholderia cenocepacia*. *J Med Microbiol*. 2006;55(Pt 7):967-9.
169. Martin DW, Mohr CD. Invasion and intracellular survival of *Burkholderia cepacia*. *Infect Immun*. 2000;68(1):24-9.
170. Mason RJ. Biology of alveolar type II cells. *Respirology*. 2006;11 Suppl:S12-5.
171. Matsui H, Grubb BR, Tarran R, Randell SH, Gatzky JT, Davis CW, et al. Evidence for periciliary liquid layer depletion, not abnormal ion composition, in the pathogenesis of cystic fibrosis airways disease. *Cell*. 1998;95(7):1005-15.

172. McCarthy Y, Yang L, Twomey KB, Sass A, Tolker-Nielsen T, Mahenthiralingam E, et al. A sensor kinase recognizing the cell-cell signal BDSF (*cis*-2-dodecenoic acid) regulates virulence in *Burkholderia cenocepacia*. *Mol Microbiol.* 2010;77(5):1220-36.
173. Menard A, Monnez C, Estrada de Los Santos P, Segonds C, Caballero-Mellado J, Lipuma JJ, et al. Selection of nitrogen-fixing deficient *Burkholderia vietnamiensis* strains by cystic fibrosis patients: involvement of *nif* gene deletions and auxotrophic mutations. *Environ Microbiol.* 2007;9(5):1176-85.
174. Mendes R, Pizzirani-Kleiner AA, Araujo WL, Raaijmakers JM. Diversity of cultivated endophytic bacteria from sugarcane: genetic and biochemical characterization of *Burkholderia cepacia* complex isolates. *Appl Environ Microbiol.* 2007;73(22):7259-67.
175. Meng QH, Springall DR, Bishop AE, Morgan K, Evans TJ, Habib S, et al. Lack of inducible nitric oxide synthase in bronchial epithelium: a possible mechanism of susceptibility to infection in cystic fibrosis. *J Pathol.* 1998;184(3):323-31.
176. Meyers E, Bisacchi GS, Dean L, Liu WC, Minassian B, Slusarchyk DS, et al. Xylocandin: a new complex of antifungal peptides. I. Taxonomy, isolation and biological activity. *J Antibiot.* 1987;40(11):1515-9.
177. Miche L, Faure D, Blot M, Cabanne-Giuli E, Balandreau J. Detection and activity of insertion sequences in environmental strains of *Burkholderia*. *Environ Microbiol.* 2001;3(12):766-73.
178. Middleton B, Rodgers HC, Camara M, Knox AJ, Williams P, Hardman A. Direct detection of N-acylhomoserine lactones in cystic fibrosis sputum. *FEMS Microbiol Lett.* 2002;207(1):1-7.
179. Mil-Homens D, Fialho AM. A BCAM0223 mutant of *Burkholderia cenocepacia* is deficient in hemagglutination, serum resistance, adhesion to epithelial cells and virulence. *PLOS One.* 2012;7(7):e41747.
180. Mil-Homens D, Rocha EP, Fialho AM. Genome-wide analysis of DNA repeats in *Burkholderia cenocepacia* J2315 identifies a novel adhesin-like gene unique to epidemic-associated strains of the ET-12 lineage. *Microbiology.* 2010;156(Pt 4):1084-96.
181. Mira NP, Madeira A, Moreira AS, Coutinho CP, Sa-Correia I. Genomic expression analysis reveals strategies of *Burkholderia cenocepacia* to adapt to cystic fibrosis patients' airways and antimicrobial therapy. *PLOS One.* 2011;6(12):e28831.
182. Moriarty TF, Mullan A, McGrath JW, Quinn JP, Elborn JS, Tunney MM. Effect of reduced pH on inorganic polyphosphate accumulation by *Burkholderia cepacia* complex isolates. *Lett Appl Microbiol.* 2006;42(6):617-23.
183. Moura JA, Cristina de Assis M, Ventura GC, Saliba AM, Gonzaga L, Jr., Si-Tahar M, et al. Differential interaction of bacterial species from the *Burkholderia cepacia* complex with human airway epithelial cells. *Microbes Infect.* 2008;10(1):52-9.
184. Muhammad I. LH, Miao L, Zhu B., Bin L., Xie G.L., Zhang G. Prevalence of potential pathogenicity and molecular characterizations of *Burkholderia cepacia*

- complex (BCC) among isolates from bamboo rhizosphere in China. *Res J Chem Environ.* 2011;15:998-1005.
185. Mullan A, Quinn JP, McGrath JW. Enhanced phosphate uptake and polyphosphate accumulation in *Burkholderia cepacia* grown under low pH conditions. *Microb Ecol.* 2002;44(1):69-77.
186. Mullen T, Callaghan M, McClean S. Invasion of *Burkholderia cepacia* complex isolates into lung epithelial cells involves glycolipid receptors. *Microb Pathog.* 2010;49(6):381-7.
187. Mullen T, Markey K, Murphy P, McClean S, Callaghan M. Role of lipase in *Burkholderia cepacia* complex (Bcc) invasion of lung epithelial cells. *Eur J Clin Microbiol Infect Dis.* 2007;26(12):869-77.
188. Nagano Y, Millar BC, Goldsmith CE, Elborn JS, Rendall J, Moore JE. Emergence of *Scedosporium apiospermum* in patients with cystic fibrosis. *Arch Dis Child.* 2007;92(7):607.
189. Nakata PA, He C. Oxalic acid biosynthesis is encoded by an operon in *Burkholderia glumae*. *FEMS Microbiol Lett.* 2010;304(2):177-82.
190. Nakazawa T, Yamada Y, Ishibashi M. Characterization of hemolysin in extracellular products of *Pseudomonas cepacia*. *J Clin Microbiol.* 1987;25(2):195-8.
191. Nierman WC, DeShazer D, Kim HS, Tettelin H, Nelson KE, Feldblyum T, et al. Structural flexibility in the *Burkholderia mallei* genome. *Proc Natl Acad Sci U S A.* 2004;101(39):14246-51.
192. Niyonsaba F, Iwabuchi K, Someya A, Hirata M, Matsuda H, Ogawa H, et al. A cathelicidin family of human antibacterial peptide LL-37 induces mast cell chemotaxis. *Immunology.* 2002;106(1):20-6.
193. O'Grady EP, Nguyen DT, Weisskopf L, Eberl L, Sokol PA. The *Burkholderia cenocepacia* LysR-type transcriptional regulator ShvR influences expression of quorum-sensing, protease, type II secretion, and *afc* genes. *J Bacteriol.* 2011;193(1):163-76.
194. O'Grady EP, Sokol PA. *Burkholderia cenocepacia* differential gene expression during host-pathogen interactions and adaptation to the host environment. *Front Cell Infect Microbiol.* 2011;1:15.
195. O'Grady EP, Viteri DF, Malott RJ, Sokol PA. Reciprocal regulation by the CepIR and CciIR quorum sensing systems in *Burkholderia cenocepacia*. *BMC Genomics.* 2009;10:441.
196. O'Neill LA, Golenbock D, Bowie AG. The history of Toll-like receptors - redefining innate immunity. *Nat Rev Immunol.* 2013;13(6):453-60.
197. O'Quinn AL, Wiegand EM, Jeddeloh JA. *Burkholderia pseudomallei* kills the nematode *Caenorhabditis elegans* using endotoxin-mediated paralysis. *Cell Microbiol.* 2001;3(6):381-93.
198. Ohtsubo Y, Genka H, Komatsu H, Nagata Y, Tsuda M. High temperature-induced transposition of insertion elements in *Burkholderia multivorans* ATCC 17616. *Appl Environ Microbiol.* 2005;71(4):1822-8.
199. Ortega X, Silipo A, Saldias MS, Bates CC, Molinaro A, Valvano MA. Biosynthesis and structure of the *Burkholderia cenocepacia* K56-2 lipopolysaccharide core oligosaccharide: truncation of the core oligosaccharide

- leads to increased binding and sensitivity to polymyxin B. *J Biol Chem.* 2009;284(32):21738-51.
200. Ostedgaard LS, Meyerholz DK, Chen JH, Pezzulo AA, Karp PH, Rokhlina T, et al. The DeltaF508 mutation causes CFTR misprocessing and cystic fibrosis-like disease in pigs. *Sci Transl Med.* 2011;3(74):74ra24.
201. Palmer KL, Aye LM, Whiteley M. Nutritional cues control *Pseudomonas aeruginosa* multicellular behavior in cystic fibrosis sputum. *J Bacteriol.* 2007;189(22):8079-87.
202. Parke JL, Gurian-Sherman D. Diversity of the *Burkholderia cepacia* complex and implications for risk assessment of biological control strains. *Annu Rev Phytopathol.* 2001;39:225-58.
203. Peix A, Mateos, P.F., Rodriguez-Barrueco, C., Martinez-Molina, E., Velasquez, E. Growth promotion of common bean (*Phaseolus vulgaris* L.) by a strain of *Burkholderia cepacia* under growth chamber conditions. *Soil Biol Biochem.* 2001;33:1927-35.
204. Pessi G, Haas D. Transcriptional control of the hydrogen cyanide biosynthetic genes *hcnABC* by the anaerobic regulator ANR and the quorum-sensing regulators LasR and RhlR in *Pseudomonas aeruginosa*. *J Bacteriol.* 2000;182(24):6940-9.
205. Pezzulo AA, Tang XX, Hoegger MJ, Alaiwa MH, Ramachandran S, Moninger TO, et al. Reduced airway surface pH impairs bacterial killing in the porcine cystic fibrosis lung. *Nature.* 2012;487(7405):109-13.
206. Porter LA, Goldberg JB. Influence of neutrophil defects on *Burkholderia cepacia* complex pathogenesis. *Front Cell Infect Microbiol.* 2011;1:9.
207. Prithiviraj B, Weir T, Bais HP, Schweizer HP, Vivanco JM. Plant models for animal pathogenesis. *Cell Microbiol.* 2005;7(3):315-24.
208. Pullar JM, Vissers MC, Winterbourn CC. Living with a killer: the effects of hypochlorous acid on mammalian cells. *IUBMB Life.* 2000;50(4-5):259-66.
209. Punj V, Sharma R, Zaborina O, Chakrabarty AM. Energy-generating enzymes of *Burkholderia cepacia* and their interactions with macrophages. *J Bacteriol.* 2003;185(10):3167-78.
210. Quan CS, Zheng W, Liu Q, Ohta Y, Fan SD. Isolation and characterization of a novel *Burkholderia cepacia* with strong antifungal activity against *Rhizoctonia solani*. *Appl Microbiol Biotechnol.* 2006;72(6):1276-84.
211. Rabin HR, Surette MG. The cystic fibrosis airway microbiome. *Current opinion in pulmonary medicine.* 2012;18(6):622-7.
212. Rahme LG, Stevens EJ, Wolfort SF, Shao J, Tompkins RG, Ausubel FM. Common virulence factors for bacterial pathogenicity in plants and animals. *Science.* 1995;268(5219):1899-902.
213. Rahme LG, Tan MW, Le L, Wong SM, Tompkins RG, Calderwood SB, et al. Use of model plant hosts to identify *Pseudomonas aeruginosa* virulence factors. *Proc Natl Acad Sci U S A.* 1997;94(24):13245-50.
214. Ramos CG, Grilo AM, da Costa PJ, Feliciano JR, Leitao JH. MtvR is a global regulatory sRNA in *Burkholderia cenocepacia*. *J Bacteriol.* 2013.

215. Ramos CG, Sousa SA, Grilo AM, Eberl L, Leitao JH. The *Burkholderia cenocepacia* K56-2 pleiotropic regulator Pbr, is required for stress resistance and virulence. *Microb Pathog.* 2010;48(5):168-77.
216. Rao S, Grigg J. New insights into pulmonary inflammation in cystic fibrosis. *Arch Dis Child.* 2006;91(9):786-8.
217. Rashid MH, Rumbaugh K, Passador L, Davies DG, Hamood AN, Iglewski BH, et al. Polyphosphate kinase is essential for biofilm development, quorum sensing, and virulence of *Pseudomonas aeruginosa*. *Proc Natl Acad Sci U S A.* 2000;97(17):9636-41.
218. Reid DW, Lam QT, Schneider H, Walters EH. Airway iron and iron-regulatory cytokines in cystic fibrosis. *The European respiratory journal.* 2004;24(2):286-91.
219. Riedel K, Hentzer M, Geisenberger O, Huber B, Steidle A, Wu H, et al. N-acylhomoserine-lactone-mediated communication between *Pseudomonas aeruginosa* and *Burkholderia cepacia* in mixed biofilms. *Microbiology.* 2001;147(Pt 12):3249-62.
220. Robinson CV, Elkins MR, Bialkowski KM, Thornton DJ, Kertesz MA. Desulfurization of mucin by *Pseudomonas aeruginosa*: influence of sulfate in the lungs of cystic fibrosis patients. *J Med Microbiol.* 2012;61(Pt 12):1644-53.
221. Rogers CS, Hao Y, Rokhlina T, Samuel M, Stoltz DA, Li Y, et al. Production of CFTR-null and CFTR-DeltaF508 heterozygous pigs by adeno-associated virus-mediated gene targeting and somatic cell nuclear transfer. *J Clin Invest.* 2008;118(4):1571-7.
222. Ronald PC, Beutler B. Plant and animal sensors of conserved microbial signatures. *Science.* 2010;330(6007):1061-4.
223. Rosales-Reyes R, Aubert DF, Tolman JS, Amer AO, Valvano MA. *Burkholderia cenocepacia* type VI secretion system mediates escape of type II secreted proteins into the cytoplasm of infected macrophages. *PLOS One.* 2012;7(7):e41726.
224. Rosales-Reyes R, Saldias MS, Aubert DF, El-Halfawy OM, Valvano MA. The *suhB* gene of *Burkholderia cenocepacia* is required for protein secretion, biofilm formation, motility and polymyxin B resistance. *Microbiology.* 2012;158(Pt 9):2315-24.
225. Rosales-Reyes R, Skeldon AM, Aubert DF, Valvano MA. The Type VI secretion system of *Burkholderia cenocepacia* affects multiple Rho family GTPases disrupting the actin cytoskeleton and the assembly of NADPH oxidase complex in macrophages. *Cell Microbiol.* 2012;14(2):255-73.
226. Rubin BK. Mucus structure and properties in cystic fibrosis. *Paediatr Respir Rev.* 2007;8(1):4-7.
227. Rubins JB. Alveolar macrophages: wielding the double-edged sword of inflammation. *Am J Respir Crit Care Med.* 2003;167(2):103-4.
228. Ryall B, Davies JC, Wilson R, Shoemark A, Williams HD. *Pseudomonas aeruginosa*, cyanide accumulation and lung function in CF and non-CF bronchiectasis patients. *The European respiratory journal.* 2008;32(3):740-7.

229. Ryall B, Lee X, Zlosnik JE, Hoshino S, Williams HD. Bacteria of the *Burkholderia cepacia* complex are cyanogenic under biofilm and colonial growth conditions. *BMC Microbiol.* 2008;8:108.
230. Ryley HC. *Burkholderia cepacia* complex infection in cystic fibrosis patients: mechanisms of pathogenesis. *Med Microbiol.* 2004;15(3):93-101.
231. Sajjan SU, Forstner JF. Identification of the mucin-binding adhesin of *Pseudomonas cepacia* isolated from patients with cystic fibrosis. *Infect Immun.* 1992;60(4):1434-40.
232. Sajjan U, Corey M, Humar A, Tullis E, Cutz E, Ackerley C, et al. Immunolocalisation of *Burkholderia cepacia* in the lungs of cystic fibrosis patients. *J Med Microbiol.* 2001;50(6):535-46.
233. Sajjan U, Keshavjee S, Forstner J. Responses of well-differentiated airway epithelial cell cultures from healthy donors and patients with cystic fibrosis to *Burkholderia cenocepacia* infection. *Infect Immun.* 2004;72(7):4188-99.
234. Sajjan U, Thanassoulis G, Cherapanov V, Lu A, Sjolín C, Steer B, et al. Enhanced susceptibility to pulmonary infection with *Burkholderia cepacia* in *Cftr(-/-)* mice. *Infect Immun.* 2001;69(8):5138-50.
235. Sajjan US, Forstner JF. Role of a 22-kilodalton pilin protein in binding of *Pseudomonas cepacia* to buccal epithelial cells. *Infect Immun.* 1993;61(8):3157-63.
236. Sajjan US, Hershenson MB, Forstner JF, LiPuma JJ. *Burkholderia cenocepacia* ET12 strain activates TNFR1 signalling in cystic fibrosis airway epithelial cells. *Cell Microbiol.* 2008;10(1):188-201.
237. Sanderson K, Wescombe L, Kirov SM, Champion A, Reid DW. Bacterial cyanogenesis occurs in the cystic fibrosis lung. *The European respiratory journal.* 2008;32(2):329-33.
238. Schikora A, Virlogeux-Payant I, Bueso E, Garcia AV, Nilau T, Charrier A, et al. Conservation of *Salmonella* infection mechanisms in plants and animals. *PLOS One.* 2011;6(9):e24112.
239. Schmerk CL, Bernards MA, Valvano MA. Hopanoid production is required for low-pH tolerance, antimicrobial resistance, and motility in *Burkholderia cenocepacia*. *J Bacteriol.* 2011;193(23):6712-23.
240. Schmerk CL, Valvano MA. *Burkholderia multivorans* survival and trafficking within macrophages. *J Med Microbiol.* 2013;62(Pt 2):173-84.
241. Schmidt S, Blom JF, Pernthaler J, Berg G, Baldwin A, Mahenthiralingam E, et al. Production of the antifungal compound pyrrolnitrin is quorum sensing-regulated in members of the *Burkholderia cepacia* complex. *Environ Microbiol.* 2009;11(6):1422-37.
242. Schoustra SE, Dench J, Dali R, Aaron SD, Kassen R. Antagonistic interactions peak at intermediate genetic distance in clinical and laboratory strains of *Pseudomonas aeruginosa*. *BMC Microbiol.* 2012;12:40.
243. Schwab U, Leigh M, Ribeiro C, Yankaskas J, Burns K, Gilligan P, et al. Patterns of epithelial cell invasion by different species of the *Burkholderia cepacia* complex in well-differentiated human airway epithelia. *Infect Immun.* 2002;70(8):4547-55.

244. Schwab UE, Ribeiro CM, Neubauer H, Boucher RC. Role of actin filament network in *Burkholderia multivorans* invasion in well-differentiated human airway epithelia. *Infect Immun*. 2003;71(11):6607-9.
245. Seed KD, Dennis JJ. Isolation and characterization of bacteriophages of the *Burkholderia cepacia* complex. *FEMS Microbiol Lett*. 2005;251(2):273-80.
246. Seed KD, Dennis JJ. Development of *Galleria mellonella* as an alternative infection model for the *Burkholderia cepacia* complex. *Infect Immun*. 2008;76(3):1267-75.
247. Seed KD, Dennis JJ. Experimental bacteriophage therapy increases survival of *Galleria mellonella* larvae infected with clinically relevant strains of the *Burkholderia cepacia* complex. *Antimicrob Agents Chemother*. 2009;53(5):2205-8.
248. Sharma S, Sharma S., Singh, R.K., Vaishampayan, A. . Colonization behavior of bacterium *Burkholderia cepacia* inside the *Oryza sativa* roots visualized using green fluorescent protein reporter. *World J Microbiol Biotechnol* 2008;24:1169-75.
249. Shaw D, Poxton IR, Govan JR. Biological activity of *Burkholderia (Pseudomonas) cepacia* lipopolysaccharide. *FEMS Immunol Med Microbiol*. 1995;11(2):99-106.
250. Shoseyov D, Brownlee KG, Conway SP, Kerem E. *Aspergillus* bronchitis in cystic fibrosis. *Chest*. 2006;130(1):222-6.
251. Sibley CD, Parkins MD, Rabin HR, Duan K, Norgaard JC, Surette MG. A polymicrobial perspective of pulmonary infections exposes an enigmatic pathogen in cystic fibrosis patients. *Proc Natl Acad Sci U S A*. 2008;105(39):15070-5.
252. Sibley CD, Sibley KA, Leong TA, Grinwis ME, Parkins MD, Rabin HR, et al. The *Streptococcus milleri* population of a cystic fibrosis clinic reveals patient specificity and intraspecies diversity. *J Clin Microbiol*. 2010;48(7):2592-4.
253. Silva IN, Ferreira AS, Becker JD, Zlosnik JE, Speert DP, He J, et al. Mucoid morphotype variation of *Burkholderia multivorans* during chronic cystic fibrosis lung infection is correlated with changes in metabolism, motility, biofilm formation and virulence. *Microbiology*. 2011;157(Pt 11):3124-37.
254. Simmonds NJ, Gyi KM. Cystic fibrosis, a *Burkholderia cenocepacia* chest wall abscess and rapid clinical deterioration. *J R Soc Med*. 2008;101 Suppl 1:S46-50.
255. Singh PK, Jia HP, Wiles K, Hesselberth J, Liu L, Conway BA, et al. Production of beta-defensins by human airway epithelia. *Proc Natl Acad Sci U S A*. 1998;95(25):14961-6.
256. Smalley JW, Charalabous P, Birss AJ, Hart CA. Detection of heme-binding proteins in epidemic strains of *Burkholderia cepacia*. *Clin Diagn Lab Immunol*. 2001;8(3):509-14.
257. Smith AW, Green J, Eden CE, Watson ML. Nitric oxide-induced potentiation of the killing of *Burkholderia cepacia* by reactive oxygen species: implications for cystic fibrosis. *J Med Microbiol*. 1999;48(5):419-23.
258. Smith DL, Smith EG, Pitt TL, Stableforth DE. Regional microbiology of the cystic fibrosis lung: a post-mortem study in adults. *J Infect*. 1998;37(1):41-3.

259. Somvanshi VS, Viswanathan P, Jacobs JL, Mulks MH, Sundin GW, Ciche TA. The type 2 secretion pseudopilin, *gspJ*, is required for multihost pathogenicity of *Burkholderia cenocepacia* AU1054. *Infect Immun*. 2010;78(10):4110-21.
260. Song H, Hwang J, Yi H, Ulrich RL, Yu Y, Nierman WC, et al. The early stage of bacterial genome-reductive evolution in the host. *PLoS Pathog*. 2010;6(5):e1000922.
261. Sousa SA, Ramos CG, Almeida F, Meirinhos-Soares L, Wopperer J, Schwager S, et al. *Burkholderia cenocepacia* J2315 acyl carrier protein: a potential target for antimicrobials' development? *Microb Pathog*. 2008;45(5-6):331-6.
262. Sousa SA, Ramos CG, Moreira LM, Leitao JH. The *hfq* gene is required for stress resistance and full virulence of *Burkholderia cepacia* to the nematode *Caenorhabditis elegans*. *Microbiology*. 2010;156(Pt 3):896-908.
263. Souza CE, Maitra D, Saed GM, Diamond MP, Moura AA, Pennathur S, et al. Hypochlorous acid-induced heme degradation from lactoperoxidase as a novel mechanism of free iron release and tissue injury in inflammatory diseases. *PLOS One*. 2011;6(11):e27641.
264. Springman AC, Jacobs JL, Somvanshi VS, Sundin GW, Mulks MH, Whittam TS, et al. Genetic diversity and multihost pathogenicity of clinical and environmental strains of *Burkholderia cenocepacia*. *Appl Environ Microbiol*. 2009;75(16):5250-60.
265. Sriramulu DD, Lunsdorf H, Lam JS, Romling U. Microcolony formation: a novel biofilm model of *Pseudomonas aeruginosa* for the cystic fibrosis lung. *J Med Microbiol*. 2005;54(Pt 7):667-76.
266. Starke JR, Edwards MS, Langston C, Baker CJ. A mouse model of chronic pulmonary infection with *Pseudomonas aeruginosa* and *Pseudomonas cepacia*. *Pediatr Res*. 1987;22(6):698-702.
267. Steinert M, Birkness K, White E, Fields B, Quinn F. Mycobacterium avium bacilli grow saprozoically in coculture with Acanthamoeba polyphaga and survive within cyst walls. *Appl Environ Microbiol*. 1998;64(6):2256-61.
268. Stites SW, Plautz MW, Bailey K, O'Brien-Ladner AR, Wesselius LJ. Increased concentrations of iron and isoferritins in the lower respiratory tract of patients with stable cystic fibrosis. *Am J Respir Crit Care Med*. 1999;160(3):796-801.
269. Stockbauer KE, Foreman-Wykert AK, Miller JF. *Bordetella* type III secretion induces caspase 1-independent necrosis. *Cell Microbiol*. 2003;5(2):123-32.
270. Stotz H.U. W, F., Wang, K. Innate immunity in plants: the role of antimicrobial peptides. In: Hiemstra PS, editor. *Antimicrobial Peptides and Innate Immunity*. Progress in Inflammation Research. Basel, Switzerland: Springer Basel; 2013. p. 29-51.
271. Stover GB, Drake DR, Montie TC. Virulence of different *Pseudomonas species* in a burned mouse model: tissue colonization by *Pseudomonas cepacia*. *Infect Immun*. 1983;41(3):1099-104.

272. Subramoni S, Agnoli K, Eberl L, Lewenza S, Sokol PA. Role of *Burkholderia cenocepacia* *afcE* and *afcF* genes in determining lipid-metabolism-associated phenotypes. *Microbiology*. 2013;159(Pt 3):603-14.
273. Suppiger A, Schmid, N., Aguilar, C., Pessi, G., and Eberl, L. Two quorum sensing systems control biofilm formation and virulence in members of the *Burkholderia cepacia* complex. *Virulence*. 2013;4(5):1-10.
274. Tan MW, Rahme LG, Sternberg JA, Tompkins RG, Ausubel FM. *Pseudomonas aeruginosa* killing of *Caenorhabditis elegans* used to identify *P. aeruginosa* virulence factors. *Proc Natl Acad Sci U S A*. 1999;96(5):2408-13.
275. Tawfik KA, Jeffs P, Bray B, Dubay G, Falkinham JO, Mesbah M, et al. Burkholdines 1097 and 1229, potent antifungal peptides from *Burkholderia ambifaria* 2.2N. *Org Lett*. 2010;12(4):664-6.
276. Thomson EL, Dennis JJ. A *Burkholderia cepacia* complex non-ribosomal peptide-synthesized toxin is hemolytic and required for full virulence. *Virulence*. 2012;3(3):286-98.
277. Thorn G. The fungi in soil. In: Van Elsas JD, Trevors, J.T., Wellington, E.M.H. , editor. *Modern Soil Microbiology*. New York, NY: Marcel Dekker, Inc.; 1997. p. 708.
278. Thornton DJ, Rousseau K, McGuckin MA. Structure and function of the polymeric mucins in airways mucus. *Annu Rev Physiol*. 2008;70:459-86.
279. Thwaite JE, Humphrey S, Fox MA, Savage VL, Laws TR, Ulaeto DO, et al. The cationic peptide magainin II is antimicrobial for *Burkholderia cepacia*-complex strains. *J Med Microbiol*. 2009;58(Pt 7):923-9.
280. Tirouvanziam R, Conrad CK, Bottiglieri T, Herzenberg LA, Moss RB, Herzenberg LA. High-dose oral N-acetylcysteine, a glutathione prodrug, modulates inflammation in cystic fibrosis. *Proc Natl Acad Sci U S A*. 2006;103(12):4628-33.
281. Tomich M, Griffith A, Herfst CA, Burns JL, Mohr CD. Attenuated virulence of a *Burkholderia cepacia* type III secretion mutant in a murine model of infection. *Infect Immun*. 2003;71(3):1405-15.
282. Tomich M, Herfst CA, Golden JW, Mohr CD. Role of flagella in host cell invasion by *Burkholderia cepacia*. *Infect Immun*. 2002;70(4):1799-806.
283. Tomich M, Mohr CD. Transcriptional and posttranscriptional control of cable pilus gene expression in *Burkholderia cenocepacia*. *J Bacteriol*. 2004;186(4):1009-20.
284. Turi JL, Yang F, Garrick MD, Piantadosi CA, Ghio AJ. The iron cycle and oxidative stress in the lung. *Free Radic Biol Med*. 2004;36(7):850-7.
285. Twomey KB, O'Connell OJ, McCarthy Y, Dow JM, O'Toole GA, Plant BJ, et al. Bacterial *cis*-2-unsaturated fatty acids found in the cystic fibrosis airway modulate virulence and persistence of *Pseudomonas aeruginosa*. *ISME J*. 2012;6(5):939-50.
286. Udine C, Brackman G, Bazzini S, Buroni S, Van Acker H, Pasca MR, et al. Phenotypic and genotypic characterisation of *Burkholderia cenocepacia* J2315 mutants affected in homoserine lactone and diffusible signal factor-based quorum sensing systems suggests interplay between both types of systems. *PLOS One*. 2013;8(1):e55112.

287. Uehlinger S, Schwager S, Bernier SP, Riedel K, Nguyen DT, Sokol PA, et al. Identification of specific and universal virulence factors in *Burkholderia cenocepacia* strains by using multiple infection hosts. *Infect Immun*. 2009;77(9):4102-10.
288. Urban TA, Goldberg JB, Forstner JF, Sajjan US. Cable pili and the 22-kilodalton adhesin are required for *Burkholderia cenocepacia* binding to and transmigration across the squamous epithelium. *Infect Immun*. 2005;73(9):5426-37.
289. Valvano MA, Keith KE, Cardona ST. Survival and persistence of opportunistic *Burkholderia* species in host cells. *Curr Opin Microbiol*. 2005;8(1):99-105.
290. Van Acker H, Sass A, Bazzini S, De Roy K, Udine C, Messiaen T, et al. Biofilm-grown *Burkholderia cepacia* complex cells survive antibiotic treatment by avoiding production of reactive oxygen species. *PLOS One*. 2013;8(3):e58943.
291. Vandamme P, Dawyndt P. Classification and identification of the *Burkholderia cepacia* complex: Past, present and future. *Syst Appl Microbiol*. 2011;34(2):87-95.
292. Vandamme P, Holmes B, Vancanneyt M, Coenye T, Hoste B, Coopman R, et al. Occurrence of multiple genomovars of *Burkholderia cepacia* in cystic fibrosis patients and proposal of *Burkholderia multivorans* sp. nov. *Int J Syst Bacteriol*. 1997;47(4):1188-200.
293. Vanlaere E, Baldwin A, Gevers D, Henry D, De Brandt E, LiPuma JJ, et al. Taxon K, a complex within the *Burkholderia cepacia* complex, comprises at least two novel species, *Burkholderia contaminans* sp. nov. and *Burkholderia lata* sp. nov. *Int J Syst Evol Microbiol*. 2009;59(Pt 1):102-11.
294. Vasil ML, Krieg DP, Kuhns JS, Ogle JW, Shortridge VD, Ostroff RM, et al. Molecular analysis of hemolytic and phospholipase C activities of *Pseudomonas cepacia*. *Infect Immun*. 1990;58(12):4020-9.
295. Venturi V, Bertani I, Kerenyi A, Netotea S, Pongor S. Co-swarming and local collapse: quorum sensing conveys resilience to bacterial communities by localizing cheater mutants in *Pseudomonas aeruginosa*. *PLOS One*. 2010;5(4):e9998.
296. Vergunst AC, Meijer AH, Renshaw SA, O'Callaghan D. *Burkholderia cenocepacia* creates an intramacrophage replication niche in zebrafish embryos, followed by bacterial dissemination and establishment of systemic infection. *Infect Immun*. 2010;78(4):1495-508.
297. Vergunst AC, Meijer AH, Renshaw SA, O'Callaghan D. *Burkholderia cenocepacia* creates an intramacrophage replication niche in zebrafish embryos, followed by bacterial dissemination and establishment of systemic infection. *Infect Immun*. 2010;78(4):1495-508.
298. Vial L, Groleau MC, Dekimpe V, Deziel E. *Burkholderia* diversity and versatility: an inventory of the extracellular products. *J Microbiol Biotechnol*. 2007;17(9):1407-29.
299. Vilella VR, Esposito S, Bruscia EM, Maiuri MC, Raia V, Kroemer G, et al. Targeting the intracellular environment in cystic fibrosis: Restoring autophagy as a novel strategy to circumvent the CFTR defect. *Front Pharmacol*. 2013;4:1.

300. Vinion-Dubiel AD, Goldberg JB. Lipopolysaccharide of *Burkholderia cepacia* complex. J Endotoxin Res. 2003;9(4):201-13.
301. Visser MB, Majumdar S, Hani E, Sokol PA. Importance of the ornibactin and pyochelin siderophore transport systems in *Burkholderia cenocepacia* lung infections. Infect Immun. 2004;72(5):2850-7.
302. Waite RD, Curtis MA. *Pseudomonas aeruginosa* PAO1 pyocin production affects population dynamics within mixed-culture biofilms. J Bacteriol. 2009;191(4):1349-54.
303. Walsh CT. Antibiotics: Actions, Origins, Resistance. ASM Press; 2003. p. 335.
304. Wan H, Winton HL, Soeller C, Stewart GA, Thompson PJ, Gruenert DC, et al. Tight junction properties of the immortalized human bronchial epithelial cell lines Calu-3 and 16HBE14o. The European respiratory journal. 2000;15(6):1058-68.
305. Wang JH, Quan CS, Qi XH, Li X, Fan SD. Determination of diketopiperazines of *Burkholderia cepacia* CF-66 by gas chromatography-mass spectrometry. Anal Bioanal Chem. 2010;396(5):1773-9.
306. Watt AP, Courtney J, Moore J, Ennis M, Elborn JS. Neutrophil cell death, activation and bacterial infection in cystic fibrosis. Thorax. 2005;60(8):659-64.
307. Whipps JM. Developments in the biological control of soil-borne plant pathogens. In: Callow JA, editor. Advances in Botanical Research--Incorporating Advances in Plant Pathology. 40. Waltham, MA: Academic Press-Elsevier; 1997. p. 1-134.
308. Whitby PW, Vanwagoner TM, Springer JM, Morton DJ, Seale TW, Stull TL. *Burkholderia cenocepacia* utilizes ferritin as an iron source. J Med Microbiol. 2006;55(Pt 6):661-8.
309. Willner D, Haynes MR, Furlan M, Hanson N, Kirby B, Lim YW, et al. Case studies of the spatial heterogeneity of DNA viruses in the cystic fibrosis lung. Am J Respir Cell Mol Biol. 2012;46(2):127-31.
310. Willner D, Haynes MR, Furlan M, Schmieder R, Lim YW, Rainey PB, et al. Spatial distribution of microbial communities in the cystic fibrosis lung. ISME J. 2012;6(2):471-4.
311. Worlitzsch D, Tarran R, Ulrich M, Schwab U, Cekici A, Meyer KC, et al. Effects of reduced mucus oxygen concentration in airway *Pseudomonas* infections of cystic fibrosis patients. J Clin Invest. 2002;109(3):317-25.
312. Wright C, Herbert G, Pilkington R, Callaghan M, McClean S. Real-time PCR method for the quantification of *Burkholderia cepacia* complex attached to lung epithelial cells and inhibition of that attachment. Lett Appl Microbiol. 2010;50(5):500-6.
313. Wright C, Pilkington R, Callaghan M, McClean S. Activation of MMP-9 by human lung epithelial cells in response to the cystic fibrosis-associated pathogen *Burkholderia cenocepacia* reduced wound healing *in vitro*. Am J Physiol Lung Cell Mol Physiol. 2011;301(4):L575-86.
314. Yang D, Chen Q, Chertov O, Oppenheim JJ. Human neutrophil defensins selectively chemoattract naive T and immature dendritic cells. J Leukoc Biol. 2000;68(1):9-14.

315. Yoder-Himes DR, Konstantinidis KT, Tiedje JM. Identification of potential therapeutic targets for *Burkholderia cenocepacia* by comparative transcriptomics. PLOS One. 2010;5(1):e8724.
316. Yohalem D.S. LJW. Distribution of *Burkholderia cepacia* phenotypes by niche, method of isolation and pathogenicity to onion. . Ann Appl Biol. 1997. ;130:467-79.
317. Yoon SS, Hennigan RF, Hilliard GM, Ochsner UA, Parvatiyar K, Kamani MC, et al. *Pseudomonas aeruginosa* anaerobic respiration in biofilms: relationships to cystic fibrosis pathogenesis. Dev Cell. 2002;3(4):593-603.
318. Zemanick ET, Sagel SD, Harris JK. The airway microbiome in cystic fibrosis and implications for treatment. Current opinion in pediatrics. 2011;23(3):319-24.
319. Zgair AK. Flagellin administration protects respiratory tract from *Burkholderia cepacia* infection. J Microbiol Biotechnol. 2012;22(7):907-16.
320. Zhu Y, Chidekel A, Shaffer TH. Cultured human airway epithelial cells (Calu-3): a model of human respiratory function, structure, and inflammatory responses. Crit Care Res Pract. 2010;2010.

# Chapter 1 – *Lemna minor* (Common duckweed) as model host for the *Burkholderia cepacia* complex

---

A version of this chapter has been submitted: Thomson and Dennis, 2013. PLoS One.

## **Introduction**

In the General Introduction, a number of infection models and cell lines were outlined that have been adopted for use in Bcc studies. Differences exist between the susceptibility to infection of wild type and *CFTR*-deficient cell lines as well as their responses to invading bacteria, but there are also higher-level effects of the *CFTR* mutations in humans that so far only appear to be modeled accurately by the *CFTR* mutant pig. These effects include a vast migration of neutrophils to the lung and their overproduction of elastase and other serine proteases that give rise to additional complications, such as the release of iron resources into the lung through disrupted epithelium (5, 12). Since Bcc virulence investigations are generally limited to the lower infection models, which do not accurately portray the CF lung environment, an alternative strategy is to embrace the multihost pathogenicity of the Bcc and discover more about the possible crossover among the various hosts. An infection model that could be manipulated to model certain physiologically relevant characteristics of the CF lung, such as low oxygen or a temperature of 37°C (explored further in Chapter 4) would provide additional advantages.

## **Common duckweed as a model host for the *Burkholderia cepacia* complex**

Monocotyledon flowering plants include cereal crops and onions, and are highly divergent from dicotyledon plants, which include the previously established Bcc infection models, lettuce and alfalfa (4, 16). The onion (37) and

lettuce models require wounding of tissue, while alfalfa infections have been carried out with or without wounding.

Common duckweed (*Lemna minor*) is one of the smallest known flowering plants and can be found growing on the surfaces of freshwater bodies throughout the world. These monocotyledon plants reproduce both sexually *via* flower fertilization and asexually by budding, and the latter strategy provides a means by which to generate a large clonal population from a single plant. By eliminating the genetic variability common to current plant and animal infection models, the duckweed model allows the infection process to be studied with greater reproducibility. Axenic cultures of duckweed are easily obtained, thereby permitting the examination of an isolated, bipartite infection process. So far, several human pathogens have been studied using this model system (38). For example, chromosomal disruption of the *lasIR* and *rhlIR* quorum sensing in *Pseudomonas aeruginosa* eliminated bacterial inhibition of the plants, indicating that the tissue-degrading proteases and other virulence factors known to be governed by these systems may have malignant effects on the plants as well. In the same study, the clinically relevant *Staphylococcus aureus* RN4220 strain was compared with an attenuated strain (ATCC 25923), and RN4220 was found to exhibit extremely high virulence against the plants, while ATCC 25923 had no observable effect. Enterohemorrhagic *Escherichia coli* 0157:H7 also displayed enhanced virulence relative to attenuated *E. coli* strain DH5 $\alpha$  (38).

## **Advantages and disadvantages of using a plant model host**

By infecting hosts derived from a single organism, more reproducible results are obtained and the infection process is more clearly isolated. Furthermore, the adaptability of the model is evidenced by duckweed's tolerance to a wide range of incubation conditions, described in the Results section of this chapter and in Chapter 4. The financial efficacy and speed with which experiments can be carried out using duckweed also open the possibility for large-scale virulence factor screening, as outlined in Chapter 3; again, the clonality of the population from which plants are drawn provides a highly reproducible backdrop for such a screening. Finally, a more broadly scientific advantage of using such a model is to delineate any possible conserved mechanisms of pathogenesis employed by Bcc bacteria for the vastly different circumstances of plant and animal infection.

The disadvantages of using a plant to model human pathogenesis primarily centre on cell-cell interaction and immunology. While several pathogens have long been known to use conserved pathways to infect both plant and animal hosts, including *P. aeruginosa*, *Enterococcus faecalis*, and *S. aureus* (6), there are reasonable doubts about using infection models lacking both roaming defender cells and an adaptive immune system for human pathogens. Nonetheless, in these early stages of understanding Bcc pathogenesis, it is appropriate to gather data on the general virulence pathways of these bacteria using rapid, high-throughput tools, particularly known environmental hosts of these bacteria such as monocotyledon plants, which include onion, cereal crops and duckweed.

Furthermore, the adaptive immune system has not yet been shown to play an important role in the subversion of CF patients by bacterial airway pathogens.

## **Objectives**

In this study, I investigated the potential of duckweed as a Bcc infection model by several different approaches. First, a 50% lethal dose (LD<sub>50</sub>) -based virulence experiment was developed for plant infection and used to investigate the relationship between LD<sub>50</sub> values obtained with a panel of Bcc strains in the *L. minor* model versus the established *G. mellonella* model. In doing so, the multihost versatility of the Bcc was further demonstrated, with certain Bcc clades highlighted for their ability to cause disease in unrelated hosts. A possible mechanism of plant killing was demonstrated using lyophilized supernatants of *Burkholderia cenocepacia* strain K56-2 and a mutant (50D9) obtained in a virulence screen described in Chapter 3 that is deficient in the production of a known phytotoxin. Bacteriophage rescue of *B. cenocepacia*-infected plants was then explored, and this therapeutic approach was demonstrated as a possible means by which to investigate infection dynamics such as tissue invasion. These results prompted the adaptation of the duckweed infection model to other human bacterial pathogens, including a panel of enteropathogenic *E. coli* (EPEC) mutants.

## Materials and Methods

### Strains, plasmids and culture conditions

Bacterial strains used in this study are listed in Table 1. All strains were grown in 2 mL ½ Luria-Bertani (½ LB) broth in 15 mL conical tubes (VWR International, Radnor, PA) for 18 hours shaking at 225 rpm and 30°C unless otherwise noted.

**Table 1. Bacterial strains used in this study.**

Species	Strain	Source or relevant genotype or phenotype <sup>a</sup>	LD <sub>50</sub> in <i>L. minor</i> , cfu/ml +/- SE <sup>bc</sup>	LD <sub>50</sub> in <i>G. mellonella</i> , cfu (ref.)
<i>Burkholderia cepacia</i>	LMG 18821	CF, Australia	1.9x10 <sup>2</sup> +/- 1.2x10 <sup>2</sup>	3.0x10 <sup>1</sup> (29)
	LMG 2161	Soil, Trinidad	2.5x10 <sup>0</sup> +/- 5.3x10 <sup>-1</sup>	1.0x10 <sup>0</sup> (29)
<i>B. multivorans</i>	C5393	CF, Canada	>1.0x10 <sup>9</sup>	>3.0x10 <sup>6</sup> (29)
	C3430	CF, Canada	>1.0x10 <sup>9</sup>	>3.0x10 <sup>6</sup> (29)
	C5274	CF, Canada	3.1x10 <sup>9</sup> +/- 2.4x10 <sup>9</sup>	1.0x10 <sup>6</sup> (29)
	C5568	CF, Canada	1.1x10 <sup>8</sup> +/- 8.8x10 <sup>6</sup>	>3.0x10 <sup>6</sup> (29)
	PC715j	CF, Canada	5.0x10 <sup>0</sup> +/- 5.0x10 <sup>-1</sup>	4.0x10 <sup>3</sup> (29)
<i>B. cenocepacia</i>	J2315	CF-e, United Kingdom	1.6x10 <sup>6</sup> +/- 7x10 <sup>5</sup>	1.0x10 <sup>5</sup> (29)
	K56-2	CF-e, Canada	1.2x10 <sup>1</sup> +/- 7.0x10 <sup>0</sup>	9.0x10 <sup>2</sup> (29)
	C1257	CF, Canada	8.8x10 <sup>0</sup> +/-	4.0x10 <sup>4</sup> (29)

			5.7x10 <sup>0</sup>	
	C4455	CF, Canada	1.01x10 <sup>5</sup> +/- 3.9x10 <sup>4</sup>	1.0x10 <sup>5</sup> (29)
	C5424	CF, Canada	5.3x10 <sup>3</sup> +/- 4.5x10 <sup>3</sup>	2.0x10 <sup>5</sup> (29)
	C6433	CF, Canada	2.8x10 <sup>4</sup> +/- 2.2x10 <sup>4</sup>	3.0x10 <sup>4</sup> (29)
	Cep511	CF, Australia	7.6x10 <sup>0</sup> +/- 3.4x10 <sup>0</sup>	8.0x10 <sup>8</sup> (29)
	50D9	Plasposon screening (Chapter 3)	>2.6x10 <sup>8</sup>	n.d.
<i>B. stabilis</i>	LMG 14294	CF, Belgium	>1.0x10 <sup>9</sup>	2.0x10 <sup>6</sup> (29)
	LMG 18870	CF, Canada	>1.0x10 <sup>9</sup>	>2.0x10 <sup>6</sup> (29)
<i>B. vietnamiensis</i>	DBO1	Soil, United States	3.7x10 <sup>2</sup> +/- 2.5x10 <sup>2</sup>	2.0x10 <sup>5</sup> (29)
	PC259	CF, United States	>1.0x10 <sup>9</sup>	>3.0x10 <sup>6</sup> (29)
<i>B. dolosa</i>	AU0645	CF, United States	>1.0x10 <sup>10</sup>	>4.0x10 <sup>6</sup> (29)
	STM1441	Rhizosphere, Senegal	4.8x10 <sup>7</sup> +/- 1.3x10 <sup>7</sup>	4.0x10 <sup>4</sup> (29)
<i>B. ambifaria</i>	Cep0996	CF, Australia	5.8x10 <sup>8</sup> +/- 4.4x10 <sup>8</sup>	8.0x10 <sup>5</sup> (29)
	AMMD	Rhizosphere, United States	2.5x10 <sup>0</sup> +/- 4.0x10 <sup>-1</sup>	n.d.
<i>B. anthina</i>	J2552	Rhizosphere, United Kingdom	4.5x10 <sup>8</sup> +/- 5.2x10 <sup>7</sup>	3.0x10 <sup>5</sup> (29)
<i>B. pyrrocinia</i>	ATCC 15958	Soil, Japan	2.5x10 <sup>0</sup> +/-  7.9x10 <sup>-1</sup>	3.0x10 <sup>2</sup> (29)
<i>Acinetobacter baumannii</i>	AYE	Clinical, France	>1.0x10 <sup>9</sup>	2.01x10 <sup>5</sup> (2)
	ACICU	Clinical, Italy	>1.0x10 <sup>9</sup>	5.58x10 <sup>5</sup> (2)
	ATCC 17978	Clinical, France	>1.0x10 <sup>9</sup>	2.42x10 <sup>5</sup> (2)
	SDF	Human body louse	>1.0x10 <sup>9</sup>	4.84x10 <sup>7</sup> (2)
<i>Escherichia coli</i>	E2348/69	Parent strain	9.0x10 <sup>1</sup> +/- 3.8x10 <sup>1</sup>	2.57x10 <sup>3</sup> (21)
	JPN15	E2348/69 cured of EAF plasmid	7.9x10 <sup>4</sup> +/- 3.0x10 <sup>4</sup>	1.2x10 <sup>8</sup> (21)
	<i>ΔescN</i>	E2348/69 deficient in	6.9x10 <sup>2</sup> +/-	1.82x10 <sup>5</sup> (21)

		type III secretion	4.7x10 <sup>2</sup>	
	<i>ΔbfpA</i>	E2348/69 deficient in bundle forming pilus	6.0x10 <sup>2</sup> +/- 5.9x10 <sup>2</sup>	4.9x10 <sup>3</sup> (21)
	<i>ΔcpxR</i>	E2348/69 deficient in Cpx pathway activation	1.0x10 <sup>2</sup> +/- 9.7x10 <sup>1</sup>	4.17x10 <sup>4</sup> (21)
	<i>cpxA24*</i>	E2348/69 with constitutive ON Cpx pathway	6.3x10 <sup>5</sup> +/- 4.9x10 <sup>5</sup>	2.5x10 <sup>10</sup> (21)
	<i>perA::Km<sup>R</sup></i>	E2348/69 deficient in type III secretion and bundle forming pilus	<1.0x10 <sup>3</sup>	n.d.
<i>Campylobacter jejuni</i>	11168	Feces of diarrheic patient	>1.0x10 <sup>9</sup>	n.d. (9)
	81-176	Feces of diarrheic patient	>1.0x10 <sup>9</sup>	n.d. (9)
<i>Ralstonia solanacearum</i>	GMI1000	Tomato plant	>1.0x10 <sup>9</sup>	n.d.

<sup>a</sup>CF, cystic fibrosis; CF-e, strain that has spread epidemically.

<sup>b</sup>S.E., standard error of the mean, included where applicable

<sup>c</sup> LD<sub>50</sub> value of 2.5 cfu/ml reflects the lowest possible LD<sub>50</sub> of 1 cfu/well starting inoculum.

## Duckweed growth and sterilization

Duckweed plants were obtained from a water barrel in the Biological Sciences greenhouse at the University of Alberta. To sterilize the plant surfaces for axenic growth, plants were submerged in 10% v/v bleach for ten seconds, transferred into 70% v/v ethanol for 10 seconds, then transferred into sterile Shenck-Hildebrant medium supplemented with 1% w/v sucrose (SHS) to recover. Plants were grown statically in 24 well plates at 30°C, as previously described (Zhang et al., 2010). Maintaining the plants under a light/dark cycle of 18/6 hours promotes asexual reproduction by division, and under these conditions plants undergo three to four generations per week.

## **Duckweed infection**

Each well of a 96-well plate was filled with 180  $\mu$ l of SHS and one duckweed plant comprising 2-3 fronds (i.e., at an intermediate stage of its growth). One millilitre of an overnight bacterial culture was centrifuged for 5 min at  $5,000 \times g$ , resuspended in 1 ml SHS to wash the cells, centrifuged again and then resuspended in a final volume of 1 ml SHS. For strains exhibiting higher lethality, cells were then diluted in SHS to an appropriate concentration for the infection. Twenty microlitres of the final cell suspension was added to the first column of 8 wells in a 96-well plate and serially diluted using a Research multichannel micropipettor (Eppendorf, Hamburg, Germany), leaving a final volume of 180  $\mu$ l in each well. Ten microlitre spot plate counts were placed on  $\frac{1}{2}$  LB agar using a Research Plus multichannel micropipettor (Eppendorf) following cell dilution, and incubated at 37°C overnight. Infection plates were wrapped in cellophane to reduce evaporation of liquid from wells and placed at 30°C. Plant survivors were counted at 96 h. Plants were identified as “alive” when more than 10% of the plant remained green after 96 h, and plants that displayed >90% loss of green pigmentation were considered dead. Each independent trial consisted of 4-8 replicate infections serially diluted 5 times, and separate overnight cultures were grown for each trial. Calculated LD<sub>50</sub> values represent the average of replicate trials, and LD<sub>50</sub> values among the strains were compared using Student’s T-tests.

## **EPEC infections**

EPEC strains were grown similarly to Bcc strains but in full-strength LB and infections were performed as described for Bcc, except that plant survival was measured at 7 days instead of 96 h as a result of EPEC-mediated killing having a delayed onset ( $\geq 5$  days) relative to that observed with Bcc strains. Two to four trials were carried out for all strains, and LD<sub>50</sub> values represent the average of replicates. Student's T-tests were used to compare LD<sub>50</sub> values among the strains.

## **Concentration of culture supernatants**

To test for secreted toxin activity,  $\sim 10^6$  cfu *B. cenocepacia* K56-2 and mutant 50D9, carrying a plasposon insertion into *bcal0225* or *shvR*, were inoculated into flasks containing 25 ml SHS and grown statically at 30°C. After 5 days, cultures were transferred to 50 ml polystyrene conical tubes (VWR International) and centrifuged for 10 minutes at 5,000  $\times g$ . Supernatants were transferred to new 50 ml polystyrene tubes and centrifuged again. Final supernatants were then filtered through a nonsterile 0.22- $\mu\text{m}$  polyvinylidene difluoride (PVDF) membrane filter (Millipore, Billerica, MA), lyophilized for 2 days, resuspended in 500  $\mu\text{l}$  water and stored at -20°C. For standardization purposes, crude protein concentrations of the concentrated supernatants were measured by A<sub>230 nm</sub> referenced to a control containing only lyophilized SHS media using a Nanodrop 2000c spectrophotometer (Thermo Scientific, Waltham, MA); these varied by less than 12.5% (2.8 – 3.2 mg/ml). Fifty microlitres of these suspensions were added to 96-well plate wells containing 150  $\mu\text{l}$  SHS and single duckweed plants, then diluted 4-fold several times to reduce toxin concentrations.

Plates were incubated at 30°C and plant morbidity was monitored every 24 h. Supernatants were obtained from duplicate cultures and tested in 2 independent trials.

### **Heat inactivation of bacteria**

To test for hypersensitivity of plants to bacterial surface structures, a  $10^9$  cfu/ml suspension of *B. cenocepacia* K56-2 in SHS was heat-inactivated at 65°C for 5 min, with bacterial killing confirmed by lack of growth on LB agar. Ten microlitres of the resulting suspension was inoculated into plant wells containing 150 µl SHS and a single plant. Plant morbidity was monitored every 24 h. Controls included non-heat-killed bacteria from the same original suspension and cell-free SHS.

### **Bacteriophage rescue**

Ninety-six well plates were prepared as above, but only 160 µl of SHS was added to each well. For the preliminary trials, 20 µl of a dilution of bacteria corresponding to  $\sim 100 \times LD_{50}$  was added to each infection well. Follow-up trials used inocula of  $\sim 10^6 \times LD_{50}$ . An additional 20 uL of  $4 \times 10^8$  pfu/ml phage KS12 in sterile mQ H<sub>2</sub>O was added to each infection well. Control trials included uninfected plants with and without phage and infected plants without phage. Each group of six plants infected with a given overnight culture of bacteria was counted as a single trial.

## **Surface sterilization of infected plants**

Using a sterile inoculating loop, each infected plant was transferred to a well containing 200  $\mu$ l 8% bleach. A sterile pipette tip was used to submerge the plant for 30 s, and the plant was transferred 3 times into wells containing 200  $\mu$ l SHS media, each time briefly submerging the plant, to remove all traces of bleach. Plants were left in the third wash well while replicate plants were surface-sterilized, and each plant was then transferred into a microfuge tube containing 25  $\mu$ l SHS. Using an ethanol-sterilized plastic micropestle (Sigma-Aldrich, St. Louis, MO), plants were homogenized until no trace of plant tissue was visible (usually 30 – 60 s). Twenty microlitres of this homogenate was transferred into 180  $\mu$ l SHS, serially diluted and spotted onto LB agar to obtain plate counts. To count bacterial survivors of the bleach treatment that could contaminate the invading bacterial numbers, the final wash solutions of each replicate were plated on LB agar. Three independent trials were carried out with four replicates of each sample per trial.

## **LD<sub>50</sub> calculations**

To determine LD<sub>50</sub> values for duckweed and wax moth larval infections, the protocol described by Randhawa (2009) was followed with the exception that standard error was calculated from the mean of trials, rather than as an inherent deviation from cumulative LD<sub>50</sub> values, which seemed somewhat artificial, given that conducting additional trials would not lower the error using that method. Data from independent trials were plotted on a Probit versus bacterial dose graph from which slope formulae were obtained for each trial. A Probit is a statistical

representation of the surviving proportion of organisms from a given test group. A sample calculation is shown in Figure 1.

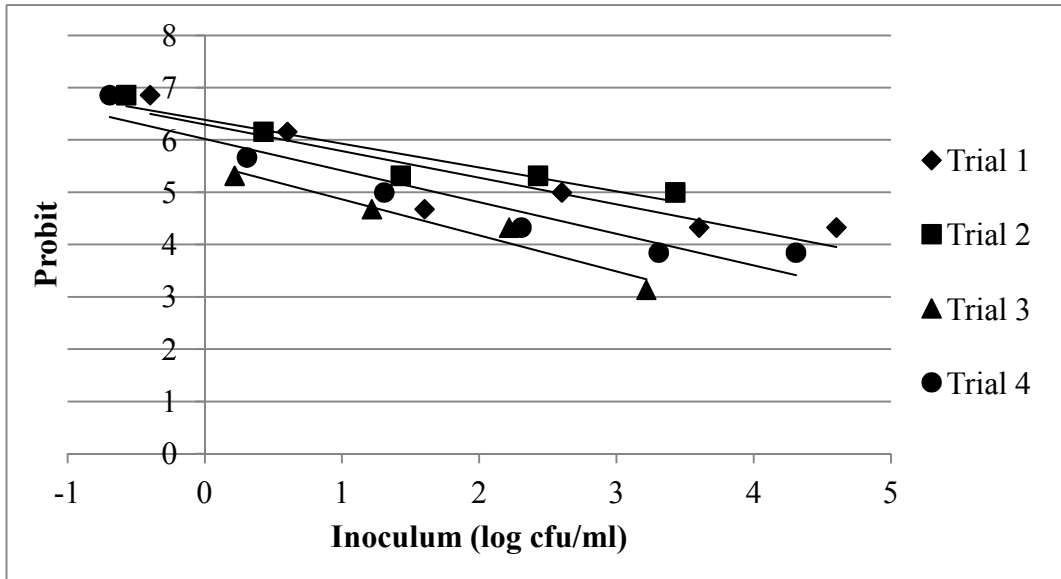


**Figure 1. Sample data for determination of *B. vietnamiensis* DBO1 LD<sub>50</sub>.** Data from individual trials were plotted and individual trendline equations were obtained to solve for  $y = 5$  (i.e. 50% survival in probit format). The derived  $x$  value was then converted from  $\log(\text{cfu/ml})$  into  $\text{cfu/ml}$ . Data points falling between 0 and 100% survival plus one point each at 0% and 100% survival were included, where available. The method utilized was adapted from Randhawa (2009). Trendline equations were as follows: Trial 1,  $y = -0.5091x + 6.2969$ ; Trial 2,  $y = -0.456x + 6.3832$ ; Trial 3,  $y = -0.689x + 5.5508$ ; Trial 4,  $y = -0.6051x + 6.0205$ .

## Results

### Development of duckweed as a model host for the *B. cepacia* complex

To generate an accurate, reproducible 96-well plate-based infection assay, single axenically-grown duckweed plants derived by asexual reproduction from a single plant were placed into individual wells of a 96-well plate containing SHS media and infected with serial dilutions of a *B. cepacia* complex pathogen, *B. cenocepacia* K56-2. Plants begin to show signs of morbidity at high doses by 24 h, with Bcc infections reaching completion at 4 days. After this time, surviving plants tend to persist, having resisted the initial infection. Figure 2a shows a typical result at 96 h: none of the plants survived the highest bacterial loads, half the plants survived the third dilution, and all of the plants survived the fourth dilution. Zhang *et al.* (2010) demonstrated that infection with *S. aureus* RN4220 resulted in dramatic drops in both plant fresh weight and chlorophyll concentration. Since our infections were performed in the absence of light, there was minimal plant growth following the infection periods, and therefore single plants showed little contrast in fresh weight. However, the bleaching effect we observed in the dead plants was also the result of chlorophyll degradation, as measured following the ethanol extraction protocol described by Zhang *et al.* (2010). Infections were also attempted using SH media without sucrose added, and no signs of morbidity were observed, indicating that *B. cenocepacia* requires an exogenous energy source to establish plant infection.

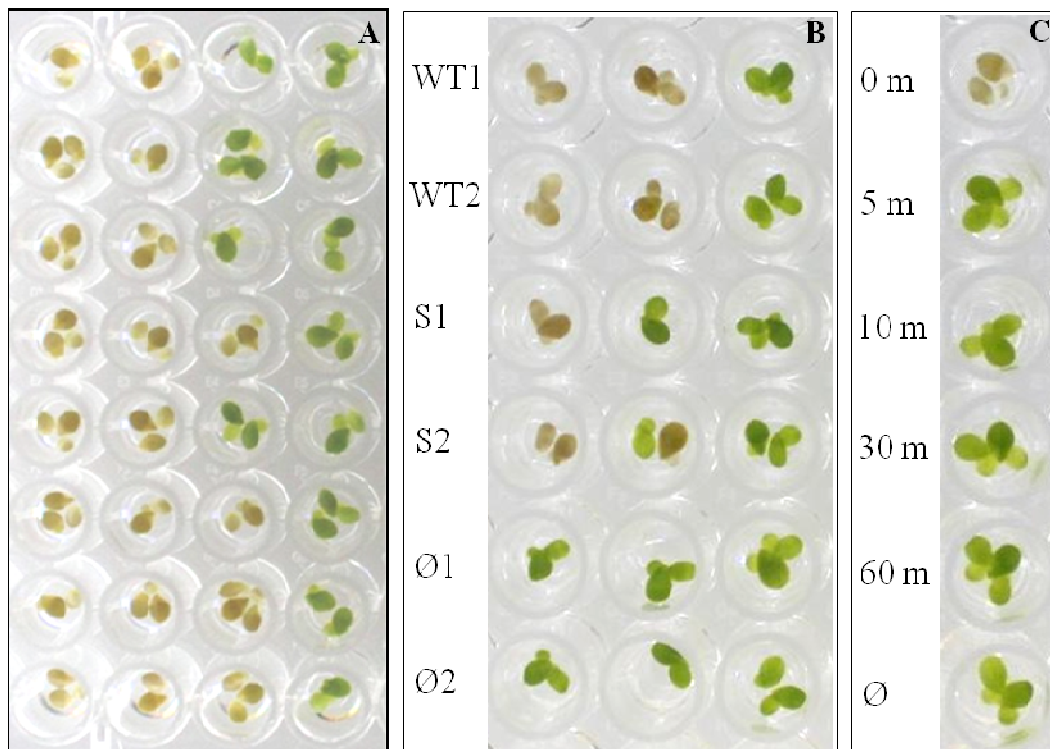


**Figure 2. *Lemna minor* provides both quantitative and qualitative assessments of bacterial strain lethality.** **A.** 50% lethal dose can be determined by assessing plant survival after a given timepoint. An overnight culture of a given strain was washed and inoculated into each well of the left-most column, then serially diluted into each subsequent column using a multichannel pipette. Bacterial counts were generated using a multichannel pipette by spotting 10  $\mu$ l from each well on agar. For Bcc infections, surviving plants were counted after 96 h. **B.** Supernatants of wild type and *shvR*-deficient *B. cenocepacia* mutant 50D9 affect duckweed at different dilutions. Supernatants from two 5-day cultures were lyophilized, resuspended in deionized water and 4-fold serially diluted into duckweed-containing wells for each strain: WT, wild type *B. cenocepacia* K56-2;

S, K56-2 mutant 50D9, harbouring a plasposon insertion in *shvR*; Ø, blank SHS media control. Results are shown at 72 h post-inoculation. C. Heat-killed *B. cenocepacia* K56-2 has no effect on duckweed. A dense ( $\sim 1 \times 10^9$  cfu/ml) K56-2 suspension was incubated at 65°C for different lengths of time (shown in min beside each well) and then inoculated into a plant-containing well. A lack of viable cells from a 5-min incubation onward was shown by spotting the suspensions on LB agar.

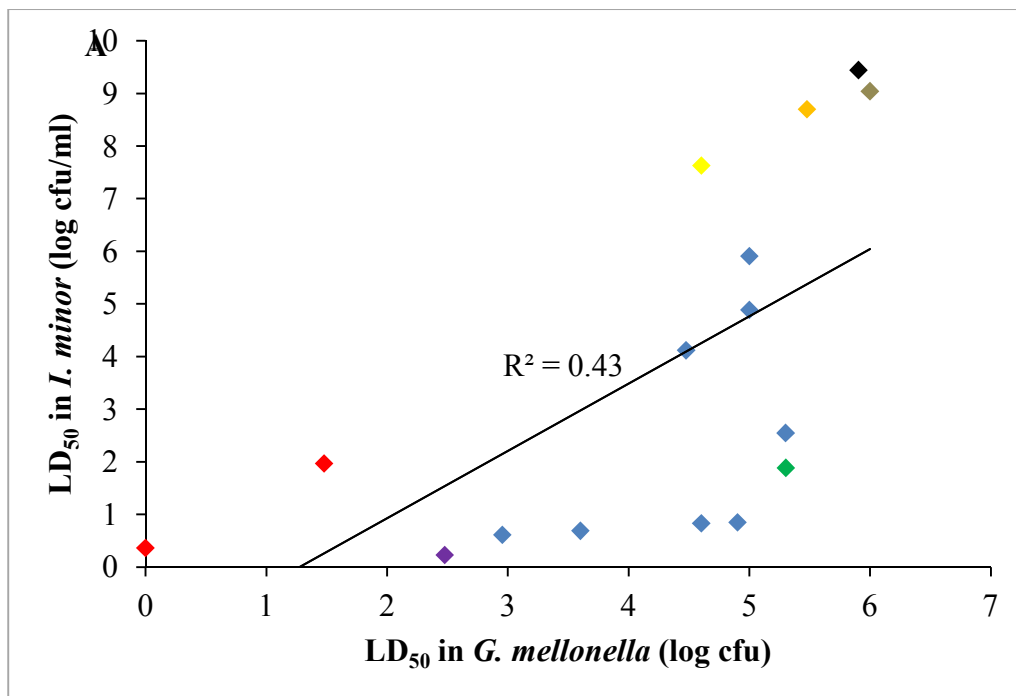
In *Bcc* infection of duckweed, the data suggest two possibilities: first, that the hypersensitive response (HR) is not responsible for plant death; second, that *Bcc* strains engage the HR to varying extents and the total chlorophyll bleaching that leaves the plants brown is simply an extreme HR. In the first case, it would be expected as an alternative that invasion or toxin production would be required to cause plant mortality. It was suspected that the product of the *afc* gene cluster, previously characterized in both *B. cepacia* BC11 (Kang *et al.*, 1998) and *B. cenocepacia* K56-2 (Subramoni *et al.*, 2011), could be responsible for this effect, so exported toxin production was tested by lyophilizing and concentrating culture supernatants from both wild type *B. cenocepacia* K56-2 and mutant 50D9 obtained during preliminary trials of a plasposon mutant screening. While wild type K56-2 supernatants killed plants at 16 -fold dilution (i.e., 0.18 mg/ml protein), supernatants of 50D9 killed plants only at 4-fold dilution (i.e., 0.775 mg/ml protein; Figure 2b), though some morbidity was observed at the 16-fold dilution in the 50D9 concentrate. This result demonstrates that K56-2 kills plants

in part through exported toxin production but that additional factors beyond those regulated by *shvR* may affect the plants. The second case proposed above, involving extreme HR by the plants, would be initiated by plant responses to pathogen-associated molecular patterns (PAMPs) found on bacterial cell surfaces (18). This was tested by inoculating plants with roughly  $10^9$  cfu/ml heat-killed bacteria, which had no effect on the plants (Figure 2c). A later factor activating the HR is the detection of effector proteins in the plant cytosol. As will be shown in Chapter 3, there is no evidence that a secretion system able to deliver effector proteins into the plant cells is responsible for plant killing by *B. cenocepacia* (18). Therefore, *B. cenocepacia* K56-2 kills duckweed through a combination of exported toxin and contact-dependent mechanisms, but likely does not activate a lethal HR.

The adaptability of this model was provided context by incubation of duckweed in temperatures as low as 4°C and as high as 37°C, oxygen levels as low as 5%, and ASMDM media simulating the cystic fibrosis lung, a recipe for which can be found in Fung *et al.* (2010). Considering the changes in gene expression shown in *Pseudomonas aeruginosa* when incubated in ASMDM, which included upregulation of iron scavenging and other metabolic pathways, there could be pathologically relevant effects on Bcc bacteria when incubated under such conditions. It is therefore tempting to imagine that the physical conditions described above also affect the bacteria's metabolic state and perhaps virulence factor expression; the effects of oxygen and temperature on *B. multivorans* pathogenesis will be discussed at length in Chapter 4.

## Correlation between Bcc virulence in plant and insect models

We investigated the relationship between LD<sub>50</sub> values of these representative Bcc strains in both models. Consistent with our early findings, the most virulent strains against wax moth larvae were also the most virulent against duckweed, and the same trend was observed for the least virulent strains (Figure 3a). Although a weak correlation was found between the raw LD<sub>50</sub> values in duckweed and larvae ( $R^2 = 0.43$ ), transforming the LD<sub>50</sub> values into rank format yielded much stronger agreement ( $R^2 = 0.81$ ), showing that the relative virulence of members of the Bcc is consistent between the two models (Figure 3b).



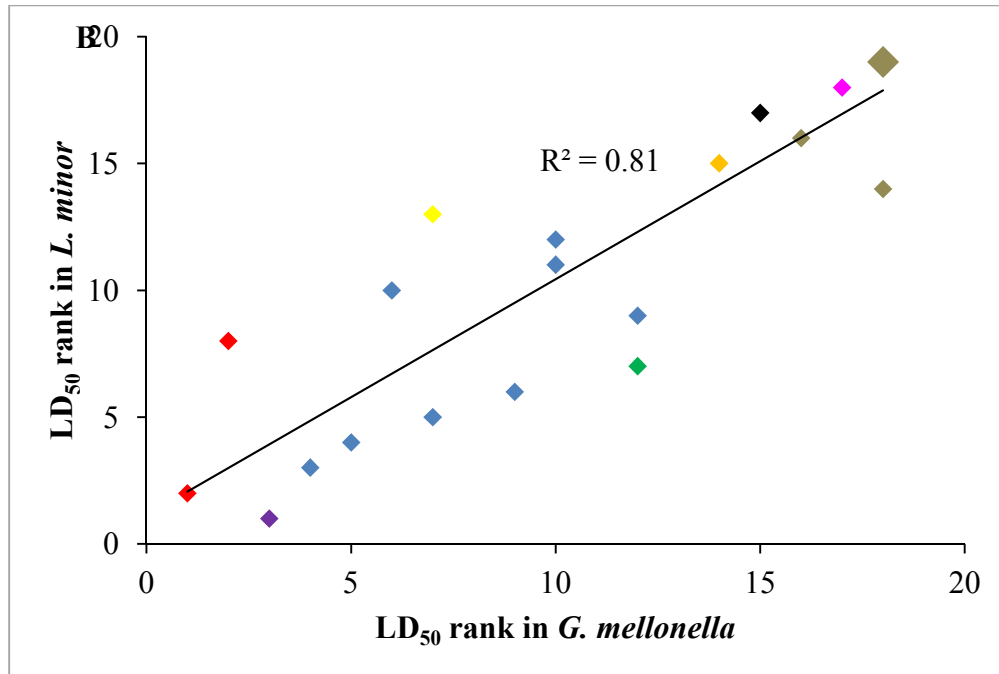


**Figure 3. The virulence of Bcc strains in duckweed correlates with their virulence in wax moth larvae. A.** Each point represents the LD<sub>50</sub> of a Bcc strain in duckweed determined from the compiled data of 2-6 independent trials plotted against LD<sub>50</sub> values determined in wax moth larvae (29). **B.** LD<sub>50</sub> values for all strains in both infection models placed in order of rank. The large brown point in **B** represents four *B. multivorans* strains (C7322, C3430, C5393, and PC249), one *B. dolosa* strain (AU0645) for which bacterial loads high enough for killing were not attained. Data points are coloured by Bcc species as follows: red, *B. cepacia*; brown, *B. multivorans*; blue, *B. cenocepacia*; green, *B. vietnamiensis*; yellow, *B. dolosa*; orange, *B. anthina*; purple, *B. pyrrocinia*; black, *B. ambifaria*; pink, *B. stabilis*.

## **Extension of the duckweed model to enteropathogenic *Escherichia coli***

The same approach used to analyze the Bcc was applied to other bacterial pathogens with LD<sub>50</sub> values established in wax moth larvae. Of the assayed bacteria, *Acinetobacter baumannii*, *Campylobacter jejuni*, and enteropathogenic *Escherichia coli* (EPEC), only EPEC showed virulence against duckweed. We also tested the tomato pathogen *Ralstonia solanacearum* against duckweed, and even after plant wounding, the bacteria were unable to establish an infection. EPEC virulence was expected, as Zhang *et al.* (38) observed virulence of enterohemorrhagic *E. coli* (EHEC) but avirulence of lab strain DH5 $\alpha$  against duckweed. Figure 4 shows LD<sub>50</sub> values determined in duckweed and plotted against values previously determined in wax moth larvae (21) for wild type EPEC and five isogenic mutants deficient in bundle forming pilus (*bfp*), a type III secretion system (*escN*; T3SS), the EAF virulence plasmid (JPN15; deficient in T3SS activation and BFP), the CpxR response regulator (*cpxR*; inactive Cpx stress response pathway), and CpxA phosphatase activity (*cpxA24\**; results in a constitutively activated Cpx pathway). T-tests revealed that only the LD<sub>50</sub> of JPN15 differs significantly from wild type EPEC ( $p = 0.06$ ); despite the large gap between the values of *cpxA24\** and EPEC, this level of significance was not attained, likely because enough trials were not conducted.

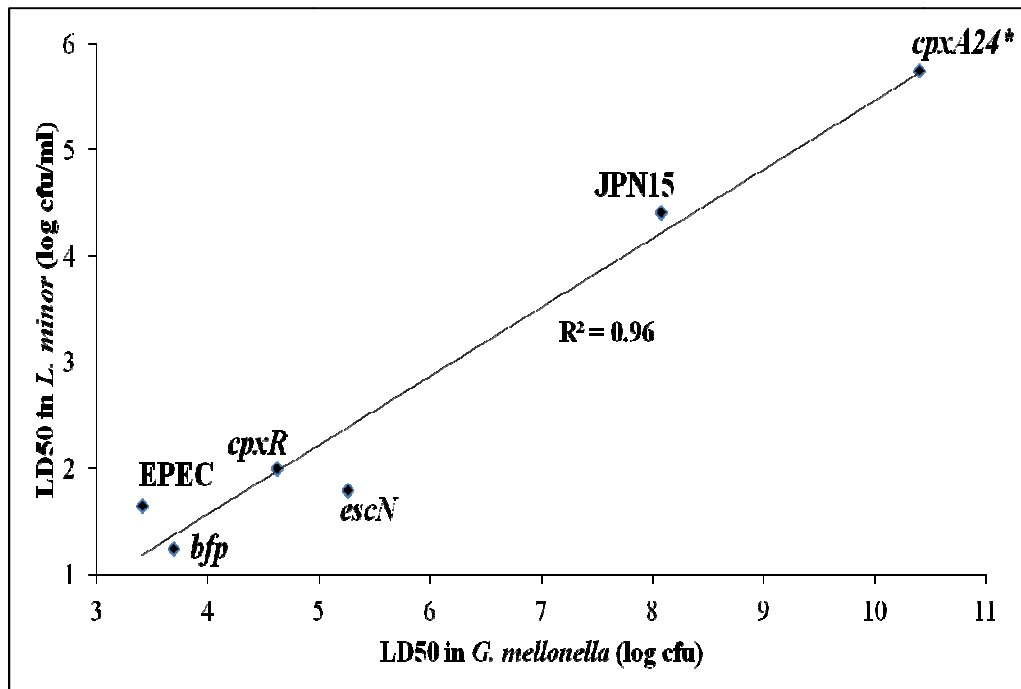


**Figure 4. The virulence of enteropathogenic *Escherichia coli* (EPEC) strains in duckweed correlates with their virulence in wax moth larvae.** Wild type EPEC and five mutant strains deficient in bundle forming pilus (*bfp*), type III secretion (*escN*), the EAF virulence plasmid (JPN15), the CpxR response regulator (*cpxR*; inactive Cpx stress response pathway), and CpxA phosphatase activity (*cpxA24\**) were inoculated into wells containing duckweed and left to incubate at 30°C for 7 days. Each point represents the LD<sub>50</sub> determined in duckweed from the compiled data of 2-4 independent trials plotted against values determined in wax moth larvae by Leuko and Raivio (21).

## **Dynamics of bacteriophage rescue of plants from *B. cenocepacia* infection**

Finally, we sought to determine whether bacteriophage treatment could rescue duckweed plants from *B. cenocepacia* K56-2 infection, and if so, whether a timeline exists for effective treatment. A preliminary experiment suggested that when phages were added at 4 h post-infection, plants showed considerably higher survival rates than when phage were added at 24 h post-infection. Therefore, we investigated the phenomenon at a finer scale, applying phage every 6 h up to 24 h. We used high bacterial loads in these experiments to investigate tissue invasion as a possible Bcc escape strategy. After 12 h, no difference exists between the survival of treated and untreated plants (Figure 5a), despite the fact that bacterial counts in the medium surrounding the plants reach their peak at 12 h (Figure 5b). Bacterial invasion of plant tissue was measured by surface-sterilization of the plants with bleach, followed by homogenization of the plants and viable plate counts of crushed plant matter. Bacteria were observed at high numbers inside the plants by 18 h, increasing approximately 10-fold by 24 h (Figure 5c).

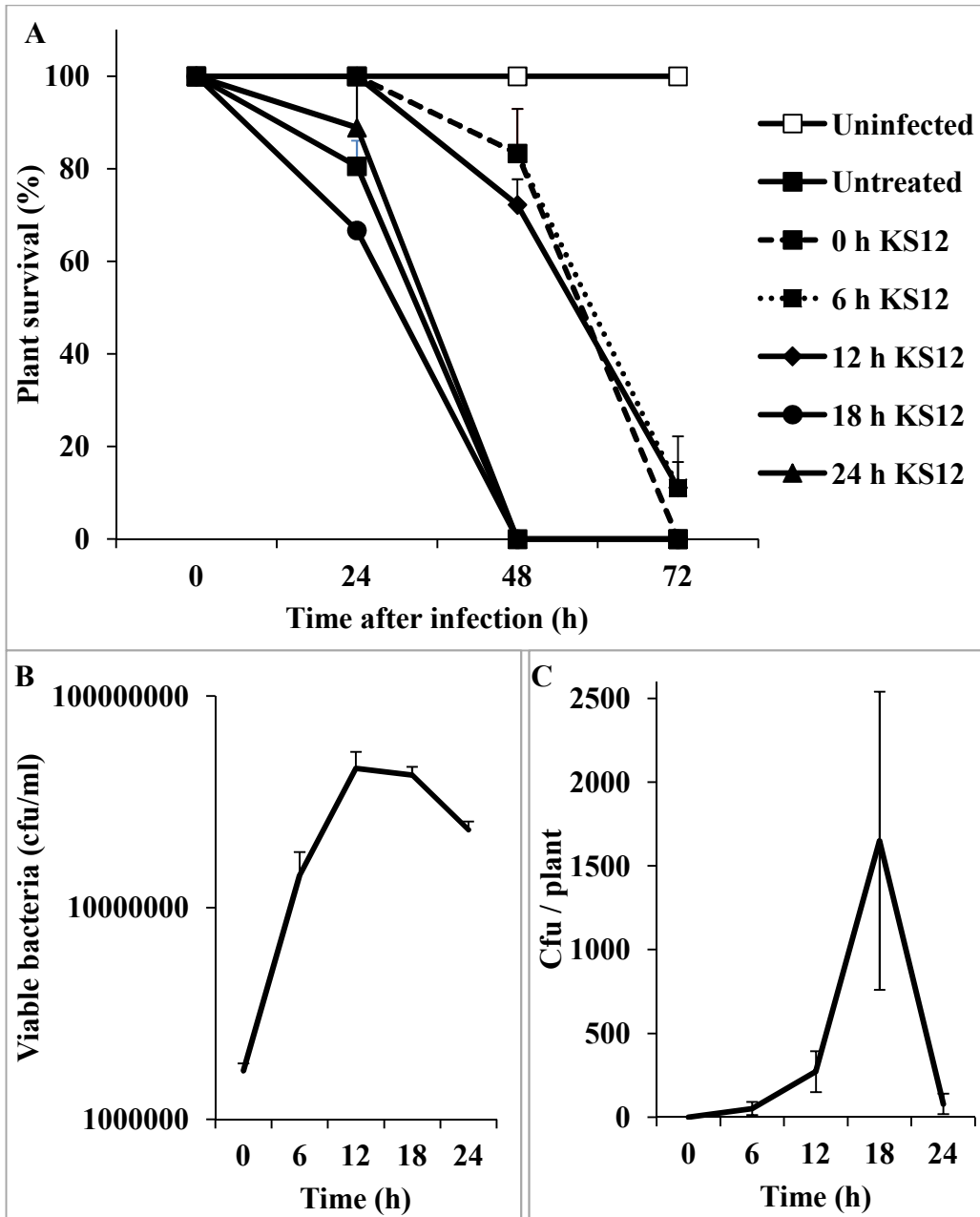


**Figure 5. *B. cenocepacia* infection of duckweed is alleviated by bacteriophage treatment up to 12 h but not after 18 h. A.** *B. cenocepacia* K56-2 was inoculated into plant-containing wells at  $2 \times 10^6$  cfu/ml, with  $4 \times 10^8$  pfu/ml of phage KS12 (i.e. MOI = 200) applied at 0, 6, 12, 18, and 24 h. Results shown are averages of 3 biological replicates using 6 plants per trial performed over 2

independent trials +/- SE. “Untreated” refers to both phage-treated and mock-treated plants, as both showed 100% survival. **B.** Bacterial counts from media surrounding plants during the infections in the absence of phage treatment. Results shown are averages of 3 biological replicates performed in triplicate over 2 independent trials +/- SE. **C.** Bacterial counts from crushed surface-sterilized plants in the absence of phage treatment. Results shown are averages of 3 biological replicates performed in quadruplicate +/- SE.

## Discussion

This study was prompted by the emerging realization that bacteria able to infect both plants and animals use some conserved virulence factors in both processes. The foundational study in this field showed that mutant strains of *P. aeruginosa* showing virulence attenuation in the mouse model were also attenuated in plant models (27). These findings launched a transposon screen of *P. aeruginosa* mutants inoculated into lettuce leaves in which nine attenuated mutants were identified, eight of which showed decreased virulence in mice (28). It was thereafter realized that virulence factors of pathogens demonstrating a similar propensity to infect both plants and animals could be similarly identified and characterized. For the Bcc, three plant models have been developed to study Bcc virulence, including wounded onion (37), alfalfa (4), and wounded lettuce midrib (23). The majority of studies using these models have compared the

virulence of Bcc isolates (4, 17, 23, 32, 37) and assessed the importance of previously-identified Bcc virulence factors to infection (31, 36). One study carried out a plasposon mutant screen using the onion model (14), and will be discussed in Chapter 3. However, all of these studies rely on comparing the virulence of bacterial strains within a narrow range of cell densities, and none has generated a comprehensive numerical assessment by which the virulence of a given strain could be accurately predicted.

Virulence of the different Bcc species in duckweed is consistent with the findings of Bernier *et al.* (4), who used alfalfa seedlings as a model host. Virulent species included *B. cepacia*, *B. cenocepacia*, *B. vietnamiensis*, *B. dolosa* and *B. ambifaria*, while *B. multivorans* and *B. stabilis* were relatively avirulent. One exception to this is that *B. ambifaria* Cep0996 shows low virulence against duckweed, while *B. ambifaria* AMMD is highly virulent ( $LD_{50} = 2.5$  cfu/ml; not shown in Figure 3 as it was not included in the analysis of Seed and Dennis (29)). We extended this analysis to place *B. pyrrocinia* and *B. anthina* in the virulent and avirulent categories, respectively, and provide an alternative quantitative approach by which to directly compare strain virulence among different infection models. Neither these results nor those of Bernier *et al.* (4) are consistent with the findings of Yohalem and Lorbeer (37), who found that Bcc strains of clinical origin were unable to cause maceration upon onion tissue inoculation, while many environmental strains, particularly isolates from onion rot, were highly pathogenic. The results in the present study demonstrate no apparent difference between the plant pathogenicity of clinical and environmental strains. In fact, the

two most virulent strains in the duckweed model (*B. cepacia* LMG 2161 and *B. pyrrocinia* ATCC 15958) are soil isolates, and in species with representative clinical and environmental strains, such as *B. ambifaria* and *B. dolosa*, the environmental strains are more virulent. The discrepancy between the studies could be a result of the inoculation method: while the alfalfa seedlings and duckweed plants are left intact following inoculation with bacteria, the onion method requires inoculating bacteria into incisions in a halved onion. Alternatively, this discrepancy could simply be an indication of common Bcc virulence factors at play for clinical infections, duckweed and alfalfa that are not significant factors in the onion rot model.

A useful quantitative gauge of Bcc virulence is the *Galleria mellonella* (Greater wax moth) larval infection model, introduced for the Bcc by Seed and Dennis (29). This study established LD<sub>50</sub> values for a panel of Bcc strains representing 9 of the 17 established Bcc species. *B. cepacia*, *B. cenocepacia* and *B. pyrrocinia* strains were the most virulent in wax moth larvae, while *Burkholderia dolosa*, *Burkholderia ambifaria* and *Burkholderia multivorans* were the least virulent. Following the establishment of LD<sub>50</sub> values in duckweed for all strains tested by Seed and Dennis (30), correlations were observed between the raw LD<sub>50</sub> values in both models ( $r^2 = 0.43$ ) and the LD<sub>50</sub> ranks of the strains in the two models ( $r^2 = 0.81$ ). This result suggests two possibilities. The first is that throughout the Bcc there are key traits with varying prevalence conferring virulence in these two models; bacteria encoding these key traits should demonstrate similar decreases in virulence in the two models when these traits are

disrupted through mutagenesis. A second possibility is that Bcc strains show variability in their resistance to host innate immune factors. However, this is discounted by the fact that *B. cenocepacia* J2315 demonstrates relatively high resistance to most antimicrobial compounds tested by Caraher *et al.* (7), while this strain is among the least virulent *B. cenocepacia* strains tested in both duckweed and wax moth larvae (30). Therefore, it is expected that conserved virulence factors confer virulence to the two models in Bcc strains, as seen in other organisms. For example, a homolog of *Pseudomonas syringae* virulence factor identified in plants was characterized in *P. aeruginosa* following the initial discovery of this bacterium's multihost pathogenicity. This work led to the identification of a master regulator of the *P. aeruginosa* quorum sensing systems, which control many mammalian virulence genes, by first identifying it and characterizing the *P. aeruginosa* homolog in *Arabidopsis* infection (26). A similar story has emerged for *B. cenocepacia*, in which the LysR-like regulator *shvR*, which was initially identified as a major virulence factor in alfalfa (3), has now been determined to control a regulon of over 1,000 *B. cenocepacia* genes that includes quorum sensing genes (25).

The mechanism of plant mortality in these infections was not determined. Although plants lack roaming defender cells and adaptive immune systems, their innate immune systems comprise two interacting pathways to defend against bacterial pathogens: effector-triggered immunity and pathogen-associated molecular pattern (PAMP)-triggered immunity. Built into these oscillating pathways is the hypersensitive response (HR), which is associated with reactive

oxygen species (ROS) production, ion flux, localized cell death and other events in the presence of an overwhelming infection (18). If plant mortality was the result of HR, it would be expected that a large dose of heat-killed bacteria would suffice to trigger a systemic, lethal HR throughout the plant. This possibility is not supported by the finding that heat-killed *B. cenocepacia* K56-2 did not induce visible plant morbidity at a high dose, despite its high lethality in the absence of heat-killing (Figure 2c). Therefore, the mechanism by which members of the Bcc induce plant mortality probably involves factors produced by the bacteria. These could involve soluble factors released into the media, as shown in Figure 2b, such as the semi-soluble antifungal compound produced by the *afc* genes encoded by *B. cenocepacia* (34) and *B. pyrrocinia* (19). Virulence factors underpinning *B. cenocepacia* pathogenicity in duckweed will be explored in Chapter 3, and build on these findings by demonstrating the presence of a multifactorial virulence mechanism.

Although most tested pathogens produced no visible morbidity during incubation with duckweed, the LD<sub>50</sub> values obtained for all six EPEC strains strongly reflect the trend observed by Leuko and Raivio (21) using the wax moth larva model (Figure 4). A mutation in *bfpA*, which knocks out the bundle-forming pilus (BFP) was found to be dispensible for EPEC virulence in both plant and insect infection (21). Since the main contributions of the BFP to EPEC pathogenesis are to initial intestinal brush border adhesion (11) and to biofilm formation through bacterium-bacterium interactions (15), it is possible that EPEC causes plant morbidity following the production of secreted toxic factors. This

partly explains the results of the present study, since a T3SS knockout strain (*escN*) showed partial virulence decreases in both plant and wax moth larvae (21) infection. However, the most surprising observation emerging from these experiments was that the elimination of the EAF virulence plasmid (strain *JPN15*) causes a larger increase in LD<sub>50</sub> than either the elimination of either type III secretion, which depends on the plasmid-encoded regulators PerA, PerB and PerC for transcriptional activation of the T3SS, or the bundle-forming pilus, which is genetically encoded by the plasmid. This suggests that the EAF plasmid carries additional virulence factors other than the well-characterized T3SS activator *perA* and BFP genes (10). The identification of such a virulence factor might explain the phenotype identified by Lin and Guttman (22), who demonstrated global deubiquitylation of human cell proteins by EPEC that is conferred by the EAF plasmid but independent of both the BFP and T3SS.

Evidence of *B. cenocepacia* K56-2 invasion of plant tissues or cells was provided by the detection of bacteria in relatively high numbers inside the plants by 18 h (Figure 5c), combined with the inefficacy of phage treatment after 12 h (Figure 5a). K56-2 invasion into plant tissues would not be surprising given the invasiveness of *B. cenocepacia* strains into a variety of cell lines (13, 20, 24, 35), though *B. cenocepacia* has demonstrated a reduced ability to transmigrate across epithelial layers relative to other Bcc species (13), which could correspond to a reduced ability to invade other tissue types. The reduction in bacterial counts at 24 h is suspected to be the result of bleach penetrating damaged plant tissues or toxic HR activity within the plant tissues as a result of infection (1). An

alternative explanation for the inability of phages to rescue plants beyond 12 h is that a bacterial toxin is released at high enough doses to cause plant death after this timepoint. This possibility is raised by the result shown in Figure 1b, where plant death is brought about by an exported toxin likely under control of the *shvR* regulator. One such toxin is synthesized by the *afc* enzymes encoded adjacent to *shvR* on the *Bc* megaplasmid. This region has been shown to be responsible for the synthesis of a membrane-associated lipopeptide likely produced by a nonribosomal peptide synthetase / polyketide synthetase hybrid that promotes phenotypes such as swarming motility, antifungal activity and plant destruction (19, 25, 33). However, the compound partitions more readily into the lipophilic fraction than the soluble following cell disruption (19), which suggests that lyophilization of the supernatant in the present study did not isolate the majority of the compound. The possibility therefore exists that toxin production early in the co-incubation of bacteria with plants causes the failure of phages rescue after 12 h.

Overall, this study presents a new infection model host for the *Burkholderia cepacia* complex and other potentially pathogenic bacteria that is inexpensive, reliable, rapid and easy to manipulate. The quantitative relationships between the virulence of both Bcc isolates and EPEC mutants in the *L. minor* infection model versus the *G. mellonella* model indicate conserved mechanisms of pathogenesis between these two vastly different hosts, with novel virulence factors encoded by the EAF plasmid implied by a substantial virulence reduction in the EAF-deficient strain. A potential mechanism of plant killing by *B.*

*cenocepacia* was demonstrated using extracted supernatants of strain K56-2 and isogenic mutant 50D9 (with a disruption of *shvR*), though the extracellular factor thought to be produced by the *afc* region encoded adjacent to *shvR* likely does not cause the full killing effect by the bacteria. The failure of bacteriophage rescue following the 12 h mark may point to a mechanism of bacterial escape into plant tissues or cells. If *B. cenocepacia* uses such a strategy, it may help explain some of the difficulties experienced by researchers in applying phage therapy to treat infections in mice (8). Regardless, duckweed represents a useful high-throughput host for testing the efficacy of therapeutic agents.

## References

1. Agrios G. Plant pathology. 5 ed. Waltham, Massachusetts: Academic Press; 2005. p. 221.
2. Antunes LC, Imperi F, Carattoli A, Visca P. Deciphering the multifactorial nature of *Acinetobacter baumannii* pathogenicity. PLOS One. 2011;6(8):e22674.
3. Bernier SP, Nguyen DT, Sokol PA. A LysR-type transcriptional regulator in *Burkholderia cenocepacia* influences colony morphology and virulence. Infect Immun. 2008;76(1):38-47.
4. Bernier SP, Silo-Suh L, Woods DE, Ohman DE, Sokol PA. Comparative analysis of plant and animal models for characterization of *Burkholderia cepacia* virulence. Infect Immun. 2003;71(9):5306-13.
5. Brea D, Meurens F, Dubois AV, Gaillard J, Chevaleyre C, Jourdan ML, et al. The pig as a model for investigating the role of neutrophil serine proteases in human inflammatory lung diseases. Biochem J. 2012;447(3):363-70.
6. Cao H, Baldini RL, Rahme LG. Common mechanisms for pathogens of plants and animals. Ann Rev Phytopath. 2001;39:259-84.
7. Caraher E, Reynolds G, Murphy P, McClean S, Callaghan M. Comparison of antibiotic susceptibility of *Burkholderia cepacia* complex organisms when grown planktonically or as biofilm in vitro. Eur J Clin Microbiol Infect Dis. 2007;26(3):213-6.
8. Carmody LA, Gill JJ, Summer EJ, Sajjan US, Gonzalez CF, Young RF, et al. Efficacy of bacteriophage therapy in a model of *Burkholderia cenocepacia* pulmonary infection. J Infect Dis. 2010;201(2):264-71.
9. Champion OL, Karlyshev AV, Senior NJ, Woodward M, La Ragione R, Howard SL, et al. Insect infection model for *Campylobacter jejuni* reveals that O-methyl phosphoramidate has insecticidal activity. J Infect Dis. 2010;201(5):776-82.
10. Clarke SC, Haigh RD, Freestone PP, Williams PH. Virulence of enteropathogenic *Escherichia coli*, a global pathogen. Clin Microbiol Rev. 2003;16(3):365-78.
11. Cleary J, Lai LC, Shaw RK, Straatman-Iwanowska A, Donnenberg MS, Frankel G, et al. Enteropathogenic *Escherichia coli* (EPEC) adhesion to intestinal epithelial cells: role of bundle-forming pili (BFP), EspA filaments and intimin. Microbiology. 2004;150(Pt 3):527-38.
12. Cosgrove S, Chotirmall SH, Greene CM, McElvaney NG. Pulmonary proteases in the cystic fibrosis lung induce interleukin 8 expression from bronchial epithelial cells via a heme/meprin/epidermal growth factor receptor/Toll-like receptor pathway. J Biol Chem. 2011;286(9):7692-704.
13. Duff C, Murphy PG, Callaghan M, McClean S. Differences in invasion and translocation of *Burkholderia cepacia* complex species in polarised lung epithelial cells in vitro. Microb Pathog. 2006;41(4-5):183-92.
14. Engledow AS, Medrano EG, Mahenthiralingam E, LiPuma JJ, Gonzalez CF. Involvement of a plasmid-encoded type IV secretion system in the plant tissue watersoaking phenotype of *Burkholderia cenocepacia*. J Bacteriol. 2004;186(18):6015-24.

15. Hicks S, Frankel G, Kaper JB, Dougan G, Phillips AD. Role of intimin and bundle-forming pili in enteropathogenic *Escherichia coli* adhesion to pediatric intestinal tissue *in vitro*. *Infect Immun*. 1998;66(4):1570-8.
16. Ibrahim M, Tang Q, Shi Y, Almoneafy A, Fang Y, Xu L, et al. Diversity of potential pathogenicity and biofilm formation among *Burkholderia cepacia* complex water, clinical, and agricultural isolates in China. *World J Microbiol Biotechnol*. 2012;28(5):2113-23.
17. Jacobs JL, Fasi AC, Ramette A, Smith JJ, Hammerschmidt R, Sundin GW. Identification and onion pathogenicity of *Burkholderia cepacia* complex isolates from the onion rhizosphere and onion field soil. *Appl Environ Microbiol*. 2008;74(10):3121-9.
18. Jones JD, Dangl JL. The plant immune system. *Nature*. 2006;444(7117):323-9.
19. Kang Y, Carlson R, Tharpe W, Schell MA. Characterization of genes involved in biosynthesis of a novel antibiotic from *Burkholderia cepacia* BC11 and their role in biological control of *Rhizoctonia solani*. *Appl Environ Microbiol*. 1998;64(10):3939-47.
20. Keig PM, Ingham E, Vandamme PA, Kerr KG. Differential invasion of respiratory epithelial cells by members of the *Burkholderia cepacia* complex. *Clin Microbiol Infect*. 2002;8(1):47-9.
21. Leuko S, Raivio TL. Mutations that impact the enteropathogenic *Escherichia coli* Cpx envelope stress response attenuate virulence in *Galleria mellonella*. *Infect Immun*. 2012;80(9):3077-85.
22. Lin AE, Guttman JA. The *Escherichia coli* adherence factor plasmid of enteropathogenic *Escherichia coli* causes a global decrease in ubiquitylated host cell proteins by decreasing ubiquitin E1 enzyme expression through host aspartyl proteases. *Int J Biochem Cell Biol*. 2012;44(12):2223-32.
23. Muhammad I. LH, Miao L, Zhu B., Bin L., Xie G.L., Zhang G. Prevalence of potential pathogenicity and molecular characterizations of *Burkholderia cepacia* complex (BCC) among isolates from bamboo rhizosphere in China. *Res J Chem Environ*. 2011;15:998-1005.
24. Mullen T, Callaghan M, McClean S. Invasion of *Burkholderia cepacia* complex isolates into lung epithelial cells involves glycolipid receptors. *Microb Pathog*. 2010;49(6):381-7.
25. O'Grady EP, Nguyen DT, Weisskopf L, Eberl L, Sokol PA. The *Burkholderia cenocepacia* LysR-type transcriptional regulator ShvR influences expression of quorum-sensing, protease, type II secretion, and *afc* genes. *J Bacteriol*. 2011;193(1):163-76.
26. Rahme LG, Ausubel FM, Cao H, Drenkard E, Goumnerov BC, Lau GW, et al. Plants and animals share functionally common bacterial virulence factors. *Proc Natl Acad Sci U S A*. 2000;97(16):8815-21.
27. Rahme LG, Stevens EJ, Wolfort SF, Shao J, Tompkins RG, Ausubel FM. Common virulence factors for bacterial pathogenicity in plants and animals. *Science*. 1995;268(5219):1899-902.

28. Rahme LG, Tan MW, Le L, Wong SM, Tompkins RG, Calderwood SB, et al. Use of model plant hosts to identify *Pseudomonas aeruginosa* virulence factors. Proc Natl Acad Sci U S A. 1997;94(24):13245-50.
29. Seed KD, Dennis JJ. Development of *Galleria mellonella* as an alternative infection model for the *Burkholderia cepacia* complex. Infect Immun. 2008;76(3):1267-75.
30. Seed KD, Dennis JJ. Development of *Galleria mellonella* as an alternative infection model for the *Burkholderia cepacia* complex. Infect Immun. 2008;76(3):1267-75.
31. Somvanshi VS, Viswanathan P, Jacobs JL, Mulks MH, Sundin GW, Ciche TA. The type 2 secretion pseudopilin, gspJ, is required for multihost pathogenicity of *Burkholderia cenocepacia* AU1054. Infect Immun. 2010;78(10):4110-21.
32. Springman AC, Jacobs JL, Somvanshi VS, Sundin GW, Mulks MH, Whittam TS, et al. Genetic diversity and multihost pathogenicity of clinical and environmental strains of *Burkholderia cenocepacia*. Appl Environ Microbiol. 2009;75(16):5250-60.
33. Subramoni S, Agnoli K, Eberl L, Lewenza S, Sokol PA. Role of *Burkholderia cenocepacia* *afcE* and *afcF* genes in determining lipid-metabolism-associated phenotypes. Microbiology. 2013;159(Pt 3):603-14.
34. Subramoni S, Nguyen DT, Sokol PA. *Burkholderia cenocepacia* ShvR-regulated genes that influence colony morphology, biofilm formation, and virulence. Infect Immun. 2011;79(8):2984-97.
35. Tomich M, Herfst CA, Golden JW, Mohr CD. Role of flagella in host cell invasion by *Burkholderia cepacia*. Infect Immun. 2002;70(4):1799-806.
36. Uehlinger S, Schwager S, Bernier SP, Riedel K, Nguyen DT, Sokol PA, et al. Identification of specific and universal virulence factors in *Burkholderia cenocepacia* strains by using multiple infection hosts. Infect Immun. 2009;77(9):4102-10.
37. Yohalem D.S. LJW. Distribution of *Burkholderia cepacia* phenotypes by niche, method of isolation and pathogenicity to onion. . Ann Appl Biol. 1997. ;130:467-79.
38. Zhang Y, Hu Y, Yang B, Ma F, Lu P, Li L, et al. Duckweed (*Lemna minor*) as a model plant system for the study of human microbial pathogenesis. PLOS One. 2010;5(10):e13527.

## Chapter 2 – *Burkholderia vietnamiensis* produces a glycosylated hemolytic virulence factor *via* a non-ribosomal peptide synthetase

---

A version of this chapter has been published: Thomson and Dennis 2012. *Virulence* 3(3): 286-98.

## Introduction

### *Burkholderia vietnamiensis*

*B. vietnamiensis* (*Bv*) is the third most prevalent Bcc species in CF (14). Although it is typically not associated with cepacia syndrome or epidemic spread, *Bv* stands out among Bcc pathogens with its ability to gain aminoglycoside resistance during chronic infection through active efflux (28). Among its agricultural and environmental benefits are its ability to degrade environmental contaminants (27), suppress fungal phytopathogens (1, 16, 30, 35, 36) and fix nitrogen (19, 44), and its ubiquitous presence on roots of common crops, including maize, rice, sorghum and coffee (19) are testament to these capabilities. Clinical *Bv* isolates display a 17% decrease in nitrogenase prevalence versus environmental isolates, suggesting that adaptation to the amino acid-rich lung environment selects against metabolically expensive nitrogen fixation (44). *Bv* is unique among the Bcc in its capacity for nitrogen fixation, although several other nitrogen-fixing *Burkholderia* species have been described (42).

For these reasons, *Bv* has been identified as a powerful bioremediation and plant growth-promoting agent (50). However, its industrial application has so far been precluded by its extensive antibiotic and biocide resistance (5, 6, 55), its intermediate levels of virulence in standard infection models, and its prevalence among the CF community, which stands at 2-6% in North America (14).

## ***Bv* virulence pathways**

Like other Bcc species, it appears that *Bv* utilizes its versatile lifestyle strategies in the CF lung infection process. Cellular invasion, toxin production, resistance to antimicrobial compounds and siderophore production are traits that are suggested to play a role in *Bv* pathogenesis and can be linked to the *Bv* soil niche. This section will build on the virulence pathways outlined in the General Introduction by describing these pathways as they apply specifically to *Bv*; where research is lacking, the pathways are generally omitted from discussion.

### *Iron acquisition*

As discussed in the General Introduction, it is not clear whether iron is a limiting factor in the lungs of CF patients; nonetheless, transcriptomic data from *Burkholderia cenocepacia* suggests that the bacterial iron acquisition machinery is upregulated during chronic infection. This is perhaps a result of bacterial competition or localized iron limitation within the biofilm communities. In any case, the lysis of erythrocytes may represent a useful and relatively cheap solution to the difficult challenge of iron acquisition in the lung environment. *Bv* is somewhat variable from strain to strain in hemolysin production, and it is difficult to assign to the different species many of the hemolysins described prior to species delineation of the Bcc. For these reasons, this section will focus on hemolysin production within the Bcc as a whole, as well as pointing out any that are known to be produced by *Bv*.

Early reports suggested that only approximately 4% of Bcc isolates exhibit  $\beta$ -hemolytic activity when sheep erythrocytes were tested (48). However, later

studies showed that up to 39% of clinical Bcc isolates possessed hemolytic activity when using sheep erythrocytes (66). One source of this hemolytic activity may arise from a  $\beta$ -hemolysin (66), although unlike *Pseudomonas aeruginosa*, Bcc phospholipase activity does not correlate with the presence of this hemolytic activity. In 1994, the isolation and purification of two related hemolysins with antifungal properties was published by Abe and Nakazawa (1). The hemolytic activity of these “cephalysins” was inhibited by sterols, suggesting that they require an interaction with cholesterol in the erythrocyte membrane to produce a biological effect. Fehlner-Gardiner *et al.* (20) identified components of the *Bv* general secretory pathway that were involved in the secretion of hemolytic and phospholipase C activities, but these were not necessary for intracellular survival within *Acanthamoeba polyphaga*. More recently, Bevivino *et al.* (3), using ram erythrocytes, found that almost all *Burkholderia ambifaria* isolates were hemolytic and that the percentage of hemolytic environmental *B. cenocepacia* isolates was markedly higher than the percentage of hemolytic clinical isolates. In contrast, Carvalho *et al.* (8) found that almost all of the 59 clinical *Burkholderia multivorans*, *B. cenocepacia*, *B. ambifaria* and *Bv* isolates from a reference CF centre in Brazil produced several different exoproducts except for hemolysin (as tested against human erythrocytes), which was only detected in *Bv*. From these results, it is evident that some Bcc members produce hemolytic toxins, although their importance towards pathogenicity is unclear.

### *Resistance to host defences*

The main study that closely examined the antimicrobial resistance of *Bv* found that it is generally more susceptible to aminoglycoside antibiotics than other Bcc species, but *Bv* can develop tobramycin resistance during the course of chronic CF infection as increasing minimum inhibitory concentration values were shown both *in vivo* and *in vitro* over the course of three separate *Bv* infections of CF patients (28). Interestingly, this trend did not hold for polymyxin B, another cationic antimicrobial drug, which suggested to the authors that the mechanism of resistance was not related to cell surface chemistry, such as that described throughout the Bcc with cAMP resistance *via* cationic LPS modifications. Rather, *Bv* can apparently make use of its extensive network of efflux pumps (likely in addition to uncharacterized means) to prevent accumulation of these drugs inside the cell. In addition, the resistance of environmental, CF and clinical non-CF *Bv* isolates to aminoglycosides were compared and clinical isolates were generally more resistant to the drugs, indicating that the activation of efflux pumps is the norm during chronic *Bv* infection in CF. Although aminoglycoside antibiotics are not host defences, this study reveals a possible mechanism by which *Bv* can resist toxic compounds in general, in addition to reinforcing the existing knowledge on the extreme cAMP resistance of the Bcc, which pertains specifically to major human innate defence molecules, cathelicin and defensins. While it is tempting to suggest that this aspect of *Bv* biology relates to its status as a bioremediation agent, there is little data to support the notion; rather, the only study examining *Bv*

contaminant resistance found that trichloroethylene degradation requires a suite of DNA repair enzymes to protect the cells (70).

A partial proteome of *Bv* G4 has been published, and it reveals two possible means by which *Bv* resists host oxidative and proteolytic factors. *Bv* produces both superoxide dismutase (SOD) and catalase, which help combat oxidative stress inside phagocytic vacuoles. The protease inhibitor ecotin was also identified in the *Bv* proteome; this enzyme was shown to be a neutrophil elastase inhibitor in *Escherichia coli*, *Yersinia pestis* and *Pantoea citrea*, but not in *P. aeruginosa* (15). Interestingly, this study showed evidence that neutrophil elastase causes bacteriostatic effects from inside the periplasm following OmpA cleavage and increased cell permeability, and ecotin likely helps protect the cell against periplasmic, rather than extracellular, elastase. SOD, catalase and ecotin would all likely serve *Bv* in defending against the army of neutrophils and their extracellular products in the CF lung.

#### *Inflammation and epithelial destruction*

Exported toxic factors produced by the Bcc that occur in *Bv* include lipase and type III, IV and VI secretion system effector proteins (40). The proteases ZmpA and ZmpB, which were outlined in the General Introduction and appear to help with antimicrobial peptide resistance and virulence, respectively, are not present in *Bv* (22, 31). Meanwhile, lipases may play a role in transepithelial migration through uncharacterized mechanisms that have been demonstrated in *B. cenocepacia* and *B. multivorans*. Lipase production by *Bv* is strain-variable but

comparable to that seen in *B. cenocepacia* (47), suggesting that these invasive effects may apply to some *Bv* strains.

The limited evidence suggesting that type III secretion (T3SS) systems play an important role in Bcc pathogenesis will be discussed in Chapter 3, but for now it should be noted that the *Bv* T3SS has not been studied but that it is present and intact within the genome (23). The type VI secretion system (T6SS) also has not been studied in *Bv* but it, too is present in the genome. The type IV secretion system (T4SS) described in the General Introduction as being responsible for plant tissue water-soaking (PTW) phenotype in onions by *B. cenocepacia* and *B. cepacia* is likely also present in *Bv*, since a *Bv* strain was shown to produce the PTW phenotype (18). The *Bv* G4 genome indicates that there are 2 T4SSs in *Bv*. In *B. cenocepacia*, a chromosomally-encoded T4SS produces the PTW phenotype, while a plasmid-borne T4SS appears to allow conjugal DNA transfer (71). It is possible that the *Bv* systems fulfill similar functions.

#### *Cellular invasion*

*Bv* is no exception to the invasion of cells described in the General Introduction. It seems likely that this propensity shares its genetic basis with the ability of *Bv* to invade fungal spores, plant roots and amoebae. Despite these abilities, *Bv* invasion has not been studied in epithelial or phagocytic cell lines, or animal tissues in general, likely as a result of the keen focus among researchers on understanding the multifactorial mechanism of *B. cenocepacia* invasion.

Although the events leading to invasion by *Bv* have not been characterized in these systems, its intracellular survival within amoebae (32) appears to rely on a similar type VI secretion system-mediated delay of autophagy as that demonstrated by *B. cenocepacia* in macrophages (54). *Bv* does not replicate within the amoebal vacuole, contrasting its behaviour within fungal spores. Following spore infection, which occurred at a rate of 15% through an uncharacterized mechanism, *Bv* was able to grow to densities of  $10^6$  cfu/spore (34), while its growth in maize roots approximated  $4 \times 10^5$  cfu/g root tissue (19).

#### *Social behaviours*

In addition to the *cepIR* system present throughout the Bcc, *Bv* has a quorum sensing system that has not been found in other Bcc species. *BviIR* are responsible for the synthesis and detection of C10-HSL in addition to the roles of *CepIR* in C6-HSL and C8-HSL, and *bviIR* are activated by *CepR* (41). The authors found that C10-HSL was detected in the three tested environmental isolates, but the molecule was absent in three of four clinical isolates despite all isolates containing the biosynthetic machinery. They determined that this was due to lack of *bviI* expression, and suggested that another factor plays an intervening role in the system. However, *bviIR* regulation has not been studied further. The only phenotype so far assigned to *BviIR* is the production of an uncharacterized antibacterial compound in *Bv* G4 (51), but this activity was refuted by Malott *et al.* (41); other phenotypes associated with quorum sensing in Bcc such as biofilm formation, swarming, and siderophore production were found to be unaffected by *bviI* or *bviR* mutations.

## **Non-ribosomal peptide synthetases**

Many bacterial secondary metabolites, including antibiotics (21), siderophores (13), and toxins (65), are synthesized with diverse structural modifications. Non-ribosomal peptide synthetases (NRPS) are modular enzyme complexes arranged as assembly lines (57) that parallel the ribosomal translation pathway and promote this structural versatility.

The minimum domain requirements for a NRPS module include an adenylation-thiolation domain (A domain; the core domain of a NRPS module which recognizes and activates amino acids), a condensation domain (C domain; responsible for creating peptide bonds between adjacent amino acids), and a thiolation domain (T domain; responsible for fastening peptide intermediates to the NRPS). In addition, a termination or thioesterase domain (Te domain) may cyclise the final peptide, while an epimerization domain (E domain) can isomerize amino acids or incorporate alternative residues, such as carbonyl acids (Figure 6). Other structural modifications emerging from NRPS include peptide branching, glycosylation, and halogenation.

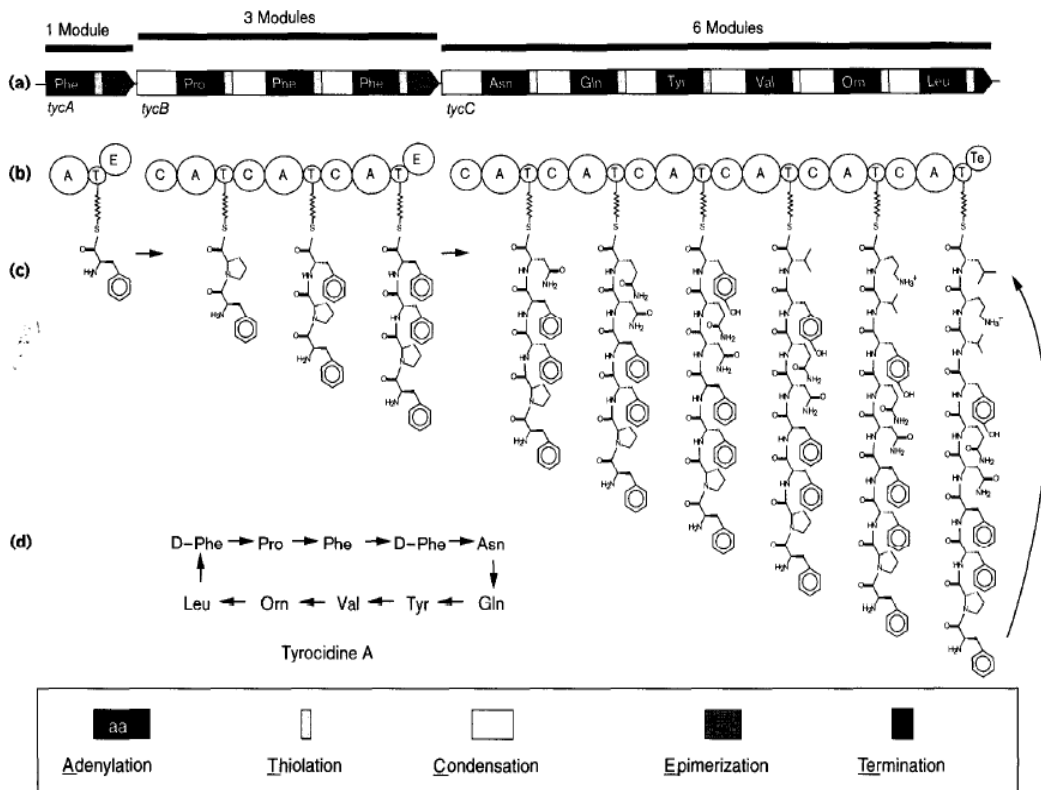


**Figure 6. Extension of a nonribosomal peptide, illustrated with the example of tyrocidine A synthesis in *Bacillus brevis*.** Three peptide synthetases, (a) encoded by the genes *tycA*, *tycB*, and *tycC*, act in concert for the stepwise assembly of the cyclic decapeptide. (b) The enzymes are composed of modules that can be subdivided into domains. The substrates are recognized and adenylated by the action of the A-domains and subsequently transferred to a thioester linkage on the T-domain (shown as a zigzag), which serves as the anchor of the nascent chain on the protein template. (c) C-domains then catalyze the condensation with the aminoacyl- or peptidyl-moieties on the neighbouring modules. At positions one and four, an epimerization domain converts L-Phe into its stereochemical isomer. (d) A thioesterase-like domain is believed to act as

a cyclase to give the final product. ©Elsevier Ltd., 1999; permission obtained.

(46)

Methods have been developed by which the substrate specificity of adenylation domains may be determined (10, 53, 59). These developments initially stemmed from the realization that all adenylation domains contain a ten-residue binding pocket that recognizes a particular amino acid to be added to the peptide chain (9,56). Building upon this discovery, the adenylation specificity code was refined by considering all amino acids within 8 Å of the amino acid binding pocket, which comprises 34 amino acids in total (50).

### **Secondary metabolites in *Bv* and the *Bcc***

Several secondary metabolite compounds with biological effects are also produced by *Bv*, either through polyketide synthetase (PKS) or non-ribosomal peptide synthetase (NRPS) enzyme complexes. These include siderophores, signaling molecules, and molecules with inhibitory effects against competing microbes.

Iron represents one of the primary limiting factors for life on Earth because it is insoluble in its oxidized form,  $\text{Fe}^{3+}$ . Siderophores are  $\text{Fe}^{3+}$ -chelating compounds generally upregulated by bacteria during iron starvation. Typically, siderophores form trimers to bind a single iron molecule, and can only be taken up into a cell by interaction with a cognate trimeric outer membrane receptor followed by active transport. Therefore, siderophores represent a means by which

a bacterial population can secure a supply of iron without providing a communal resource for competing organisms. Most known siderophores are synthesized through NRPS complexes, but others are formed as offshoots of pre-existing metabolic pathways or by NRPS-independent means involving alternating condensation of amino acids with dicarboxylic acids (9). There are four known siderophores produced by the Bcc: ornibactin, pyochelin, cepabactin, and cepaciachelin. Ornibactin is the most prevalent of these among the Bcc, comprising 4 amino acids condensed into a peptide by a NRPS complex that acylates both terminal peptides. Pyochelin is produced to varying levels in ~50% of Bcc strains and is formed by the NRPS-mediated condensation of two cysteine residues with salicylic acid. Cepabactin appears to be quite rare among the Bcc, and may be limited to *B. cepacia*. It is a cyclic hydroxamate, formed from the insertion of a hydroxylamine into a carboxylic acid, and is not produced *via* NRPS. Cepaciachelin is so far only known in *B. ambifaria*, and is formed by heavily modifying lysine with putrescine and two 2,3-dihydroxybenzoic acid residues as sidegroups. Salicylic acid is a precursor to pyochelin, but appears to have its own receptor and may function as a siderophore (67). Of the confirmed Bcc siderophores, only ornibactin is produced by *Bv*, and its role in the virulence of this species has not been examined.

In addition to their signalling roles discussed in the General Introduction, the cyclic dipeptides known as diketopiperamines (DKPs) can exhibit strong antimicrobial activity. For example, cyclo(L-Arg-D-Pro) was found to inhibit a chitinase produced by *Serratia marcescens* by mimicking a reaction intermediate;

further work then demonstrated cell wall synthesis-inhibition against the yeast *Saccharomyces cerevisiae*. In some cases DKPs form important components to larger bioactive molecules. DKPs effective against both bacteria and fungi have been isolated from both bacteria and fungi, indicating that these molecules represent an element of the vast repertoire of bioactive metabolites involved with intermicrobial competition (43). Recently, five DKPs were identified in *Bv*, all of which were directly synthesized and secreted by the bacteria (69). These include cyclo(Pro-Phe), cyclo(Pro-Tyr), cyclo(Ala-Val), cyclo(Pro-Leu), and cyclo(Pro-Val). Four were previously known in Gram negative bacteria, but cyclo(Pro-Phe) was novel. Surprisingly, the addition of exogenous DKPs from culture supernatant inhibited the antifungal activity of the *Bv* culture supernatant. This indicates that the molecules are interfering with the biological activity, rather than the production, of an antifungal compound.

Known secondary metabolite toxins produced by the Bcc but not by *Bv* include the broad-spectrum antifungal agent pyrrolnitrin (16); a group of antifungal and antitumor agents deemed cepafungins (58); hemolytic peptides named cepalysins (1); related antifungal compounds cepacidine A1 and A2 (33, 36); and the recently described antifungal cyclic peptide occidiofungin or burkholdine (24-26, 38, 63), which may be similar to xylocandins, previously isolated from *B. pyrrocinia* strain LMG 21822 (4, 45). The biosynthetic pathways of pyrrolnitrin and occidiofungin have been characterized, and both are produced using NRPS complexes.

## Objectives

While many of these NRPS/PKS-synthesized compounds show activity against fungi, the present study identified through random and directed mutagenesis a NRPS gene cluster in *Bv* strain DBO1 that is homologous to the gene cluster that synthesizes occidiofungin / burkholdine (henceforth referred to as occidiofungin) in other Bcc strains, and demonstrate that the compound synthesized by the products of this gene cluster is not only antifungal but also strikingly  $\beta$ -hemolytic and required for full virulence of *Bv* in wax moth larvae. This study also uses molecular tools to expand our knowledge on the prevalence of this gene cluster within the Bcc.

## Materials and Methods

### Bacterial strains, plasmids, antibiotics and culture conditions

Luria-Bertani (LB) broth was prepared in distilled water to half concentration for Bcc strains and full concentration for *Escherichia coli* strains. Sheep, horse, bovine, and rabbit blood broth (Dalynn Biologicals, Calgary, AB) and human blood broth (Canadian Blood Services, Edmonton, AB) were prepared to 5% v/v blood in trypticase soy broth (TSB). Agar plates were prepared with 1.5% w/v agar. Antibiotics were included where necessary to the following concentrations: Ampicillin (amp), 100  $\mu\text{g}/\text{mL}$ ; Trimethoprim (Tp), 100  $\mu\text{g}/\text{mL}$ ; Tetracycline (Tc), 100  $\mu\text{g}/\text{mL}$ . All antibiotics were purchased from Difco through BD - Canada (Mississauga, ON). *Escherichia coli* DH5 $\alpha$  was used for plasmid manipulation. *E. coli* strains were grown at 37 °C, while DBO1 was grown at 30

°C. All liquid cultures were shaken at 225 rpm. High-copy number plasmid pJET (Amp<sup>R</sup>) was employed in cloning experiments. For random plasposon mutagenesis, pTnMod-OTp' (Tp<sup>R</sup>) (12) was used. To complement gene *6466*, pSCRhaB2 (9) was used. A complete list of bacterial strains and plasmids is shown in Table 2.

**Table 2. Strains and plasmids used in this study.**

<i>Bacterial strain</i>	<i>Genotype or relevant phenotype</i>	<i>Hemolytic activity</i>	<i>Source</i>
<i>B. vietnamiensis</i>			
DBO1	Parent strain	+	Soil
<i>6465::Tp<sup>R</sup></i>	DBO1 with targeted oriTp' insertion in gene <i>6465</i> , encoding an FAD-linked dioxygenase	+	This study
<i>6466::Tp<sup>R</sup></i>	DBO1 with targeted oriTp' insertion in gene <i>6466</i> , encoding a putative LuxR regulator	-	This study
<i>6468::Tp<sup>R</sup></i>	DBO1 with oriTp' plasposon insertion in gene <i>6468</i> , encoding a putative LuxR regulator	-	This study
<i>6469::Tp<sup>R</sup></i>	DBO1 with oriTp' plasposon insertion in gene <i>6469</i> , encoding a putative peptide transporter	-	This study
<i>6470::Tp<sup>R</sup></i>	DBO1 with targeted oriTp' insertion in gene <i>6470</i> , encoding a hypothetical protein	+	This study
<i>6471::Tp<sup>R</sup></i>	DBO1 with targeted oriTp' insertion in gene <i>6471</i> , encoding a putative glycosyltransferase within the NRPS gene cluster	+/-	This study
<i>6472::Tp<sup>R</sup></i>	DBO1 with oriTp' plasposon insertion in gene <i>6472</i> , encoding a putative adenylation domain-containing protein	-	This study
<i>6473::Tp<sup>R</sup></i>	DBO1 with oriTp' plasposon insertion in gene <i>6473</i> , encoding a putative adenylation domain-containing protein	-	This study
<i>6474::Tp<sup>R</sup></i>	DBO1 with oriTp' plasposon	-	This study

	insertion in gene <i>6474</i> , encoding a putative adenylation domain-containing protein		
<i>6476::Tp<sup>R</sup></i>	DBO1 with oriTp' plasposon insertion in gene <i>6476</i> , encoding a putative adenylation domain-containing protein and polyketide synthetase	-	This study
<i>6477::Tp<sup>R</sup></i>	DBO1 with targeted oriTp' insertion in gene <i>6477</i> , encoding a putative polyketide synthetase	-	This study
<i>6478::Tp<sup>R</sup></i>	DBO1 with oriTp' plasposon insertion in gene <i>6478</i> , encoding a putative polyketide synthetase within the NRPS gene cluster	-	This study
<i>6479::Tp<sup>R</sup></i>	DBO1 with targeted oriTp' insertion in gene <i>6479</i> , encoding a putative taurine metabolism protein	+	This study
DBO1/pSCRhaTc	DBO1 carrying pSCRhaTc	+	
<i>6466::Tp<sup>R</sup>/pSCRhaTc</i>	DBO1 mutant <i>6466::Tp<sup>R</sup></i> carrying pSCRhaTc	-	
<i>6466::Tp<sup>R</sup>/p6466</i>	<i>6466::Tp<sup>R</sup></i> carrying pSCRha- <i>6466<sup>His</sup></i>	+	This study
<i>E. coli</i>			
DH5α	Cloning host strain	NA	
Plasmid			
pJET1.2/blunt	Cloning vector, Amp <sup>R</sup>	NA	Fermentas
pTnMod-OTp'	Plasposon used for random mutagenesis, Tp <sup>R</sup>	NA	10
pSCRhaB2	Rhamnose-inducible plasmid carrying Tp <sup>R</sup>	NA	(7)
pSCRhaTc	pSCRhaB2 with Tc <sup>R</sup> cassette inserted at the ClaI site within <i>dhfr</i> promoter to eliminate Tp <sup>R</sup>	NA	This study
pSCRha- <i>6466<sup>His</sup></i>	pSCRhaTc carrying <i>bamb6466</i> with a 6x polyhistidine tag	NA	This study

+ = full clearing, +/- = partial clearing, - = no clearing; NA = not applicable

## Random plasposon mutagenesis

This portion of the project was carried out by Dr. Dennis with help from a summer student. A random plasposon insertion mutant library was created in *Bv* DBO1 using plasposon pTn*Mod*-OTp' as previously described (12), and sequencing of rescued plasposons with flanking DNA was carried out using primers Ori and Tp (Table 3). Cells containing integrated plasposons were selected on 1/2 LB + 100 µg /mL trimethoprim. Twenty thousand mutants were patched onto 5% sheep blood TSA agar, incubated at 30 °C, and observed for hemolysis after 48 h. Mutants exhibiting loss of hemolysis were carried forward and their plasposon insertion sites were isolated as previously described (12). To ensure that the random plasposon mutants obtained carried authentic mutations responsible for the observed phenotype, plasposon site of insertion plasmid clones were reintroduced into wildtype DBO1, and following recombination and selection on 1/2 LB + 100 µg /mL trimethoprim, and PCR analysis to ensure proper integration, the reconstructed mutants were again tested for hemolytic activity on 5% sheep blood TSA agar.

**Table 3. Oligonucleotides used in this study.**

Oligonucleotide	Sequence
<i>Mutagenesis*</i>	
m6465-1	GGTTCGACATTCTGACGTT
m6465-2	CCTCTATGTGCCGAACAG
m6466-1	AGAGTCAGATGTTTCGCGAAG
m6466-2	GTCTCGACCGTGCTTTCC

m6470-1	AAGCGGCGTTCGTCAAGTC
m6470-2	AGGTGGCTGAGTTCGACATTG
m6471-1	AAGGTCTGCATCAATCTGG
m6471-2	AGGGAATAGGTCAGCGGC
m6477-1	GCCGTTCTGCAACTACATCC
m6477-2	AGGCGGTCGGTCAGTTCG
m6479-1	ATGGTACCGGCGTCCTTCGAATC
m6479-2	ATAAGCTTGGCAGACGTCGGGTT
<i>Complementati on*</i>	
c6466-1	ATAATACATATGCATCATCACCATCACCACGTTTCGCG AAGCTTG
c6466-2	ATTCTAGACTACGCCGCCGACGCGCAC
<i>Sequencing</i>	
Ori	GGGGAAACGCCTGGTATC
TP <sup>R</sup>	TTTATCCTGTGGCTGC
pJET-F	CGACTCACTATAGGGAGAGCGGC
pJET-R	AAGAACATCGATTTTCCATGGCAG
pSCRha-F	GGCCATTTTCCTGTC
pSCRha-R	GCTTCTGCGTTCTGA
<i>Bcc cluster screening</i>	
s6472-1	TACATGCTCGACGACGCGCT
s6472-2	ATGTTGTAGGTGGCCGACGGG
s6474-1	TCTCGACCAGCGGGCAATACC
s6474-2	TCCTCGATCATGAAGCGCAG
s6476-1	AAGGTCACGTGGTTCGGCTCG

s6476-2	<b>ATTTCGCGGACCAGTTCGGC</b>
---------	-----------------------------

\*Restriction sites shown in bold. 6x histidine tag underlined.

## Targeted mutagenesis

Once the NRPS cluster had been identified through random plasposon mutagenesis, mutations in the remaining genes within the cluster were created through a targeted insertion mutagenesis strategy using homologous recombination. Primers were designed to amplify open reading frames (ORFs) and XbaI sites at either end. A full list of primers is shown in Table 3, and all primers were ordered from Sigma-Alrich (St. Louis, MO). PCR amplification was carried out using TopTaq (Qiagen Inc., Oakville, ON). In many cases, because of imperfect local homology between the AMMD and DBO1 sequences, techniques were used to enhance primer binding in order to obtain PCR products. DNA bands were extracted from agarose gel using GeneClean (Fermentas, Burlington, ON), ligated to pJET1.2 (Fermentas, Burlington, ON) and cloned in *E. coli* DH5 $\alpha$  (Invitrogen Corp., Carlsbad, CA), and DNA sequencing of the cloned fragments was carried out to confirm the identity of the product. To generate plasmids containing insertions, the OriTp<sup>R</sup> region was extracted from pTnMod-OTp' by digestion with BglII and XbaI, ligated to the PCR products using T4 ligase (Promega Corp., Madison, WI) and the 3-way ligation product was cloned into *E. coli* DH5 $\alpha$ , with selection of transformants on LB + 100  $\mu$ g/ml Tp. OriTp-insert plasmids were subsequently extracted from their DH5 $\alpha$  hosts, electroporated into *B. vietnamiensis* DBO1, and transformants were selected on 1/2 LB + 100  $\mu$ g/ml Tp. Mutations were confirmed by PCR amplification using mutagenesis primers.

## Genetic complementation

To restore the mutated hemolysis phenotype to DBO1 mutant *6466::Tp<sup>R</sup>*, I generated a PCR product of *B. ambifaria* AMMD gene *6466*, a putative LuxR regulator of the NRPS gene cluster, and cloned this into the rhamnose-inducible plasmid pSCRhaB2 (7) modified with a tetracycline cassette from p34S-Tc (12) with *Sma*I and ligated into the unique *Eco*RV site of pSCRhaB2. The *6466<sup>His</sup>* PCR construct was amplified with an N-terminal 6x histidine tag and *Nde*I and *Xba*I sites at the 5' and 3' termini (Table 3), respectively, and inserted into the *Nde*I and *Xba*I sites of pSCRhaB2 following its *Nde*I + *Xba*I digestion and purification from a 0.8% agarose gel using GeneClean. Triparental mating (7) was carried out to transform mutant *6466::Tp<sup>R</sup>* with the plasmid; meanwhile, wild type DBO1 and *6466::Tp<sup>R</sup>* were similarly transformed with a blank version of the same Tc<sup>R</sup>-carrying plasmid, produced by digestion with *Nde*I + *Xba*I, purification with GeneClean, digestion with Mung Bean exonuclease (Promega Corp.) and self-ligation, to control for the physiological effects of the vector. Fifty pSCRhaTc-*6466<sup>His</sup>* transformants were screened on blood agar with and without 0.2% rhamnose to identify transformants expressing hemolysin; of these, approximately half showed rhamnose-dependent hemolytic activity. Two complemented mutants were carried forward, and one of these was used in virulence experiments.

## Liquid hemolysis assay

To quantitatively compare hemolytic activity produced by *B. vietnamiensis* DBO1 with that produced by mutants of the NRPS cluster constructed in DBO1 (and subsequently, other strains exhibiting positive PCR

results for genes 6472, 6474 and 6476), a liquid hemolysis assay was developed. DBO1 and mutants were grown in 2 mL sheep blood broth for 48 h in duplicate. One millilitre of supernatant was assayed at 24 h and 48 h and absorbance was measured using an Ultrospec 3000 (Pharmacia Biotech, Cambridge, UK) at a range of wavelengths from 350 nm to 700 nm (Fig. 3). Viable bacterial plate counts were obtained by serial dilution and plating on ½ LB and red blood cell counts were taken using a Bright-Line Hemacytometer (Hausser Scientific, Horsham, PA). This method measured released heme at the optimal wavelengths of 540 nm and 570 nm. A higher-throughput assay was then developed based on these results. The strains were grown for 24 h in four separate 200 µL TSB with appropriate antibiotics in a Costar® 3599 96 Well Culture Cluster (Corning Inc., Corning, NY). Complemented mutant 6466::*Tp<sup>R</sup>/pSCRhaTc-6466<sup>His</sup>* was grown with and without 0.2% rhamnose. OD<sub>600</sub> was taken of all cultures, and three cultures falling within 10% of OD<sub>600</sub> = 1.1 were selected for each strain; cultures of mutant 6473::*Tp<sup>R</sup>* did not grow within this cut-off, so this strain was not used in the experiment. Five microlitres of each cell suspension was added to quadruplicates of 200 µL 5% sheep blood in TSB in 96 well plates and incubated with shaking at 30 °C; to reduce evaporation from wells, plates were plastic-wrapped. After 48 h, 180-200 µL was removed from each well to a microfuge tube and centrifuged at 1,000 x g for 15 minutes. Carefully, avoiding any cell pellet, 140 µL of each supernatant was removed into a 96 well plate and OD<sub>570</sub> was measured. Averages of quadruplicates for each trial were taken and each quadruplicate average statistically represented a value of *n*. Student's T-tests were

carried out to determine statistical significance; to determine T-test type, an F-test was carried out for each comparison.

### **Wax moth larva killing assay**

To compare *in vivo* virulence of wild type *Bv* DBO1 with NRPS cluster gene insertion mutants, *Galleria mellonella* (Greater wax moth) larvae were infected. The standard protocol from Seed and Dennis (56) was followed with several adjustments. Bacterial inocula were  $5 \times 10^6$  cfu and were OD<sub>600</sub> standardized prior to injection. Ampicillin was omitted from the buffer due to its inhibitory activity against DBO1; to compensate for the lack of antibiotic, larvae were dipped in ethanol and dried on paper towel prior to injection. DBO1/pSCRhaTc, 6466::Tp<sup>R</sup>/pSCRhaTc and 6466::Tp<sup>R</sup>/pSCRhaTc-6466<sup>His</sup> were grown at 37 °C for 24 h on LB agar + Tp + Tc + 0.2% rhamnose, and an additional 6466::Tp<sup>R</sup>/pSCRhaTc-6466<sup>His</sup> culture was grown without rhamnose for reduced 6466 expression. All strains except 6466::Tp<sup>R</sup>/pSCRhaTc-6466<sup>His</sup> grown without rhamnose were injected with 0.4% rhamnose added to the 10 mM MgSO<sub>4</sub> suspension. The control injections included 10 mM MgSO<sub>4</sub>, Tp, Tc, and 0.4% rhamnose. Injections were spread over a period of 4 days. Separate cultures were grown, suspended in buffer, and diluted to OD<sub>595</sub> = 0.170 (200 μL in a 96-well plate) for each set of 10 larvae to be injected, with each set of 10 larvae statistically representing a value of *n*. Infected larvae were then incubated at 30 °C for 120 hr. Mortality data were analyzed statistically by a Student's T-test; to determine T-test type, an F-test was carried out for each comparison.

## Prevalence of the hemolysin NRPS cluster in the Bcc

To determine the prevalence of the NRPS cluster among clinical and environmental Bcc isolates, 47 Bcc strains, one untyped *Burkholderia* species, and two *Ralstonia pickettii* strains were screened using primers (Table 3) based on regions of homology between the known sequences of *Burkholderia contaminans* and *B. ambifaria* AMMD but displaying no homology beyond those known sequences. Genes corresponding to *B. ambifaria* strain AMMD genes 6472, 6474 and 6476 were chosen for this screen because these appear to be three of the most significant NRPS biosynthetic genes of the cluster, and their larger size offered more options for primers fitting the above criteria. Colony PCR was performed on each isolate and the PCR products were separated on a 0.8% agarose gel. Strains exhibiting correctly sized products for at least two of the three primer pairs were analyzed further using the liquid hemolysis assay. Strains analyzed are shown in the Results section, Table 3.

## Results

### Identification of an NRPS cluster through plasposon mutagenesis

The hemolytic patterns of the Bcc species *Bv* DBO1 and *B. ambifaria* AMMD, which form  $\beta$ -hemolysis (yellow clearing) on sheep blood agar, were investigated by randomly mutagenizing DBO1 with plasposon pTn*Mod*-OTp<sup>7</sup> (12). Mutants were screened on sheep blood agar + 100  $\mu$ g / mL Tp, and those deficient in hemolysis were carried forward for analysis, which revealed plasposon insertion sites in an uncharacterized gene cluster containing NRPS-

encoding genes, as well as regulator and transporter-encoding genes (Figure 7). Further insertion mutation analysis identified genes essential to the hemolytic activity, and allowed delineation of the ends of the gene cluster. DNA sequence analysis of the *Bv* DBO1 gene cluster demonstrated high homology to a nearly identical gene cluster in the sequenced genome of *B. ambifaria* strain AMMD. The core Bcc NRPS gene cluster is approximately 50.5 kb in length and comprises 13 ORFs arranged identically in both strains. In *B. ambifaria* AMMD, the NRPS cluster located on chromosome 3 and was predicted to extend from basepair 1,101,558 to 1,152,073 for a total of 50,515 base pairs. BLASTN analysis (2) identified only one other closely related gene cluster in the GenBank database, a gene cluster of Bcc member *B. contaminans* strain MS14 encoding occidiofungin biosynthesis proteins. Not only are these 13 genes in MS14 syntenous to the NRPS genes in AMMD/DBO1, each ORF in the AMMD/DBO1 gene cluster has as its most closely related database entry an ORF in the MS14 occidiofungin biosynthetic cluster. For example, the *B. ambifaria* AMMD 3176 amino acid adenylation protein Bamb\_6472 is 89% identical to the same protein in *B. contaminans* MS14, along the entire sequence. For comparison, the next closest database relative is an uncharacterized protein identified in *Acidobacterium capsulatum* ATCC 51196 that is 52% identical to Bamb\_6472. This analysis indicates that the gene clusters identified to be responsible for the hemolytic activity observed in strain DBO1 (and by homology AMMD), are closely related to the occidiofungin biosynthesis gene cluster identified in *B.*

*contaminans* MS14, and to few other genes in the known bacterial genetic sequences.

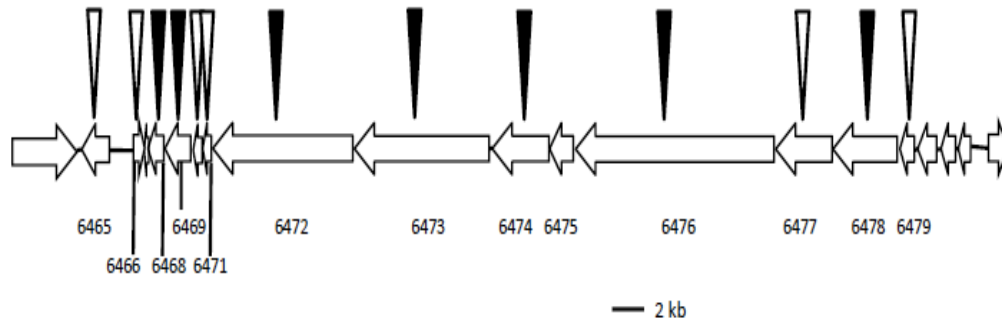


**Figure 7. The NRPS cluster responsible for toxic activity in *B. vietnamiensis* DBO1.** The cluster appears similar to that described in *B. contaminans* MS14 by Gu *et al.* (26), except that an additional two genes, homologues of 6477 and 6478 in *B. ambifaria* AMMD, are present upstream of the described MS14 cluster that are required for virulence in DBO1. Filled vertical arrows indicate genes disrupted by plasposon mutagenesis; unfilled vertical arrows indicate genes disrupted through targeted mutagenesis. Genes are named according to the sequenced *B. ambifaria* AMMD genome: 6465, encoding an FAD-linked dioxygenase homologue; 6466, encoding a LuxR homologue; 6467, encoding a hypothetical protein with a DNA binding motif; 6468, encoding a LuxR homologue; 6469, encoding a cyclic peptide transporter; 6470, encoding a hypothetical protein; 6471, encoding a glycosyltransferase; 6472, encoding an adenylation domain-containing protein (ADCP); 6473, encoding an ADCP; 6474, encoding an ADCP; 6475, encoding a  $\beta$ -lactamase; 6476, encoding an ADCP-polyketide synthetase (PKS) hybrid; 6477, encoding a PKS; 6478, encoding a

PKS; 6479, encoding a taurine dioxygenase. Only genes 6466 through 6478 appear to be involved in toxin production.

### **Uniquely structured toxin is a broad-specificity hemolysin**

Bcc strains DBO1 and AMMD were grown on blood agar with erythrocytes from various sources, including bovine, rabbit, sheep, horse and human, to determine whether hemolysis was limited to certain mammals. Both strains exhibited hemolytic activity on all types of blood agar. Clearing on sheep blood agar produced large yellow zones of lysis, indicative of a  $\beta$ -hemolysis (Figure 8), while cleared zones on other blood types appeared colorless. Mutants in DBO1 defective in producing zones of clearing on one type of blood agar were defective in producing zones of clearing on the other types of blood agar. In order to determine whether the diffusible hemolytic activity observed was active against bacterial cells, Bcc strains producing hemolytic activity were streaked on sheep blood plates and cross-streaked (either concurrently or after one day's growth) with a panel of Gram negative and Gram positive bacterial species including various pseudomonads, *E. coli*, *Staphylococcus* and *Bacillus* species, and 25 different Bcc strains. In both conditions, the Bcc hemolytic activity was not inhibitory to the growth of any other bacterial strain tested, even though hemolytic activity was observable in the underlying blood agar.



**Figure 8. Bcc hemolytic activity on TSA 5% sheep blood agar. *B.***

*vietnamiensis* strain DBO1 and *B. ambifaria* strain AMMD (“V” streaked) produce large transparent yellow hemolytic zones of clearing on an inverted sheep blood plate following overnight growth at 30°C. *B. cenocepacia* strains C4455 and C6433 and *B. multivorans* strain C3430 produce no such hemolytic zones of clearing and are barely visible through the opaque growth media. (64)

To quantify the effect of different NRPS mutations on hemolytic activity, we developed a high-throughput liquid human blood hemolysis assay using hemoglobin release (absorbance at wavelength 570 nm) as a marker. As shown in Figure 3, we first tested this assay against wildtype strain DBO1, and two constructed mutants including *6466::Tp<sup>R</sup>*, a putative *luxR* homologue mutant and

*6477::Tp<sup>R</sup>*, a putative polyketide synthetase mutant, neither of which produce zones of clearing on sheep blood agar. Although hemocytes were inoculated with similar numbers of bacterial cells (Figure 9b), only wildtype strain DBO1 was able to release substantial amounts of hemoglobin (Figure 3a) or reduce the counted number of red blood cells (Figure 9c).

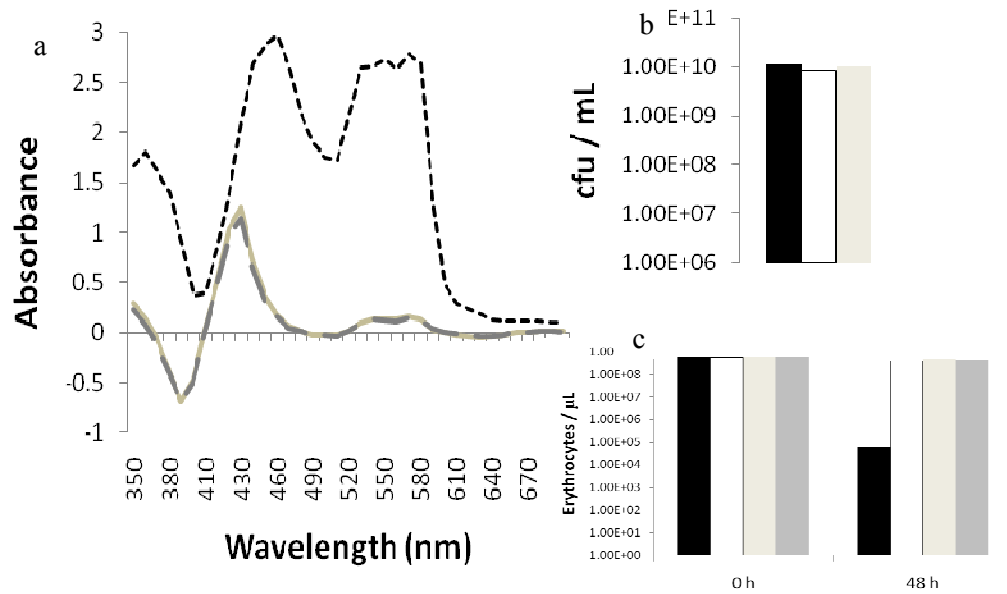


**Figure 9. Development of a high-throughput liquid hemolysis assay. A.**

Absorbance of blood broth supernatants across a range of wavelengths after 24 hour incubation with wt DBO1 and two NRPS cluster mutants. Wild type DBO1 = dotted black line, *6466::oriTp<sup>R</sup>* (*luxR* mutant) = solid grey line, *6477::oriTp<sup>R</sup>* (polyketide synthetase mutant) = dotted grey line. B. Viable plate counts after 24 h. Wild type DBO1 = black, *6466::oriTp<sup>R</sup>* = white, *6477::oriTp<sup>R</sup>* = grey. B. Erythrocyte counts. Wild type DBO1 = black, *6466::oriTp<sup>R</sup>* = white, *6477::oriTp<sup>R</sup>* = light grey, blank control (no bacteria added) = dark grey. (64)

As described previously (38, 63), the NRPS product occidiofungin is a cyclic lipopeptide comprising eight amino acids. At least two forms of the peptide exist. One form contains a xylose side chain (occidiofungin 1229), which is presumably added to the peptide by the predicted glycosyltransferase encoded within the NRPS gene cluster. The other form contains no xylose side chain (burkholdine 1097). While the xylose-containing peptide was shown to have antifungal activity, the peptide lacking xylose displayed little activity (38, 63). To determine whether we would observe differences in hemolytic activity produced by the different *Bv* DBO1 NRPS cluster mutants, including the glycosyltransferase mutant *6471::Tp<sup>R</sup>*, DBO1 mutants were incubated with human erythrocytes for a period of two days, and the absorbance at 570 nm of the supernatants was taken each day. As shown in Figure 10, there are three potential hemolytic phenotypes demonstrated by the strains. First, there is a fully hemolytic phenotype characteristic of both wild type DBO1 and strains containing mutations to genes outside of the NRPS gene cluster (*6465* and *6479*). In addition, genes *6469* and *6470*, although by location included as a part of the NRPS gene cluster, are not essential to the production of hemolytic activity, as their mutation does not significantly alter wildtype hemolytic activity. Secondly, there is an intermediate hemolytic phenotype exhibited by mutant *6471::Tp<sup>R</sup>*, likely due to the lack of a xylose addition to the final product, as described for occidiofungin (38, 63). Whereas xylose addition to occidiofungin appears to be essential for antifungal activity, the absence of NRPS product glycosylation in DBO1 reduces but does

not eliminate the hemolytic activity of the NRPS-derived compound in *Bv* DBO1. Finally, there is a complete abrogation of hemolysis in strains containing mutations to genes *6466* (encoding a LuxR regulator), *6469* (encoding a cyclic peptide transporter), *6472* (encoding an adenylation domain-containing protein [ADCP]), *6473* (encoding an ADCP), *6474* (encoding an ADCP), *6476* (encoding an ADCP-polyketide synthetase [PKS]), *6477* (encoding a PKS), and *6478* (encoding a PKS). To prove that the DBO1 genes identified by mutagenesis were indeed responsible for the defect in hemolytic activity observed, genetic complementation was achieved for cluster gene *6466* (Figure 4), and partial complementation to wildtype hemolytic activity was obtained for gene *6469* (data not shown). When gene *6466* is cloned behind a rhamnose inducible promoter in plasmid pSCRhaTc-*6466*<sup>His</sup> (forming plasmid p66), and introduced into DBO1 mutant *6466::Tp*<sup>R</sup>, the addition of 0.2% rhamnose results in full restoration of hemolytic activity as measured by hemoglobin release, whereas *6466::Tp*<sup>R</sup>/p66 without added rhamnose remains non-hemolytic.

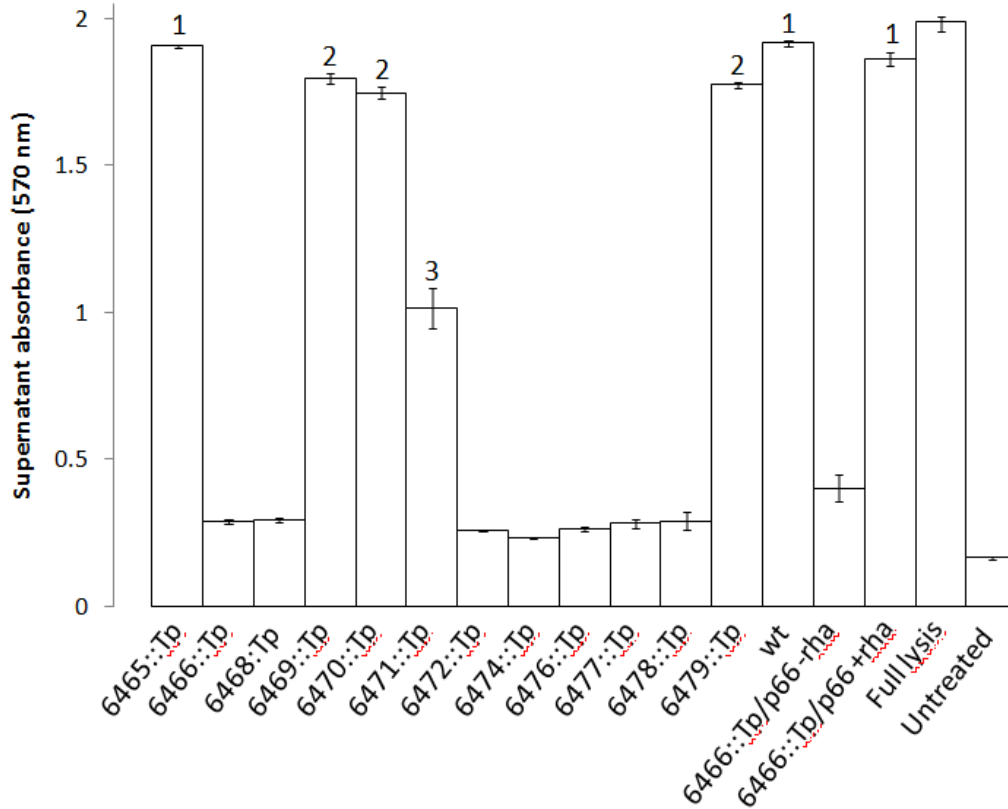


**Figure 10. Lysis of human erythrocytes by *B. vietnamiensis* DBO1 requires the intact NRPS cluster, including biosynthetic genes and Lux regulators.**

Supernatant absorbance (570 nm) was taken of each strain incubated in TSB + 5% human erythrocytes after shaking at 30 °C for 48 h. Wt = wild type; 6466::Tp<sup>R</sup>/p66 -rha and 6466::Tp<sup>R</sup>/p66 +rha = complemented mutant 6466::Tp<sup>R</sup>/pSCRhaTc-6466<sup>His</sup> incubated with and without 0.2% rhamnose, respectively. Error bars denote standard deviation from three independent trials performed in triplicate. Digits above bars indicate statistically different groups (p<0.05, n=3). (64)

## Virulence in multiple model hosts

To explore the importance of the NRPS product in virulence, *Bv* DBO1 strains (wild type, 6466::Tp<sup>R</sup>, 6469::Tp<sup>R</sup>, 6470::Tp<sup>R</sup>, 6471::Tp<sup>R</sup>, and 6472::Tp<sup>R</sup>) were grown overnight and inoculated at 1.2-1.7x10<sup>7</sup> cfu into *G. mellonella* (Greater wax moth) larvae. The results shown in Figure 11 indicate that the DBO1 NRPS product is toxic to the *G. mellonella* moth larvae, and the absence of the predicted xylose residue in the 6471::Tp<sup>R</sup> mutant has no apparent impact on this toxicity. Mutants demonstrating decreased virulence include the putative NRPS cluster regulator mutant 6466::Tp<sup>R</sup>, the cyclic peptide transporter mutant 6469::Tp<sup>R</sup>, and the NRPS enzyme mutant 6472::Tp<sup>R</sup>. Gene 6470, which encodes a hypothetical protein, has no apparent effect on the toxicity of the compound.

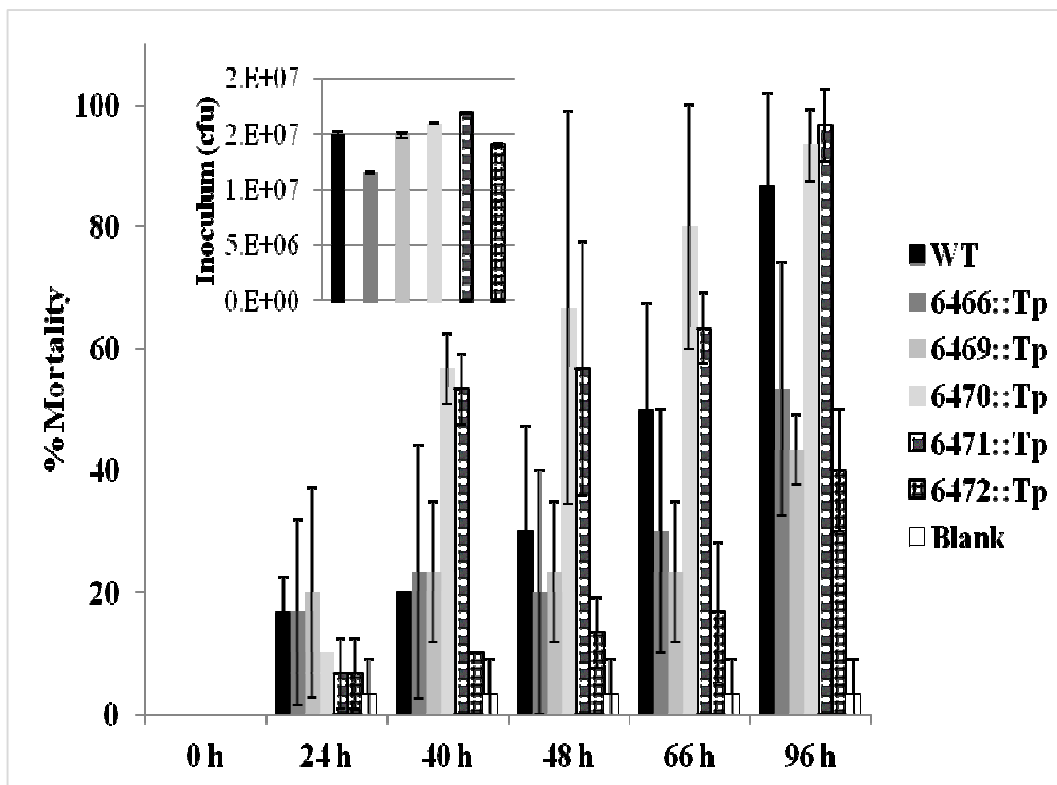


**Figure 11. *B. vietnamiensis* DBO1 requires intact NRPS cluster genes for full virulence against *Galleria mellonella* larvae.** Five microlitres of suspensions of the bacterial strains containing inocula shown in the embedded graph were inoculated into 10 larvae in 3 biological replicates. Strains are described in Table 2. The infected larvae were incubated at 30 °C and survival counts were taken at the timepoints shown. Results are shown as average larval mortality (%) +/- SD.

To demonstrate the restoration of the virulence phenotype by genetic complementation, *Bv* DBO1 strains (wildtype, *6466::Tp<sup>R</sup>* and *6466::Tp<sup>R</sup>/p66*) were grown overnight and inoculated at  $5 \times 10^6$  cfu into *G. mellonella* (Greater wax moth) larvae. Larval death counts were taken every 24 h. The results indicate that the DBO1 NRPS product is toxic to the *G. mellonella* moth larvae, whereas a gene *6466* LuxR knockout mutant (*6466::Tp*) lacking the ability to produce the hemolysin has reduced virulence. Genetic complementation of this gene knockout, as described above for hemoglobin release, showed similar restoration of the toxic effects towards *G. mellonella* upon the addition of rhamnose. Since moth larvae do not contain red blood cells, the results illustrated in Figure 12 suggest that the hemolytic NRPS product is not strictly a hemolysin, but rather a cytotoxin, possibly active against several cell types including fungi (as demonstrated for *B. contaminans* MS14 occidiofungin), insects, amoebae, and higher organisms.

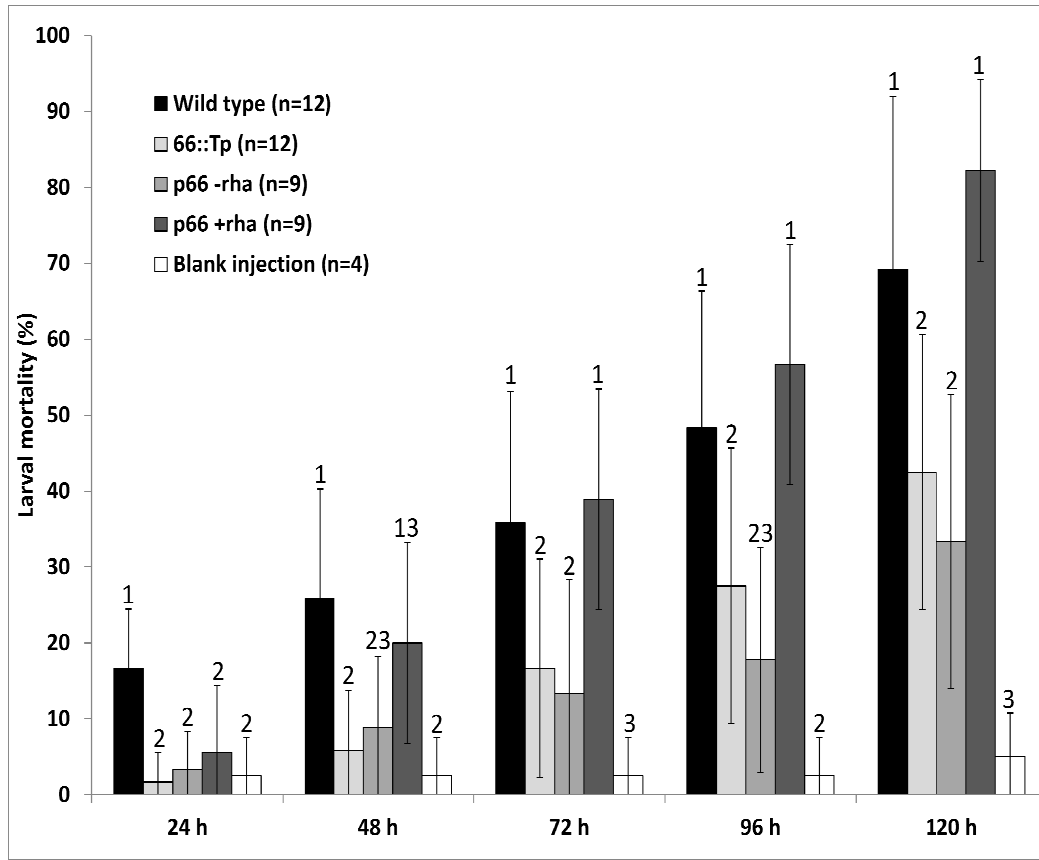


**Figure 12. Genetic complementation of a putative NRPS cluster regulator in *B. vietnamiensis* DBO1 restores full virulence against *Galleria mellonella***

**larvae.** Five microlitres of bacterial suspension, corresponding to  $5 \times 10^6$  colony forming units, was inoculated into 10 larvae in  $n$  independent trials. The infected larvae were incubated at 30 °C and viability counts were taken at 24 h intervals.

[66Tp<sup>R</sup> = strain 6466::Tp<sup>R</sup>; p66 = 6466::Tp<sup>R</sup> carrying complementation vector pSCRha-6466<sup>His</sup>]. Error bars = +/- SD. Digits above bars indicate statistical differences as determined by a Student's t-test ( $p < 0.01$ ).

(64)

To further this hypothesis, DBO1 strains exhibiting NRPS hemolytic activity, as well as isogenic mutants defective in hemolysin production, were tested in a *Dictyostelium discoideum* feeding infection model (52). We were unable to detect differences in virulence towards grazing *D. discoideum* in DBO1 strains either producing or not producing the NRPS toxin, possibly because the type VI secretion system of *Bv*, which likely contributes in large part to the toxicity of these bacteria toward amoebae, was still functional. Finally, the virulence of DBO1 and 6466::Tp were compared in the duckweed infection model described in Chapter 1. Although only a single trial was carried out for the mutant, the results suggest that 6466::Tp is attenuated relative to the wild type strain (Figure 13). Further work should clarify the role of the NRPS toxin in plant pathogenesis.

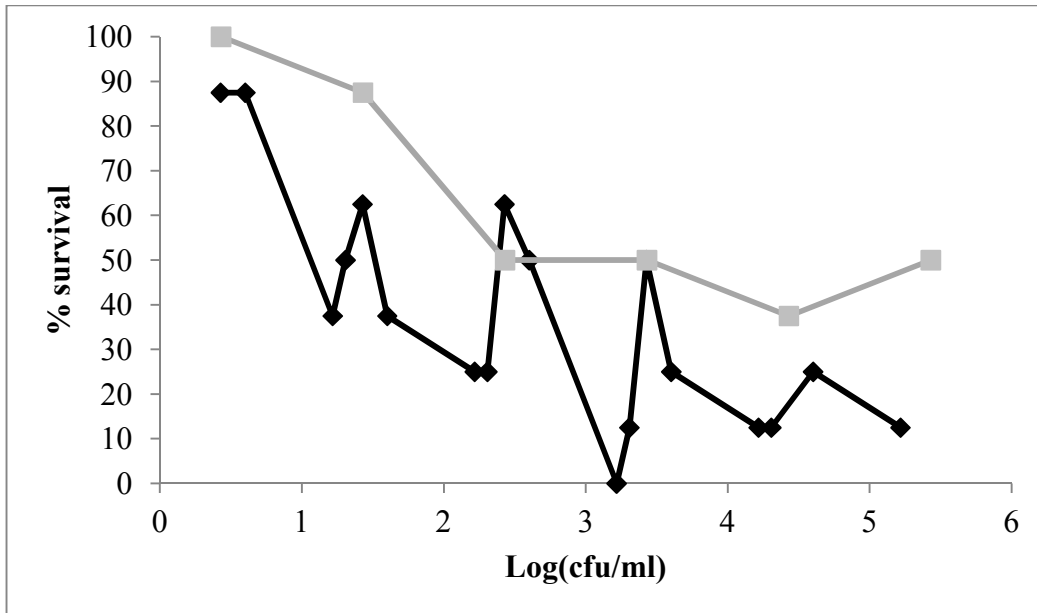


**Figure 13. *B. vietnamiensis* DBO1 may require a putative NRPS cluster regulator for full virulence against *Lemna minor*.** Bacteria were inoculated into plant-containing wells of a 96 well plate which was placed at 30 °C for 4 days. Black, plant survival during co-incubation with wild type DBO1 ( $n = 4$ ); grey, plant survival during co-incubation with *6466::Tp* ( $n = 1$ ).

### Prevalence of the NRPS gene cluster in the Bcc species

In order to determine how prevalent occidiofungin compounds are across members of the Bcc, we screened all available Bcc isolates in our library using PCR primers designed from homologous regions between known sequences of *B. contaminans* MS14 and *B. ambifaria* AMMD. The primers were also designed to amplify the regions within these genes showing no homology to other sequenced genes. Of 54 isolates screened, thirteen yielded PCR products for at least two of the primer sets, and of those thirteen, ten yielded products in all three primer sets

(Table 4). Using the same assay as described above, hemolysis of human erythrocytes by each of the thirteen strains was investigated. Of the ten Bcc strains positive for all three PCR products, seven of them demonstrated high levels of hemolytic activity against human erythrocytes. Of the three Bcc strains positive for only two of the three PCR products, only one of these exhibited any hemolytic activity, and this was at a low level (Figure 14). In addition, analysis of other *Burkholderia* genomes currently available in the GenBank database indicate that no additional Bcc genomes contain NRPS genes or gene clusters similar to those identified in AMMD, DBO1, or MS14 (Table 4). It is important to note that the apparent presence of these NRPS genes is required for hemolytic activity but does not guarantee its production, possibly due to small, acquired mutations in the NRPS gene cluster in some Bcc strains. Overall, hemolytic or toxic activity produced by an NRPS-derived occidiofungin-like compound appears to be limited to the Bcc species *B. ambifaria*, *B. contaminans*, *B. pyrrocinia*, and *Bv*.

**Table 4. Bcc and related strains analyzed in this study. (64)**

<b>Species</b>	<b>Strain</b>	<b>PCR products</b>	<b>Hemolysis</b>	<b>Source/info</b>
<i>B. cepacia</i>	ATCC25416 <sup>T</sup>	ND	NT	Onion rot
<i>B. cepacia</i>	LMG18821	ND	None	CF isolate
<i>B. cepacia</i>	ATCC17759	ND	None	Soil
<i>B. cepacia</i>	CEP521	ND	None	CF isolate
<i>B. multivorans</i>	LMG13010 <sup>T</sup>	ND	None	CF isolate
<i>B. multivorans</i>	ATCC17616	ND	None	Anthranilate enrichment

<i>B. multivorans</i>	PC249-2	ND	None	ATCC17616 mutant
<i>B. multivorans</i>	C5393	ND	None	CF isolate
<i>B. multivorans</i>	C3430	ND	None	CF isolate
<i>B. multivorans</i>	C5274	ND	None	CF isolate
<i>B. multivorans</i>	C5568	ND	NT	CF isolate
<i>B. multivorans</i>	CGD1	ND*	NT	CGD isolate
<i>B. multivorans</i>	CGD2	ND*	NT	CGD isolate
<i>B. cenocepacia</i>	J2315 <sup>T</sup>	ND <sup>(*)</sup>	None	CF isolate
<i>B. cenocepacia</i>	K56-2	ND	None	CF isolate
<i>B. cenocepacia</i>	PC184	ND	NT	CF isolate
<i>B. cenocepacia</i>	715j	6472	None	CF isolate
<i>B. cenocepacia</i>	K63-3	6472	NT	CF isolate
<i>B. cenocepacia</i>	C1257	ND	None	CF isolate
<i>B. cenocepacia</i>	C4455	ND	None	CF isolate
<i>B. cenocepacia</i>	C5424	ND	NT	CF isolate
<i>B. cenocepacia</i>	C6433	ND	None	CF isolate
<i>B. cenocepacia</i>	BC7	ND	None	CF isolate
<i>B. cenocepacia</i>	CEP511	ND	None	CF isolate
<i>B. cenocepacia</i>	AU1045	ND*	NT	CF isolate
<i>B. cenocepacia</i>	HI2424	ND*	NT	Soil
<i>B. cenocepacia</i>	MC0-3	ND*	NT	Soil
<i>B. cenocepacia</i>	D1	ND	NT	Environmental isolate
<i>B. stabilis</i>	LMG14294 <sup>T</sup>	6472, 6474,	None	CF isolate

		6476		
<i>B. stabilis</i>	LMG18870	ND	None	CF isolate
<i>B. vietnamiensis</i>	LMG10929 <sup>1</sup>	6472, 6474, 6476	None	Soil rhizosphere
<i>B. vietnamiensis</i>	DB01	6472, 6474, 6476	High	Phthalate enrichment
<i>B. vietnamiensis</i>	LMG18835	6472, 6474, 6476	High	CF isolate
<i>B. vietnamiensis</i>	G4	ND <sup>(*)</sup>	NT	Trichloroethene enrichment
<i>B. dolosa</i>	LMG18943 <sup>1</sup>	ND	None	CF isolate
<i>B. dolosa</i>	L06	ND	NT	CF isolate
<i>B. dolosa</i>	AU0645	ND	NT	CF isolate
<i>B. dolosa</i>	STM1441 / LMG21443	ND	None	Soil
<i>B. dolosa</i>	CEP021	ND	NT	CF isolate
<i>B. dolosa</i>	E12	ND	NT	CF isolate
<i>B. ambifaria</i>	AMMD <sup>1</sup>	6472, 6474, 6476	High	Soil
<i>B. ambifaria</i>	CEP0996	6472, 6474, 6476	High	CF isolate
<i>B. ambifaria</i>	LMG17828	6472, 6474, 6476	None	Soil
<i>B. ambifaria</i>	M53	6472,	High	Soil

		6474, 6476		
<i>B. pyrrocinia</i>	LMG14191 <sup>T</sup>	6472, 6474	Low	Soil
<i>B. pyrrocinia</i>	LMG21822	6472, 6474, 6476	Moderate	Soil
<i>B. pyrrocinia</i>	LMG21823	6472, 6474, 6476	None	Water
<i>B. pyrrocinia</i>	LMG21824	6472, 6474, 6476	High	CF isolate
<i>B. anthina</i>	W92 <sup>T</sup>	ND	NT	Soil
<i>B. anthina</i>	J2552	ND	NT	Soil
<i>B. anthina</i>	C1765	ND	NT	CF isolate
<i>B. anthina</i>	AU1293	6472	NT	CF isolate
<i>B. ubonensis</i>	Bu	ND*	NT	Soil
<i>B. contaminans</i>	MS14	6472, 6474, 6476*	NT	Soil
<i>B. lata</i>	383	ND*	NT	Soil
<i>B. sp.</i>	JS150	ND	NT	<i>p</i> - dichlorobenzen e enrichment
<i>R. pickettii</i>	ATCC27511 <sup>T</sup>	ND	NT	Patient isolate
<i>R. pickettii</i>	YH105	6472, 6474	None	<i>p</i> - nitrobenzoate enrichment

Superscript “T” following the strain name denotes the Type strain of each species. “ND” = Not Detected. “NT” = Not Tested. Asterisks indicate the result was

obtained using genomic analysis. “CF” = cystic fibrosis. “CGD” = chronic granulomatous disease.

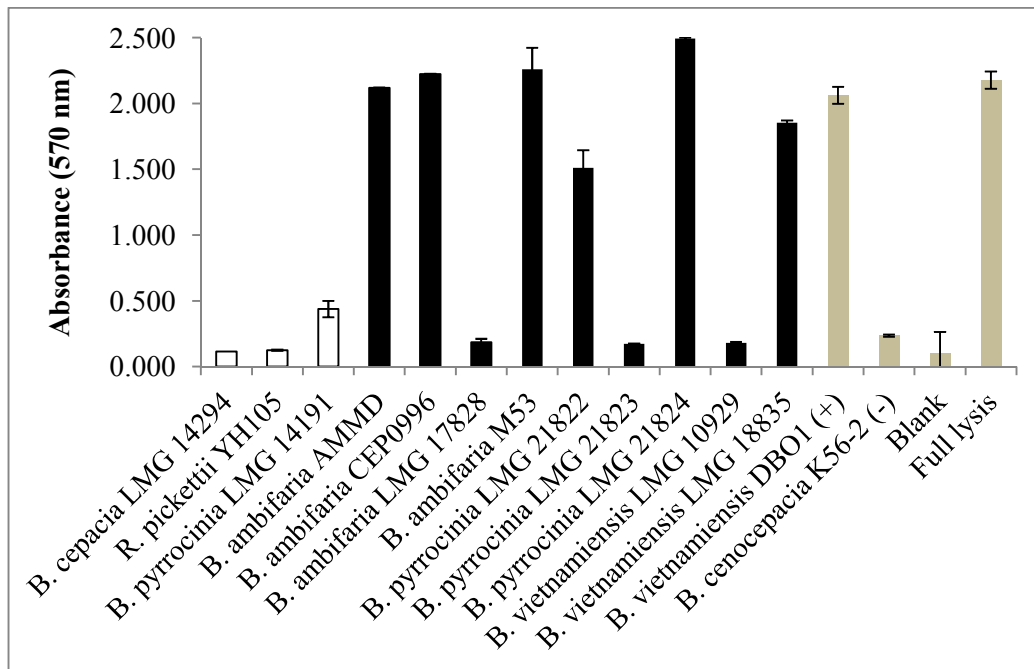


**Figure 14. Human erythrocyte lysis requires the presence of the NRPS cluster in *B. cepacia* complex isolates.** Forty-seven Bcc strains, one untyped *Burkholderia* species, and two *R. pickettii* strains and were screened using PCR primers for three of the non-ribosomal peptide biosynthesis genes within the cluster. Of the 50 strains, 13 were positive for at least two of the genes, and 10 were positive for all three genes tested. White columns = strains positive for two of the genes, black columns = strains positive for all three genes tested.  $A_{570}$  of the supernatants were taken after 48 hr incubation of the strains in TSB + 5% human erythrocytes in triplicate. Controls are shown in grey, including *B. vietnamiensis* DBO1 as positive control (+) and *B. cenocepacia* K56-2 as negative control (-).

Error bars = +/- SD of triplicates. Similar results were observed in a second trial.

(64)

## Discussion

Bcc species *B. contaminans* MS14 produces cellular toxins that are synthesized using a non-ribosomal peptide synthase pathway, which is characteristic of complex secondary metabolite compounds. These compounds, known as occidiofungins or burkholdines, have been previously shown to have antifungal activity (39, 63), but herein we show that these compounds, or compounds closely related to occidiofungins (based partially on biosynthetic gene cluster similarities), also possess high levels of hemolytic activity. Besides individual ORF homology and syntenic organization between the gene clusters in MS14, *B. ambifaria* AMMD, and *Bv* DBO1, the hemolysis results from the glycosyltransferase mutant in DBO1 suggest that the NRPS-derived compounds from the three Bcc strains are similar. Prior structural analysis of the MS14 NRPS compound suggests that the ring peptide can be glycosylated by xylose, and that without this glycosylation, the antifungal properties of occidiofungin are lost. However, genetic inactivation of *Bv* DBO1 NRPS gene cluster homologue *6471*, encoding the putative glycosyltransferase, reduces hemolytic activity by approximately half but has no effect on the toxicity of the compound toward *G. mellonella* larvae. This suggests that the natural target of both forms of occidiofungin may be towards eukaryotic cells in general (including

erythrocytes), but that the unglycosylated form of the NRPS peptide is only capable of killing a subset of cell types, including insect and fungal cells.

To examine whether other Bcc strains possess the NRPS gene cluster, PCR primer sets localized to unique sequences were used to probe for the presence of two NRPS genes. This analysis identified 13 of 54 Bcc strains potentially carrying the NRPS gene cluster. Further analysis with another unique PCR primer pair reduced this number to ten strains that carried three NRPS genes. Upon functional testing, only seven of these ten strains exhibited hemolysis of human erythrocytes, suggesting that two strains (*B. pyrrocinia* LMG 14294 and *Bv* LMG 10929) possessed undefined mutations to the hemolytic gene cluster or do not express the NRPS cluster genes under the experimental conditions. In addition, only two PCR products were amplified from *B. ambifaria* CEP0996, although this strain exhibited hemolytic activity in this assay. This suggests that either one set of primer pairs was divergent from the CEP0996 genomic sequence, inhibiting amplification of the NRPS orthologue from this strain, or that this strain produces a hemolytic toxin different from occidiofungin. A noteworthy finding is the probable unification of the recently described occidiofungin or burkholdine with the much earlier xylocandins. The likelihood of their shared identity rests on the experimental amplification of the occidiofungin-synthesizing NRPS genes in *B. pyrrocinia* LMG 21822 in conjunction with this strain's hemolytic activity demonstrated in this study.

In terms of medical relevance, this NRPS gene cluster has not been identified in the two most clinically prevalent Bcc species, *Burkholderia*

*multivorans* and *B. cenocepacia*. Although clinical Bcc strains can exhibit little difference from strains found in the environment (3), the identification of this NRPS gene cluster in Bcc species better adapted to soil environments than to association with humans suggests that this gene cluster evolved to protect the Bcc from ecological niche predators such as fungi and amoeba rather than as a virulence factor to assist invasion of human tissue. A virulence-linked secondary metabolite produced by *B. cenocepacia* is synthesized by the gene products of the *afc* cluster in strain J2315. The cluster is positively regulated by the LysR-like global regulator ShvR (49) and the metabolite, which is expected to resemble a lipopeptide initially identified in *B. pyrrocinia* (29), contributes to biofilm formation, antifungal activity and virulence in both plants and chronic rat infection (61). These phenotypes have recently been linked to lipid metabolism, since relative cellular lipid concentrations vary between wild type *B. cenocepacia* and various *afc* cluster mutants (60). The authors suggest that such modification could alter other phenotypes dependent on lipids, such as swarming motility.

The literature on NRPS and PKS systems indicates that associated dedicated glycosyltransferases are not uncommon. Although the xylose moiety appears to enhance hemolytic activity of the Bcc NRPS-derived compound, the exact mechanism through which this is achieved awaits further investigation. Walsh *et al.* (68) describe a possible function of such glycosyltransferases as having a role in imparting polarity or solubility to hydrophobic compounds, thus improving their access into target cell surfaces. The combined results of this and

previous studies on occidiofungin (25, 63) suggest that glycosylation is important for full toxicity of the compound only against certain host cells.

At the time of this study's publication, several key questions remained with respect to the function of some ORFs found within the NRPS cluster, and some of these questions have since been answered in recent publications. First, the determination that occidiofungin has hemolytic and virulence roles indicates that it may not be suitable as an antifungal therapy in humans. However, one study examined the hemolytic and antifungal properties of five occidiofungin variants from a single *B. cepacia* strain, finding that while all variations on the compound permit both antifungal activity and hemolysis, one variation produces much greater activity against fungal cells than erythrocytes (37). This is a desirable trait for a potential therapeutic agent. Another study provided some support for the possible therapeutic role of occidiofungins by demonstrating that at a 1 mg/kg dose, the compound produced no significant deleterious effects on mice, though all doses higher than 1 mg caused decreased body and organ weight and all doses caused cytotoxicity in a rat cell line (62). A second unanswered question concerned occidiofungin's mechanism of action. It was determined that the compound activates apoptosis in yeast cells, thereby joining a new class of antifungal agents (17). The existing classes target cell membrane integrity and cell wall biosynthesis without activating apoptosis. This novel mechanism of action is exciting, since apoptosis in fungi occurs through a different pathway than in mammalian cells.

Other lingering questions following the publication of this study concerned the genetic structure of the NRPS cluster. Two genes within the cluster contain thioesterase (TE) domains (*6482* and *6472*), which is unusual for the enzyme complexes, which are typically cyclized by a single terminal thioesterase domain. (The alternate TE domain-containing protein *6482*, along with *6479*, *6480*, and *6481*, had been ignored during our study as a result of the analysis of the structure of the gene cluster and the data collected from a *6479* mutant indicating it had no role in the observed hemolytic phenotype. This was a mistake rooted in the singular focus on identifying the hemolytic properties of the compound.) However, it was discovered that having two TE domains provides added variation to the compounds that arises at the final stages of synthesis, when two forms of the peptide are already present as a result of the incorporation of a hydroxy group on a variable amino acid within the peptide. At this point in synthesis, the two TE domains have different preferences for cyclizing the peptide based on the presence or absence of a hydroxy group at the variable site. The implications for this variability manifest themselves in bioactivity, since one form of the compound has greater effects on fungi. It remains to be seen whether these isoforms vary in their bioactivity against other cell types, such as erythrocytes. Another peptide-modifying enzyme is encoded by *6471*. This glycosyltransferase was recently confirmed to add a xylose to the peptide that has no role in its antifungal activity (11). However, this leaves unsolved a primary finding of the present study showing a partially attenuating effect on hemolysis when *6471* is disrupted. Because of the hemolysis-attenuating effect of mutagenizing the

glycosyltransferase, it seems likely that the peptide has greater surface-active properties when glycosylated, consistent with the polarity-enhancing effects of peptide glycosylation proposed by Walsh *et al.* (68). While this modification could provide greater access to the cell surface for membrane disruption, it has no apparent effect on the fungal apoptotic activation. This access to the cell surface could be tested through solvent partitioning experiments, to show increased solubility of the glycopeptide in water versus the unglycosylated form. Gene 6470, immediately downstream of 6471, encodes a hypothetical protein that has no effect on hemolytic activity. Gene 6467, overlapping the two *luxR* homologue ORFs, is a small ORF encoding a potential product of only 110 amino acids, with no homology to any known protein. This may be a truncated ORF that was introduced along with the upstream *luxR* family transcriptional regulator gene 6468 during acquisition and assembly of the NRPS cluster. However, this ORF has not been characterized in the recent literature. Gene 6475, situated between two large genes encoding proteins with amino acid adenylation domains, encodes a 538 amino acid protein that contains a  $\beta$ -lactamase domain. Rather than providing cellular resistance to antibiotics, this protein is likely involved in the synthesis of  $\beta$ -hydroxytyrosine, as suggested by a homology study performed by Gu *et al.* (24). Because we were unable to amplify PCR constructs to mutagenize gene 6475, a role in hemolysis for this gene remains to be determined. All other genes in the strain DBO1 NRPS gene cluster are essential for hemolytic activity.

Our results suggest that the Bcc occidiofungin-like cyclic peptide targets and disrupts components of the membranes of eukaryotic cells, but not

prokaryotic cells. Subsequent analysis by other groups suggest that while higher doses of the compound are harmful to mammals, there exist several isoforms of the compound that have highly variable effects on mammalian and fungal toxicity. In any case, the compound does not appear to be prevalent among Bcc species that commonly infect CF patients, nor was it commonly found in clinical isolates. Therefore, it is likely that occidiofungin-like compounds have evolved for predation defence in the soil habitats of the Bcc and have not been maintained to provide any particular pathogenesis-related advantage to these bacteria.

## References

1. Abe M, Nakazawa T. Characterization of hemolytic and antifungal substance, cepalycin, from *Pseudomonas cepacia*. *Microbiol Immunol*. 1994;38(1):1-9.
2. Altschul SF, Gish W, Miller W, Myers EW, Lipman DJ. Basic local alignment search tool. *J Mol Biol*. 1990;215(3):403-10.
3. Bevivino A, Dalmastrì C, Tabacchioni S, Chiarini L, Belli ML, Piana S, et al. *Burkholderia cepacia* complex bacteria from clinical and environmental sources in Italy: genomovar status and distribution of traits related to virulence and transmissibility. *J Clin Microbiol*. 2002;40(3):846-51.
4. Bisacchi GS, Hockstein DR, Koster WH, Parker WL, Rathnum ML, Unger SE. Xylocandin: a new complex of antifungal peptides. II. Structural studies and chemical modifications. *J Antibiot*. 1987;40(11):1520-9.
5. Burns JL, Wadsworth CD, Barry JJ, Goodall CP. Nucleotide sequence analysis of a gene from *Burkholderia (Pseudomonas) cepacia* encoding an outer membrane lipoprotein involved in multiple antibiotic resistance. *Antimicrob Agents Chemother*. 1996;40(2):307-13.
6. Buroni S, Pasca MR, Flannagan RS, Bazzini S, Milano A, Bertani I, et al. Assessment of three Resistance-Nodulation-Cell Division drug efflux transporters of *Burkholderia cenocepacia* in intrinsic antibiotic resistance. *BMC Microbiol*. 2009;9:200.
7. Cardona ST, Valvano MA. An expression vector containing a rhamnose-inducible promoter provides tightly regulated gene expression in *Burkholderia cenocepacia*. *Plasmid*. 2005;54(3):219-28.
8. Carvalho AP, Ventura GM, Pereira CB, Leao RS, Folescu TW, Higa L, et al. *Burkholderia cenocepacia*, *B. multivorans*, *B. ambifaria* and *B. vietnamiensis* isolates from cystic fibrosis patients have different profiles of exoenzyme production. *APMIS*. 2007;115(4):311-8.
9. Challis GL. A widely distributed bacterial pathway for siderophore biosynthesis independent of nonribosomal peptide synthetases. *Chembiochem*. 2005;6(4):601-11.
10. Challis GL, Ravel J, Townsend CA. Predictive, structure-based model of amino acid recognition by nonribosomal peptide synthetase adenylation domains. *Chem Biol*. 2000;7(3):211-24.
11. Chen KC, Ravichandran A, Guerrero A, Deng P, Baird SM, Smith L, et al. The *Burkholderia contaminans* MS14 ocfC gene encodes a xylosyltransferase for production of the antifungal occidiofungin. *Appl Environ Microbiol*. 2013;79(9):2899-905.
12. Dennis JJ, Zylstra GJ. Plasposons: modular self-cloning minitransposon derivatives for rapid genetic analysis of gram-negative bacterial genomes. *Appl Env Microbiol*. 1998;64(7):2710-5.
13. Di Lorenzo M, Poppelaars S, Stork M, Nagasawa M, Tolmasky ME, Crosa JH. A nonribosomal peptide synthetase with a novel domain organization is essential for siderophore biosynthesis in *Vibrio anguillarum*. *J Bacteriol*. 2004;186(21):7327-36.

14. Drevinek P, Mahenthiralingam E. *Burkholderia cenocepacia* in cystic fibrosis: epidemiology and molecular mechanisms of virulence. *Clin Microbiol Infect.* 2010;16(7):821-30.
15. Eggers CT, Murray IA, Delmar VA, Day AG, Craik CS. The periplasmic serine protease inhibitor ecotin protects bacteria against neutrophil elastase. *Biochem J.* 2004;379(Pt 1):107-18.
16. el-Banna N, Winkelmann G. Pyrrolnitrin from *Burkholderia cepacia*: antibiotic activity against fungi and novel activities against streptomycetes. *J Appl Microbiol.* 1998;85(1):69-78.
17. Emrick D, Ravichandran A, Gosai J, Lu S, Gordon DM, Smith L. The antifungal occidiofungin triggers an apoptotic mechanism of cell death in yeast. *J Nat Prod.* 2013;76(5):829-38.
18. Engledow AS, Medrano EG, Mahenthiralingam E, LiPuma JJ, Gonzalez CF. Involvement of a plasmid-encoded type IV secretion system in the plant tissue watersoaking phenotype of *Burkholderia cenocepacia*. *J Bacteriol.* 2004;186(18):6015-24.
19. Estrada-De Los Santos P, Bustillos-Cristales R, Caballero-Mellado J. *Burkholderia*, a genus rich in plant-associated nitrogen fixers with wide environmental and geographic distribution. *Appl Environ Microbiol.* 2001;67(6):2790-8.
20. Fehlner-Gardiner CC, Hopkins TM, Valvano MA. Identification of a general secretory pathway in a human isolate of *Burkholderia vietnamiensis* (formerly *B. cepacia* complex genomovar V) that is required for the secretion of hemolysin and phospholipase C activities. *Microb Path.* 2002;32(5):249-54.
21. Galm U, Wendt-Pienkowski E, Wang L, George NP, Oh TJ, Yi F, et al. The biosynthetic gene cluster of zorbamycin, a member of the bleomycin family of antitumor antibiotics, from *Streptomyces flavoviridis* ATCC 21892. *Mol Biosyst.* 2009;5(1):77-90.
22. Gingues S, Kooi C, Visser MB, Subsin B, Sokol PA. Distribution and expression of the ZmpA metalloprotease in the *Burkholderia cepacia* complex. *J Bacteriol.* 2005;187(24):8247-55.
23. Glendinning KJ, Parsons YN, Duangsonk K, Hales BA, Humphreys D, Hart CA, et al. Sequence divergence in type III secretion gene clusters of the *Burkholderia cepacia* complex. *FEMS Microbiol Lett.* 2004;235(2):229-35.
24. Gu G, Smith L, Liu A, Lu SE. Genetic and biochemical map for the biosynthesis of occidiofungin, an antifungal produced by *Burkholderia contaminans* strain MS14. *Appl Environ Microbiol.* 2011;77(17):6189-98.
25. Gu G, Smith L, Wang N, Wang H, Lu SE. Biosynthesis of an antifungal oligopeptide in *Burkholderia contaminans* strain MS14. *Biochem Biophys Res Commun.* 2009;380(2):328-32.
26. Gu G, Wang N, Chaney N, Smith L, Lu SE. AmbR1 is a key transcriptional regulator for production of antifungal activity of *Burkholderia contaminans* strain MS14. *FEMS Microbiol Lett.* 2009;297(1):54-60.
27. Jacobsen CS, Pedersen JC. Mineralization of 2,4-dichlorophenoxyacetic acid (2,4-D) in soil inoculated with *Pseudomonas cepacia* DBO1(pRO101), *Alcaligenes eutrophus* AEO106(pRO101) and *Alcaligenes eutrophus*

- JMP134(pJP4): effects of inoculation level and substrate concentration. *Biodeg.* 1991;2(4):253-63.
28. Jassem AN, Zlosnik JE, Henry DA, Hancock RE, Ernst RK, Speert DP. In vitro susceptibility of *Burkholderia vietnamiensis* to aminoglycosides. *Antimicrob Agents Chemother.* 2011;55(5):2256-64.
29. Kang Y, Carlson R, Tharpe W, Schell MA. Characterization of genes involved in biosynthesis of a novel antibiotic from *Burkholderia cepacia* BC11 and their role in biological control of *Rhizoctonia solani*. *Appl Env Microbiol.* 1998;64(10):3939-47.
30. Kerr J. Inhibition of fungal growth by *Pseudomonas aeruginosa* and *Pseudomonas cepacia* isolated from patients with cystic fibrosis. *J Infect.* 1994;28(3):305-10.
31. Kooi C, Subsin B, Chen R, Pohorelic B, Sokol PA. *Burkholderia cenocepacia* ZmpB is a broad-specificity zinc metalloprotease involved in virulence. *Infect Immun.* 2006;74(7):4083-93.
32. Lamothe J, Thyssen S, Valvano MA. *Burkholderia cepacia* complex isolates survive intracellularly without replication within acidic vacuoles of *Acanthamoeba polyphaga*. *Cell Microbiol.* 2004;6(12):1127-38.
33. Lee CH, Kim S, Hyun B, Suh JW, Yon C, Kim C, et al. Cepacidine A, a novel antifungal antibiotic produced by *Pseudomonas cepacia*. I. Taxonomy, production, isolation and biological activity. *J Antibiot (Tokyo).* 1994;47(12):1402-5.
34. Levy A, Chang BJ, Abbott LK, Kuo J, Harnett G, Inglis TJ. Invasion of spores of the arbuscular mycorrhizal fungus *Gigaspora decipiens* by *Burkholderia* spp. *Appl Environ Microbiol.* 2003;69(10):6250-6.
35. Li X, Yu HY, Lin YF, Teng HM, Du L, Ma GG. Morphological changes of *Fusarium oxysporum* induced by CF66I, an antifungal compound from *Burkholderia cepacia*. *Biotechnol Lett.* 2010;32(10):1487-95.
36. Lim Y, Suh JW, Kim S, Hyun B, Kim C, Lee CH. Cepacidine A, a novel antifungal antibiotic produced by *Pseudomonas cepacia*. II. Physico-chemical properties and structure elucidation. *J Antibiot.* 1994;47(12):1406-16.
37. Lin Z, Falkinham JO, 3rd, Tawfik KA, Jeffs P, Bray B, Dubay G, et al. Burkholdines from *Burkholderia ambifaria*: antifungal agents and possible virulence factors. *J Nat Prod.* 2012;75(9):1518-23.
38. Lu SE, Novak J, Austin FW, Gu G, Ellis D, Kirk M, et al. Occidiofungin, a unique antifungal glycopeptide produced by a strain of *Burkholderia contaminans*. *Biochem.* 2009;48(35):8312-21.
39. Lu SE, Novak J, Austin FW, Gu G, Ellis D, Kirk M, et al. Occidiofungin, a unique antifungal glycopeptide produced by a strain of *Burkholderia contaminans*. *Biochem.* 2009;48(35):8312-21.
40. Mahenthiralingam E, Urban TA, Goldberg JB. The multifarious, multireplicon *Burkholderia cepacia* complex. *Nat Rev Microbiol.* 2005;3(2):144-56.
41. Malott RJ, Sokol PA. Expression of the *bviIR* and *cepIR* quorum-sensing systems of *Burkholderia vietnamiensis*. *J Bacteriol.* 2007;189(8):3006-16.

42. Martinez-Aguilar L, Diaz R, Pena-Cabriales JJ, Estrada-de Los Santos P, Dunn MF, Caballero-Mellado J. Multichromosomal genome structure and confirmation of diazotrophy in novel plant-associated *Burkholderia* species. *Appl Environ Microbiol.* 2008;74(14):4574-9.
43. Martins MB, Carvalho, I. Diketopiperazines: biological activity and synthesis. *Tetrahedron.* 2007;63(40):9923-32.
44. Menard A, Monnez C, Estrada de Los Santos P, Segonds C, Caballero-Mellado J, Lipuma JJ, et al. Selection of nitrogen-fixing deficient *Burkholderia vietnamiensis* strains by cystic fibrosis patients: involvement of *nif* gene deletions and auxotrophic mutations. *Environ Microbiol.* 2007;9(5):1176-85.
45. Meyers E, Bisacchi GS, Dean L, Liu WC, Minassian B, Slusarchyk DS, et al. Xylocandin: a new complex of antifungal peptides. I. Taxonomy, isolation and biological activity. *J Antibiot.* 1987;40(11):1515-9.
46. Mootz HD, Marahiel MA. Design and application of multimodular peptide synthetases. *Current opinion in biotechnology.* 1999;10(4):341-8.
47. Mullen T, Markey K, Murphy P, McClean S, Callaghan M. Role of lipase in *Burkholderia cepacia* complex (Bcc) invasion of lung epithelial cells. *Eur J Clin Microbiol Infect Dis.* 2007;26(12):869-77.
48. Nakazawa T, Yamada Y, Ishibashi M. Characterization of hemolysin in extracellular products of *Pseudomonas cepacia*. *J Clin Microbiol.* 1987;25(2):195-8.
49. O'Grady EP, Nguyen DT, Weisskopf L, Eberl L, Sokol PA. The *Burkholderia cenocepacia* LysR-type transcriptional regulator ShvR influences expression of quorum-sensing, protease, type II secretion, and *afc* genes. *J Bacteriol.* 2011;193(1):163-76.
50. O'Sullivan LA, Weightman AJ, Jones TH, Marchbank AM, Tiedje JM, Mahenthiralingam E. Identifying the genetic basis of ecologically and biotechnologically useful functions of the bacterium *Burkholderia vietnamiensis*. *Environ Microbiol.* 2007;9(4):1017-34.
51. Park JH, Hwang, I., Kim, J.-W., Lee, S.O., Conway, B., Greenberg, E.P., Kyoung, L. Characterization of quorum-sensing signaling molecules produced by *Burkholderia cepacia* G4. *J Microbiol Biotechnol.* 2001;11(5):804-11.
52. Pukatzki S, Ma AT, Sturtevant D, Krastins B, Sarracino D, Nelson WC, et al. Identification of a conserved bacterial protein secretion system in *Vibrio cholerae* using the *Dictyostelium* host model system. *PNAS USA.* 2006;103(5):1528-33.
53. Rausch C, Weber T, Kohlbacher O, Wohlleben W, Huson DH. Specificity prediction of adenylation domains in nonribosomal peptide synthetases (NRPS) using transductive support vector machines (TSVMs). *Nucleic Acids Res.* 2005;33(18):5799-808.
54. Rosales-Reyes R, Skeldon AM, Aubert DF, Valvano MA. The Type VI secretion system of *Burkholderia cenocepacia* affects multiple Rho family GTPases disrupting the actin cytoskeleton and the assembly of NADPH oxidase complex in macrophages. *Cell Microbiol.* 2012;14(2):255-73.

55. Rose H, Baldwin A, Dowson CG, Mahenthiralingam E. Biocide susceptibility of the *Burkholderia cepacia* complex. *J Antimicrob Chemother.* 2009;63(3):502-10.
56. Seed KD, Dennis JJ. Development of *Galleria mellonella* as an alternative infection model for the *Burkholderia cepacia* complex. *Infect Immun.* 2008;76(3):1267-75.
57. Shaw-Reid CA, Kelleher NL, Losey HC, Gehring AM, Berg C, Walsh CT. Assembly line enzymology by multimodular nonribosomal peptide synthetases: the thioesterase domain of *E. coli* EntF catalyzes both elongation and cyclolactonization. *Chem Biol.* 1999;6(6):385-400.
58. Shoji J, Hino H, Kato T, Hattori T, Hirooka K, Tawara K, et al. Isolation of cepafungins I, II and III from *Pseudomonas* species. *J Antibiot.* 1990;43(7):783-7.
59. Stachelhaus T, Mootz HD, Marahiel MA. The specificity-conferring code of adenylation domains in nonribosomal peptide synthetases. *Chem Biol.* 1999;6(8):493-505.
60. Subramoni S, Agnoli K, Eberl L, Lewenza S, Sokol PA. Role of *Burkholderia cenocepacia* *afcE* and *afcF* genes in determining lipid-metabolism-associated phenotypes. *Microbiology.* 2013;159(Pt 3):603-14.
61. Subramoni S, Nguyen DT, Sokol PA. *Burkholderia cenocepacia* ShvR-regulated genes that influence colony morphology, biofilm formation, and virulence. *Infect Immun.* 2011;79(8):2984-97.
62. Tan W, Cooley J, Austin F, Lu SE, Pruett SB, Smith L. Nonclinical toxicological evaluation of occidiofungin, a unique glycolipopeptide antifungal. *Int J Toxicol.* 2012;31(4):326-36.
63. Tawfik KA, Jeffs P, Bray B, Dubay G, Falkinham JO, Mesbah M, et al. Burkholdines 1097 and 1229, potent antifungal peptides from *Burkholderia ambifaria* 2.2N. *Org Lett.* 2010;12(4):664-6.
64. Thomson EL, Dennis JJ. A *Burkholderia cepacia* complex non-ribosomal peptide-synthesized toxin is hemolytic and required for full virulence. *Virulence.* 2012;3(3):286-98.
65. Toh M, Moffitt MC, Henrichsen L, Raftery M, Barrow K, Cox JM, et al. Cereulide, the emetic toxin of *Bacillus cereus*, is putatively a product of nonribosomal peptide synthesis. *J Appl Microbiol.* 2004;97(5):992-1000.
66. Vasil ML, Krieg DP, Kuhns JS, Ogle JW, Shortridge VD, Ostroff RM, et al. Molecular analysis of hemolytic and phospholipase C activities of *Pseudomonas cepacia*. *Infect Immun.* 1990;58(12):4020-9.
67. Visser MB, Majumdar S, Hani E, Sokol PA. Importance of the ornibactin and pyochelin siderophore transport systems in *Burkholderia cenocepacia* lung infections. *Infect Immun.* 2004;72(5):2850-7.
68. Walsh CT, Losey HC, Freel Meyers CL. Antibiotic glycosyltransferases. *Biochem Soc Transact.* 2003;31(Pt 3):487-92.
69. Wang JH, Quan CS, Qi XH, Li X, Fan SD. Determination of diketopiperazines of *Burkholderia cepacia* CF-66 by gas chromatography-mass spectrometry. *Anal Bioanal Chem.* 2010;396(5):1773-9.

70. Yeager CM, Bottomley, P.J., Arp, D.J. Requirement of DNA repair mechanisms for survival of *Burkholderia cepacia* G4 upon degradation of trichloroethylene. *Appl Env Microbiol.* 2001;67(12):5384-91.
71. Zhang R, LiPuma JJ, Gonzalez CF. Two type IV secretion systems with different functions in *Burkholderia cenocepacia* K56-2. *Microbiology.* 2009;155(Pt 12):4005-13.

## Chapter 3 – Identification of *Burkholderia cenocepacia* virulence factors

---

## Introduction

### *Burkholderia cenocepacia*

In Western nations between 1985 and 2004, *Bc* infections of CF patients accounted for between 45-92% of the total Bcc infections and coincide with lower survival rates among patients. Furthermore, *Bc* is the only Bcc species that causes epidemics; in addition to the ET-12 (henceforth referred to as sequence type-28 or ST-28) strain that devastated the U.K. and Canada in the 1980s-90s, the more recent epidemic strain ST-32 has appeared in a number of countries and has the apparent propensity to spread rapidly among patients in a clinical setting. These characteristics appear limited to *Bc* strains, although their genetic origins have not been determined. Interestingly, the *Bc* IIIA strains, which include the most important epidemic clones, are rarely isolated outside of clinical settings, which is unusual among the Bcc, since there are few defining features between environmental and clinical isolates of the other Bcc species (24).

One feature of the *Bc* IIIA genome that sets it apart from *Bc* IIIB is a preponderance of genomic islands (GIs): the *Bc* J2315 (a *Bc* IIIA epidemic strain of the ET-12 or ST-28 lineage) genome contains 14 GIs, none of which appear in either sequenced *Bc* IIIB strain. Furthermore, ST-28 contains multiple copies of insertion sequence IS407 (41), which was discussed in the General Introduction in the context of extensive *B. mallei* genome reduction. IS407 is absent from ST-32, another *Bc* IIIA epidemic lineage. Recently, ISs of the ST-28 and ST-32 strains were mapped and compared, and a number of similarities emerged, including the

high frequency of insertion into GIs (32). ISs of different origin in different *Bc* strains were even shown to have disrupted the same genes, and multiple ISs within ST-28 were found to disrupt two different copies of a helicase gene. These results could indicate selective convergence built into the genomic plasticity of *Bc* epidemic strains.

An important feature of the *Bc* GIs is their recently-described tendency to transpose in response to oxidative stress (22). This effect has implications both for the adaptability of the organisms, since genetic diversity would increase under the conditions of high oxidative stress characterizing chronic CF lung infection, and for clinicians' ability to correctly identify those using traditional molecular fingerprinting approaches. The *Bc* GIs remain largely uncharacterized, with the exception of the *Bc* epidemic strain marker (BCESM), which was originally described as the marker for epidemic clones. It carries genes for the *cciIR* quorum sensing system – the first description of a GI-encoded quorum sensing system – and other virulence-linked genes encoding a porin and an amidase, among others (7).

### ***Bc* virulence pathways**

A large number of *Bc* virulence determinants have been identified in isolation, although it is becoming increasingly apparent that there is interplay among many of these through both sequential and cooperative means. Furthermore, the vast discrepancy between the virulence of *B. cenocepacia* and other important Bcc species in most infection models is only beginning to be understood through comparative genomics. Because an array of *Bc* virulence

factors were already presented in the General Introduction, this section will summarize those pathways but focus primarily on traits specific to *Bc* within the context of CF-relevant infection models.

Underscoring the above-described importance of mobile elements in the *Bc* genome, a study conducted in 2005 used suppression-subtractive genomic hybridization to identify genetic elements in *Bc* that are absent from *B. stabilis* or *B. multivorans* and found that nearly half of such genes are DNA-modification, phage or IS-related. Ten percent of these genes were found within the *BcenGI5* island (11).

#### *Iron acquisition*

As discussed in the General Introduction, it is not clear whether iron is a limiting factor in the lungs of CF patients; nonetheless, transcriptomic data from *Bc* isolates suggests that the bacterial iron acquisition machinery is up-regulated during chronic infection (56). This is perhaps a result of bacterial competition or localized iron limitation within the biofilm communities. Regardless, *Bc* produces at least 3 different siderophores, including ornibactin, salicylic acid (SA), and in lesser quantities, pyochelin. Of these, ornibactin appears to be the most important, as it is able to compensate for the loss of pyochelin uptake machinery during chronic infection of the rat lung (83). However, this study did not address the role of SA, which is produced by the vast majority of Bcc isolates from the CF lung(20), except to provide evidence that SA most likely has its own receptor, despite its role as a biosynthetic intermediate of pyochelin in other organisms.

Also discussed previously, *B. cenocepacia* was the first bacterial pathogen shown to acquire iron from ferritin. This abundant molecule could represent an important host-subversion process while providing a competitive advantage for *Bc* over other CF lung microbes. So far, no other Bcc species are known to carry out this process. The extracellular protein toxin ZmpB has been shown to cleave iron sequestration molecules lactoferrin and transferrin (45).

A hemolysin with apoptotic activity against human neutrophils was described in *Bc* ST-28 that may represent another mode of iron acquisition through the lysis of erythrocytes (35). However, this molecule has not been characterized further, nor was its biosynthetic pathway identified. BCESM-encoding *Bc* may be unique among the Bcc in encoding a protein initially thought to bind heme, although whole cell lysates of all tested Bcc strains were able to sequester heme (71). The availability of heme through microbleeds (18) and hemolysis suggests that heme binding could represent another approach for iron acquisition in *Bc*. The disruption of the operon thought to encode the putative heme-binding protein was later shown to affect *Bc* viability during chronic infection of the rat lung (34).

It appears that *Bc* is well-equipped to cope with iron starvation using a vast range of tactics, including iron sequestration through siderophore production, appropriation of iron from human iron-binding molecules, and, possibly, lysis of iron-rich erythrocytes followed by uptake of heme.

### *Resistance to host defences*

Transcriptional data have unveiled a large network of gene products involved with *Bc* resistance to oxidative stress, encompassing roughly 5% of the *Bc* genome (64). The protein originally identified as a heme-binding outer membrane protein unique to epidemic *Bc* is now understood to be a catalase-peroxidase, helping *Bc* resist oxidative stress by attenuating the effects of neutrophil-produced hydrogen peroxide (71). Another catalase protein is also encoded by *Bc* and the high homology of the two proteins (73% identity) would seem to indicate redundancy (48). However, the *in vivo* viability requirement for the first catalase-peroxidase, identified by Hunt *et al.* (34), and the more in-depth characterization of the two proteins shows their functional divergence. While KatA is involved with TCA cycle protection from oxidative stress, KatB plays a more generalized protective role from hydrogen peroxide in the cell. Supporting the more global role of KatB, this enzyme is mildly up-regulated in the above-mentioned transcriptional response to oxidative stress, while KatA is not (64).

Antimicrobial peptides represent another important host defence. ZmpA and ZmpB are able to cleave cathelicidin and  $\beta$ -defensin, respectively, likely helping *Bc* resist this central host innate defence (44). ZmpB is also able to cleave immunoglobulins (Ig) (45), further subverting the host defence through inhibition of Ig-mediated opsonization complement activity. Another factor contributing to complement resistance of *Bc* is autotransporter protein Bcam0223; a mutation in this gene results in sensitivity to the classical complement pathway by uncharacterized means (55). Meanwhile, the previously-mentioned ST-28

hemolysin was shown to cause apoptosis of both human neutrophils and murine macrophages (35), representing another possible component of the extracellular toxin arsenal deployed by *Bc* to resist phagocytosis.

While macrophages and neutrophils receive the bulk of the attention where CF lung infections are concerned, dendritic cells (DCs) are a central element of both the innate and adaptive immune systems. These phagocytes were shown to undergo not only maturation arrest as a result of exposure to *Bc*, but also necrosis. Neither effect was observed following DC exposure to *B. multivorans*, highlighting yet another difference that may help explain the prognoses typically associated with the two species. However, proinflammatory cytokine production was similar in response to both species (49).

Following bacterial phagocytosis, *Bc* has a strong tendency to persist within the macrophage vacuole. It is becoming increasingly clear that the type VI secretion system (T6SS) plays central role in this host subversion, and T6SS-associated traits will be discussed further in Chapter 4. Type IV secretion also appears to be involved with this phenotype. Two type IV secretion systems (T4SSs) are present in *Bc*: a plasmid-encoded T4SS produces the PTW phenotype, while a chromosomally-encoded T4SS appears to allow conjugal DNA transfer (86). When the plasmid-encoded T4SS is knocked out, maturation of *Bc*-containing vacuoles (BcCV) proceeds and bacteria are degraded within the mature lysosome of both CF epithelial and non-CF monocyte cell lines. This contrasts processing of wild type *Bc*, in which the BcCV is diverted harmlessly to the endoplasmic reticulum (67). It remains to be seen whether the PTW phenotype

is related to intracellular persistence; if so, this points to a compelling adaptation of a plant virulence-associated protein to human infection. One way to approach this problem would be to identify the effector molecule(s) responsible for PTW, and test mutants in these genes against a human cell line.

#### *Inflammation and epithelial destruction*

In addition to its previously-described role in antimicrobial peptide resistance, ZmpA is active against a range of human structural and signalling proteins, including fibronectin, collagen and  $\gamma$ -interferon (43). This degradation of matrix proteins is perhaps associated with lipase production, which is prevalent among *Bc* strains and known to play an uncharacterized role in transepithelial migration (57).

While self-mediated migration is likely one strategy adopted by *Bc*, the abundant release of elastase by neutrophils is one of the most damaging processes by host or microbe that occurs within the CF lung and may provide alternative means of invasion into underlying tissues for *Bc*. The ST-28 hemolysin described by Hutchison *et al.* (35) was shown to cause degranulation and release of elastase by human neutrophils, which could represent an aggravating factor in this already severe inflammatory and destructive process.

Other toxins produced by *Bc* inducing inflammation and cell destruction may include type III-secreted effectors. Although such effectors have yet to be identified, knockout of the *Bc* T3SS is associated with greater bacterial clearance and lower inflammatory cell migration in mice (77).

### *Cellular invasion*

The steps to cellular invasion are typically thought to begin with adherence by the bacteria to the cell layer. Adhesins expressed by *Bc* include the cable pilus and an associated 22 kDa adhesin, several other pili that remain genetically uncharacterized, and the autotransporter encoded by *bcam0223*. Although knocking out the *Bc* autotransporter *Bcam0223* causes decreased adherence to both 16HBE14o- (CFTR<sup>+</sup>) and CFBE41o- (CFTR<sup>-</sup>) bronchial epithelial cells, the mutation does not affect invasion (55). Therefore, invasion may not depend on adherence in all cases; it is conceivable that different modes of invasion exist, for example, through biofilm formation, receptor-mediated uptake, and tight junction disruption.

Through a transposon screening of 4,000 J2315 mutants, Tomich *et al.* (78) identified a single mutant with a reduced ability to invade A549 squamous epithelial cells, carrying an insertion in a flagellar biosynthesis gene. The fact that of 4,000 mutants, only a single relevant gene was identified suggests that cellular invasion likely occurs through passive means in *Bc*, which is able to survive intracellularly using both T6S and the above-described means. Following this work, another group showed that a flagellar mutation severely attenuates *Bc* during chronic murine lung infection but does not reduce the number of bacteria appearing in the spleen or bloodstream, indicating that bacterial dissemination throughout the body is unaffected (82). The same study demonstrated the flagellar-mediated activation of TLR-5 and subsequent release of IL-8, a neutrophil chemotactic chemokine which has also been shown to promote growth

of a clinical *Bc* isolate both extracellularly and intracellularly (39). Additional research has not been performed to establish a solid role for the *Bc* flagellum in invasion of relevant, polarized cell lines, but together, these results do suggest an important virulence role for the flagellum that may be more closely linked to immune stimulation than to invasion.

High iron availability was outlined as an invasion-stimulating condition, and although its exact mechanism has not been determined, increased biofilm formation on the epithelium is likely involved (9). This may be the primary pathway by which *Bc* invades lung tissues; although *Bc* is able to disrupt tight junctions of Calu-3 and 16HBE14o- cells by unidentified factors, paracellular invasion of the monolayers was not observed (25). However, a later study using a different *Bc* strain infecting cytokeratin 13-enriched lung epithelial cells demonstrated that the *Bc* cable pilus and associated 22-kDa adhesin are able to bind CK13, and that this interaction promotes transepithelial migration (81). The authors justified their use of these specialized cell lines by explaining that in tissues undergoing chronic repair, such as the CF lung, CK13 is up-regulated and available for binding at the epithelial surface, supporting the relevance of their results.

### *Virulence regulation*

As outlined in the General Introduction, most of the work in characterizing *Bcc* quorum sensing (QS) systems has been carried out in *Bc*. Several QS systems have been identified, including CepIR, CciIR, and the BDSF system. In addition,

an orphan regulator CepR2 has been identified with a role in virulence (51). While CepR typically behaves as a positive regulator, CciR negatively operates on the same regulon (60). Genes regulated by the *Burkholderia* diffusible signal factor (BDSF) overlap with CepR-regulated genes, although the two systems appear to operate independently, without hierarchical control (70). Unique to *Bc*, the CciIR quorum sensing system is found on the BCESM island, and CciR negatively regulates the expression of hundreds of genes, including known virulence factors. The CciIR system is thought to have been acquired by horizontal gene transfer and subsequently incorporated into the *Bc* genetic circuitry, including its placement under positive regulation by CepR (50).

The *Bc* quorum sensing systems are interlaced with some global regulators. ShvR is a LysR-like regulator that positively regulates over 1,000 genes in *Bc*, including virulence-linked genes such as those comprising the two divergently-transcribed *afc* clusters, type II protein secretion and the associated *zmpA* and *zmpB* proteases (58). ShvR was also found to negatively regulate both the *cepIR* and *cciIR* quorum sensing systems, illustrating the complexity of virulence gene regulation in *Bc*. This complexity is further confounded by the recently-discovered role of AtsR, a sensor kinase hybrid encoded by *bcam0379*, in modulating expression of quorum sensing-controlled genes independently of the quorum sensing systems (4). These genes include the proteases *zmpA* and *zmpB* and the *cepI* and *cciR* quorum sensing genes themselves. AtsR was initially characterized as a repressor of type VI secretion and biofilm formation in *Bc*, with mutants of this gene showing more pronounced disruption of the macrophage

actin cytoskeleton mediated through T6SS activity (3). Another LysR-like regulator, encoded by *bcam1871*, has been implicated in virulence and shown to positively regulate *zmpA* and *zmpB*, both through the enhancement of AHL activity and through AHL-independent gene activation (61).

The fine-tuning of virulence gene regulation has recently been given some context by a study showing whole-genome transcription profiles of *Bc* J2315 under a range of physicochemical conditions. The effects of physicochemical conditions on transcription of the various virulence-linked regulators described above are summarized in

Table 5 along with *zmpA* and *zmpB*, which are regulated by most of these. The data in this table illustrate a complex interplay between environmental cues and gene regulation in *Bc* and imply a host of environmental sensors acting upstream of these regulators to drive their expression under appropriate circumstances. For example, *zmpA* is transcribed at high levels during incubation at stationary phase, in low oxygen, and during heat stress, each case coinciding

with the upregulation of at least two regulators known to activate its transcription (CepR, Bcam1871, and ShvR).

**Table 5. Transcriptional changes of virulence-linked *B. cenocepacia* regulators and exported toxins under varying physiological conditions versus normal growth controls.** Adapted from Sass *et al.* (69). Genes under strong regulation (>10-fold change) are shown in bold.

Gene ID	Annotation	Stationary phase in min. medium	Stationary phase in rich medium	6% oxygen	Oxidative stress (organic peroxide)	Oxidative stress (inorganic peroxide)	Heat stress 42.5°C	Physiological temperature 37°C vs. 20°
<i>BCAM0379</i>	AtsR	Down			Down	Down		
<i>BCAM0227</i>	BDSF sensor	Down			Down	Down		
<i>BCAM0581</i>	BDSF synthase			Down				
<i>BCAM0240</i>	CciR	Up						Down
<i>BCAM0188</i>	CepR2	Up	Up				Up	Down
<i>BCAM1868</i>	CepR	Up		Up	Down	Down		

<i>BCAM1870</i>	CepI	Up		Up	Down		Up	Up
<i>BCAM1871</i>	LysR regulator	Up	Up	Up	Down		Up	Up
<i>BCAS0225</i>	ShvR	Up	Up	Down				Up
<i>BCAS0409</i>	ZmpA	<b>Up</b>	<b>Up</b>	<b>Up</b>			<b>Up</b>	Up
<i>BCAM2307</i>	ZmpB	Up		Up	Down			

## Objectives

Although a number of *Bc* virulence factors have been discovered and tested in the various infection models, the poor prognosis associated specifically with *Bc* infection for CF patients and, particularly, lung transplant recipients has yet to be fully explained at a genotypic level. The relationship between the phytopathogenic and zoopathogenic characteristics of the Bcc have been studied to limited extents, with only a few virulence factors characterized in alfalfa, onion and lettuce plant models, some of which (the LysR regulator ShvR, the pseudopilin gene GspJ, *cepIR* quorum sensing system) appear to play roles in animal infection. Therefore, this study makes use of both the high-throughput and clonal characteristics of the newly-developed duckweed model to attempt to identify Bcc virulence determinants from a phytopathogenic perspective. This approach is hypothesized to produce novel determinants, since it is only the second high-throughput screening for attenuated mutants carried out in Bcc studies, the first having used *C. elegans* (72). The identification of such virulence determinants is expected to contribute to a broader understanding of the higher-level and CF-relevant context of *Bc* virulence.

## Materials and Methods

### Bacterial strains, plasmids, antibiotics and culture conditions

Luria-Bertani (LB) broth was prepared in deionized water to half concentration for *Bcc* strains and full concentration for *Escherichia coli* strains. Agar plates were prepared with 1.5% w/v agar. Antibiotics were included where necessary to the following concentrations: Chloramphenicol (Cm), 25 µg/mL; Trimethoprim (Tp), 100-300 µg/mL; Tetracycline (Tc), 100 µg/mL. All antibiotics were purchased from Difco through BD - Canada (Mississauga, ON). *Escherichia coli* DH5α was used for plasmid manipulation. *E. coli* strains were grown at 37 °C, while *Bc* was grown at 30 °C. All liquid cultures were shaken at 225 rpm. High-copy number plasmid pJET (Amp<sup>R</sup>) was employed in cloning experiments. For random plasposon mutagenesis, pTnMod-OTp' (Tp<sup>R</sup>) (21) was used. For genetic complementation of gene *bcal1124*, a modified form of pSCRhaB2 (9) was used carrying Tc resistance. A complete list of bacterial strains and plasmids is shown in Table 6.

**Table 6. Strains and plasmids used in this study.**

<i>Bacterial strain</i>	<i>Genotype or relevant phenotype</i>	<i>Source</i>
<i>B. cenocepacia</i>		
K56-2	Parent strain	Clinical, CF
11G10	K56-2 with <i>oriTp</i> insertion into <i>bcas0210</i>	This study
12C9	K56-2 with <i>oriTp</i> insertion into <i>bcal0311</i>	This study
16A11	K56-2 with <i>oriTp</i> insertion into <i>bcal2159</i>	This study
32B11	K56-2 with <i>oriTp</i> insertion into intergenic region between <i>bcal0549</i> and <i>bcal0550</i>	This study

42H4	K56-2 with <i>oriTp</i> insertion into an unknown location	This study
46B2	K56-2 with <i>oriTp</i> insertion into <i>bcal1124</i>	This study
50D9	K56-2 with <i>oriTp</i> insertion into <i>bcas0225</i>	This study
51H6	K56-2 with <i>oriTp</i> insertion into <i>bcas0134</i>	This study
62F12	K56-2 with <i>oriTp</i> insertion into <i>bcal0870</i>	This study
K56-2/pSCRhaTc	K56-2 carrying pSCRhaTc	
46B2/pSCRhaTc	K56-2 mutant 46B2 ( <i>bcal1124::Tp<sup>R</sup></i> ) carrying pSCRhaTc	
46B2/p1124	K56-2 mutant 46B2 carrying pSCRhaTc- <i>bcal1124<sup>His</sup></i>	This study
46B2/p1124 <sup>''</sup>	K56-2 mutant 46B2 carrying pSCRhaTc- <i>bcal1124<sup>His</sup></i> with point mutations at R204H and E336G	This study
<i>E. coli</i>		
DH5 $\alpha$	Cloning host strain	
Plasmids		
pJET1.2/blunt	Cloning vector, Amp <sup>R</sup>	Fermentas
pTnMod-OTp <sup>'</sup>	Plasposon used for random mutagenesis, Tp <sup>R</sup>	(21)
pSCRhaTc	pSCRhaB2 modified with a Tc resistance cassette inserted within <i>dhfr</i> promoter	(75)
p1124	Rhamnose-inducible plasmid pSCRhaTc carrying N-terminally 10x polyhistidine-tagged <i>bcal1124</i>	This study
p1124 <sup>R204H</sup>	Rhamnose-inducible plasmid pSCRhaTc carrying N-terminal 10x polyhistidine-tagged <i>bcal1124</i> with point mutations at R204H and E336G	This study

### Random plasposon mutagenesis and virulence screening

A mutant library carrying random genomic insertions was produced by electroporating *B. cenocepacia* K56-2 with plasposon pTnModO-Tp<sup>'</sup> and plating transformants on LB containing  $\mu\text{g/ml}$  trimethoprim (LB + Tp), as previously described (75). This library was originally created by Sarah Routier and Gerardo

Juarez-Lara and later condensed by Bridget Casey. Duckweed plants were placed individually into wells of a 96-well plate containing 200  $\mu$ l SHS. Mutant strains were grown in 96-well plates for 40 h in 200  $\mu$ l  $\frac{1}{2}$  LB + Tp100 at 30°C with shaking at 225 rpm, then ~5  $\mu$ l from each well were transferred to the plant-containing wells using a sterile 96-pin Multi-Blot Replicator (VP Scientific, San Diego, CA). Inoculated plants were then incubated at 30°C for 4 days, and surviving plants were recorded. Plasposon insertion sites were determined by plasposon rescue, as previously described (21), using restriction enzymes such as EcoRI, PstI and SphI, with target sites every ~1,000-4,000 bp in the *Bc* J2315 genome. Sequencing of the resulting plasmids was performed using BigDye Terminator v3.1 (Life Technologies, Carlsbad, CA) with sequencing primers Ori and Tp<sup>R</sup> (Table 7).

**Table 7. Oligonucleotides used in this study.**

Oligonucleotide*	Sequence (5' to 3')
<i>Complementation</i>	
1124-F	TTATTACATATGAATAACGTTAATGAAGACCAG G
1124-R	ATAAAGCTTTTAATGATGGTGATGGTGATGATG <u>GTGATGGTGTTTCATTCTGGTCCTTATCC</u>
<i>Sequencing</i>	
pJET-F	CGACTCACTATAGGGAGAGCGGC
pJET-R	AAGAACATCGATTTTCCATGGCAG
Ori	GGGGAAACGCCTGGTATC

Tp <sup>R</sup>	TTTATCCTGTGGCTGC
pSCRha-F	GGCCCATTTTCCTGTC
pSCRha-R	GCTTCTGCGTTCTGA

\*Restriction sites shown in bold; 10x polyhistidine tag underlined.

## Genetic complementation of mutant 46B2

To restore the virulence phenotype of mutant 46B2, *bcal1124* was amplified by colony PCR from *B. cenocepacia* K56-2 according to manufacturer's instructions using TopTaq (Qiagen, Inc., Hilden, Germany) and oligonucleotides (Sigma-Aldrich) 1124-F and 1124-R (Table 7). The resulting PCR construct and plasmid pSCRhaTc (75) were digested with FastDigest enzymes NdeI and HindIII (Thermo Fisher Scientific, Ltd., Waltham, MA), separated by gel electrophoresis, and purified using GeneJET Gel Extraction Kit (Thermo Fisher Scientific). The products were then ligated using T4 DNA ligase (Promega Corp., Fitchburg, WI) at 16°C overnight. *E. coli* DH5α was transformed with 5 μl of the ligation mixture and transformants were selected on LB + Tc. Plasmids were then extracted and compared by restriction digestion and gel electrophoresis as well as BigDye sequencing. *B. cenocepacia* K56-2 was transformed by electroporation and selection on LB + Tc. Plasmid isolations were carried out using GeneJET plasmid miniprep kit (Thermo Fisher Scientific).

## Duckweed infection

The standard protocol outlined in Chapter 1, Materials & Methods was followed with slight modifications. For *bcal1124* experiments, strains were grown at 30 °C for 18 h in ½ LB broth + Tc with 0.02% rhamnose. No antibiotic was

added to the plant wells, since the plants were found to be sensitive to varying degrees to tetracycline, trimethoprim, and the solvents in which they were suspended. For strains grown with rhamnose, cells were washed in SHS with 0.02% rhamnose and serial dilutions were carried out in plant-containing wells with 0.02% rhamnose.

### **Wax moth larval infection**

To compare *in vivo* virulence of wild type *Bc* K56-2 with mutants *bcal1124::Tp<sup>R</sup>* and  $\Delta$ *tssF*, *Galleria mellonella* (Greater wax moth) larvae were infected. The standard protocol from Seed and Dennis (38) was followed with several adjustments. Ampicillin was omitted from the buffer because of uncertainties surrounding its effect on the mutant; to compensate for this omission, larvae were dipped in 95% ethanol and dried on paper towel prior to injection. For *bcal1124* experiments, all strains were grown at 30 °C for 18 h in ½ LB broth + Tc + 0.02% w/v rhamnose, washed three times in 10 mM MgSO<sub>4</sub> containing 0.05% rhamnose, then serially diluted in the same buffer. The control injections included 10 mM MgSO<sub>4</sub> and 0.05% rhamnose. Infected larvae were then incubated at 30 °C for up to 96 hr. Survival data were compiled into single probit vs. inoculum graphs to determine LD<sub>50</sub>, as described in Chapter 1, Materials & Methods.

## Phenotypic characterization of mutants

### *Overgrowth phenotype*

To quantify the visual observation of dense growth during duckweed infection by mutant 46B2, overnight cultures of K56-2/pSCRhaTc, 46B2/pSCRhaTc, 46B2/p1124 and 46B2/p1124<sup>R204H</sup> were grown as described above with the addition of 100 Tc and 0.02% rhamnose and an infection was carried out as per normal. At 4 days post-infection, 150 µl samples were taken from the wells of each strain at 2 separate dilutions and placed in another 96 well plate for OD<sub>600</sub> readings. Blank SHS medium was used as a reference. The suspensions of each strain were then combined and the combined suspension was serially diluted for viable plate counts and spotted on LB agar. To eliminate the possibility of contamination in these experiments, cells were plated on both *Burkholderia cepacia* selection agar (85) and LB agar, and no evidence was seen of differential colony morphotypes, with the exception of a small proportion of *Bc* K56-2 shiny colony variants.

### *Polymyxin B minimum inhibitory concentration*

Duplicate overnight cultures were prepared as described above with 100 Tc and 0.02% rhamnose. OD<sub>600</sub> was taken for each strain, and they were found to be equal to within 5%. Five microlitres of each culture were added to 150 µl of serial doubling dilutions of polymyxin B (Pmx) suspension in a 96 well plate. The highest Pmx concentration was 8 mg/ml. The 96 well plate was placed at 30°C shaking for 16 h at which point OD<sub>600</sub> was taken.

### *Swimming motility*

Duplicate overnight cultures were prepared as described above with 100 Tc and 0.02% rha and 2 µl of each culture was spotted onto triplicate LB agar (0.3% agar) plates poured fresh the day of the experiment. Each strain was spotted onto each plate to ensure consistency. Plates were incubated at 37°C. Motility was assessed at 48 h by measuring swim zone diameters.

### *Electron microscopy*

To visualize the morphology of overgrowing 46B2 mutant cells, bacteria were pelleted from a 4 day infection experiment with duckweed plants. The cells were resuspended in 4% paraformaldehyde, and samples were then prepared by Arlene Oatway at the Advanced Microscopy Unit of the Biological Sciences Department in the University of Alberta. Cells were imaged using a Philips / FEI (Morgagni) Transmission Electron Microscope with Gatan Digital Camera.

### *Immunoblotting*

To identify proteins produced by *B. cenocepacia* K56-2, 46B2/pSCRhaTc, and 46B2/pI124, whole cell lysates were obtained. Fifty microlitres of overnight culture were centrifuged at 5,000 × g, the supernatant was discarded and pellet was resuspended in electrophoresis sampling buffer (ESB: 62.5 mM Tris-HCl (pH 6.8), 1% SDS, 10% glycerol, 5% β-mercaptoethanol, 0.001% bromophenol blue). Samples were boiled for five minutes and either used promptly in one-dimensional sodium dodecyl sulfate polyacrylamide gel electrophoresis (SDS-PAGE) or stored at -20 °C for later use. SDS-PAGE was performed according to Laemmli (47). Buffer solution used in SDS-PAGE was composed of 25 mM Tris,

192 mM glycine and 0.1% sodium dodecyl sulfate in distilled water. To transfer the separated proteins onto a nitrocellulose membrane (Bio-Rad Laboratories, Inc.) for immunoblotting, the gel was subjected to electrotransfer and immunoblotting according to manufacturer's instructions using a Mini Trans-Blot cell (Bio-Rad, Inc.). Primary antibody (polyclonal rabbit anti-His, Rockland Immunochemicals) was prepared to 1/2,000 in TBS while secondary antibody (DyLight 488 goat anti-rabbit, Sigma-Aldrich) was prepared to 1/10,000 in TBS. After the final wash, the membrane was imaged using a ChemiDoc image platform (Bio-Rad) by fluorescence detection at 488 nm.

## **Bioinformatics**

Several genes identified in the virulence screening were annotated as hypothetical proteins in the NCBI database, so their protein sequences were submitted to the PHYRE2 database (40). This software uses Hidden Markov Models to identify folds within the proteins based on an extensive database of solved protein structures. To determine the prevalence of the virulence genes among *Burkholderia* strain, orthologs of the *B. cenocepacia* J2315 genes were searched in the *Burkholderia* Genome Database (84). STRING was used to identify possible interacting partners of these proteins; this database draws information concerning conserved genetic arrangements, co-appearances of genes in sequenced genomes, experimental interaction data (generally in *Saccharomyces cerevisiae* and *E. coli*), and several other categories.

## Statistical analysis

To compare the LD<sub>50</sub> data from different strains, Student's t-tests were carried out. Parameters were two-tailed and, since sample sizes were typically low (2-4), equal variance was assumed.

## Results

### Identification of putative *Bc* virulence factors through plasposon mutagenesis

Following the screening of 5,980 *Bc* K56-2 mutant strains in a series of high-throughput duckweed virulence experiments, nine mutants were carried forward for further characterization. There were an additional three mutants with slight attenuations (~2-fold) that were cryogenically stored but not characterized. Plasposon insertion sites, brief descriptions of the disrupted genes and the virulence attenuations caused by the disruptions are shown in Table 8. Repeated attempts at recovering plasposon and flanking DNA from mutant 42H4 following by sequencing produced only plasposon sequence without the accompanying insertion locus, and due to time constraints the insertion site was not determined.

**Table 8. *B. cenocepacia* K56-2 plasposon mutants attenuated against duckweed plants.**

Strain	LD50 cfu/mL +/- SE <sup>a</sup>	Plasposon insertion locus <sup>b</sup>	Characteristics
--------	---------------------------------------	--	-----------------

WT	1.2x10 <sup>1</sup> +/- 7.0x10 <sup>0</sup>	n/a	n/a
11G10	>10 <sup>9</sup>	<i>bcas0210</i> : Putative AMP-binding enzyme	
12C9	2.1x10 <sup>5</sup> +/- 4.6x10 <sup>4</sup>	<i>bcal0311</i> : HisG (ATP phosphoribosyltransferase)	Part of histidine biosynthesis cluster; up-regulated 2-fold during chronic CF infection (56)
16A11	~1x10 <sup>6</sup>	<i>bcal2159</i>	Hypothetical $\alpha/\beta$ barrel domain-containing protein; downstream from SuhB <sub>Bc</sub> (66)
32B11	1.9x10 <sup>3</sup> +/- 1.5x10 <sup>3</sup>	Intergenic between <i>bcal0549</i> and <i>bcal0550</i>	
42H4	3.5x10 <sup>4</sup> +/- 1.7x10 <sup>4</sup>	n.d.	
46B2	7.7x10 <sup>1</sup> +/- 1.8x10 <sup>1</sup>	<i>bcal1124</i> : Hypothetical protein in BcenGI5 genomic island	Immediately downstream from a CepR box (13)
50D9	>2.6x10 <sup>8</sup>	<i>bcas0225</i> : ShvR	LysR-like protein regulates AFC cluster, quorum sensing, protein secretion, protease and lipase production, and virulence (58, 74)
51H6	~10 <sup>3</sup>	<i>bcas0134</i> : LysR-like regulator	Putative LysR-like regulator, regulated by BDSF signalling (53)
62F12	1.6x10 <sup>5</sup> – 2.2x10 <sup>6</sup>	<i>bcal0870</i>	Putative oxidoreductase, identified as an essential gene in <i>B. cenocepacia</i> H111 (37)

<sup>a</sup>S.E., standard error of the mean, included where applicable

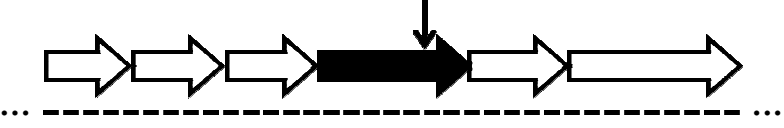
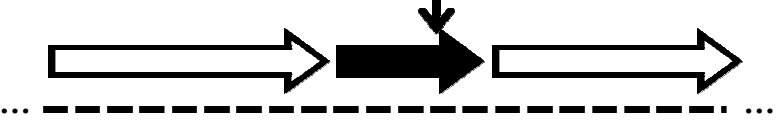
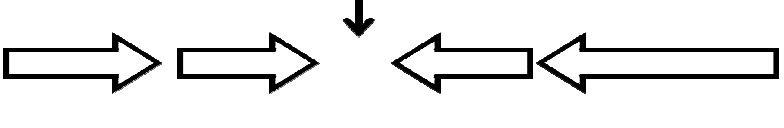
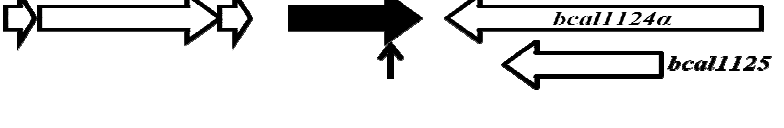
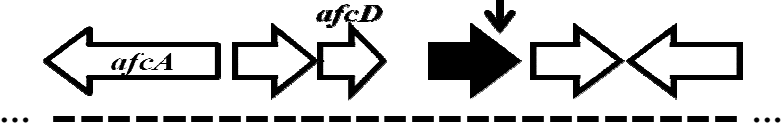
<sup>b</sup>n.d., not determined.

## ***In silico* characterization of putative virulence factors**

To establish directions for investigation of these putative virulence factors, the genes surrounding the plasposon insertions were examined. The genetic loci are summarized in Table 9. Studies examining transcriptomic responses of *B. cenocepacia* to a range of environmental cues (8, 23, 29, 51, 53, 56, 58, 59, 64, 69, 76) were explored to identify co-expression patterns of genes surrounding the disrupted virulence genes. Of these, the most wide-reaching analysis carried out by Sass *et al.* (69) provided evidence for their co-regulation with nearby genes, suggesting greater functional contexts for these virulence genes. Both *bcal0311* and *bcas0210* were found to be co-regulated with neighbouring genes during stationary phase incubation in minimal medium versus growth in LB for both gene clusters and also at low oxygen versus ambient oxygen for the *bcas0210* / *afc* cluster. The same set of microarrays found that that at stationary phase in minimal medium, *bcal0870* is co-regulated with *bcal0868* and *bcal0869*, which face the opposite direction on the *Bc* J2315 chromosome. *Bcal2159* and *bcal2157* (*suhB<sub>Bc</sub>*) are similarly down-regulated at 37°C versus 20°C, but divergently regulated in minimal medium stationary phase incubation, while *bcal2159* and *bcal2162* are up-regulated in both minimal and rich medium stationary phase incubation. *Bcal1124* and *bcas0134* do not appear to be co-regulated with surrounding genes under the physicochemical conditions tested, although McCarthy *et al.* showed that knocking out the BDSF signalling system caused 3-fold up-regulation of *bcal0134* (53). The same study found consistent down-regulation of *afc* genes in the BDSF knockout strain, indicating that either BDSF

exerts direct effects on this cluster or it acts as a positive regulator of *shvR*, whose gene product is an activator of the *afc* cluster (58).

**Table 9. Genetic loci of virulence-attenuating plasposon insertions.**

Strain / gene	Locus and plasposon insertion site <sup>a</sup>	Ref.
11G10 / <i>bcas0210</i>		(69)
12C9 / <i>bcal0311</i>		(69)
16A11 / <i>bcal2159</i>		(69)
32B11 / intergenic		
46B2 / <i>bcal1124</i>		
50D9 / <i>bcas0225</i>		(69) (53)

51H6 / <i>bcas0134</i>		
62F12 / <i>bcal0870</i>		(69)

<sup>a</sup>Plasposon insertion shown by small black arrow. Disrupted genes are black; surrounding genes are white. Ellipses indicate extended genetic context for the likely co-regulation based on transcriptomics studies indicated by dotted lines.

A variety of bioinformatic analyses were then carried out to determine homologies (BLASTP and PHYRE2), subcellular localization (PSORT v.3.0.2), possible interactions with other proteins (STRING), prevalence of orthologs among *Burkholderia* bacteria (*Burkholderia* genome database), and other characteristics where appropriate. Bioinformatic analyses are summarized in Table 10. Most of the gene products were predicted to be localized to the cytoplasm, though that does not rule out Sec-independent secretion. Two hypothetical proteins, Bcal1124 and Bcal2159, were assigned putative function based on PHYRE2 analysis. While Bcal1124 was predicted to have both DNA binding and cell scaffolding domains, Bcal2159 has strong fold homology to an ethyl *tert*-butyl ether degradation protein with possible oxygenase catalytic activity. Interestingly, Bcal1124 is only found in *Bc* and *B. pseudomallei*, while the putative LysR regulator Bcas0134 has homologs only in epidemic ET-12 *Bc* strains. Bcas0134 did not appear to be associated with ShvR (Bcas0225), which co-occurs in organisms with many other LysR-like regulators encoded throughout

the *Bc* genome. As expected based on the above-described transcriptional analyses, the interaction networks of the operon-encoded genes, *bcal0311* and *bcas0210*, suggest interactions with their neighbouring genes. Bioinformatic analysis of the oxidoreductase *bcal0870* provides few clues concerning its function, though one gene with which may be co-transcribed in stationary phase starvation is a GTP cyclohydrolase I, which in eukaryotes is involved with amino acid biosynthesis (5).

**Table 10. Bioinformatical analysis of virulence genes.**

<b>Strain / gene</b> Predicted protein size (a.a / kDa)	<b>Predicted domains (NCBI or PHYRE2)</b>	<b>Predicted subcellular localization (PSORT v3.0.2)</b>	<b>Predicted interaction network (STRING score &gt; 0.5)</b>	<b>Prevalence in <i>Burkholderia</i> (<i>Burkholderia</i> Genome Database)</b>
11G10 / <i>bcas0210</i> 527 / 56	Acyl-CoA ligase; adenylate-forming domain	Cytoplasmic	<i>bcas0206</i> – <i>bcas0216</i>	<i>B. cenocepacia</i> , <i>B. ambifaria</i> , <i>B. lata</i> , <i>B. pseudomallei</i> , <i>B. mallei</i>
12C9 / <i>bcal0311</i> 217 / 23	ATP phosphoribosyl transferase (Histidine biosynthesis)	Cytoplasmic	<i>hisABCDEFGHIJ</i> , <i>murA</i>	Ubiquitous
16A11 / <i>bcal2159</i> 108 / 12	EthD (ethyl <i>tert</i> -butyl ether degradation)	Unknown, but contains putative $\alpha/\beta$ barrel domain	<i>bcam1117</i> , <i>bcam0058</i> , <i>bcal3159</i>	<i>B. cenocepacia</i> , <i>B. lata</i> , <i>B. multivorans</i> , <i>B. gladioli</i> , <i>B.</i>

				<i>xenovorans</i>
32B11 / intergenic  <b>n/a</b>	n/a	n/a	n/a	Limited to the Bcc (BLASTN)
46B2 / <i>bcal1124</i>  <b>399 / 47</b>	Origin of replication- binding domain; spectrin repeat- like or calponin domain	Cytoplasmic	None	<i>B. cenocepacia</i> , <i>B. pseudomallei</i>
50D9 / <i>bcas0225</i>  <b>330 / 36</b>	Helix-turn- helix; periplasmic binding fold	Cytoplasmic	LysR-coding genes: <i>bcal1817</i> , <i>bcam1666</i> , <i>bcam0464</i> , <i>bcas0226</i> , <i>bcam0658</i> , ( <i>bcas0134</i> )	<i>B. cenocepacia</i> , <i>B. ambifaria</i> , <i>B.</i> <i>lata</i> , <i>B. gladioli</i>
51H6 / <i>bcas0134</i>  <b>316 / 35</b>	Helix-turn- helix; periplasmic binding fold	Cytoplasmic	Transporter: <i>bcas0133</i>	Limited to <i>B.</i> <i>cenocepacia</i> ET- 12 epidemic lineage
62F12 / <i>bcal0870</i>  1431 / 149	FAD-binding domain; iron- sulfur binding and oxidoreductase domains	Cytoplasmic	Diverse: <i>bcal1461</i> , <i>panC</i> , <i>bcal2947</i> , <i>bcal0872</i> , <i>bcal0871</i> , <i>bcal</i> <i>4375</i> , <i>bcal1264</i> , <i>serC</i> , <i>bcal3264</i> , <i>bcal3266</i>	Ubiquitous

To obtain fold predictions for Bcal1124, which is annotated as a hypothetical protein, its amino acid sequence was submitted to the PHYRE2 database. Three putative folds were identified within Bcal1124, which comprises 312 amino acids. The most reliable of these, with 82% confidence, was an origin of replication-binding domain from Geminivirus virus of tomato plants. This

domain is predicted to extend from residue 212 to residue 266. Other motifs predicted within Bcal1124 are a spectrin repeat-like domain (residue 86-137, 56% confidence) and a calponin-binding domain (residue 99-154, 55% confidence).

Bcal2159 was matched by PHYRE2 to an ethyl *tert*-butyl ether (ETBE) degradation protein domain (residue 1-107, 100% confidence). ETBE is a gasoline additive that has been recognized as a prevalent and persistent soil and groundwater contaminant (28). Four proteins have been identified in *Rhodococcus ruber* that are both induced by and allow for the degradation of ETBE (14). While homologs of this pathway's proteins are found in *Bc* with varying levels of identity (EthA - Bcal0923, 46%; EthB – Bcam2591, 27%; EthC - Bcal2193, 35%), they are scattered throughout the genome with the exception of one possible EthA homolog, encoded by *bcal2158* and sharing 19% amino acid identity. Overall, the distribution of these genes, their apparent integration into functional gene clusters, and their failure to appear in STRING analysis for potential interacting genes suggest that they have evolved for other purposes in *Bc*.

The plasposon insertion in mutant 32B11 disrupts an intergenic region that is not predicted to encode any small regulatory RNAs by any recent studies examining these molecules using both bioinformatics and experimental methods (16, 17, 65). Attempts at genetic complementation by introducing this intergenic region to 32B11 *in trans* were unsuccessful.

## Genetic complementation of mutant 46B2

It was predicted that genes located within gene clusters, such as *bcal0210*, would prove problematic for complementation as a result of polar mutations. Mutant 46B2 was chosen for complementation both to avoid this pitfall (because *bcal1124* is the final gene of a cluster, as shown in Table 9), and because this mutant displayed a curious overgrowth phenotype during duckweed infection, described later. It is located inside genomic island BcenGI5, and our research group has a general interest in non-native genomic regions, particularly prophages. In addition, BcenGI5 stood out among *Bc* genomic islands in demonstrating differential regulation of several genes (not including *bcal1124*) during bacterial growth in CF sputum relative to minimal medium (23), indicating that BcenGI5 may play a role in bacterial adaptation to the CF lung environment.

These mutants were complemented by cloning PCR constructs in pSCRhaTc, a low copy vector providing rhamnose inducibility. A first attempt for *bcal1124* revealed that two point mutations were introduced in the PCR construct: R204H and E336G. Since R204H is both predicted to be on the outskirts of the putative DNA binding domain and is semi-conserved among *B. cenocepacia* strains (212-266), this construct was named p1124” and carried forward while other clones were screened for the desired error-free construct. The E336G mutation does not occur in a conserved residue, nor does it fall within a predicted functional domain.

Colonies obtained from transformation of the mutants with the complementation vectors (p1124 and p1124”) were then screened for the

restoration of duckweed killing. Clones showing fully restored phenotypes were obtained for 46B2/p1124, but 46B2/p1124" remained attenuated in virulence. LD<sub>50</sub> values were determined for each strain under rhamnose induction, and are shown in Figure 15. K56-2/pSCRhaTc and 46B2/pSCRhaTc were inoculated into wax moth larvae under rhamnose induction, and the mutant was attenuated nearly 4-fold relative to its parent strain (Figure 16). Therefore, *bcal1124* is involved with virulence in multiple hosts, though the virulence defect observed in duckweed far exceeds that observed in wax moth larvae.

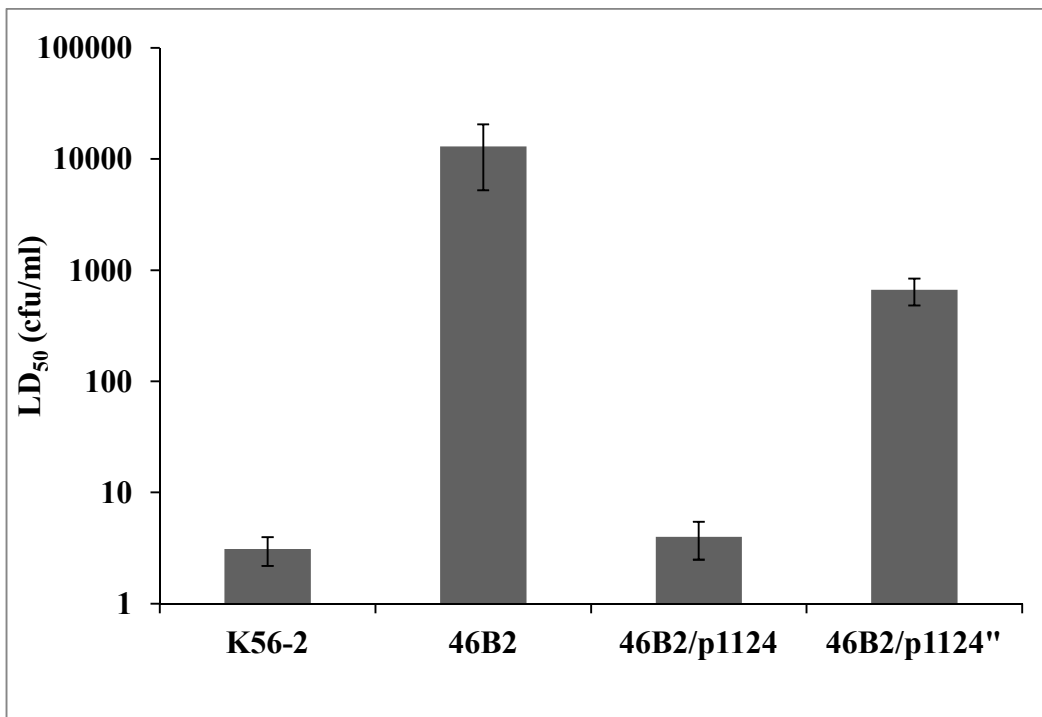


**Figure 15. Complementation of mutant 46B2 with *bcal1124* restores plant killing.** Infection experiments were performed as described above following overnight growth of all strains (K56-2/pSCRhaTc, 46B2/pSCRhaTc, 46B2/p1124,

46B2/p1124<sup>wt</sup>) in ½ LB + Tc100 + 0.02% w/v rhamnose. While p1124 carries the wild-type version of *bca1124*, p1124<sup>mut</sup> carries two point mutations in the gene, including R204H and E336G. Infections omitted antibiotics but included 0.02% rhamnose to continue induction of the pSCRha promoter.

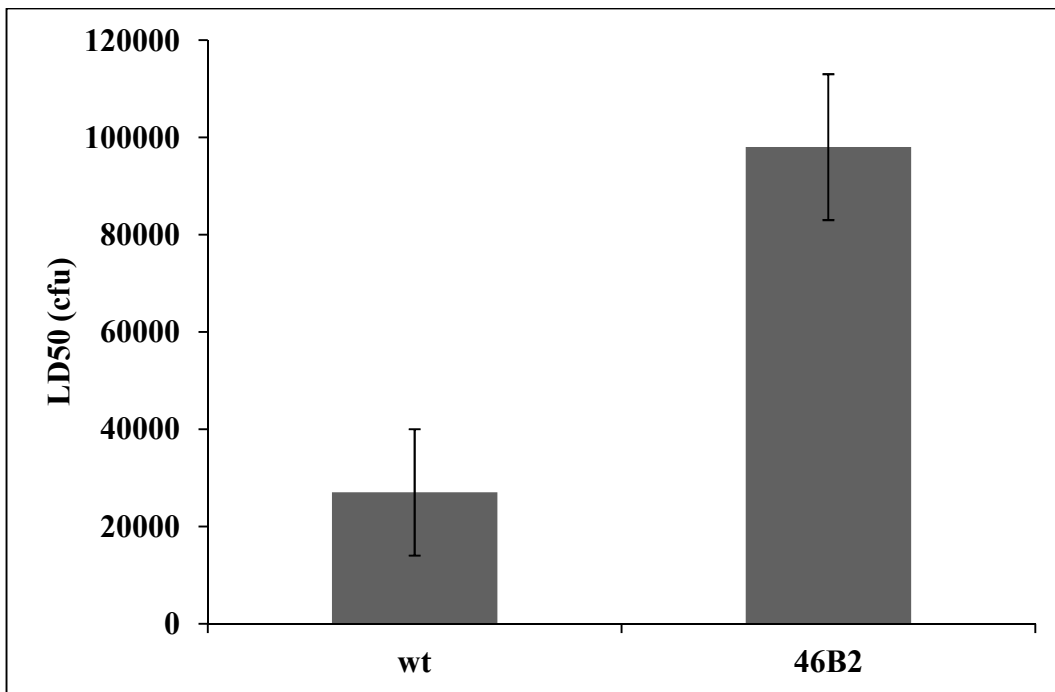


**Figure 16. Mutant 46B2 is attenuated in wax moth larval model.** Bacterial strains (wt, wild type *B. cenocepacia* K56-2; 46B2, mutant 46B2 carrying pSCRhaB2) were grown overnight in 2 ml ½ LB + 100Tc + 0.02% rhamnose, washed in 10 mM MgSO<sub>4</sub>, serially diluted and injected into the penultimate hindlimb of wax moth larvae rinsed with 95% ethanol. Results shown are averages of 2 independent trials +/- SE.

To confirm the expression of Bcal1124 and Bcal1124<sup>''</sup> in the complement strains, Western blot analysis was performed using rabbit  $\alpha$ -polyhistidine primary and goat  $\alpha$ -rabbit secondary antibodies. Both Bcal1124 and Bcal1124<sup>''</sup> were detected and are shown in Figure 17. The expected size for Bcal1124 with a 10x polyhistidine tag is 48 kDa, but the signal for both Bcal1124 variants was detected between 50 and 75 kDa.

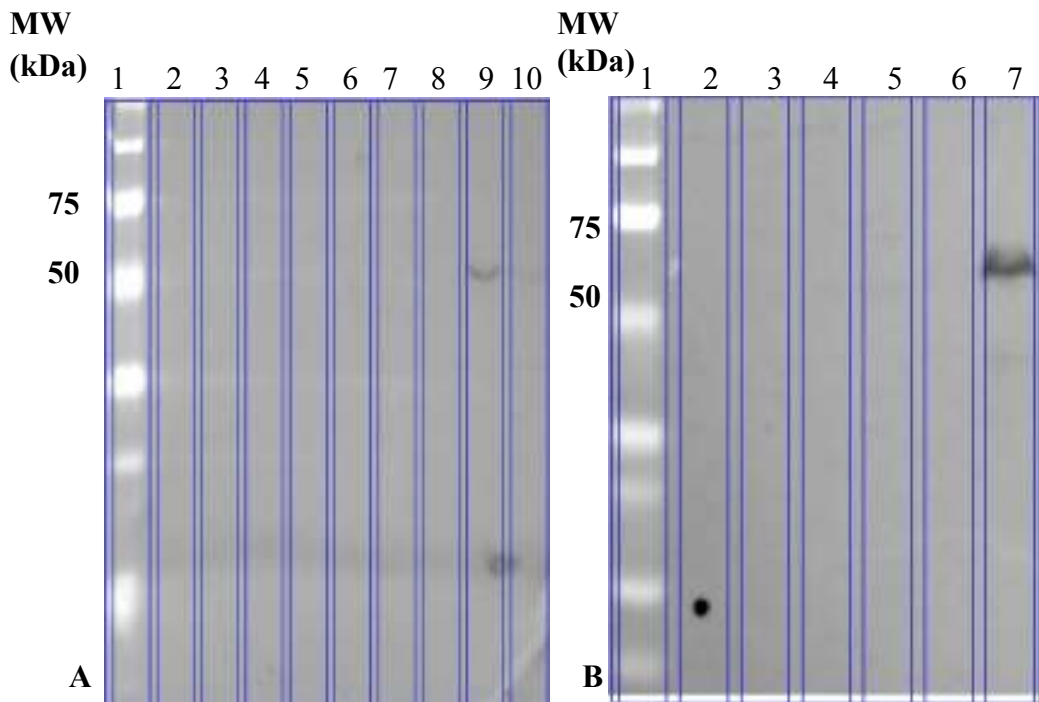


**Figure 17. Western blots showing expression of Bcal1124 and Bcal1124<sup>''</sup> from whole cell lysates of strains 46B2/p1124 and 46B2/p1124<sup>''</sup>.** A. All strains grown with 0.02% rhamnose. Lanes: 1, protein standard ladder; 2, K56-2/pSCRhaTc; 3, 46B2/pSCRhaTc clone A; 4, 46B2/pSCRhaTc clone B; 5, 46B2/pSCRhaTc clone C; 6, 46B2/p1124<sup>''</sup> clone A; 7, 46B2/p1124<sup>''</sup> clone B; 8, 46B2/p1124<sup>''</sup> clone C; 9,

46B2/p1124" clone D; 10, 46B2/p1124" clone E. **B.** Lanes: 1, protein standard ladder; 2, K56-2/pSCRhaTc grown without 0.02% rhamnose; 3, K56-2/pSCRhaTc grown with 0.02% rhamnose; 4, 46B2/pSCRhaTc grown without 0.02% rhamnose; 5, 46B2/pSCRhaTc grown with 0.02% rhamnose; 6, 46B2/p1124 grown without 0.02% rhamnose; 7, 46B2/p1124 grown with 0.02% rhamnose.

### **Additional phenotypic characterization of 16A11 and 46B2**

#### *16A11*

Since *bcal2159* is situated near the phenotypically-characterized *suhB<sub>Bc</sub>* (*bcal2157*), it was hypothesized that mutant 16A11 may share some of its phenotypes. The most easily tested phenotypes were motility and polymyxin B (Pmx) resistance. 16A11/pSCRhaTc produced a swim zone equal to that of K56-2/pSCRhaTc, and both strains were resistant to Pmx up to 8 mg/ml. Therefore, it appears that these genes are involved with divergent phenotypes. This finding is consistent with the general inconsistencies in the transcription patterns of the two genes under a wide range of conditions (69). No additional phenotypes were tested for this mutant, though its substantial attenuation against duckweed merits further attention.

#### *46B2*

Mutant 46B2 produces an unusual growth phenotype when grown in the presence of duckweed in the SHS medium. The bacteria appeared to grow to

extreme density, easily visible to the naked eye, while the parent strain generally only grew approximately 10-fold and its growth was not easily discernible. Dense 46B2 growth generally appeared after the third day of co-incubation with duckweed. Therefore, the growth of 46B2 and the complement strains was examined more closely by comparing both  $OD_{600\text{ nm}}$  and viable plate counts among the various strains. By Day 4, the growth trend was clearly visible in 46B2/pSCRhaTc, 46B2/p1124 and 46B2/p1124<sup>R204H</sup> but not in K56-2/pSCRhaTc, and significant differences were observed between OD values of K56-2/pSCRhaTc and both 46B2/pSCRhaTc and 46B2/p1124<sup>R204H</sup> ( $p < 0.01$ ), but not between K56-2/pSCRhaTc and 46B2/p1124 ( $p = 0.08$ ). The strongest growth was observed in both 46B2/pSCRhaTc and 46B2/p1124<sup>R204H</sup> (Figure 18). There was agreement between  $OD_{600}$  values and viable plate counts, indicating that the absorbance data are due to true cell growth and not to a morphological change in the mutant. The phenotype was only observed during growth in the presence of duckweed; there was no difference between the growth of strains when plants were absent. Another observation worth noting is that the phenotype was variable – in some infection wells, the bacteria produced dense turbidity, while others from the same initial culture at the same dilution produced only thin turbidity.

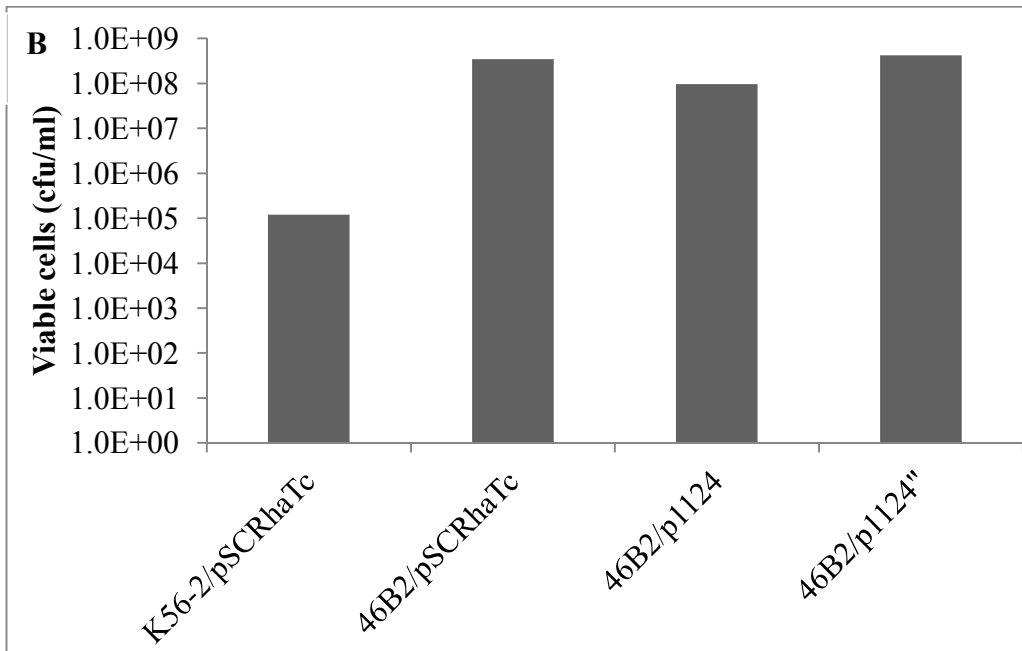
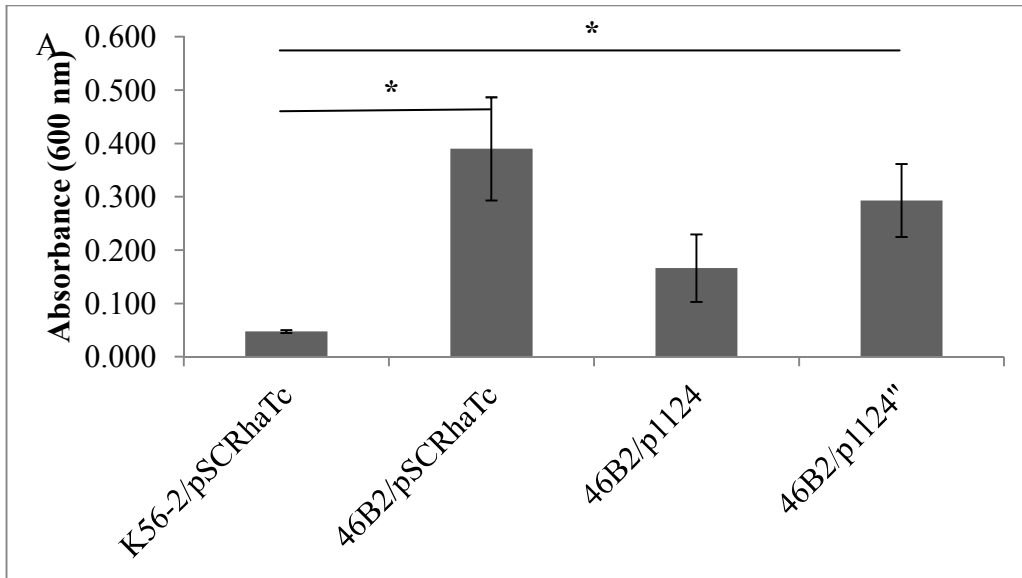


**Figure 18. Overgrowth phenotype of mutant 46B2 is partially relieved by constitutive expression of *bca1124* in trans.** **A.** Optical density of 150  $\mu$ l samples taken from wells of each strain co-incubated with duckweed. Results shown are the averages of 8 biological replicates  $\pm$  SE. **B.** Viable plate counts of

each strain from 8 biological replicates compiled into one suspension and serially diluted in triplicate. \* $p < 0.01$

Because of this growth aberration, a morphological effect of the *bcal1124* mutation was hypothesized, and cell samples were prepared for scanning electron microscopy. Imaging of the cells by scanning electron microscopy revealed no difference in morphology between K56-2/pSCRhaTc and 46B2/pSCRhaTc (Figure 19). In addition to morphological characteristics such as cell size and shape, a difference that was anticipated between the two strains was a relatively high percentage of dividing cells in 46B2, which was not observed.

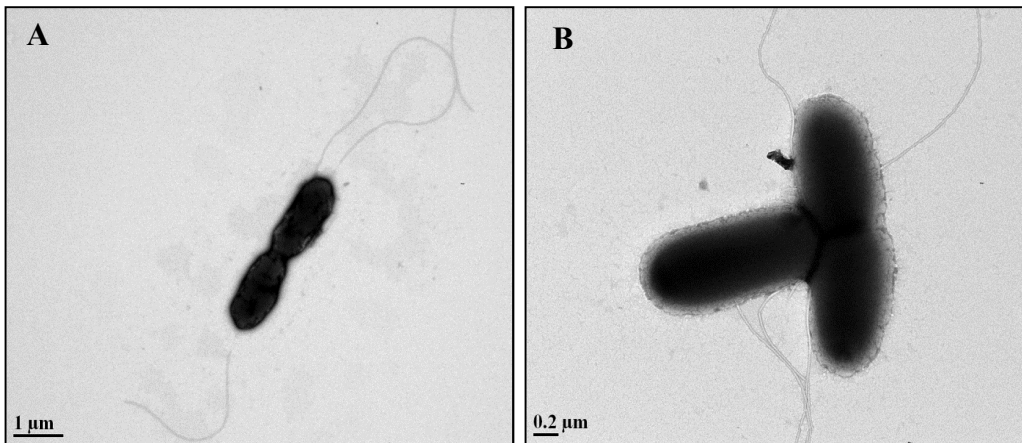


**Figure 19. Mutagenesis of *bcal1124* has no obvious morphological effects on *B. cenocepacia* K56-2.** Samples of K56-2/pSCRhaTc (A) and 46B2/pSCRhaTc (B) were taken from 4-day duckweed infections supplemented with 0.02% rhamnose and centrifuged; pelleted cells were fixed in 4% paraformaldehyde for transmission electron microscopy. Intact polar flagella can be seen in both images.

## Discussion

Despite the importance of delineating the genetic bases for pathogenesis in the Bcc, few tools exist for the high-throughput identification of virulence genes. *Bc* strains are among the most virulent in Bcc infection models, including plants (10, 79), and, therefore, plants could represent useful models to identify the genes underpinning the ability of *Bc* to cause disease in a wide variety of organisms. The clonal nature of duckweed grown under proper lighting conditions makes it an ideal host for a high-throughput virulence screen, since each plant should respond identically to challenge from different mutant strains.

The *Bc* K56-2 plasposon mutant library used in this study was previously screened for mutant strains resistant to bacteriophage infection. This screen identified several resistant mutants carrying plasposon insertions in different genes, indicating a high degree of insertion randomness throughout the library.

The screening of 5,980 *Bc* K56-2 mutants yielded nine with large virulence deficiencies (>10-fold increase in LD<sub>50</sub>). Five of these mutants have insertions in loci that have not been implicated in virulence of Bcc or other organisms prior to this study, while the disrupted gene of mutant 42H4 was not determined and another mutant, 32B11, carried a plasposon insertion in an intergenic region. In addition to the five uncharacterized virulence genes, two additional genes were identified and strains carrying disruptions in both genes showed complete avirulence against duckweed. One of these genes (*bcas0225/shvR*, disrupted in mutant 50D9) is a known positive regulator of many *Bc* genes including two divergently-transcribed gene clusters represented by

*bcas0223-0224* (which comprises *afcCD*) and *bcas0201-0222* (which includes *afcABEF*). *Bcas0225* was recently shown to be co-transcribed under various conditions along with a large cluster of surrounding genes stretching from *bcal0202* to *bcal0226* (68). The main inducing cues for genes within this cluster are stationary phase growth in minimal medium and, to a lesser extent, growth in low iron. Low oxygen is a repressive cue for most of these genes. Since the CF lung is generally a nutrient-rich environment (with the possible exception of iron availability), induction in minimal medium but not in rich medium may not be especially relevant to the CF lung; however, low oxygen is almost certainly a prevalent feature of both the CF lung and intracellular environments experienced by the Bcc, as discussed in more detail in Chapter 4. Therefore, both *shvR* and the associated *afc* gene-containing operons are likely not up-regulated during chronic infection of the CF lung.

The other fully attenuated strain, 57H6, carries an insertion in *bcas0210*. *Bcas0210* encodes a cytoplasmic AMP-binding enzyme with 4 inverted repeats of 10 bp. This gene falls within the *afcABEF*-containing cluster under control of ShvR and follows the same general transcription patterns as *shvR*, described above. The *afc* genes, which include *afcC* and *afcD* along with *bcas0223* (*afcA*), *bcas0222* (*afcB*), *bcas0208* (*afcE*) and *bcas0201* (*afcF*) are now known to give rise to antifungal activity through the nonribosomal synthesis of a lipopeptide previously characterized in *B. pyrrocinia* (38). Mutations in *afcE* and *afcF* also cause modulations in the cellular lipid profile (73) that correlate with increases in membrane permeability and decreases in swarming motility. Strains carrying

mutations in non-*afc* genes of this operon, *bcas0207* and *bcas0204* do not share these phenotypes, although they were previously implicated in virulence against alfalfa, biofilm formation, protein secretion, and colony morphology (74). Therefore, further experimentation with mutant 57H6 should identify the phenotypes to which *bcas0210* contributes in addition to the virulence phenotype delineated in the present study. It is expected that mutant 50D9 would show a lack of antifungal activity, lipid profile changes, and decreased swarming, consistent with the results found for *shvR* mutants in the above-described studies.

*Bcal0311* is disrupted in mutant 12C9, which displays a considerable decrease in virulence relative to the parent strain. This gene encodes HisG, a cytoplasmic ATP phosphoribosyltransferase that catalyzes the first reaction in histidine biosynthesis (1). HisG is encoded within a conserved histidine biosynthesis cluster that has not been implicated in virulence in the Bcc or other pathogens, but one study confirmed its role in histidine biosynthesis in *B. multivorans*, showing histidine auxotrophy resulting from the disruption of *hisA*, *hisB*, *hisE*, and *hisF* (42). The histidine biosynthesis cluster was shown to be down-regulated during stationary phase growth in minimal medium, and to a lesser extent in rich medium, and the cluster was not induced under any conditions. Therefore, chronic infection in the CF lung may repress these genes. However, induction of the genes in *Escherchia coli* and *Salmonella enterica* is known to occur *via* ppGpp, which signals starvation within the cell, while histidine molecules repress the biosynthetic pathway at the first reaction step. This tight regulation reflects the high metabolic cost of synthesizing histidine (1), and

it is therefore not surprising that Sass *et al.* found no inducing conditions for this cluster in their analysis (68).

Meanwhile, disruption of *bcal0870* (disrupted in mutant 62F12) also causes a large virulence decrease. This gene encodes a putative oxidoreductase and is co-transcribed in minimal media with *bcal0868* and *bcal0869*, which are implicated in amino acid biosynthesis. Bcal0868 is annotated as GTP cyclohydrolase I, which in eukaryotes is a crucial component of the synthesis of a cofactor for phenylalanine hydroxylase, tyrosine hydroxylase and tryptophan hydroxylase (5). Meanwhile, Bcal0869 is annotated as a threonine dehydratase, which is involved in the conversion of threonine into other amino acids (63). Therefore, amino acid biosynthesis likely plays a role in the pathogenesis of *Bc* against duckweed under these infection conditions. Another *Bc* virulence screen using *Caenorhabditis elegans* identified 3-4 amino acid metabolism genes out of 14 total virulence genes, supporting the duckweed screening results and showing that amino acid metabolism has important roles in *Bc* virulence in diverse hosts (72). Attenuation due to amino acid auxotrophy likely takes effect during amino acid starvation, but since the CF lung is generally rich in amino acids, particularly of the aromatic variety (62), amino acid auxotrophy may not be important during CF infection. Virulence attenuation of amino acid biosynthesis mutants has been shown in other airway pathogens, including *B. pseudomallei* (2) and *M. tuberculosis* (52), and such mutants are generally considered good candidates for live vaccines. The use of live vaccines to generate effective immune response in the airways of CF patients shows some early promise, with nasal and oral

vaccination of healthy human adults with an attenuated *Salmonella* strain expressing *P. aeruginosa* antigens triggering significant increases in mucosal IgA (12). Live attenuated vaccines have not been attempted for the Bcc, though several Bcc antigens have been identified that confer protection in mice (15).

*Bcal2159* encodes a homolog of an ethyl *tert*-butyl ether (ETBE) degrading enzyme EthD. Disruption of this gene in mutant 16A11 causes a large decrease in virulence. ETBE is a gasoline additive and a common and persistent groundwater contaminant. Microbes able to degrade this compound and the related MTBE are highly sought-after, and characterization of the pathway has been carried out in *Rhodococcus ruber* (14). The gene cluster required for degradation comprises four genes, *ethABCD*, which share homology with *bcal0923*, *bcam2591*, *bcal2193* and *bcal2159*, respectively. Without experimental evidence, it is difficult to speculate on whether these genes have a similar ETBE-degradation function in *Bc*, but their genomic scattering suggests that they have evolved for other purposes. *Bcal2159* is located near *bcal2157*, which encodes SuhB<sub>Bc</sub>, an inositol monophosphatase homolog recently implicated in polymyxin B resistance, biofilm formation, type II and VI protein secretion, and motility through a mechanism proposed to involve modulation of RNA polymerase activity as seen in *E. coli* (66). However, mutant 16A11 showed wild type levels of polymyxin resistance as well as full swimming motility. Therefore, these genes are likely not functionally related, despite being similarly regulated during incubation at physiological temperature (69). SuhB<sub>Bc</sub> was not implicated directly in virulence and its mutation had no effect on cellular invasion, although its

associated phenotypes indicate that disruption of this gene would likely manifest in a virulence defect (66). *Bcal2159* is encoded on the opposite strand of *suhB<sub>Bc</sub>* and was shown to be divergently transcribed from *suhB<sub>Bc</sub>* during stationary phase incubation in minimal medium, instead showing similar upregulation as the protein chaperone-encoding *bcal2162* in this condition as well as in rich medium stationary phase incubation (69).

*Bcas0134* is disrupted in mutant 51H6, which displays a moderate virulence attenuation. This gene encodes a putative LysR-like regulator whose expression increases upon disruption of the BDSF synthase *bcam0581*, though no effect on this gene was observed as a result of disruption of the proposed BDSF sensor *bcam0270* (53). Therefore, *bcas0134* may be under negative control of an alternative BDSF response regulator. Bioinformatical analysis and recent microarray data provide little information concerning the cellular role or the conditions under which this gene is differentially regulated, but cross-referencing on the *Burkholderia* Genome Database and BLASTN analysis reveal that this gene is limited to ET-12 epidemic *Bc* strains. The emergence of the ET-12 lineage is proposed to have occurred as a result of horizontal gene transfer, given its 14 genomic islands found throughout the 2 chromosomes and megaplasmid that make up approximately half of the 21% of genes unique to *Bc* J2315 relative to other sequenced *Bc* strains (33). *Bcas0134* is not found within one of these genomic islands, and BLASTN does not suggest that it arose from duplication of another gene within the J2315 genome.

Mutant 32B11 is moderately attenuated but carries a plasposon insertion in noncoding region between *bcal0549*, the terminal gene of a dipeptide transporter gene cluster, and *bcal0550*, which encodes a homolog of LamB, an osmoresponsive outer membrane porin in *E. coli* (31). The insertion is found ~250 bp from either gene and is downstream from both, indicating that polar mutations on either gene are unlikely. An initial study on *Bc* identified 213 putative small noncoding RNAs (sRNAs) using an *in silico* approach, and confirmed four of these experimentally (16). None of the predicted sRNAs aligned with the region disrupted in mutant 32B11. Furthermore, computational prediction has proved somewhat unreliable in identifying true sRNA, since most experimentally-identified sRNAs do not match those previously identified by computational methods (65). Ramos *et al.* (65) identified 24 putative sRNAs in *Bc* through their interaction with the two RNA chaperone Hfq homologs encoded by *Bc*, and showed differential levels of 21 of these in a *hfq* knockout strain. None of these predicted sRNAs overlaps the *bcal0549-bcal0550* intergenic region. Therefore, there is no evidence suggesting that the disrupted intergenic region in mutant 32B11 encodes a sRNA, though effects on DNA stability or interactions with neighbouring genes cannot be ruled out. Finally, a second plasposon insertion not detected during plasposon rescue could be present within this strain. To determine whether this has occurred, Southern blot analysis should be carried out on this strain and any others for which genetic complementation does not work.

*Bcal1124* is disrupted in mutant 46B2, with a corresponding virulence attenuation of roughly 100-fold – the smallest change among the virulence genes

identified. This gene is found within genomic island *BcenGI5*, which carries a disproportionately large number of genes differentially expressed during growth in CF sputum (23), indicating that genes within *BcenGI5* may help *Bc* adapt to chronic infection. Furthermore, *BcenGI5* was shown to contain the largest proportion of genes unique to *Bc* compared with the relatively attenuated *B. multivorans* and *B. stabilis* species in a genome subtraction analysis, implying a role for this genomic island in the divergence of *Bc* from the other Bcc species. In the comprehensive microarray analysis of *Bc* J2315 recently carried out, *bcal1124* was not co-regulated with any surrounding genes under the seven conditions tested, only showing slight upregulation during oxidative stress (68), and *bcal1124* was not found to be differentially regulated under conditions tested in other transcriptomics studies. Chambers *et al.* (13) identified a CepR motif directly upstream of *bcal1124*, indicating that the gene is under quorum sensing control. CepR is also known as a typical gene activator rather than repressor (60). Given this context of population dynamics—that is, *bcal1124* is normally expressed at high cell density—the disruption of this gene could conceivably produce a missing step in the regulation of the cell cycle. Upon restoration and constitutive induction of *bcal1124 in trans*, the cells still produce a partial overgrowth phenotype. It is therefore reasonable to expect that if *Bcal1124* is involved with fine-tuning of the cell cycle, its expression is under strict control and disruption of this control through gene inactivation or constitutive expression causes a similar overgrowth effect. As additional regulatory motifs are identified in *Bc*, particularly for repressors, it will be worth determining whether *bcal1124* is

subject to negative control that is alleviated at high cell density. One approach that could yield useful data in this regard would be to perform qPCR to measure *bcal1124* transcript levels at various growth stages.

Homologs of Bcal1124 are found only in *Bc* and *B. pseudomallei*, which are two of the most important human pathogens of the *Burkholderia* genus. Although Bcal1124 is annotated as a cytoplasmic hypothetical protein, PHYRE2 analysis produced a strong fold homology with an origin of replication-binding domain (ORBD) in the REP protein of a Geminivirus that causes tomato yellow leaf curl, as well as moderate overlapping fold homologies with phosphoinositide-binding clathrin adaptor (PBCA) and calponin homology (CH) domains. Geminiviruses are ssDNA viruses that undergo rolling-strand replication and are proposed to have descended from Gram positive bacterial plasmids (46). REP protein is the only Geminivirus protein essential for replication (26) and its ORBD is a key driver of this process (30). The PBCA domain links clathrin to the membranes of clathrin-coated vesicles during intracellular trafficking (19), while CH domains are found in a wide variety of actin-binding proteins (80).

Mutant 46B2 produces a unique overgrowth phenotype when incubated with duckweed in SHS media (Figure 18). This phenotype was found to produce considerably higher OD<sub>600</sub> and cell counts, with an increase in cell density exceeding 1,000-fold in 46B2. The growth phenotype was only observed during growth in the presence of duckweed; there was no detectable increase in optical density when plants were absent. This implies the presence of a plant-produced compound to which 46B2 responds with cell growth. Compounds mediating

plant-bacterial interactions are not unknown, and the most striking examples of these are AHL mimics, which are produced in a wide range of plants, modulating bacterial behaviours such as plant root and algal surface colonization. Perhaps more relevant to the present study is a direct effect of a plant flavonoid on the rhizobial LysR-like regulator NodD. NodD senses flavonoids produced by legume plants that are suitable for nodulation by undergoing a conformational change, then induces the expression of the Nod factors for invasion of the root and adoption of the highly specialized root nodule lifestyle (6). Although duckweed does not have true roots or form root nodules, the ubiquity of plant-produced compounds modulating bacterial behaviour suggests that duckweed could alter *Bc* growth through such means. Applying HPLC fractions of a duckweed supernatant to the mutant cells and looking for overgrowth would be one approach to identifying this factor.

Cell morphology was examined by electron microscopy, which revealed no difference in cell shape or relative numbers of dividing cells between 46B2 and the parent strain at 4 days following duckweed infection (Figure 19). Since cell growth was already known to be occurring, the lack of dividing mutant cells in this analysis indicates that the extent of growth was already reached by this timepoint, and cells should have been examined at previous timepoints to capture this phenotype. Indeed, the growth phenotype does not generally appear in the infections until after 3 days and is clearly visible by 4 days. Interestingly, the overgrowth phenotype was not fully abolished in the complement strain, which produced intermediate growth between the mutant and parent strains during mild

induction with rhamnose (Figure 18). This suggests that *bcal1124* requires either specific timing or extent of expression, and that modulating either of these will give rise to the growth phenotype. Also noteworthy is that the calculated LD<sub>50</sub> for these strains reflects the initial inoculum, yet the dense population of 46B2 cells accumulating in the media is still unable to produce wild type levels of plant morbidity or mortality. Therefore, the true measure of lethality for this strain is not reflected within the calculated LD<sub>50</sub>.

Complementation of 46B2 with wild type *bcal1124 in trans* caused restored virulence, but a version of the construct carrying two point mutations introduced during PCR amplification produced no such phenotypic restoration (Figure 15). The point mutations were introduced at R204H, which is found near the predicted DNA binding domain, and E336G, which is near the C-terminus and not close to the other predicted ORBD and CH domains. Therefore, the working hypothesis is that a defective DNA binding domain gives rise to the growth phenotype in response to a plant signal, and that this may be related to dysregulation of the cell cycle. One example of a plant signal that manipulates the cell cycle of bacteria occurs in rhizobia, where nodulating bacteria undergo rapid DNA accumulation and terminally differentiate in response to host plant cues (54).

A virulence defect was observed during wax moth larval infection of 46B2 versus wild type K56-2, indicating that *bcal1124* likely contributes to multihost pathogenicity (Figure 16). However, the increase in LD<sub>50</sub> observed in this strain was approximately 4-fold, whereas the mutation causes a ~100-fold LD<sub>50</sub> increase

in duckweed infection. Meanwhile, a previous study examined the effect of a *shvR* mutation (which is carried by strain 50D9 in the present study) on a range of model organisms, finding that while *Bc* K56-2 virulence in the nematode and wax moth larval models was unaffected, the mutant strain showed complete attenuation in the alfalfa model that corresponded to decreased inflammation during chronic rat lung infection (79). This study also showed that all mutations causing attenuation in the alfalfa model were accompanied by attenuations in at least one other model, and often two.

Among the most interesting findings of this screen are the absence of genes that have previously been implicated in plant pathogenesis. In alfalfa, the only mutations causing complete or near-complete bacterial attenuation were *shvR* in *Bc* K56-2 and *cepIR* in *Bc* H111, though several other mutations (disrupting genes encoding nematode fast killing protein AidA and type II secretion protein GspE in *Bc* H111, and pyoverdine synthesis and type III secretion in *Bc* K56-2) caused moderate attenuation. In the present duckweed screen, no type II secretion, type III secretion or siderophore biosynthesis genes were identified. Even a partial-coverage genome screening such as that executed in this study would be expected to draw virulence links to large gene clusters such as these. Similarly, the present study's findings contrast the virulence factors found using the onion model, in which mutations causing attenuation encoded a T2SS, T4SS, and a polygalacturonase (27, 72). While the polygalacturonase, which is secreted through the T2SS but encoded by a single gene, might not emerge in a mutant screen, one would expect to see a larger cluster such as a secretion system. The

sensitivity of the duckweed screen (which identified genes causing LD<sub>50</sub> increases from 100-fold to 100,000,000-fold) indicates that even genes playing only small virulence roles in these other models should have been anticipated. This is especially true given the prior use of this mutant library by M.Sc. student Gerardo Juarez-Lara, who identified a wide variety of genes involved in bacteriophage sensitivity to *Bc* K56-2 (36). Therefore, the best explanation for the differences observed using these models lies in the differences among the models themselves. The onion model relies on inoculating bacteria into wounded tissue, while alfalfa infections are carried out on water agar and inocula comprise bacteria suspended in depleted overnight culture medium (10), which would provide all but limiting nutrients as well as an abundance of quorum sensing molecules carried over from growth. Both models inoculate with high densities of bacteria, rather than using a serial dilution-based method as adopted in the present study. Finally, the type of tissue encountered by the bacteria at the plant surfaces varies considerably: onion is a bulb and therefore differentiated as a root, and wounding likely exposes cytoplasmic material from these cell types as well as intercellular spaces; alfalfa seedlings are differentiated with roots, shoots and the accompanying diversity of cell and tissue types; duckweed is a more uniform surface for colonization, lacking both roots and any other form of subterranean adaptation, since its entire life cycle is spent in water. These differences could potentially account for the different virulence factors required for pathogenesis, since the bacterial inocula (signal molecules and suspension media) and the plant tissues that the bacteria encounter (cell and tissue types and wounding) vary among the models.

The only *Bc* mutant screen for virulence using intact organisms prior to the current study was carried out with *Caenorhabditis elegans*. This study discovered several virulence-linked genes by inoculating 96 well plates containing ten worms in each well with mutant strain cultures and counting the numbers of surviving worms following incubation. In addition to the amino acid metabolism genes mentioned previously, virulence genes identified in this screen included other core metabolic enzymes, a T2SS prepilin, and two putative regulators (72).

The use of duckweed to identify virulence genes was validated by the discovery during this screen of two previously-identified virulence genes, the global regulator *shvR* and an *afc* cluster gene, *bcas0210* (Table 8). This validation progressed through the determination that, consistent with results found in alfalfa, mutations in these genes caused complete virulence attenuation. Beyond these, five novel virulence genes are linked to amino acid metabolism, gene regulation, and two proteins of unknown function. Bioinformatic analysis permitted the further exploration of one of these genes of unknown function, which was identified as a likely DNA binding protein with orthologs limited to *B. pseudomallei* and *B. cenocepacia*. A unique overgrowth phenotype was observed in this mutant that begins to appear at 3 days post-infection and depends on the presence of duckweed. Restoration of virulence in this mutant failed when two point mutations were introduced into the complementation construct; one of these mutations was found near the putative DNA binding fold, providing some validation for the function of this domain. The mutant was compared with wild type *Bc* K56-2 in the wax moth larval model and found to be attenuated.

Therefore, this screen identified a suite of new virulence genes including at least one conferring multihost pathogenicity.

While the screen demonstrated some genetic bases for plant pathogenesis in *Bc*, the discovery that a mutation in *bcal1124* may permit the manipulation of the bacterial cell cycle by plant factors highlights the ecological origins of Bcc human pathogens. Future work to determine the function of this protein should first aim to eliminate the overgrowth phenotype by providing the proper timing and pressure in driving expression of *bcal1124* in the complement strain. If the overgrowth phenotype can be corrected in the complement, further work could characterize the expression of the native protein in the wild type strain and correlate perturbations of its expression in the complement with the overgrowth phenotype. A simple approach to identify additional factors in this phenotype would involve repeating the duckweed screen with additional mutants to find strains producing this same phenotype. This strategy would provide the added possibility of identifying more virulence genes.

## References

1. Alifano P, Fani R, Lio P, Lazcano A, Bazzicalupo M, Carlomagno MS, et al. Histidine biosynthetic pathway and genes: structure, regulation, and evolution. *Microbiol Rev.* 1996;60(1):44-69.
2. Atkins T, Prior RG, Mack K, Russell P, Nelson M, Oyston PC, et al. A mutant of *Burkholderia pseudomallei*, auxotrophic in the branched chain amino acid biosynthetic pathway, is attenuated and protective in a murine model of melioidosis. *Infect Immun.* 2002;70(9):5290-4.
3. Aubert DF, Flannagan RS, Valvano MA. A novel sensor kinase-response regulator hybrid controls biofilm formation and type VI secretion system activity in *Burkholderia cenocepacia*. *Infect Immun.* 2008;76(5):1979-91.
4. Aubert DF, O'Grady EP, Hamad MA, Sokol PA, Valvano MA. The *Burkholderia cenocepacia* sensor kinase hybrid AtsR is a global regulator modulating quorum-sensing signalling. *Environ Microbiol.* 2013;15(2):372-85.
5. Bader G, Schiffmann S, Herrmann A, Fischer M, Gutlich M, Auerbach G, et al. Crystal structure of rat GTP cyclohydrolase I feedback regulatory protein, GFRP. *J Mol Biol.* 2001;312(5):1051-7.
6. Bais HP, Weir TL, Perry LG, Gilroy S, Vivanco JM. The role of root exudates in rhizosphere interactions with plants and other organisms. *Annu Rev Plant Biol.* 2006;57:233-66.
7. Baldwin A, Sokol PA, Parkhill J, Mahenthiralingam E. The *Burkholderia cepacia* epidemic strain marker is part of a novel genomic island encoding both virulence and metabolism-associated genes in *Burkholderia cenocepacia*. *Infect Immun.* 2004;72(3):1537-47.
8. Bazzini S, Udine C, Sass A, Pasca MR, Longo F, Emiliani G, et al. Deciphering the role of RND efflux transporters in *Burkholderia cenocepacia*. *PLOS One.* 2011;6(4):e18902.
9. Berlutti F, Morea C, Battistoni A, Sarli S, Cipriani P, Superti F, et al. Iron availability influences aggregation, biofilm, adhesion and invasion of *Pseudomonas aeruginosa* and *Burkholderia cenocepacia*. *Int J Immunopathol Pharmacol.* 2005;18(4):661-70.
10. Bernier SP, Silo-Suh L, Woods DE, Ohman DE, Sokol PA. Comparative analysis of plant and animal models for characterization of *Burkholderia cepacia* virulence. *Infect Immun.* 2003;71(9):5306-13.
11. Bernier SP, Sokol PA. Use of suppression-subtractive hybridization to identify genes in the *Burkholderia cepacia* complex that are unique to *Burkholderia cenocepacia*. *J Bacteriol.* 2005;187(15):5278-91.
12. Bumann D, Behre C, Behre K, Herz S, Gewecke B, Gessner JE, et al. Systemic, nasal and oral live vaccines against *Pseudomonas aeruginosa*: a clinical trial of immunogenicity in lower airways of human volunteers. *Vaccine.* 2010;28(3):707-13.
13. Chambers CE, Lutter EI, Visser MB, Law PP, Sokol PA. Identification of potential CepR regulated genes using a cep box motif-based search of the *Burkholderia cenocepacia* genome. *BMC Microbiol.* 2006;6:104.

14. Chauvaux S, Chevalier F, Le Dantec C, Fayolle F, Miras I, Kunst F, et al. Cloning of a genetically unstable cytochrome P-450 gene cluster involved in degradation of the pollutant ethyl tert-butyl ether by *Rhodococcus ruber*. J Bacteriol. 2001;183(22):6551-7.
15. Choh LC, Ong GH, Vellasamy KM, Kalaiselvam K, Kang WT, Al-Maleki AR, et al. *Burkholderia* vaccines: are we moving forward? Front Cell Infect Microbiol. 2013;3:5.
16. Coenye T, Drevinek P, Mahenthiralingam E, Shah SA, Gill RT, Vandamme P, et al. Identification of putative noncoding RNA genes in the *Burkholderia cenocepacia* J2315 genome. FEMS Microbiol Lett. 2007;276(1):83-92.
17. Coenye T, Van Acker H, Peeters E, Sass A, Buroni S, Riccardi G, et al. Molecular mechanisms of chlorhexidine tolerance in *Burkholderia cenocepacia* biofilms. Antimicrob Agents Chemother. 2011;55(5):1912-9.
18. Cosgrove S, Chotirmall SH, Greene CM, McElvaney NG. Pulmonary proteases in the cystic fibrosis lung induce interleukin 8 expression from bronchial epithelial cells via a heme/meprin/epidermal growth factor receptor/Toll-like receptor pathway. J Biol Chem. 2011;286(9):7692-704.
19. Daboussi L, Costaguta G, Payne GS. Phosphoinositide-mediated clathrin adaptor progression at the trans-Golgi network. Nat Cell Biol. 2012;14(3):239-48.
20. Darling P, Chan M, Cox AD, Sokol PA. Siderophore production by cystic fibrosis isolates of *Burkholderia cepacia*. Infect Immun. 1998;66(2):874-7.
21. Dennis JJ, Zylstra GJ. Plasposons: modular self-cloning minitransposon derivatives for rapid genetic analysis of gram-negative bacterial genomes. Appl Env Microbiol. 1998;64(7):2710-5.
22. Drevinek P, Baldwin A, Lindenbug L, Joshi LT, Marchbank A, Vosahlikova S, et al. Oxidative stress of *Burkholderia cenocepacia* induces insertion sequence-mediated genomic rearrangements that interfere with macrorestriction-based genotyping. J Clin Microbiol. 2010;48(1):34-40.
23. Drevinek P, Holden MT, Ge Z, Jones AM, Ketchell I, Gill RT, et al. Gene expression changes linked to antimicrobial resistance, oxidative stress, iron depletion and retained motility are observed when *Burkholderia cenocepacia* grows in cystic fibrosis sputum. BMC Infect Dis. 2008;8:121.
24. Drevinek P, Mahenthiralingam E. *Burkholderia cenocepacia* in cystic fibrosis: epidemiology and molecular mechanisms of virulence. Clin Microbiol Infect. 2010;16(7):821-30.
25. Duff C, Murphy PG, Callaghan M, McClean S. Differences in invasion and translocation of *Burkholderia cepacia* complex species in polarised lung epithelial cells in vitro. Microb Pathog. 2006;41(4-5):183-92.
26. Elmer JS, Brand L, Sunter G, Gardiner WE, Bisaro DM, Rogers SG. Genetic analysis of the tomato golden mosaic virus. II. The product of the AL1 coding sequence is required for replication. Nucleic Acids Res. 1988;16(14B):7043-60.
27. Engledow AS, Medrano EG, Mahenthiralingam E, LiPuma JJ, Gonzalez CF. Involvement of a plasmid-encoded type IV secretion system in the plant

- tissue watersoaking phenotype of *Burkholderia cenocepacia*. J Bacteriol. 2004;186(18):6015-24.
28. Fayolle-Guichard F, Durand J, Cheucle M, Rosell M, Michelland RJ, Tracol JP, et al. Study of an aquifer contaminated by ethyl tert-butyl ether (ETBE): site characterization and on-site bioremediation. J Hazard Mater. 2012;201-202:236-43.
29. Ferreira AS, Silva IN, Oliveira VH, Becker JD, Givskov M, Ryan RP, et al. Comparative transcriptomic analysis of the *Burkholderia cepacia* tyrosine kinase bceF mutant reveals a role in tolerance to stress, biofilm formation, and virulence. Appl Environ Microbiol. 2013;79(9):3009-20.
30. Fontes EP, Eagle PA, Sipe PS, Luckow VA, Hanley-Bowdoin L. Interaction between a geminivirus replication protein and origin DNA is essential for viral replication. J Biol Chem. 1994;269(11):8459-65.
31. Gowrishankar J. Identification of osmoreponsive genes in *Escherichia coli*: evidence for participation of potassium and proline transport systems in osmoregulation. J Bacteriol. 1985;164(1):434-45.
32. Graindorge A, Menard A, Monnez C, Cournoyer B. Insertion sequence evolutionary patterns highlight convergent genetic inactivations and recent genomic island acquisitions among epidemic *Burkholderia cenocepacia*. J Med Microbiol. 2012;61(Pt 3):394-409.
33. Holden MT, Seth-Smith HM, Crossman LC, Sebahia M, Bentley SD, Cerdeno-Tarraga AM, et al. The genome of *Burkholderia cenocepacia* J2315, an epidemic pathogen of cystic fibrosis patients. J Bacteriol. 2009;191(1):261-77.
34. Hunt TA, Kooi C, Sokol PA, Valvano MA. Identification of *Burkholderia cenocepacia* genes required for bacterial survival *in vivo*. Infect Immun. 2004;72(7):4010-22.
35. Hutchison ML, Poxton IR, Govan JR. *Burkholderia cepacia* produces a hemolysin that is capable of inducing apoptosis and degranulation of mammalian phagocytes. Infect Immun. 1998;66(5):2033-9.
36. Juarez-Lara G. Characterization of bacteriophage receptors in the *Burkholderia cepacia* complex (Bcc): University of Alberta; 2013.
37. Juhas M, Stark M, von Mering C, Lumjiaktase P, Crook DW, Valvano MA, et al. High confidence prediction of essential genes in *Burkholderia cenocepacia*. PLOS One. 2012;7(6):e40064.
38. Kang Y, Carlson R, Tharpe W, Schell MA. Characterization of genes involved in biosynthesis of a novel antibiotic from *Burkholderia cepacia* BC11 and their role in biological control of *Rhizoctonia solani*. Appl Environ Microbiol. 1998;64(10):3939-47.
39. Kaza SK, McClean S, Callaghan M. IL-8 released from human lung epithelial cells induced by cystic fibrosis pathogens *Burkholderia cepacia* complex affects the growth and intracellular survival of bacteria. Int J Med Microbiol. 2011;301(1):26-33.
40. Kelley LASMJE. Protein structure prediction on the web: a case study using the Phyre server. Nat Protoc. 2009;4:363 - 71.

41. Kenna DT, Yesilkaya H, Forbes KJ, Barcus VA, Vandamme P, Govan JR. Distribution and genomic location of active insertion sequences in the *Burkholderia cepacia* complex. *J Med Microbiol.* 2006;55(Pt 1):1-10.
42. Komatsu H, Imura Y, Ohori A, Nagata Y, Tsuda M. Distribution and organization of auxotrophic genes on the multichromosomal genome of *Burkholderia multivorans* ATCC 17616. *J Bacteriol.* 2003;185(11):3333-43.
43. Kooi C, Corbett CR, Sokol PA. Functional analysis of the *Burkholderia cenocepacia* ZmpA metalloprotease. *J Bacteriol.* 2005;187(13):4421-9.
44. Kooi C, Sokol PA. *Burkholderia cenocepacia* zinc metalloproteases influence resistance to antimicrobial peptides. *Microbiology.* 2009;155(Pt 9):2818-25.
45. Kooi C, Subsin B, Chen R, Pohorelic B, Sokol PA. *Burkholderia cenocepacia* ZmpB is a broad-specificity zinc metalloprotease involved in virulence. *Infect Immun.* 2006;74(7):4083-93.
46. Krupovic M, Ravantti JJ, Bamford DH. Geminiviruses: a tale of a plasmid becoming a virus. *BMC Evol Biol.* 2009;9:112.
47. Laemmli UK. Cleavage of structural proteins during the assembly of the head of bacteriophage T4. *Nature.* 1970;227(5259):680-5.
48. Lefebvre MD, Flannagan RS, Valvano MA. A minor catalase/peroxidase from *Burkholderia cenocepacia* is required for normal aconitase activity. *Microbiology.* 2005;151(Pt 6):1975-85.
49. MacDonald KL, Speert DP. Differential modulation of innate immune cell functions by the *Burkholderia cepacia* complex: *Burkholderia cenocepacia* but not *Burkholderia multivorans* disrupts maturation and induces necrosis in human dendritic cells. *Cell Microbiol.* 2008;10(10):2138-49.
50. Malott RJ, Baldwin A, Mahenthalingam E, Sokol PA. Characterization of the *cciIR* quorum-sensing system in *Burkholderia cenocepacia*. *Infect Immun.* 2005;73(8):4982-92.
51. Malott RJ, O'Grady EP, Toller J, Inhulsen S, Eberl L, Sokol PA. A *Burkholderia cenocepacia* orphan LuxR homolog is involved in quorum-sensing regulation. *J Bacteriol.* 2009;191(8):2447-60.
52. McAdam RA, Weisbrod TR, Martin J, Scuderi JD, Brown AM, Cirillo JD, et al. *In vivo* growth characteristics of leucine and methionine auxotrophic mutants of *Mycobacterium bovis* BCG generated by transposon mutagenesis. *Infect Immun.* 1995;63(3):1004-12.
53. McCarthy Y, Yang L, Twomey KB, Sass A, Tolker-Nielsen T, Mahenthalingam E, et al. A sensor kinase recognizing the cell-cell signal BDSF (*cis*-2-dodecenoic acid) regulates virulence in *Burkholderia cenocepacia*. *Mol Microbiol.* 2010;77(5):1220-36.
54. Mergaert P, Uchiumi T, Alunni B, Evanno G, Cheron A, Catrice O, et al. Eukaryotic control on bacterial cell cycle and differentiation in the *Rhizobium*-legume symbiosis. *Proc Natl Acad Sci U S A.* 2006;103(13):5230-5.
55. Mil-Homens D, Fialho AM. A BCAM0223 mutant of *Burkholderia cenocepacia* is deficient in hemagglutination, serum resistance, adhesion to epithelial cells and virulence. *PLOS One.* 2012;7(7):e41747.

56. Mira NP, Madeira A, Moreira AS, Coutinho CP, Sa-Correia I. Genomic expression analysis reveals strategies of *Burkholderia cenocepacia* to adapt to cystic fibrosis patients' airways and antimicrobial therapy. PLOS One. 2011;6(12):e28831.
57. Mullen T, Markey K, Murphy P, McClean S, Callaghan M. Role of lipase in *Burkholderia cepacia* complex (Bcc) invasion of lung epithelial cells. Eur J Clin Microbiol Infect Dis. 2007;26(12):869-77.
58. O'Grady EP, Nguyen DT, Weisskopf L, Eberl L, Sokol PA. The *Burkholderia cenocepacia* LysR-type transcriptional regulator ShvR influences expression of quorum-sensing, protease, type II secretion, and *afc* genes. J Bacteriol. 2011;193(1):163-76.
59. O'Grady EP, Sokol PA. *Burkholderia cenocepacia* differential gene expression during host-pathogen interactions and adaptation to the host environment. Front Cell Infect Microbiol. 2011;1:15.
60. O'Grady EP, Viteri DF, Malott RJ, Sokol PA. Reciprocal regulation by the CepIR and CciIR quorum sensing systems in *Burkholderia cenocepacia*. BMC Genomics. 2009;10:441.
61. O'Grady EP, Viteri DF, Sokol PA. A unique regulator contributes to quorum sensing and virulence in *Burkholderia cenocepacia*. PLOS One. 2012;7(5):e37611.
62. Palmer KL, Aye LM, Whiteley M. Nutritional cues control *Pseudomonas aeruginosa* multicellular behavior in cystic fibrosis sputum. J Bacteriol. 2007;189(22):8079-87.
63. Park JH, Oh JE, Lee KH, Kim JY, Lee SY. Rational design of *Escherichia coli* for L-isoleucine production. ACS Synth Biol. 2012;1(11):532-40.
64. Peeters E, Sass A, Mahenthiralingam E, Nelis H, Coenye T. Transcriptional response of *Burkholderia cenocepacia* J2315 sessile cells to treatments with high doses of hydrogen peroxide and sodium hypochlorite. BMC Genomics. 2010;11:90.
65. Ramos CG, Grilo AM, da Costa PJ, Leitao JH. Experimental identification of small non-coding regulatory RNAs in the opportunistic human pathogen *Burkholderia cenocepacia* J2315. Genomics. 2012.
66. Rosales-Reyes R, Saldias MS, Aubert DF, El-Halfawy OM, Valvano MA. The *suhB* gene of *Burkholderia cenocepacia* is required for protein secretion, biofilm formation, motility and polymyxin B resistance. Microbiology. 2012;158(Pt 9):2315-24.
67. Sajjan SU, Carmody LA, Gonzalez CF, LiPuma JJ. A type IV secretion system contributes to intracellular survival and replication of *Burkholderia cenocepacia*. Infect Immun. 2008;76(12):5447-55.
68. Sass A, Marchbank A, Tullis E, Lipuma JJ, Mahenthiralingam E. Spontaneous and evolutionary changes in the antibiotic resistance of *Burkholderia cenocepacia* observed by global gene expression analysis. BMC Genomics. 2011;12:373.
69. Sass AM, Schmerk C, Agnoli K, Norville PJ, Eberl L, Valvano MA, et al. The unexpected discovery of a novel low-oxygen-activated locus for the anoxic persistence of *Burkholderia cenocepacia*. ISME J. 2013;7(8):1568-81.

70. Schmid N, Pessi G, Deng Y, Aguilar C, Carlier AL, Grunau A, et al. The AHL- and BDSF-dependent quorum sensing systems control specific and overlapping sets of genes in *Burkholderia cenocepacia* H111. PLOS One. 2012;7(11):e49966.
71. Smalley JW, Charalabous P, Birss AJ, Hart CA. Detection of heme-binding proteins in epidemic strains of *Burkholderia cepacia*. Clin Diagn Lab Immunol. 2001;8(3):509-14.
72. Somvanshi VS, Viswanathan P, Jacobs JL, Mulks MH, Sundin GW, Ciche TA. The type 2 secretion pseudopilin, gspJ, is required for multihost pathogenicity of *Burkholderia cenocepacia* AU1054. Infect Immun. 2010;78(10):4110-21.
73. Subramoni S, Agnoli K, Eberl L, Lewenza S, Sokol PA. Role of *Burkholderia cenocepacia* *afcE* and *afcF* genes in determining lipid-metabolism-associated phenotypes. Microbiology. 2013;159(Pt 3):603-14.
74. Subramoni S, Nguyen DT, Sokol PA. *Burkholderia cenocepacia* ShvR-regulated genes that influence colony morphology, biofilm formation, and virulence. Infect Immun. 2011;79(8):2984-97.
75. Thomson EL, Dennis JJ. A *Burkholderia cepacia* complex non-ribosomal peptide-synthesized toxin is hemolytic and required for full virulence. Virulence. 2012;3(3):286-98.
76. Tolman JS, Valvano MA. Global changes in gene expression by the opportunistic pathogen *Burkholderia cenocepacia* in response to internalization by murine macrophages. BMC Genomics. 2012;13:63.
77. Tomich M, Griffith A, Herfst CA, Burns JL, Mohr CD. Attenuated virulence of a *Burkholderia cepacia* type III secretion mutant in a murine model of infection. Infect Immun. 2003;71(3):1405-15.
78. Tomich M, Herfst CA, Golden JW, Mohr CD. Role of flagella in host cell invasion by *Burkholderia cepacia*. Infect Immun. 2002;70(4):1799-806.
79. Uehlinger S, Schwager S, Bernier SP, Riedel K, Nguyen DT, Sokol PA, et al. Identification of specific and universal virulence factors in *Burkholderia cenocepacia* strains by using multiple infection hosts. Infect Immun. 2009;77(9):4102-10.
80. Umemoto R, Nishida N, Ogino S, Shimada I. NMR structure of the calponin homology domain of human IQGAP1 and its implications for the actin recognition mode. J Biomol NMR. 2010;48(1):59-64.
81. Urban TA, Goldberg JB, Forstner JF, Sajjan US. Cable pili and the 22-kilodalton adhesin are required for *Burkholderia cenocepacia* binding to and transmigration across the squamous epithelium. Infect Immun. 2005;73(9):5426-37.
82. Urban TA, Griffith A, Torok AM, Smolkin ME, Burns JL, Goldberg JB. Contribution of *Burkholderia cenocepacia* flagella to infectivity and inflammation. Infect Immun. 2004;72(9):5126-34.
83. Visser MB, Majumdar S, Hani E, Sokol PA. Importance of the ornibactin and pyochelin siderophore transport systems in *Burkholderia cenocepacia* lung infections. Infect Immun. 2004;72(5):2850-7.

84. Winsor GL, Khaira B, Van Rossum T, Lo R, Whiteside MD, Brinkman FS. The *Burkholderia* Genome Database: facilitating flexible queries and comparative analyses. *Bioinformatics*. 2008;24(23):2803-4.
85. Wright RM, Moore JE, Shaw A, Dunbar K, Dodd M, Webb K, et al. Improved cultural detection of *Burkholderia cepacia* from sputum in patients with cystic fibrosis. *J Clin Pathol*. 2001;54(10):803-5.
86. Zhang R, LiPuma JJ, Gonzalez CF. Two type IV secretion systems with different functions in *Burkholderia cenocepacia* K56-2. *Microbiology*. 2009;155(Pt 12):4005-13.
-

## Chapter 4: The *B. cenocepacia* antibacterial type VI secretion system

---

## Introduction

### The type VI secretion system

The initial characterization of the type VI secretion system (T6SS) in 2006 solved a long-standing puzzle concerning a cluster of genes related to the type IV secretion system (T4SS) that appeared frequently in sequenced genomes of Gram negative bacteria without assigned function. Pukatzki *et al.* (38) screened a transposon library of *V. cholerae* V52 for mutants deficient in resistance to predation by *Dictyostelium* predation, and found several genes clustered together that conferred predation resistance and appeared to give rise to the secretion of proteins lacking N-terminal hydrophobic domains. This characteristic of the proteins rules out type I and type II secretion, and sequencing of the V52 genome revealed that neither a type III nor a type IV secretion system are encoded by these bacteria, although this new gene cluster carried genes similar to those found in both systems. Suddenly, earlier findings suggesting the existence of an unidentified gene cluster involved with protein secretion in other bacteria, including *Vibrio cholerae* (18) and the root nodule producer *Rhizobium* (9), began making sense.

Since then, a string of studies have begun to unveil the true nature of the T6SS with increasing detail. The realization that the VgrG proteins, thought to occupy roles as effector proteins of the T6SS, share homology with phage tail spike proteins (31, 37), provided some evolutionary context for the T6SS. Some VgrG proteins were discovered to contain extended C-terminal catalytic domains. These “evolved” VgrG proteins were identified *in silico* in *V. cholerae*, *P. aeruginosa*, *B. cenocepacia*, *Yersinia pestis* and the plant pathogen *Xanthomonas*

*oryzae*. Structural work detailed ancestral relationships between Hcp and phage tail tubes and between Vca0109 and phage baseplate proteins (31). Another parallel to bacteriophage activity is the production of a contractile sheath formed by VipA and VipB, which are proposed to surround the T6SS in the cytoplasm and, during contraction, eject the tube into a target cell (4). Depolymerization and recycling of the VipA-VipB complex is carried out by ClpV (12, 35), and formation of the sheath relies on the presence of the baseplate protein Vca0109 (4). Fluorescence microscopy captured the formation of the sheath structures, which appear to polymerize within 10-30 seconds in the published videos. Contraction of the sheaths causes thickening (~30% increase in diameter) and the appearance of ridges that suggest longitudinal squeezing within the helical polymer (4). In addition to these proteins with active roles in the propulsion of the T6SS and its activity once inside the target cell are a host of membrane, periplasmic and cytoplasmic proteins predicted to form a framework for the machine, and these have typically been characterized to lesser degrees (17).

### **Functions of the *Bc* T6SS**

Keeping pace with our ever-increasing structural understanding of the T6SS is the stunning functional diversity to which these systems have been adapted in different bacteria. While the initial discoveries pointed to potentially important roles in the invasion of and defence against eukaryotic cells, the prevalence of T6SSs in non-pathogenic bacteria suggested that these machines have additional roles.

As mentioned above, the T6SS was initially characterized for its role in predation resistance against amoebae. Early reports showed that this phenotype was not limited to *V. cholerae*, as *B. cenocepacia* is also able to resist predation using its T6SS (2). Although the full details of the predation resistance pathways have yet to be elucidated, the mechanism by which bacteria resist degradation within the vacuoles appears to be conserved whether the bacteria are phagocytosed by amoebae or macrophages. As will be described in more detail, in the Bcc, this occurs through the delay of phagosomal maturation. T6S has also been extensively characterized in many bacteria as a requirement for full virulence or persistence in multicellular hosts (17).

In 2010, two studies revealed the T6SS as more than a virulence determinant for bacteria by demonstrating the requirement of an intact T6SS for antibacterial activity in both *P. aeruginosa* and *V. cholerae*. In *P. aeruginosa*, a protein toxin-antitoxin system was identified and named Tse2/Tsi2 (25). Exposure of a *tsi2* knockout strain to a Tse2/Tsi2-expressing wild type strain causes a substantial growth advantage for the wild type cells, indicating that cells require immunity to some toxins they produce and that self-nonsel self recognition may not apply in T6S-mediated competition. Although the cellular target was not identified, several evolved VgrG proteins are known to contain C-terminal domains with putative bioactivity against bacteria, such as lysozyme and lipase domains (17). Furthermore, type VI-secreted toxins Tse1 and Tse3 were shown to cause cell lysis through peptidoglycan cleavage (42). Meanwhile, in *V. cholerae*, it was shown that the T6SS provides not only a growth advantage, but that prey *E.*

*coli* cells are in fact killed by T6SS-mediated action (32). The group went on to show by means of separating predator and prey by a filter that bacterial killing requires cell-cell contact between predator and prey. The killing effect is independent of VgrG1-mediated actin crosslinking that confers *V. cholerae* resistance to amoebal phagocytosis (38). Although this study did not address toxin-antitoxin systems, *V. cholerae* was determined to have no effect on itself, regardless of the presence of an intact T6SS. Antibacterial activity through T6S has also been reported for *S. marcescens* (34), *B. thailandensis* (44), and *P. syringae* (24). Interestingly, there has yet to be a demonstration of T6SS-mediated antibacterial effects against Gram positive organisms (17).

It is worth mentioning that the decreased persistence of T6SS mutants during infection studies may relate to their inability to overcome the innate microflora, rather than any direct T6SS-mediated effects on the host (17). The competitive advantages often conferred by bacterial T6SSs would support this notion, as invading bacteria would need to fight for niche space along mucosa or other sites of infection.

Another noteworthy observation is that *V. cholerae* maintains only a single T6SS through which the bacteria harm both bacterial and eukaryotic cells. This implies that even though the structure remains the same, a T6SS can be adapted to different target cells through the use of different effector proteins. Other bacteria maintain several T6SSs that appear to target different hosts, with *B. pseudomallei* currently holding the record at six (8). Only two of these systems have been

assigned functions: one is required for giant cell formation in mouse infection, while the other has antibacterial activity (17).

### **Type VI secretion in *Bc***

While most of the structural and functional characterization of the individual proteins has been carried out in other bacteria, it stands to reason that this conserved genetic element encodes similar structures in the Bcc. Exceptions to this were published in 2010 in a study demonstrating formation of an outer membrane-anchored complex by VipA and VipB, and the requirement of ClpV for the formation this complex (1), whereas studies in other organisms have shown cytosolic localization of these sheath proteins and their depolymerization by ClpV. The authors speculated that the role of ClpV could be related to the export of VipA and VipB into the periplasm. These findings have not been expanded into analyses of other structural T6SS proteins in *Bc*, but they show that in the Bcc, and probably in many bacteria, the T6SS operates by slightly different rules.

As a result of the urgency of elucidating the virulence pathways of the Bcc, most of the work on Bcc T6S has been directed at mechanistic infection modeling centred on macrophage invasion and persistence within their vacuoles. This line of work evolved in amoebal infection models, where Bcc persistence within vacuoles was initially demonstrated and related to the delay of phagosomal maturation (30). A later study made use of both *Dictyostelium discoideum* and mouse macrophages to show the centrality of a two-component system in the negative regulation of the *Bc* T6SS; by knocking out the regulator AtsR, several

T6SS-mediated phenotypes emerged, including hypervirulence against *Dictyostelium*, increased actin crosslinking in macrophages, and increased biofilm formation (2). This study also linked the newly-discovered T6SS to previous results from a study with pools of signature-tagged *Bc* transposon mutants infecting mice that yielded hits to uncharacterized proteins (26), which turned out to be T6SS proteins Bcal0338 (TssK), Bcal0347 (ClpV) and Bcal0352, an uncharacterized protein with predicted metallopeptidase activity.

Recent mechanistic studies have begun to elucidate the pathways by which the *Bc* T6SS hijacks host cell machinery to promote bacterial intracellular survival. Surprisingly, it was recently shown that *Bc* cells colocalize with non-maturing vacuoles whether or not they carry an intact T6SS, suggesting that the phagosomal maturation delay previously implicated in *Bc* survival within amoebae and macrophages is not T6SS-dependent, as previously thought. Rather, the T6SS secretes unidentified proteins that interfere with Rac1 recruitment. Rac1 is a Rho GTPase that forms part of the NADPH oxidase complex, and its disruption attenuates the threat of reactive oxygen species within the acidic vacuole (40).

Promoting the role of T6S as a multifactorial virulence pathway in *Bc*, Gavrilin *et al.* have recently demonstrated that secretion of unidentified effector proteins by the T6SS causes the activation of a crucial macrophage inflammasome that drives the production and release of IL-1 $\beta$ , leading to host cell cytotoxicity as measured by LDH release (22). This proinflammatory cytokine is found in high concentrations in the CF lung (6), and CF macrophages produce more IL-1 $\beta$  than

non-CF human macrophages in response to *Bc* exposure, an effect that was shown to occur through the sensing of *Bc* LPS by the Nod intracellular pattern recognition receptors (29). Another study showed that the T6SS is required for the escape of T2SS proteins, including ZmpA and ZmpB, into the host cytosol, where further IL-1 $\beta$  production is triggered and secreted from the host cell. The escape of type II-secreted proteins was proposed to occur through a vacuolar membrane disruption mechanism mediated by the T6SS (39). Therefore, T6S in *Bc* plays at least two distinct virulence roles, first in helping the bacteria to attenuate the extreme environment of the phagocytic vacuole, and second in promoting the destruction of the host cell and the provision of further host cells through cytokine-mediated recruitment.

## **Objectives**

The discoveries that *Bc* has a functional T6SS involved in virulence within phagocytes and that the *V. cholerae* T6SS has a role in interbacterial competition prompted the exploration into possible antibacterial roles for the *Bc* T6SS using *E. coli* as a model prey species. As a CF lung colonizer, *Bc* must compete for niche space among the dense microbial population already present, and so it was hypothesized that if the *Bc* T6SS was responsible antibacterial effects, these effects might extend to some known CF colonizers. Since the T6SS is required for effective persistence in the rat agar bead model of chronic infection, it was hypothesized that the T6SS would impact virulence in other infection models, including wax moth larvae and duckweed. *In silico* analysis of the *Bc* genome was

carried out to provide future directions for the discovery of pathways by which the T6SS is adapted for activity against eukaryotic and prokaryotic cells.

## Materials and methods

### Bacterial strains, plasmids, antibiotics and culture conditions

Luria-Bertani (LB) broth was prepared in deionized water to half concentration for Bcc strains and full concentration for *Escherichia coli* strains. Agar plates were prepared with 1.5% w/v agar. Antibiotics were included where necessary to the following concentrations: Chloramphenicol (Cm), 25 µg/mL; Trimethoprim (Tp), 100-300 µg/mL; Ampicillin (Ap), 100 µg/mL. All antibiotics were purchased from Difco through BD - Canada (Difco, Inc., Mississauga, ON). *Escherichia coli* DH5α was used for plasmid manipulation. *E. coli* strains were grown at 37 °C, while Bc was grown at 30 °C. All liquid cultures were shaken at 225 rpm. High-copy number plasmid pJET (Ap<sup>R</sup>) was employed in cloning experiments. A complete list of bacterial strains and plasmids is shown in Table 11.

**Table 11. Strains and plasmids used in this study.**

Bacterial strain	Genotype or relevant phenotype	Source
<i>B. cenocepacia</i>		
K56-2	Parent strain	Clinical, CF
K56-2/pSCRhaTc	K56-2 carrying blank pSCRhaTc plasmid	This study
K56-2/pSCRhaB2	K56-2 carrying blank pSCRhaB2 plasmid	This study
<i>tssF</i> ::Tp	Insertional K56-2 mutant containing Tp resistance cassette disruption of <i>tssF</i> ( <i>bcal0345</i> )	This study
<i>tssF</i> ::Tp/pSCRhaTc	<i>tssF</i> ::Tp carrying blank pSCRhaTc	This

	plasmid	study
<i>tssF</i> ::Tp/ <i>ptssF</i>	<i>tssF</i> ::Tp carrying pSCRhaTc- <i>tssF</i> with C-terminal 6x polyhistidine tag	This study
$\Delta$ <i>tssF</i>	K56-2 with unmarked clean deletion of <i>tssF</i>	This study
$\Delta$ <i>tssF</i> /pSCRhaB2	$\Delta$ <i>tssF</i> carrying blank pSCRhaB2	This study
$\Delta$ <i>tssF</i> / <i>ptssF</i> -1	$\Delta$ <i>tssF</i> carrying pSCRhaB2- <i>tssF</i> with C-terminal 6x polyhistidine tag	This study
$\Delta$ <i>tssF</i> / <i>ptssF</i> -2	$\Delta$ <i>tssF</i> carrying pSCRhaB2- <i>tssF</i> with N-terminal 10x polyhistidine tag	This study
$\Delta$ <i>tssF</i> / <i>ptssFG</i>	$\Delta$ <i>tssF</i> carrying pSCRhaB2- <i>tssFG</i> with N-terminal 10x polyhistidine tag on <i>tssF</i> and C-terminal 10x polyhistidine tag on <i>tssG</i>	This study
$\Delta$ <i>tssF</i> / <i>ptssDEFG</i>	$\Delta$ <i>tssF</i> carrying pSCRhaB2- <i>tssDEFG</i> with C-terminal 10x polyhistidine tag on <i>tssG</i>	This study
$\Delta$ <i>tssF</i> -2	K56-2 with unmarked deletion of <i>tssF</i> that maintains putative transcription start sites by eliminating only the middle ~60% of <i>tssF</i>	This study
$\Delta$ <i>tssF</i> -2/pSCRhaB2	$\Delta$ <i>tssF</i> -2 carrying blank pSCRhaB2	This study
$\Delta$ <i>tssF</i> -2/ <i>ptssF</i> -2	$\Delta$ <i>tssF</i> -2 carrying pSCRhaB2- <i>tssF</i> with N-terminal 10x polyhistidine tag	This study
<i>V. cholerae</i>		
V52	Parent strain with constitutive activation of T6SS	(38)
$\Delta$ <i>vasK</i>	V52 with clean deletion of <i>vasK</i>	(38)
<i>P. aeruginosa</i>		
PAO1	Clinical isolate	
PA14	Clinical isolate	
<i>S. aureus</i>		
RN4220	Clinical isolate	
<i>K. aerogenes</i>		
<i>E. coli</i>		
DH5 $\alpha$	Cloning host strain	
DH5 $\alpha$ /pBBR1MCS	Prey strain with Cm resistance for bacterial competition experiments	
Plasmids		
pJET1.2	Cloning vector carrying <i>bla</i> gene for ampicillin resistance	Thermo Scientific
pTetRA	Suicide vector carrying <i>tetA</i> and <i>tetR</i> for tetracycline resistance; derived from	In house plasmid

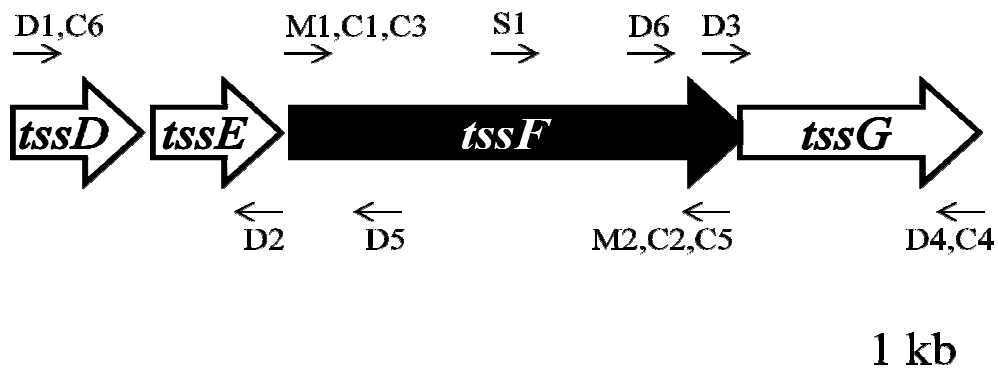
	pDD806	
pGPI	Suicide vector carrying <i>dhfr</i> gene for trimethoprim resistance; used for introduction of clean deletion construct into target genome; contains a <i>SceI</i> restriction site adjacent to the multiple cloning site	(21)
pGPI- <i>tssDEG</i>	pGPI with <i>tssDE</i> inserted at <i>EcoRV</i> - <i>EcoRI</i> and <i>tssG</i> inserted at <i>EcoRI</i> -	This study
pDAI- <i>sceI</i>	Expression vector carrying <i>sceI</i> for the digestion of <i>SceI</i> restriction site introduced to the target genome along with pGPI	(21)
pSCRhaB2	Rhamnose-inducible complementation vector carrying <i>Tp</i> resistance cassette	(14)
pSCRhaTc	pSCRhaB2 modified with a Tc resistance cassette	(45)
pTc- <i>tssF</i>	pSCRhaTc with 3' 6x polyhistidine-tagged <i>tssF</i> inserted at <i>NdeI</i> and <i>XbaI</i>	This study
<i>ptssF</i>	pSCRhaB2 with 5' 10x polyhistidine-tagged <i>tssF</i> inserted at <i>NdeI</i> and <i>HindIII</i>	This study
<i>ptssFG</i>	pSCRhaB2 with <i>tssFG</i> , including a 3' 10x polyhistidine tag on <i>tssF</i> and a 5' 10x polyhistidine tag on <i>tssG</i> , inserted at <i>NdeI</i> and <i>XbaI</i>	This study
<i>ptssDEFG</i>	pSCRhaB2 with <i>tssDEFG</i> inserted at <i>NdeI</i> and <i>XbaI</i> carrying a 5' 10x polyhistidine tag on <i>tssG</i>	This study

### Insertional mutagenesis of *tssF*

An insertional *tssF* mutant was created in Bc K56-2 using a targeted insertional mutagenesis strategy. Primers M1 and M2 (Table 12) were designed to amplify *tssF* with *StuI* restriction sites at 5' and 3' ends. PCR amplification was carried out using TopTaq (Qiagen Inc., Oakville, ON). DNA bands were extracted from agarose gel using GeneClean (Fermentas, Burlington, ON), ligated to pJET1.2 (Fermentas, Burlington, ON) and cloned in *E. coli* DH5 $\alpha$  (Invitrogen Corp., Carlsbad, CA), and DNA sequencing of the cloned fragments was carried

out to confirm the identity of the product. A trimethoprim (Tp) resistance cassette was inserted at a native PstI site within *tssF*. The disrupted *tssF* construct and an additional 200 bp at the 3' end were excised from pJET using BamHI and HindIII enzymes, and the resulting construct was ligated into pTetRA, which was also cloned in DH5 $\alpha$ . T4 ligase (Promega Corp., Madison, WI) was used for all ligation reactions. The insertional mutation was confirmed by PCR using primers M1 and M2.

**Table 12. Oligonucleotides used in this study.** Refer to Figure 20



for locations.

Process	Oligo-nucleotide	Sequence*
<i>Insertional mutagenesis</i>	M1	TTAGGCCTGCAGGAAATATTGAG
	M2	TTAGGCCTGGAAGAACTCGAAGC
<i>Unmarked gene deletion</i>	D1	TATTCTAGAGGTAGGACGTTAAAACCACC
	D2	TATGATATCCAATATTTCTGCCGGACCTG
	D3	TATGATATCACGATCGACGAGGAACACTT
	D4	TATGAATTCCAGGTTTCGATTGCGTGTGTGTT
	D5	TATGATATCGAACGACTCGATCATCCG
	D6	TATGATATCTCGATGCGCCAGATCGAC
<i>Complementation</i>	C1	CATTAGCATATGGAAGAATTGCTGCCGTA TTACGAACGCGAA
	C2	ATTCTAGACTAGTGGTGATGGTGATGATG CGCCAGGATCGATT

	C3	CATTAT <b>CATATGCATCATCACCATCACCAT</b> CATCACCATCACGAAGAATTGCTGCCGTA TTAC
	C4	ACAT <b>CTAGATCAATGATGGT</b> GATGGTGAT GATGGTGATGGTGAATCACGTGCAGTTCG TA
	C5	TT <b>CTAGACTACGCCAGGATCGATT</b> CGCC GGTTC
	C6	ATGTTACATATGCACTTGCAGT
<i>Sequencing</i>	S1	GGAAGCACGCTATACGC
	pGPI F	TTACTAAGCTGATCCGGTG
	pGPI R	GGGGAAACGCCTGGTATC
	pSCRha F	GGCCCATTTTCCTGTC
	pSCRha R	GCTTCTGCGTTCTGA

\*restriction sites are shown in bold; polyhistidine tags are underlined.

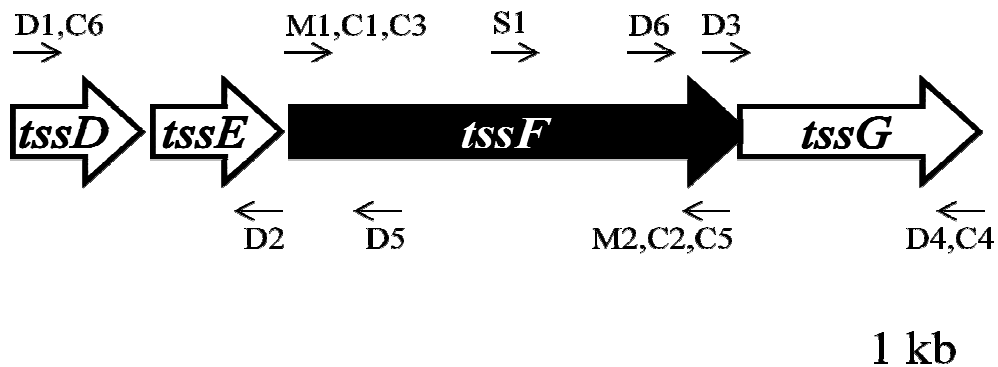


**Figure 20. Mutagenesis, complementation and sequencing oligonucleotide locations in the *tssDEFG* locus.** These genes form part of a larger operon. Small arrows show the locations of oligonucleotides described in Table 12.

### Unmarked clean deletion of *tssF*

Because of repeated failures to complement the insertional *tssF* mutant, a clean deletion strategy was designed using the system described by Flannagan *et*

*al.* (21). In short, regions flanking a target gene are cloned together on plasmid pGPI, which contains a unique site for the *SceI* restriction enzyme. Homologous recombination places the deletion construct and the plasmid on the chromosome adjacent to the target gene. By transforming cells containing the chromosomally-inserted pGPI with plasmid pDAI-*sceI*, which expresses the *SceI* homing endonuclease, the chromosome is digested. This causes a break in the DNA that must be eliminated for the cell to survive; therefore, plasmid pGPI is released by homologous recombination along with either the wild type target gene or the deletion construct. In approximately 50% of events, the wild type region will remain instead of the deletion construct (there is no selection for one or the other); clones carrying the deletion construct can be identified by PCR amplification across the target gene. Plasmid pDAI-*sceI* can then be cured by passaging such clones in liquid media for 3 days and verifying the absence of the plasmid by standard plasmid isolation and gel electrophoresis.

To generate a *tssF* clean deletion mutant, PCR amplification of *tssDE* and *tssG*, the respective upstream and downstream flanking genes of *tssF*, was carried out using primer sets D1/D2 and D3/D4 (Figure 20). The PCR products were then separated by gel electrophoresis, purified from the gel by GeneClean, digested using appropriate enzymes shown in Table 11, and then ligated to pGPI. Following overnight ligation at 16°C, the ligation mixture was used to transform *E. coli* DH5α by heat shock, and transformants were selected on LB + Tp100. Plasmid isolation was carried out using QIAprep kit (Qiagen), and BigDye sequencing of pGPI was performed using primers pGPI F and pGPI R (Table 11).

A plasmid was then selected for electroporation into *Bc* K56-2, and transformants were selected on LB + Tp100. A strain carrying pGPI-*tssDEG* was then transformed by electroporation with pDAI-*sceI* and selected on LB + Tc100. Transformants were then screened for loss of *tssF* by PCR amplification using primers D1 and D4 (Figure 20). Strains demonstrating a loss of *tssF* were then screened for the loss of the ability to kill *E. coli* by the interspecies competition assay described below; two clones demonstrating this phenotype loss were carried forward for plasmid curing in 3 daily passages in fresh LB broth. Mutants exhibiting loss of pDAI-*sceI* were identified by growing colonies from the third passage culture on LB and LB + Tc100; plasmid loss in Tc-sensitive strains was confirmed by plasmid isolation and gel electrophoresis.

### **Genetic complementation**

To restore the mutated phenotype to K56-2 mutant  $\Delta tssF$ , 4 different PCR products containing *tssF* were generated (oligonucleotides shown in parentheses):

1. containing *tssF* flanked by 5' NdeI and 3' XbaI sites with a 6x polyhistidine tag at the 3' end (C1, C2);
2. containing *tssF* flanked by 5' NdeI and 3' XbaI restriction sites and a 10x polyhistidine tag at the 5' end (C3, C5);
3. containing *tssFG* flanked by 5' NdeI and 3' XbaI sites with and 10x polyhistidine tags at the 5' end of *tssF* and 3' end of *tssG* (C3, C4);
- and 4. containing *tssDEFG* flanked by 5' NdeI and 3' XbaI sites with a 10x polyhistidine tag at the 3' end of *tssG* (C6, C4).

All constructs were cloned into the rhamnose-inducible plasmid pSCRhaB2 (14) following its digestion with the appropriate enzymes and GeneClean purification from a 0.8% agarose gel (Fermentas, Inc., Burlington, ON). PCR

construct #1 was cloned into the Tc resistance-carrying plasmid pSCRhaTc, since it was to be used for the complementation of an insertional *tssF::Tp<sup>R</sup>* mutant. Triparental mating (9) was carried out to transform  $\Delta tssF$  with the complementation plasmid, and both wild type K56-2 and the mutant were similarly transformed with blank plasmid to control for the physiological effects of the vector. The blank plasmid-carrying wild type strain was produced in collaboration with Gerardo Juarez-Lara, a former Master's student of the Dennis lab, by digestion of pXO3 (14) with NdeI + XbaI, purification with GeneClean, digestion with Mung Bean exonuclease (Promega Corp.) and self-ligation. Complementation transformants were screened for the restoration of their phenotypes with and without 0.02% rhamnose by performing the interspecies competition assay described below.

### **Interspecies competition experiment**

To evaluate the function of the Bc T6SS in interspecies competition, the method of MacIntyre *et al.* (32) was used. Briefly, predator (K56-2 or  $\Delta tssF$  mutant) and prey (DH5 $\alpha$ /pBBR1MCS) strains were grown on LB agar for 18 – 20 h at 37 °C, resuspended in 1 ml LB broth, and standardized by OD<sub>600</sub>. Predator and prey were then mixed together at a 10:1 ratio, centrifuged at 16,100 x g for 2 minutes, and resuspended in 25  $\mu$ l LB per replicate. Twenty-five microlitres of the resuspended mixtures were then spotted on LB agar, left to dry on the bench for several minutes, and then placed at 37 °C for 4 hours. After this incubation, spots were resuspended in 1 ml LB broth and serially diluted using a Deepwell 96 well plate (VWR International). To obtain plate counts for the predator and prey

strains, 10  $\mu$ l spots of each dilution were pipetted using a Research Plus multichannel micropipettor (Eppendorf, Inc. , Hamburg) onto antibiotic-containing LB agar; Ap was included to select for Bc predator strains, while Cm was included to select for *E. coli* prey. The plates were then incubated at 37 °C until colonies appeared. Results were compared by Student's t-test.

### **Susceptibility of other human pathogens to Bc T6SS-mediated killing**

To determine whether other pathogenic bacteria were susceptible to T6SS-mediated killing by Bc K56-2, the interspecies competition assay was performed using *Pseudomonas aeruginosa* PAO1 and PA14. *Klebsiella aerogenes* and *Staphylococcus aureus* RN4220 were subjected to a similar assay that was not necessarily specific to T6SS-mediated killing, where survival of prey strains was compared in the presence and absence of Bc K56-2. In addition, *B. cenocepacia* K56-2 and the isogenic mutant *tssF::Tp* were subjected to killing by *Vibrio cholerae* V52 and its isogenic  $\Delta vasK$  mutant in a manner identical to that described above.

### **Promoter prediction, protein localization and structural homology software**

To obtain information concerning likely promoter sites surrounding *tssF*, we used the Neural Network Promoter Prediction software at the Berkeley Drosophila Genome Project website ([http://www.fruitfly.org/seq\\_tools/promoter.html](http://www.fruitfly.org/seq_tools/promoter.html)). The inner membrane localization of TssF was determined to high likelihood by the PSORTb ver. 3.0 software (47), available at <http://www.psort.org/psortb/>. This information was

helpful in determining whether to include 5' or 3' polyhistidine tag on the *tssF* complementation construct. (In the end, both constructs were generated.) To identify potential structural homologs of proteins encoded by the genes surrounding predicted *vgrG* homologs in *Bc* J2315, protein sequences were submitted to PHYRE2. Generally, fold predictions with confidence levels below 40% were not included in the final analysis unless the fold encompassed a large portion of the protein (>25% of the protein).

## Results

### **The *B. cenocepacia* T6SS is homologous to T6SS-1 of *B. thailandensis***

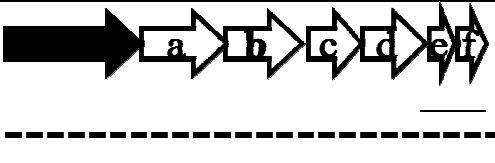
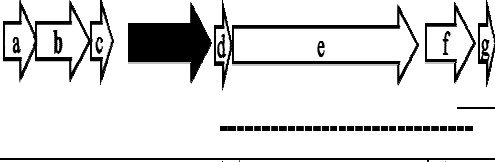
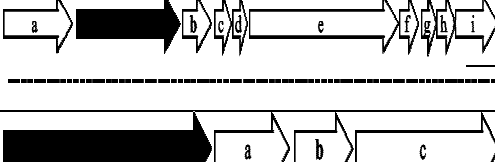
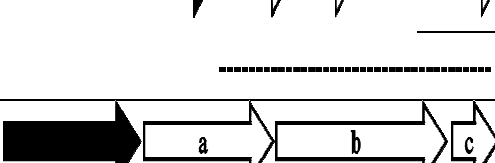
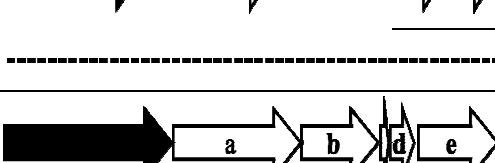
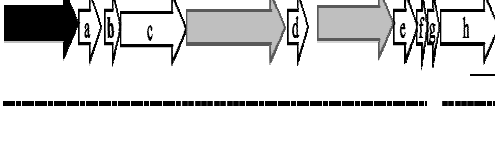
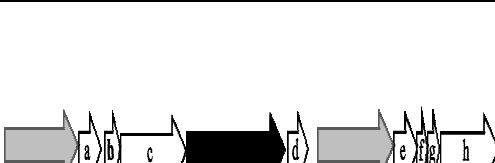
*B. thailandensis* encodes five separate T6SSs within its genome. While mutagenesis of T6SS-5 causes attenuation of the bacteria in a murine infection model, the other systems are not required for virulence in mice (44). Of these four, only T6SS-1 was assigned a putative role, as mutant in this T6SS displayed reduced competition with *Pseudomonas putida* in a mixed biofilm. BLASTN analysis reveals that the *Bc* T6SS is homologous to T6SS-1 in *B. thailandensis* (92% coverage, ~86% identity), implying that the *Bc* T6SS is also evolved for competition with other bacteria. The *Bc* T6SS gene cluster encompasses *bcal0337-bcal0352*, and carries all core T6SS genes identified in previous studies with the exception of VgrG (TssI), which will be discussed in upcoming sections. In addition to the core genes, there are several accessory genes within the core T6SS cluster, including *bcal0340* (tetratricopeptide repeat-containing lipoprotein),

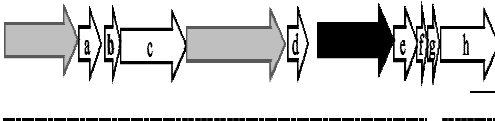
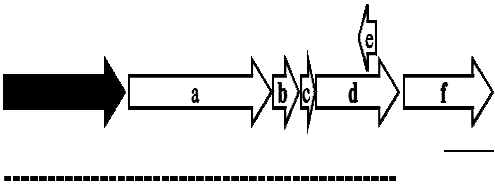
*bcal0349* (OmpA-like protein with peptidoglycan-binding domains), *bcal0350* (hypothetical protein), and *bcal0352* (metallopeptidase).

In other T6SSs, VgrG proteins are thought to act both as cell-puncturing spikes and as effector proteins. VgrG proteins containing effector domains are called “evolved” VgrGs and contain differentiated C-terminal regions with biological activity. However, evolved VgrGs are a small minority of VgrGs, suggesting that the undifferentiated protein plays the single role of capping the T6SS tube during contraction, while other effector proteins pass into the target cell following the puncturing event. In *Bc* J2315, 10 homologs of *V. cholerae* VgrG1-3 are dispersed throughout the genome, occurring on both chromosomes and the megaplasmid formerly known as chromosome 3 (Table 13); this dispersal of VgrG genes is not unusual for T6SSs (17), and secreted effector proteins are suspected to be encoded alongside them (3). An exception to this trend is found with Bcal1355, Bcal1359 and Bcal1362, VgrG homologs encoded within the same gene cluster. Interestingly, the *Bc* VgrG homologs each occur within, and usually at the 5’ end of, clusters of unidirectional genes, suggesting transcriptional and possibly functional relationships.

**Table 13. The *B. cenocepacia* J2315 genome encodes 10 putative VgrG proteins in 7 gene clusters.**

VgrG2 homolog*	% VgrG -2 homo -logy **	Size a.a.	G C %	Charac-teristics	Genetic locus. Ruler = 1 kb. Dotted lines show co-transcription (43) (5) (20). See Table 14 for information on surrounding genes.

Bcal1294	30-48	701	58	C-terminal lysozyme domain (527-662)	
Bcam2254	28-46	706	65	No evolved domain	
Bcas0667	29-47	999	62	C-terminal phospholipase domain (680-999)	
Bcam0043	26-42	834	69	No evolved domain	
Bcal2503	35-54	492	62	C-terminal lysozyme domain	
Bcam0148	23-43	948	61	C-terminal phage tail-associated lysozyme / triple-stranded β-helix*** @493-718 (99%)	
Bcal1355	24-36	931	69	C-terminal domains: 1. Phage tail-associated lysozyme / triple-stranded β-helix*** @499-831 (99%) 2. Unknown	
Bcal1359	25-40	1233	65	C-terminal domains: 1. Phage tail-associated lysozyme / triple-stranded β-helix*** @513-758 (98%) 2. Zinc metalloprotease** * @1097-1163 (79%)	

Bcal1362	22-35	934	70	C-terminal domains: 1. Phage tail-associated lysozyme / triple-stranded $\beta$ -helix*** @528-792 (99%) 2. Phage $\beta$ -helix – foldon region fusion protein*** @768-884 (67%)	
Bcal1165	22-41	835	61	C-terminal domains: 1. Phage tail-associated lysozyme / triple-stranded $\beta$ -helix*** @506-719 (99%) 2. Phage $\beta$ -helix – foldon region fusion protein*** @662-792 (66%)	

\* VgrG1 and VgrG3 produce same homologs as VgrG2

\*\*Shown as identities-positives (i.e., exact amino acid matches versus similar amino acids)

\*\*\*As suggested by PHYRE2 analysis (% confidence shown in parentheses)

Table 14 outlines the primary and tertiary amino acid sequence homology of the proteins encoded within the various VgrG clusters. The protein domains identified through these analyses include phospholipases (Bcal1296, Bcam0149, Bcam0151), endonucleases (Bcal1298, Bcas0663, Bcal1172), a diguanylate cyclase (Bcam2256), unspecified hydrolases (Bcam0046, Bcal1366), RHS repeat proteins (Bcam2252, Bcam2253, Bcas0663), possible DNA-interacting proteins (Bcam2253A, Bcas0661A, Bcas0664, Bcal2500, Bcal1357), possible host cell attachment proteins (Bcal1295, Bcam2255, Bcal2502, Bcal1360, Bcam2253), and mediators of protein-protein interactions (Bcal1297, Bcal1300, Bcas0666, Bcam0150, Bcam0152, Bcal1165), including ankyrin repeat proteins.

**Table 14. *In silico* characterization of genes neighbouring *B. cenocepacia* J2315 VgrG homologs.**

VgrG2 homolog*	Letter-gene (from Table 13)	Homology*
Bcal1294	A- <i>bcal1295</i>	Immunoglobulin-like beta-sandwich (67% / 9%) *
	B- <i>bcal1296</i>	Phospholipase
	C- <i>bcal1297</i>	Ankyrin repeat (protein-protein interactions)
	D- <i>bcal1298</i>	HNH ENDO VII nuclease toxin
	E- <i>bcal1299</i>	Chaperone / protein binding (100% / 89%)*
	F- <i>bcal1300</i>	TPR repeat (protein-protein interactions)
Bcam2254	A- <i>bcam2257</i>	Oxidoreductase (38% / 60%)*
	B- <i>bcam2256</i>	Diguanylate cyclase (cyclic di-GMP is a bacterial intracellular signal)
	C- <i>bcam2255</i>	OmpA (peptidoglycan-binding)
	D- <i>bcam2253A</i>	MogI/psbp-like putative regulator (100% / 97%)* Photosynthesis involvement
	E- <i>bcam2253</i>	YD repeat (carbohydrate-binding) and RHS repeat (toxins)
	F- <i>bcam2252</i>	Pseudogene; RHS repeat
	G- <i>bcam2251A</i>	ATP-binding (37% / 26%)*
Bcas0667	A- <i>bcas0668</i>	VasA
	B- <i>bcas0666</i>	Ankyrin repeat exported protein
	C- <i>bcas0665</i>	Unknown
	D- <i>bcas0664</i>	MogI/psbp-like putative regulator (100% / 96%)* Photosynthesis involvement
	E- <i>bcas0663</i>	HNH ENDO VII nuclease and RHS repeat
	F- <i>bcas0662</i>	SMI1 bacterial toxin immunity protein
	G- <i>bcas0661C</i>	Cystatin-like (cysteine protease inhibitor) (87% / 87%) *
	H- <i>bcas0661B</i>	Unknown
	I- <i>bcas0661A</i>	Metal-binding (86% / 14%)* Transcription (52% / 27%)* Electron transport (65% / 7%)*
Bcam0043	A- <i>bcam0044</i>	Unknown
	B- <i>bcam0045</i>	Homotrimer-forming (48% / 8%)*
	C- <i>bcam0046</i>	$\alpha/\beta$ hydrolase (91% / 22%)*
Bcal2503	A- <i>bcal2502</i>	Immunoglobulin-like $\beta$ -sandwich (60% / 9%)*
	B- <i>bcal2501</i>	Phage portal protein (35% / 15%)*
	C- <i>bcal2500</i>	DNA binding domain (60% / 8%)*

		40S ribosomal protein (44% / 55%)*
<b>Bcam0148</b>	<b>A-<i>bcam0149</i></b>	Phospholipase D
	<u>B-<i>bcam0150</i></u>	SEL1 tetratricopeptide repeat (protein-protein interactions)
	<u>C-<i>bcam0150A</i></u>	Pseudogene; lipoprotein attachment site
	<u>D-<i>bcam0151</i></u>	Pseudogene; phospholipase
	<u>E-<i>bcam0152</i></u>	Lipoprotein; SEL1 tetratricopeptide repeat
Bcal1355	<u>A-<i>bcall356</i></u>	Unknown
Bcal1359	<u>B-<i>bcall357</i></u>	Tudor domain (transcription) (43% / 24%)*
Bcal1362	<u>C-<i>bcall358</i></u>	Unknown
	<u>D-<i>bcall360</i></u>	Fibronectin-like
	<u>E-<i>bcall363</i></u>	Unknown
	<u>F-<i>bcall364</i></u>	Unknown
	<u>G-<i>bcall365</i></u>	Unknown
	<u>H-<i>bcall366</i></u>	$\alpha/\beta$ hydrolase (81% / 22%)*
Bcal1165	<u>A-<i>bcall166</i></u>	SH3 adaptor protein (protein-protein interactions)
	<u>B-<i>bcall167</i></u>	Cytokine (41% / 16%)*
	<u>C-<i>bcall168</i></u>	Unknown
	<u>D-<i>bcall169</i></u>	Pseudogene disrupted by insertion sequence
	<u>E-<i>bcall171</i></u>	Transposase
	<u>F-<i>bcall172</i></u>	HNH endonuclease (94% / 10%)* ParB/Sulfiredoxin (92% / 11%)*

\*Proteins annotated as hypothetical in NCBI were submitted for PHYRE2 fold homology analysis; % confidence and coverage shown in parentheses  
 Genes shown in bold are absent from both *B. multivorans* C5393 and *B. stabilis* LMG 14294, while underlined genes are absent only from LMG 14294, as determined by suppression-subtractive hybridization (7).

Another interesting result that emerged from this analysis is the presence of a VasA homolog upstream of the virulence plasmid-associated VgrG encoded by *bcas0667*. Alignment of *Bcas0668* with the T6SS operon-encoded VasA homolog, *Bcal0345*, shows 40% identity between the two proteins. The two proteins share particularly high homology near their N-termini, though the individual domains making up this protein have not been characterized. It is tempting to suggest that *Bcas0668* can act as an adapter molecule for assembly of a modified T6SS that uses *Bcas0667* as VgrG spike.

## **Insertional mutagenesis of *tssF* disrupts T6SS activity in *B. cenocepacia***

To generate a *Bc* mutant defective in type VI secretion (T6S), a Tp resistance cassette was inserted into the centre of the uncharacterized T6SS cluster gene *tssF*, homologs of which have yet to be characterized in other bacteria aside from the abrogation of T6SS-associated virulence phenotypes in both *V. cholerae* (38) and *Rhizobium leguminosarum* (9). Consistent with its predicted localization in other bacteria (17), TssF is predicted by PSORT analysis to localize to the cytoplasm in *Bc*.

Following the successful mutagenesis of this gene in *Bc* K56-2, the interspecies competition abilities of the wild type and mutant strain, *tssF::Tp*, were compared using a competition assay in which predator (*Bc*) and prey (*E. coli* DH5 $\alpha$  carrying pBBR1MCS conferring Cm resistance) are mixed at a ratio of 10:1 following optical density standardization and incubated on LB agar. After 4 hours, the cells are resuspended in LB, serially diluted and then plated on selective media to obtain survivor counts. Typical experiments using these strains resulted in 10<sup>2</sup> to 10<sup>4</sup>-fold survivability differences for *E. coli* when incubated with the benign *tssF::Tp* mutant as opposed to wild type K56-2, depending on the starting cell density. A representative experiment is shown in Figure 21. While the initial predator:prey ratio is 10:1, *E. coli* grows much faster than *Bc*, and so the *E. coli* prey mixed with the attenuated *tssF::Tp* strain tend to “catch up” in population density during the 4 hour incubation.

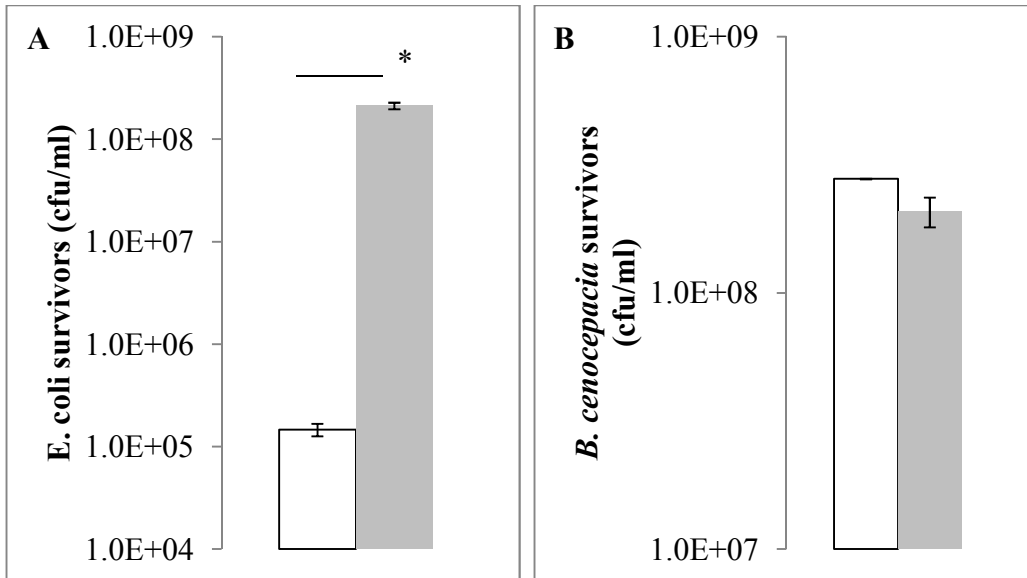


**Figure 21. Inactivation of *B. cenocepacia* K56-2 type VI secretion through mutagenesis of *tssF* results in the abolishment of *E. coli* killing.** In this representative experiment, cells were mixed at 10:1 *B. cenocepacia*:*E. coli* and co-incubated for 4 hours to allow for T6SS-mediated killing to take place. **A.** *E. coli* survivors following 4 hour co-incubation with *B. cenocepacia* K56-2 (white) or *tssF*::Tp (grey). **B.** *B. cenocepacia* K56-2 (white) and *tssF*::Tp (grey) survivors following the incubation period. Results shown are averages of three biological replicates +/- SE. \* $p < 0.0002$

Repeated failures to complement the *tssF*::Tp using both pBBR1MCS, in which *tssF* was cloned along with upstream DNA to maintain any native promoter activity, and the lower-copy pSCRhaTc, which contains a rhamnose-inducible promoter from which inserted genes can be selectively expressed, prompted the realization that a polar mutation was likely introduced following the insertion of the Tp resistance cassette into *tssF*.

## **Clean deletion of *tssF* disrupts T6SS activity by *Bc* but is not restored by genetic complementation**

To circumvent the difficulties with complementation of the insertional mutant, a new mutant was generated using an unmarked deletion system developed by Flannagan *et al.* (21) and adapted for use in the Dennis lab by Ashraf Abdu and Erin Dockery. The first attempt at creating this mutant was successful in disrupting the *E. coli* killing phenotype, yet complementation was declared unsuccessful following the screening of 15 colonies for restoration of the killing phenotype (Figure 22). This prompted the development of additional complementation strategies, including placing the polyhistidine tag at the N-terminus of *tssF*, and co-complementing with *tssF* and *tssG*. Co-complementation was attempted on the advice of Dr. Stefan Pukatzki and his student Daniel Unterweger, who suggested that some T6SS genes required co-expressing with nearby genes for functionality. In no case was restoration of the *E. coli* killing phenotype observed, and results shown in Figure 24 represent results observed using all approaches.

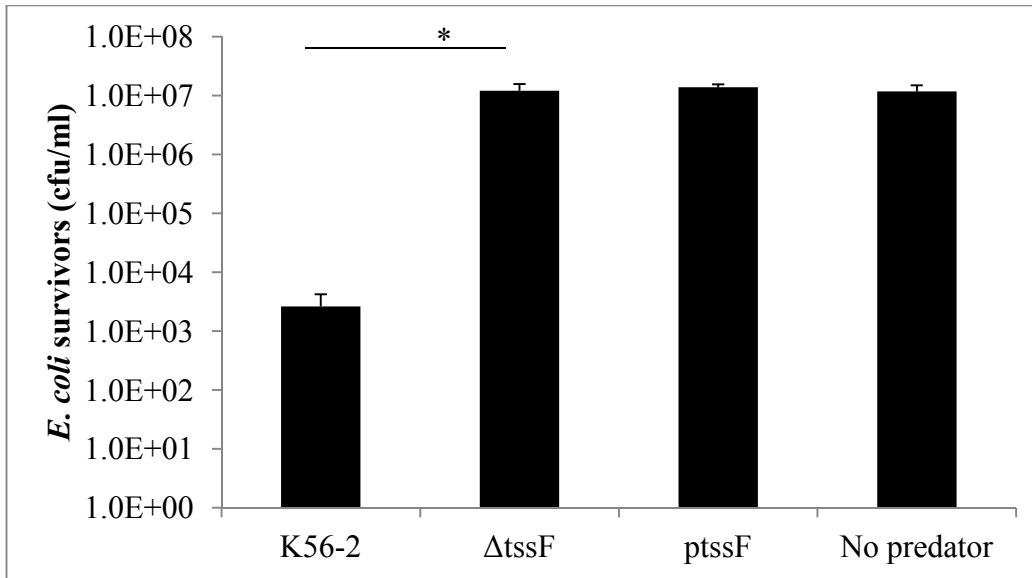


**Figure 22. Deletion of *tssF* abolishes the *E. coli* killing phenotype, but the phenotype is not restored by complementation *in trans*.** Treatments: K56-2, *E. coli* incubated with *B. cenocepacia* K56-2 parent strain; ΔtssF, *E. coli* incubated with *B. cenocepacia* K56-2 carrying in-frame clean deletion knockout of *tssF*; ptssF, *E. coli* incubated with ΔtssF carrying complementation plasmid; No predator, *E. coli* incubated in the absence of *B. cenocepacia*. Results shown are averages of 3 biological replicates from a representative trial +/- SE. \*  $p < 0.01$ . In this figure, ΔtssF is representative of the results obtained from all *tssF* insertional and deletion mutants produced.

These difficulties prompted the exploration of alternative causes for the lack of phenotype restoration, and the possibility of promoter disruption as a result of *tssF* deletion was raised. Therefore, the gene cluster from *bcal0340* to *tssG* was analyzed by Neural Network Promoter Prediction, and a number of promoters were suggested (Figure 23). Therefore, a new strategy was developed

to delete ~1410 bp from the interior of *tssF*, while maintaining an in-frame non-functional gene. This was produced using primers D5 in place of D1 and D6 in place of D3 (Table 12). The resulting construct was sequenced and shown to be in frame. The *E. coli* killing phenotype was disrupted to the same extent seen previously, but restoration of the phenotype did not occur following genetic complementation with *ptssF*.

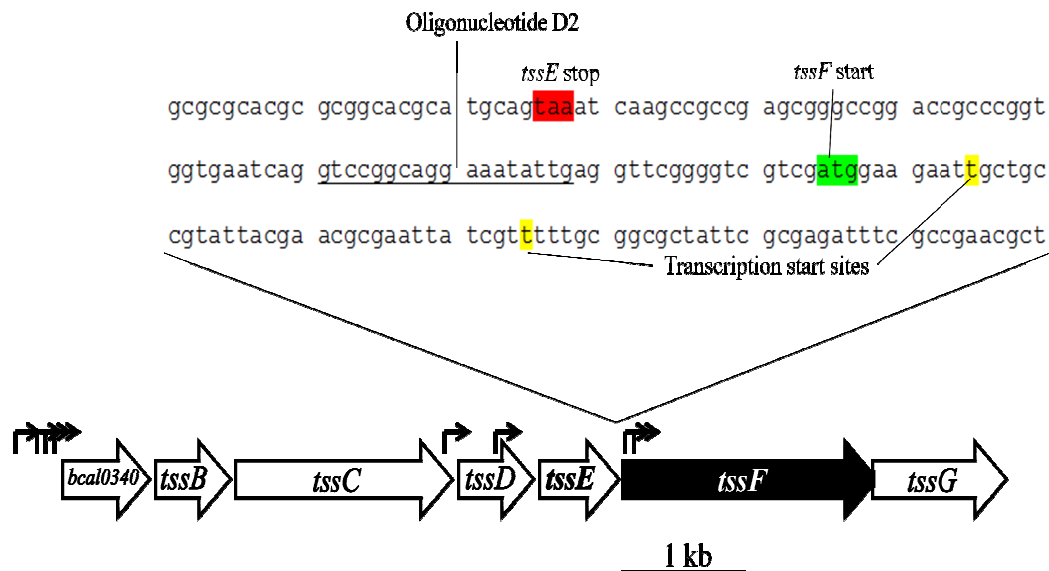


**Figure 23. Neural Network promoter analysis suggests the elimination of two putative promoters by the deletion of *tssF*.** Predicted transcription start sites are shown with raised arrows.

### Susceptibility of human pathogens to Bc T6SS-mediated killing

To explore the specificity of T6SS-mediated killing on other bacterial taxa, different prey species were used. First, it was hypothesized that Bcc bacteria use their T6SS to bring about deleterious effects on other CF pathogens, including *P. aeruginosa* and *S. aureus*. As shown in Figure 24, neither wild type nor *tssF*-mutagenized *Bc* K56-2 has any obvious effect on the survivability of *P.*

*aeruginosa* or *S. aureus*. The failure of *Bc* to kill *S. aureus* is not surprising, since Gram positive bacteria appear to be resistant to the T6SS killing effect of *V. cholerae* as well (32).

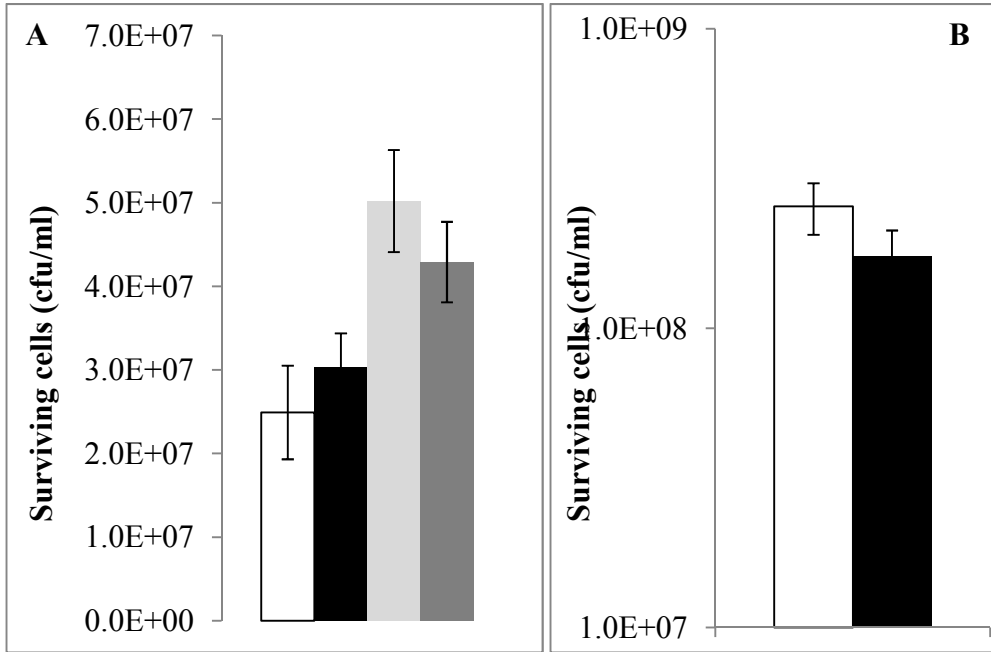


**Figure 24. An intact T6SS has no effect on CF pathogens *P. aeruginosa* or *S. aureus*.** **A.** *P. aeruginosa* PAO1 (black/white) and PA14 (grey) survivors following co-incubation with *Bc* K56-2 (light) or *tssF::Tp* (dark). **B.** *S. aureus* survivors following incubation in the presence (white) or absence (black) of *Bc* K56-2.

In the presence of *Bc* K56-2, *K. aerogenes* survivability decreased approximately 10-fold ( $p < 0.0001$ ) compared with *K. aerogenes* incubated alone, indicating a likely but unconfirmed effect of T6SS-mediated killing by *Bc* (Figure 25).

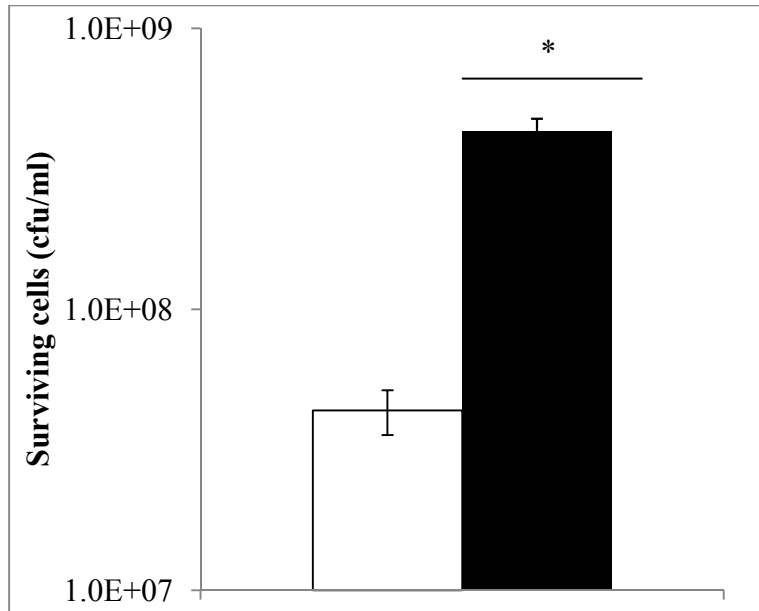


**Figure 25. Incubation with *B. cenocepacia* K56-2 reduces survivability of *K. aerogenes*, possibly through T6SS-mediated killing.** *K. aerogenes* survivor counts are shown following incubation in the presence (white) or absence (black) of *B. cenocepacia* K56-2. The experiment was performed in 3 biological replicates and results are shown as the mean +/- SE. \* $p < 0.0001$

While *Bc* demonstrated no ability to suppress *V. cholerae* in these experiments, the susceptibility of *Bc* to T6SS-mediated killing was tested by reversing the competition assay, with *Bc* K56-2 and *tssF::Tp* as prey strains and *Vibrio cholerae* V52 and an isogenic T6SS-deficient  $\Delta vasK$  mutant previously shown to be deficient in *E. coli* killing (32) as predators. The results shown in Figure 26 extend the predation range of *V. cholerae* V52 to *Bc*.

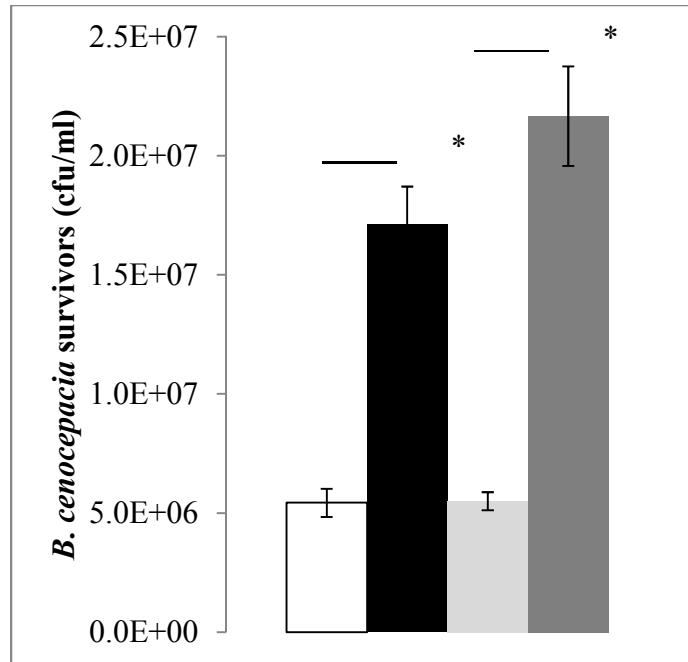


**Figure 26. The *Vibrio cholerae* V52 T6SS is active against *B. cenocepacia* K56-2.** *B. cenocepacia* K56-2 (black/white) and *tssF::Tp* (grey) survivor counts are shown following predation by *V. cholerae* V52 (light) or  $\Delta vasK$  (dark). The experiment was carried out in three biological replicates and results are shown as mean +/- SE. \*  $p < 0.005$ .

### **Type VI secretion does not contribute to duckweed or wax moth larval pathogenesis**

To assess the involvement of the *Bc* T6SS in virulence, two infection models were employed. *Bc* K56-2 and *tssF::Tp* were each injected into 20 wax moth larvae at inocula of  $9.5 \times 10^6$  and  $1.7 \times 10^7$  cfu, respectively, and surviving larvae were counted at 24 h intervals. Although survival was approximately double for *tssF::Tp* at 48 h, the difference was not significant (Figure 27a). No significant difference was observed between the LD<sub>50</sub> of K56-2 and *tssF::Tp*

against duckweed. These results indicate that although the *Bc* T6SS has a clear role in invasion and intracellular survival in phagocytes, its contribution to infection of multicellular hosts is likely limited. This finding is consistent with the revelation that only one of five functional T6SSs in *B. thailandensis* is required for full virulence in mice (44).

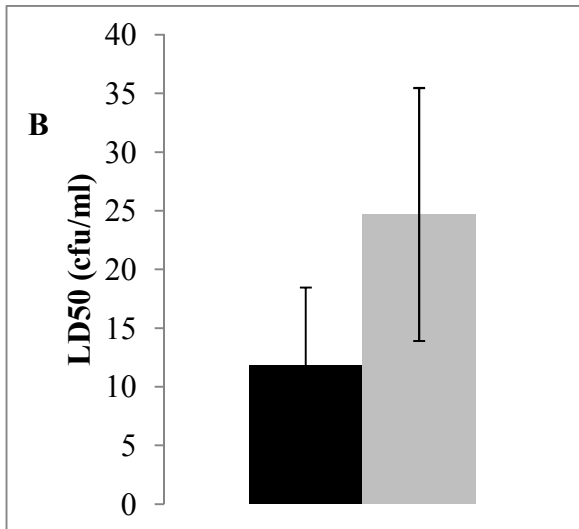
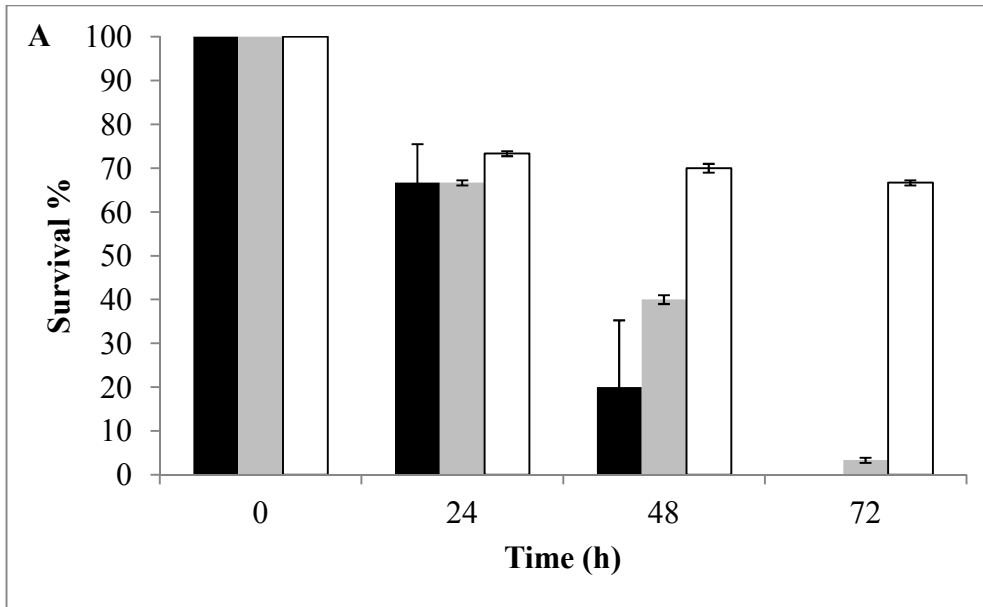


**Figure 27.** The *B. cenocepacia* T6SS has no apparent role in virulence against *Galleria mellonella* (Greater wax moth larvae) or *Lemna minor* (Common duckweed). **A.** *G. mellonella* survival following injection with  $1 \times 10^3$  cfu *B. cenocepacia* K56-2 (black),  $1 \times 10^3$  cfu *tssF::Tp* (grey), or buffer control (white). Results shown are the averages of three biological replicates  $\pm$  SE. **B.** LD<sub>50</sub> of *B. cenocepacia* K56-2 (black) and *tssF* (grey) against *L. minor*. Results shown are the averages of two (*tssF::Tp*) or four (K56-2) biological replicates  $\pm$  SE.

To determine if other Bcc species use T6S for antibacterial activity, the same insertional *tssF*::Tp mutation produced in *Bc* K56-2 was introduced into *B. multivorans* ATCC 17616. A similar trend of *E. coli* killing to that observed in *Bc* was observed (Figure 28), indicating that the Bcc T6SS may fulfill similar roles in the different species.

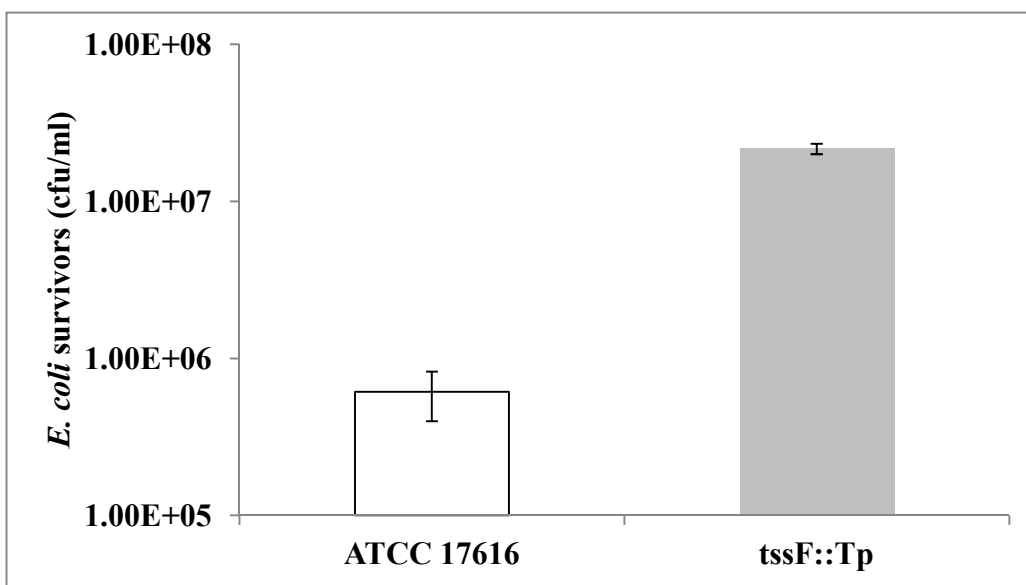


**Figure 28. Inactivation of *B. multivorans* ATCC 17616 type VI secretion through mutagenesis of *tssF* results in the abolishment of *E. coli* killing.** In this representative experiment, cells were mixed at 10:1 *B. multivorans*:*E. coli* and co-incubated for 4 hours to allow for T6SS-mediated killing to occur. Results shown are average +/- SE surviving *E. coli* cells following co-incubation with *B. multivorans* ATCC 17616 or *tssF*::Tp, performed in 3 biological replicates. \**p* = 0.0002

## Discussion

Social behaviours are central to the lifestyle of many bacteria – they build communities together, move together, and communicate amongst themselves. In addition, they devote enormous genomic and cellular infrastructure toward competition with their neighbours. Their means of competing include the release of soluble molecules into the surrounding environment. For example, microcins are antimicrobial peptides produced in Enterobacteriaceae that target phylogenetically related organisms (19), and bacteriocins are proteins containing three functional domains reliant on target cell receptor binding to initiate uptake and cell destruction, produced by *E. coli* and also targeting closely-related organisms (15). In addition to the release of such molecules, broader groups of Gram negative bacteria have been shown to elaborate surface-attached appendages called contact-dependent inhibition systems (CDI), which function as “toxins on a stick” by carrying toxins at their distal ends for passive introduction into cells contacted by the CDI<sup>+</sup> bacterium. CDI gene clusters are usually arranged in a *cdiBIA* format. CdiB forms a  $\beta$ -barrel for the export of CdiA to the cell surface, while *cdiA* encodes the “stick” that likely stretches tens of nanometres from the cell surface and carries variable C-terminal toxin domains. CdiI is a small toxin immunity protein corresponding to the C-terminal toxin of CdiA (41).

A newly-discovered mode of toxin delivery among Gram negative cells occurs through the elaboration of T6SSs, which have been shown to mediate the transfer of several characterized toxins into target cells, resulting in their

inhibition or death. In this study, we have demonstrated through the disruption of *tssF* that both the *Bc* K56-2 and *B. multivorans* ATCC 17616 T6SSs are responsible for an interbacterial competition phenotype in *Bc*. Although *E. coli* killing in the *Bc tssF* mutants was not restored through a range of genetic complementation strategies, the increasingly stringent gene knockout strategies, cumulating with an in-frame partial deletion of *tssF*, demonstrate that killing of *E. coli* cells is mediated by the *Bc* T6SS. This claim is moderated, however, by the failure of complementation. It is conceivable, though unlikely, that spontaneous gene deletions elsewhere in the genome during these mutageneses are the root of this failure. The demonstration that insertional mutagenesis of *B. multivorans tssF* causes a similar loss of *E. coli* killing indicates that the high degree of T6SS sequence conservation among Bcc species is reflected in phenotypic similarities. Despite this similarity in T6SS-mediated interbacterial competition, however, the intracellular lifestyle of *B. multivorans* may differ slightly from that of *Bc* in the growth of intracellular bacteria. While *Bc* strain C1359 was shown to survive and increase in numbers within A549 epithelial cells, *B. multivorans* 10661 was only able to invade and persist, without subsequent cell growth (27). Similar comparisons have not been carried out in phagocytes.

Since the discovery of extensive microbiomes in both CF and healthy lungs, it has become apparent that, like other mucosal surfaces, invading bacteria must displace the existing lung microflora to compete for niche space (10). Therefore, this study sought to explore beyond *E. coli* and determine if the T6SS mediates interbacterial competition with known CF lung colonizers, including *P.*

*aeruginosa*, *S. aureus* and *Klebsiella* sp. Since Gram positive bacteria are thus far understood to be resistant to T6SS-mediated killing (17), it was not surprising that *S. aureus* displayed no sensitivity during co-incubation with *Bc* K56-2 or the isogenic *tssF*::Tp mutant. *P. aeruginosa* reacted similarly to co-incubation with *Bc*, but a *K. aerogenes* strain (which is related to the CF colonizer *K. pneumoniae*) showed approximately 10-fold reduction in survivability during co-incubation. This experiment was not carried out with the *tssF* mutant to determine whether the effect was T6SS-mediated, but the outcome is consistent with results seen in positive killing trials against *E. coli*. Therefore, supporting evidence is required to ascertain whether *Bc* uses its T6SS to compete with CF airway bacteria. A screen to identify strains susceptible to *B. thailandensis* T6SS-mediated competition revealed only 3 of 32 strains that were strongly outcompeted and 4 of 32 strains that were moderately outcompeted as a result of the T6SS. One of these moderately-sensitive strains is *K. pneumoniae*, supporting the incomplete data described above suggesting *Klebsiella* bacteria are susceptible to *Burkholderia* T6SS effector activity (44). The sensitivity of additional CF airway colonizers, particularly common organisms not linked to pathology, such as *Rothia* spp. (10), should be tested to provide evidence for or against the hypothesis that CF pathogens outcompete airway bacteria using type VI secretion.

The *Bc* T6SS was tested against that of *V. cholerae* in predator-prey experiments, and it was found that while *V. cholerae* was resistant to killing by *Bc*, there was a ~3-4-fold decrease in viable *Bc* cells exposed to *V. cholerae* versus the *V. cholerae* T6SS knockout strain  $\Delta vasK$ . Therefore, at least one T6SS

toxin expressed by *V. cholerae* is active against *Bc*. One such toxin candidate is VasX, which was initially shown to cause membrane perturbations in the model amoeba *Dictyostelium discoideum* (33) but also has antibacterial activity at the periplasmic face of the Gram negative inner membrane through pore formation (Miyata *et al.*, unpublished results). Peptidoglycan degradation by the evolved VgrG-3 was also shown to occur, providing another candidate for the antibacterial effect of *V. cholerae* on *Bc* (13). In *P. aeruginosa*, three exported T6SS substrates have been identified along with putative cognate antitoxins, and one of these three substrates, Tse2, was confirmed to have *E. coli*-inhibiting activity through an as-yet uncharacterized mechanism that occurs in the cytoplasm (25). Another of these exported toxins, Tse1, carries an amidase fold normally associated with peptidoglycan degradation; this enzyme, however, was shown to have broad peptidoglycan specificity conferred by its relatively open architecture compared with typical amidase enzymes (16). Another peptidoglycan-degrading effector was recently characterized in *Pseudomonas protegens*, and was shown to have glycoside hydrolase activity similar to that observed in the *V. cholerae* VgrG-3 evolved domain (46). Lysozyme-like C-terminal domains are prevalent among the VgrG proteins identified in *Bc* (Table 13), suggesting that many of these gene clusters may be functionally directed toward interbacterial competition.

No clear role for the *Bc* T6SS in plant or insect pathogenesis could be established in this study. It is clear from previous studies that this system has negative effects on eukaryotic cellular pathways, including the disruption of cytoskeletal integrity and NADPH oxidase complex formation at the vacuolar

membrane, and manipulation of intracellular signalling to activate proinflammatory cytokines (2, 22, 39, 40). However, these are effects on single cells representing roaming defenders in mammalian hosts, while the experiments in the present study tested insect larvae and plants, neither of which produce roaming phagocytes. An earlier study did, however, identify a role for the *Bc* T6SS in persistence during chronic rat lung infection (26). It seems logical that since T6SS has not been demonstrated against Gram positive bacteria, it is the thick cell wall that prevents access by the T6SS to its cellular targets. If this proves correct, then the same concept would hold true for toxin delivery into plant cells. However, this fails to explain why the the T6SS has no contribution to virulence in the wax moth larval model.

A likely possibility is that the T6SS is reserved for use during intracellular persistence, which has thus far not been demonstrated as a *Bc* pathogenesis strategy against plants or insects. This hypothesis is compromised, however, by transcriptomic data showing strong evidence for the down-regulation of the T6SS cluster during stationary phase incubation in minimal medium, and to a lesser extent in rich medium, as well as during exposure to oxidative stress, all conditions that would be expected to drive the expression of T6SS given the harsh intracellular environment. In addition, no activation was observed at 6% oxygen, another condition in which T6SS activation would be expected, since the intracellular environment of the macrophage contains 2.6% oxygen (23). The only condition under which a majority of the cluster was up-regulated is at 37°C versus 20°C. It is particularly surprising that, despite the functional role demonstrated for

the *Bc* T6SS in shutting down the cellular autophagy machinery by preventing formation of the NADPH oxidase complex, the cells would down-regulate the T6SS during oxidative stress. This could imply that under normal circumstances of cellular invasion, the *Bc* T6SS is deployed rapidly enough that oxidative stress is averted in the vacuole, but if the first tactic fails, the bacteria abort the T6SS altogether to conserve resources for alternative tactics. Put in the context of cellular cost, it should also come as no surprise that *Bc* down-regulates the T6SS under restrictive growth conditions. A confounding variable to this hypothesis is that *AtsR*, an important T6SS repressor, is down-regulated under the same conditions as the T6SS, although *AtsR* down-regulation would be expected to permit T6SS expression. This implies the existence of an unidentified upstream activator under these conditions. Overall, the careful control of type VI secretion in *Bc* may reflect a specific ecological role for the T6SS in resisting and benefiting from phagocytic predation that relies on the proper timing of expression.

With the results of this study, *Bc* is only the second organism, after *V. cholerae*, shown to use a single T6SS cluster against both eukaryotic and prokaryotic cells. This dual functionality implies that the system is adapted in response to the need for different roles. This possibility was investigated by analyzing the *VgrG* loci scattered throughout the 2 chromosomes and megaplasmid of *Bc* J2315. BLASTP analysis using the *V. cholerae* *VgrG*-2 protein identified 10 putative *VgrG* homologs encoded by *Bc* J2315. Three of these genes are encoded within the same gene cluster. In general, the *VgrG*

homologs are encoded at or near the 5' region of a gene cluster encoding between 4 and 11 genes in total. While many of the proteins encoded within these clusters are annotated as hypothetical based on their amino acid sequences, PHYRE2 fold homology (28) strongly suggests the striking possibility that many of these VgrG-associated proteins are the T6SS effectors that have not yet been identified in *Bc*.

Type VI secretion is thought to act similarly to CDI in terms of toxin delivery, with the added benefits of a contractile mechanism to puncture the host cell envelope and a conduit through which toxins translocate into the target cell. VgrG proteins show strong homology with phage tailspike proteins, indicating that VgrGs likely carry out the task of puncturing the cell envelope following T6SS sheath contraction to prepare the T6SS for delivery of effectors into the receiving cell. Some VgrG proteins contain C-terminal effector domains, which in some cases have lysozyme-like peptidoglycan-degrading activity (16, 46). Of the 10 putative VgrG proteins identified in *Bc*, seven contain potential lysozyme-like domains, suggesting that these gene clusters are expressed for antibacterial activity. Another VgrG protein contains a phospholipase evolved domain, suggesting a role in membrane perturbations of either prokaryotic or eukaryotic target cells, although VgrG-mediated lipase activity has yet to be experimentally confirmed. True effector proteins devoid of VgrG scaffolds have proven difficult to identify, since their secretion is thought to rely on cell-cell contact, making the effectors generally undetectable in cell supernatants (17).

The results shown in Table 14 illustrate a diversity of possible effector proteins encoded within clusters immediately downstream of the identified *vgrG*

homologs that suggest toxic effects against target cells, including phospholipases, endonucleases, a diguanylate cyclase, hydrolases and RHS repeat proteins. Interestingly, both RHS-repeat proteins and nucleases are adapted for use in CDI systems. Rearrangement hotspot (RHS)-repeat toxins have been identified as functional analogues to the characterized CdiA-based CDI systems, with C-terminal toxin domains and downstream-encoded cognate antitoxin proteins (36). The identification of RHS-repeat domains within the putative effectors downstream of *vgrG* genes in *Bc* suggests either interplay between the RHS-based CDI systems or, more likely, the adoption of RHS functionality by the T6SS. Nucleases have been identified in the CDI systems of several bacteria, including *B. pseudomallei*, and have varying specificities including degradation of tRNAs and DNA. Other CDI toxin domains include metallopeptidases, adenosine deaminases, and ADP-ribosyl cyclases (41). In addition, possible transcription factors, which could confer some degree of self-regulation to the cluster, or DNA-interfering proteins, which would be expected to bind host bacterial DNA, recur through these clusters. Another protein contains a peptidoglycan-binding domain and may either relate to attachment to target cells or degradation of peptidoglycan in target cells. A larger number of proteins contain putative immunoglobulin-like domains, suggesting a possible mechanism of cell sensing. The six proteins containing domains associated with conferring protein-protein interactions could act either as antitoxin proteins or adapters for the different VgrG complexes to interact with the core T6SS. There are only three putative ankyrin repeat proteins in the J3215 genome, and two appear within VgrG clusters; the third is present

within a MFS transporter. Additional proteins of interest encoded within the *bcas0667* cluster include a toxin immunity protein and a cysteine protease inhibitor. Transcriptomics data (5, 20, 43) indicates that in general, the *vgrG* genes are co-expressed with the downstream genes of the clusters, suggesting possible functional interactions. One exception is that *bcal1171* and *bcal1172*, which encode a transposase and an endonuclease, respectively, are differentially expressed from the remainder of the *bcal1165-69* cluster. Therefore, these proteins may not be related to this *vgrG* cluster. In several cases, the *vgrGs* are differentially expressed from their downstream clusters, indicating that timing may play a role in expression of some of these gene clusters.

These data give rise to a possible model for VgrG function in *Bc* that builds on the use of evolved VgrG proteins by suggesting that the various *vgrG* clusters can be called upon and interchanged based on functional requirement, such as the destruction of bacterial cells and eukaryotic cells. As additional functions of the T6SS become evident, these gene clusters will no doubt accumulate more context. For example, the number of putative DNA binding proteins shown in Table 14 could, instead of helping to control *vgrG* cluster regulation, conceivably act inside target cells to direct transcription of select genes, thereby modifying the behaviour of neighbouring cells to the benefit of the T6SS-elaborating cell. A similar mechanism has been identified in the plant pathogen *Xanthomonas*, which injects type III-secreted TAL (transcription activator-like) effectors into host cells. One TAL effector is known to up-regulate

growth genes and cause localized overgrowth of the plant, which is thought to promote bacterial dissemination (11).

In the polymicrobial, biofilm-dominated environment of the CF lung, establishing a colonizing population involves the displacement of existing bacteria (25) and competition for niche space. This work has shown that T6S within the Bcc plays an antibacterial role, though it has yet to be shown that specific CF lung colonizers are susceptible to T6SS-mediated killing. Within the CF lung environment, where biofilms predominate and a wide range of bacteria are present, it seems likely that the Bcc T6SS provides a competitive edge to the bacteria.

Future work to follow this study could investigate the identified *vgrG* clusters in *Bc* through a variety of approaches. The first approach would be to create knockout mutations in each *vgrG* cluster and test these mutants for antibacterial and anti-amoebal predation activity. Because of the likelihood of redundancy based on the prevalence of evolved lysozyme domains among the VgrGs, several combination knockout mutants may be required. If a particular gene cluster is determined to encode the means for a given phenotype, the putative effector proteins encoded within it could be characterized through two additional lines of inquiry. To confirm suspected toxins, the effectors could be cloned on a repressible plasmid and expressed in target *E. coli* cells to assess toxicity. Meanwhile, protein-protein interactions could be demonstrated through yeast two-hybrid experiments or pulldown experiments to confirm toxin-antitoxin interactions or toxin interactions with host cellular targets. In addition to

contributing to the general understanding of these central Gram negative machines, the identification and characterization of T6SS effector proteins could open the downstream possibility of developing novel therapeutics.

## References

1. Aubert D, MacDonald DK, Valvano MA. BcsKC is an essential protein for the type VI secretion system activity in *Burkholderia cenocepacia* that forms an outer membrane complex with BcsLB. *J Biol Chem*. 2010;285(46):35988-98.
2. Aubert DF, Flanagan RS, Valvano MA. A novel sensor kinase-response regulator hybrid controls biofilm formation and type VI secretion system activity in *Burkholderia cenocepacia*. *Infect Immun*. 2008;76(5):1979-91.
3. Barret M, Egan F, Fargier E, Morrissey JP, O'Gara F. Genomic analysis of the type VI secretion systems in *Pseudomonas* spp.: novel clusters and putative effectors uncovered. *Microbiology*. 2011;157(Pt 6):1726-39.
4. Basler M, Pilhofer M, Henderson GP, Jensen GJ, Mekalanos JJ. Type VI secretion requires a dynamic contractile phage tail-like structure. *Nature*. 2012;483(7388):182-6.
5. Bazzini S, Udine C, Sass A, Pasca MR, Longo F, Emiliani G, et al. Deciphering the role of RND efflux transporters in *Burkholderia cenocepacia*. *PLOS One*. 2011;6(4):e18902.
6. Berger M. Inflammatory mediators in cystic fibrosis lung disease. *Allergy Asthma Proc*. 2002;23(1):19-25.
7. Bernier SP, Sokol PA. Use of suppression-subtractive hybridization to identify genes in the *Burkholderia cepacia* complex that are unique to *Burkholderia cenocepacia*. *J Bacteriol*. 2005;187(15):5278-91.
8. Bingle LE, Bailey CM, Pallen MJ. Type VI secretion: a beginner's guide. *Curr Opin Microbiol*. 2008;11(1):3-8.
9. Bladergroen MR, Badelt K, Spaink HP. Infection-blocking genes of a symbiotic *Rhizobium leguminosarum* strain that are involved in temperature-dependent protein secretion. *Mol Plant Microbe Interact*. 2003;16(1):53-64.
10. Blainey PC, Milla CE, Cornfield DN, Quake SR. Quantitative analysis of the human airway microbial ecology reveals a pervasive signature for cystic fibrosis. *Sci Transl Med*. 2012;4(153):153ra30.
11. Boch J, Bonas U. *Xanthomonas* AvrBs3 family-type III effectors: discovery and function. *Annu Rev Phytopathol*. 2010;48:419-36.
12. Bonemann G, Pietrosiuk A, Diemand A, Zentgraf H, Mogk A. Remodelling of VipA/VipB tubules by ClpV-mediated threading is crucial for type VI protein secretion. *EMBO J*. 2009;28(4):315-25.
13. Brooks TM, Unterweger D, Bachmann V, Kostiuik B, Pukatzki S. Lytic activity of the *Vibrio cholerae* type VI secretion toxin VgrG-3 is inhibited by the antitoxin TsaB. *J Biol Chem*. 2013;288(11):7618-25.
14. Cardona ST, Valvano MA. An expression vector containing a rhamnose-inducible promoter provides tightly regulated gene expression in *Burkholderia cenocepacia*. *Plasmid*. 2005;54(3):219-28.
15. Cascales E, Buchanan SK, Duche D, Kleanthous C, Lloubes R, Postle K, et al. Colicin biology. *Microbiol Mol Biol Rev*. 2007;71(1):158-229.
16. Chou S, Bui NK, Russell AB, Lexa KW, Gardiner TE, LeRoux M, et al. Structure of a peptidoglycan amidase effector targeted to Gram-negative bacteria by the type VI secretion system. *Cell Rep*. 2012;1(6):656-64.

17. Coulthurst SJ. The Type VI secretion system - a widespread and versatile cell targeting system. *Res Microbiol.* 2013.
18. Das S, Chaudhuri K. Identification of a unique IAHP (IcmF associated homologous proteins) cluster in *Vibrio cholerae* and other proteobacteria through *in silico* analysis. *In Silico Biol.* 2003;3(3):287-300.
19. Destoumieux-Garzon D, Peduzzi J, Rebuffat S. Focus on modified microcins: structural features and mechanisms of action. *Biochimie.* 2002;84(5-6):511-9.
20. Ferreira AS, Silva IN, Oliveira VH, Becker JD, Givskov M, Ryan RP, et al. Comparative transcriptomic analysis of the *Burkholderia cepacia* tyrosine kinase bceF mutant reveals a role in tolerance to stress, biofilm formation, and virulence. *Appl Environ Microbiol.* 2013;79(9):3009-20.
21. Flannagan RS, Linn T, Valvano MA. A system for the construction of targeted unmarked gene deletions in the genus *Burkholderia*. *Environ Microbiol.* 2008;10(6):1652-60.
22. Gavrilin MA, Abdelaziz DH, Mostafa M, Abdulrahman BA, Grandhi J, Akhter A, et al. Activation of the pyrin inflammasome by intracellular *Burkholderia cenocepacia*. *J Immunol.* 2012;188(7):3469-77.
23. Gazdik MA, McDonough KA. Identification of cyclic AMP-regulated genes in *Mycobacterium tuberculosis* complex bacteria under low-oxygen conditions. *J Bacteriol.* 2005;187(8):2681-92.
24. Haapalainen M, Mosorin H, Dorati F, Wu RF, Roine E, Taira S, et al. Hcp2, a secreted protein of the phytopathogen *Pseudomonas syringae* pv. tomato DC3000, is required for fitness for competition against bacteria and yeasts. *J Bacteriol.* 2012;194(18):4810-22.
25. Hood RD, Singh P, Hsu F, Guvener T, Carl MA, Trinidad RR, et al. A type VI secretion system of *Pseudomonas aeruginosa* targets a toxin to bacteria. *Cell Host Mic.* 2010;7(1):25-37.
26. Hunt TA, Kooi C, Sokol PA, Valvano MA. Identification of *Burkholderia cenocepacia* genes required for bacterial survival *in vivo*. *Infect Immun.* 2004;72(7):4010-22.
27. Keig PM, Ingham E, Kerr KG. Invasion of human type II pneumocytes by *Burkholderia cepacia*. *Microb Pathog.* 2001;30(3):167-70.
28. Kelley LASMJE. Protein structure prediction on the web: a case study using the Phyre server. *Nat Protoc.* 2009;4:363 - 71.
29. Kotrange S, Kopp B, Akhter A, Abdelaziz D, Abu Khweek A, Caution K, et al. *Burkholderia cenocepacia* O polysaccharide chain contributes to caspase-1-dependent IL-1beta production in macrophages. *J Leukoc Biol.* 2011;89(3):481-8.
30. Lamothe J, Thyssen S, Valvano MA. *Burkholderia cepacia* complex isolates survive intracellularly without replication within acidic vacuoles of *Acanthamoeba polyphaga*. *Cell Microbiol.* 2004;6(12):1127-38.
31. Leiman PG, Basler M, Ramagopal UA, Bonanno JB, Sauder JM, Pukatzki S, et al. Type VI secretion apparatus and phage tail-associated protein complexes share a common evolutionary origin. *Proc Natl Acad Sci U S A.* 2009;106(11):4154-9.

32. MacIntyre DL, Miyata ST, Kitaoka M, Pukatzki S. The *Vibrio cholerae* type VI secretion system displays antimicrobial properties. PNAS USA. 2010;107(45):19520-4.
33. Miyata ST, Kitaoka M, Brooks TM, McAuley SB, Pukatzki S. *Vibrio cholerae* requires the type VI secretion system virulence factor VasX to kill *Dictyostelium discoideum*. Infect Immun. 2011;79(7):2941-9.
34. Murdoch SL, Trunk K, English G, Fritsch MJ, Pourkarimi E, Coulthurst SJ. The opportunistic pathogen *Serratia marcescens* utilizes type VI secretion to target bacterial competitors. J Bacteriol. 2011;193(21):6057-69.
35. Pietrosiuk A, Lenherr ED, Falk S, Bonemann G, Kopp J, Zentgraf H, et al. Molecular basis for the unique role of the AAA+ chaperone ClpV in type VI protein secretion. J Biol Chem. 2011;286(34):30010-21.
36. Poole SJ, Diner EJ, Aoki SK, Braaten BA, t'Kint de Roodenbeke C, Low DA, et al. Identification of functional toxin/immunity genes linked to contact-dependent growth inhibition (CDI) and rearrangement hotspot (Rhs) systems. PLoS Genet. 2011;7(8):e1002217.
37. Pukatzki S, Ma AT, Revel AT, Sturtevant D, Mekalanos JJ. Type VI secretion system translocates a phage tail spike-like protein into target cells where it cross-links actin. Proc Natl Acad Sci U S A. 2007;104(39):15508-13.
38. Pukatzki S, Ma AT, Sturtevant D, Krastins B, Sarracino D, Nelson WC, et al. Identification of a conserved bacterial protein secretion system in *Vibrio cholerae* using the *Dictyostelium* host model system. PNAS USA. 2006;103(5):1528-33.
39. Rosales-Reyes R, Aubert DF, Tolman JS, Amer AO, Valvano MA. *Burkholderia cenocepacia* type VI secretion system mediates escape of type II secreted proteins into the cytoplasm of infected macrophages. PLOS One. 2012;7(7):e41726.
40. Rosales-Reyes R, Skeldon AM, Aubert DF, Valvano MA. The Type VI secretion system of *Burkholderia cenocepacia* affects multiple Rho family GTPases disrupting the actin cytoskeleton and the assembly of NADPH oxidase complex in macrophages. Cell Microbiol. 2012;14(2):255-73.
41. Ruhe ZC, Low DA, Hayes CS. Bacterial contact-dependent growth inhibition. Trends Microbiol. 2013;21(5):230-7.
42. Russell AB, Hood RD, Bui NK, LeRoux M, Vollmer W, Mougous JD. Type VI secretion delivers bacteriolytic effectors to target cells. Nature. 2011;475(7356):343-7.
43. Sass AM, Schmerk C, Agnoli K, Norville PJ, Eberl L, Valvano MA, et al. The unexpected discovery of a novel low-oxygen-activated locus for the anoxic persistence of *Burkholderia cenocepacia*. ISME J. 2013;7(8):1568-81.
44. Schwarz S, West TE, Boyer F, Chiang WC, Carl MA, Hood RD, et al. *Burkholderia* type VI secretion systems have distinct roles in eukaryotic and bacterial cell interactions. PLOS Path. 2010;6(8):e1001068.
45. Thomson EL, Dennis JJ. A *Burkholderia cepacia* complex non-ribosomal peptide-synthesized toxin is hemolytic and required for full virulence. Virulence. 2012;3(3):286-98.

46. Whitney JC, Chou S, Russell AB, Biboy J, Gardiner TE, Ferrin MA, et al. Identification, structure and function of a novel type VI secretion peptidoglycan glycoside hydrolase effector-immunity pair. *J Biol Chem*. 2013.
  47. Yu NY, Wagner JR, Laird MR, Melli G, Rey S, Lo R, et al. PSORTb 3.0: improved protein subcellular localization prediction with refined localization subcategories and predictive capabilities for all prokaryotes. *Bioinformatics*. 2010;26(13):1608-15.
-

Chapter 5: *Burkholderia multivorans* virulence is activated by physiologically relevant temperature and oxygen levels

---

## Introduction

### *Burkholderia multivorans*

Virulence studies of the Bcc have traditionally concentrated on characterizing *Burkholderia cenocepacia* (*Bc*) rather than *Burkholderia multivorans* (*Bm*) for three main reasons. First, there is a sense of urgency to identify *Bc* pathogenesis mechanisms in an effort to develop virulence-blocking drugs, since *Bc* is so far the only Bcc species to give rise to multinational epidemics within the CF community (19). Second, *Bc* typically correlates with worse prognosis than other Bcc members following lung transplant in CF patients, suggesting its greater tendency toward tissue invasion or general pervasiveness throughout the airway (8). Finally, while *Bc* strains are usually among the most virulent of the Bcc members in infection models, *Bm* tends to demonstrate substantially lower virulence in multicellular Bcc infection models (2-4, 7, 15, 33). However, despite these attenuated characteristics relative to *Bc*, *Bm* now occupies the top spot among Bcc infections in American CF patients (19). As *Bm* is a Bcc species that is linked to rapid declines in CF patient health and cepacia syndrome, this trend is worrisome and creates an urgent need to characterize *Bm* pathogenesis and the environmental factors controlling its virulent behaviour.

Acquisition of *Bm* is thought to occur from environmental, rather than clinical sources, as evidenced by the taxonomic variation of *Bm* isolates from different patients (39). However, unlike other Bcc species, *Bm* is rarely isolated

from soil and other environmental samples, suggesting that it occupies a thus far-undefined environmental niche (19).

### ***Bm* virulence factors**

Because most multicellular hosts are not susceptible to *Bm* infection, very little is understood concerning specific factors involved with *Bm* pathogenesis. However, *Bm* has a strong propensity to invade and persist within epithelial cells and macrophages, and cell lines have been instrumental in beginning to address the underlying mechanisms.

Like *Bc*, *Bm* is highly invasive toward respiratory epithelial cells, but may require basolateral receptors for full monolayer transmigration ability, since migration was reduced when polarized Calu-3 cells were used instead of unpolarized A549 cells (12). *Bm* also shows the highest rate of invasion among Bcc species during infection of BEAS-2B unpolarized monolayers. Invasion of 16HBE14o<sup>-</sup> (CFTR<sup>+</sup>) and CFBE41o<sup>-</sup> (CFTR<sup>-</sup>) polarized cells appears to be linked to *Bm* secreted lipases. *Bm* strains not only produce more lipase than all other Bcc species but also show greater lipase-dependent invasion of both cell lines than a *Bc* strain (24). This study also found no difference between the effects of lipase pre-treatment of either cell line on the invasion ability of the two tested *Bm* strains, indicating that *Bm* invasion occurs independently of CFTR. Recently, it was shown that mannitol, which is typically associated with EPS production in the Bcc, activates the expression of fimbrial and afimbrial adhesins that promote biofilm production and mucin binding in a clinical *Bm* strain. These genes are not found in an environmental *Bm* strain that is unable to produce these

EPS-independent mannitol-induced phenotypes. Mutagenesis of the genes encoding these structures had no effect on the virulence of the *Bm* strain against wax moth larvae, and the invasive ability of the mutants was not assessed.

Using an actin inhibitor to disrupt the cytoskeleton of well-differentiated bronchial epithelial cells, Schwab *et al.* (32) showed that *Bm* invasion of host cells does not depend on polymerized actin, though *Bm* biofilm formation was disrupted by inhibition of actin polymerization for unidentified reasons. This feature could contrast the invasion exhibited by *Bc*, which seems to rely on passive uptake by epithelial cells (38). Interestingly, IL-8, a potent neutrophil chemoattractant that is released in response to *Bcc* exposure, promotes growth of a clinical *Bm* isolate in a concentration-dependent manner and even promotes intracellular *Bm* survival, particularly during invasion of CFBE41o- cells (18). These trends were not observed for the environmental *Bm* isolate. Meanwhile, cytokine release and apoptosis by BEAS-2B cells were shown to be similarly triggered by *Bm* and *Bc*, but while dendritic cells showed similar cytokine release by both species, necrosis was only caused by *Bc* (22).

Although persistence within epithelial cells has not been investigated, a recent study has described *Bm* invasion of and persistence within macrophages. While *Bc* cells are known to disrupt the fusion of the lysosome to the bacterial-enclosing vacuole, *Bm* fails to prevent this from occurring and, perhaps as a consequence, demonstrates persistence within both murine and human macrophages but only growth within murine macrophages (30). Some variability was observed among the invasion rate of the three tested *Bm* strains, and this was

attributed to differences in O-antigen. An earlier study had shown that the presence of O-antigen on *Bc* K56-2 was the reason for its lower degree of macrophage internalization relative to *Bc* J2315, which lacks an O-antigen (28). T6SS-mediated prevention of NADPH complex formation at the vacuole during *Bc* invasion has not been shown to occur in *Bm*, though results shown in Chapter 4 indicate that *Bm* produces a functional T6SS.

One study investigating *Bm* virulence attenuation in a multicellular model host first showed a change from a mucoid to a nonmucoid phenotype in clonal *Bm* isolates sampled several months apart from a single CF patient. The nonmucoid isolate showed a >10-fold decrease in the 72 h LD<sub>50</sub> versus the earlier mucoid isolate (35), indicating that, as in *Bc* (44), the nonmucoid phenotype is linked to greater virulence. The underlying mechanism for this may take root in resistance to oxidative stress during phagocytosis, although the upregulation of a wide range of genes was shown in *Bc* nonmucoid isolates, including transcription factors and *bcas0293*, which encodes the nematocidal protein AidA (44). In addition, the mucoid isolate harbours a mutation in *cepR*, which is known to control a range of virulence factors in *Bc*; this was proposed to account for the lack of AHL production in this isolate and could also explain in large part its decreased virulence, particularly given that AidA is not involved with *Bc* virulence in larvae (40). However, the absence of this mutation from the nonmucoid isolate indicates that the two isolates could be highly divergent both genotypically and phenotypically, since the nonmucoid isolate was sampled at a later timepoint than the mucoid isolate during a chronic infection that lasted over ten years.

## **Objectives**

Our limited understanding of *Bm* pathogenesis stands in glaring contrast to the importance of this species in the CF community. This study makes use of the newly-established duckweed infection model to investigate the role of environmental conditions on the virulence of *Bm* and other Bcc species. To model CF lung conditions, infections were carried out in 5% oxygen and physiologically relevant temperature, with the expectation that these conditions will alter the virulence of *Bm* or other Bcc strains and reveal hidden facets of their pathogenesis.

## **Materials and Methods**

### **Bacterial strains, plasmids, antibiotics and culture conditions**

Luria-Bertani (LB) broth was prepared in deionized water to half concentration for all Bcc cultures, which were grown in 2 ml volumes in 15 ml polypropylene conical tubes at 30°C in an orbital shaker at 225 rpm. A complete list of bacterial strains is shown in Table 2.

### **Duckweed infection**

Infection assays were prepared and analyzed as described in Chapter 1, with some changes to the protocol for the 37°C infections. Infection plates were not wrapped in cellophane because of condensation build-up. After bacterial inoculation, plates were placed in a 37°C incubator at either ambient oxygen (~21%) or 5% oxygen. Plant survival was measured at 72 h; for strains producing

a large survival difference between low and high oxygen at 48 h, LD<sub>50</sub> was also calculated for this timepoint.

### **Greater wax moth larval infections**

Infections were performed as described previously (Seed and Dennis, 2008), with minor alterations. Bacteria were grown on ½ LB agar in either a 37°C, ambient O<sub>2</sub> incubator or in a 37°C, 5% O<sub>2</sub> and 10% CO<sub>2</sub> incubator. Cells were then scraped off the plate, resuspended in sterile 10 mM MgSO<sub>4</sub>, washed once and diluted. For 5% O<sub>2</sub> infections, 10 mM MgSO<sub>4</sub> was covered with gas-permeable Parafilm (Pechiney, Chicago, IL) and placed at 5% O<sub>2</sub> for one hour prior to dilutions to maintain low oxygen levels in solution. Following dilutions, cell suspensions were covered with Parafilm and placed at 5% O<sub>2</sub> until injections were performed. Larvae were dipped in 95% ethanol and dried on paper towel prior to injections, which were carried out in sets of 6-8. A set of control worms was injected with 10 mM MgSO<sub>4</sub> between each dilution series of bacterial injections to verify that bacteria were cleaned from the syringe and that worms were surviving the physical injection process. Control worms displayed 10-15% mortality, with only slight differences between ambient and low treatments.

## Results

### Manipulation of the duckweed model to mimic cystic fibrosis lung conditions

After establishing similarities between the behaviour of Bcc strains in duckweed and existing animal and plant hosts (Chapter 1), the duckweed model was adapted to gain insight into Bcc behaviour during CF lung-mimicking conditions. We tested the effects of temperature and oxygen limitation by performing the standard duckweed infection assay at 37°C and either 5% or ambient O<sub>2</sub>. Several strains showed considerable increases in virulence as a result of oxygen limitation, including clinical *Bm* isolates C5393, C5274, C5568 and LMG 13010, *B. anthina* J2552 and *B. stabilis* LMG 14294 (Table 15). *B. vietnamiensis* DBO1 and *B. cepacia* LMG 18821 underwent a temperature-dependent increase in virulence. *Bc* J2315 demonstrated a slight temperature-dependent attenuation, while *B. pyrrocinia* LMG 14191, which is among the most virulent strains at 30°C and ambient oxygen, was attenuated at 37°C and ambient oxygen but completely avirulent at 5% oxygen. Loss of virulence in LMG 14191 was likely not due to a growth defect, since this strain was able to grow on SHS agar under all conditions tested.

**Table 15. Effect of temperature and oxygen on the virulence of Bcc strains against duckweed.**

Species	Strain <sup>a</sup>	Origin	LD <sub>50</sub> (cfu/ml) +/- SE <sup>bc</sup>		
			30°C 20% O <sub>2</sub>	37°C 5% O <sub>2</sub>	37°C 20% O <sub>2</sub>
<i>B. cepacia</i>	<i>LMG 18821</i>	CF patient	188 +/- 125	2.5 +/- 0.004	3.3 +/- 0.5
<i>B. multivorans</i>	<i>C5393</i>	CF patient	>230,000,000	7.3 +/- 2.9	8,280 +/- 5,690
	ATCC 17616	Soil	>110,000,000	>340,000,000	>410,000,000
	C3430	CF patient	>242,000,000	>438,000,000	>378,000,000
	<i>C5274</i>	CF patient	6,050,000,000 +/- 3,060,000,000	2.5 +/- 0	4,310,000 +/- 2,940,000
	<i>C5568</i>	CF patient	106,000,000	2.5 +/- 0.03 (2.5 +/- 0.03)	2.5 +/- 0.4 (218 +/- 50)
	<i>LMG 13010</i>	CF patient	61,200,000 +/- 8,890,000	2.5 +/- 0.4 (2.5 +/- 0.4)	7.7 +/- 2.1 (>310)
<i>B. cenocepacia</i>	J2315	CF patient	1,640,000 +/- 664,000	6,170,000	9,760,000 +/- 9,630,000
	K56-2	CF patient	12 +/- 6.7	2.5	2.5
	C1257	CF patient	8.8 +/- 5.7	2.5 +/- 1.4	22 +/- 20
<i>B. stabilis</i>	<i>LMG 14294</i>	CF patient	>1,000,000,000	1,260,000 +/- 1,030,000	>190,000,000
<i>B. vietnamiensis</i>	<i>DBO1</i>	Soil	372 +/- 248	2.5	2.5
<i>B. ambifaria</i>	AMMD	Soil	2.5 +/- 0.4	2.5	9.8
<i>B. anthina</i>	<i>J2552</i>	Soil	452,000,000 +/- 51,700,000	<10	880,000,000 +/- 849,000,000
<i>B. pyrrocinia</i>	<i>LMG 14191</i>	Soil	2.5 +/- 0.5	>110,000,000	2,180 +/- 1,450

<sup>a</sup>**Strains** showing a large increase in virulence at low oxygen; strain showing a large decrease in virulence at low oxygen; *strains* showing a temperature-dependent change in virulence.

<sup>b</sup>Numbers in parentheses show LD<sub>50</sub> at 48 h for strains demonstrating large difference between low and high oxygen treatments at this timepoint.

<sup>c</sup> LD<sub>50</sub> value of 2.5 cfu/ml reflects the lowest possible LD<sub>50</sub> of 1 cfu/well starting inoculum.

Following the realization that oxygen limitation has no apparent adverse effects on wax moth larvae, we infected *G. mellonella* larvae with *Bm* C5274 at 37°C and 5% or 20% oxygen to determine if the strong virulence-activation trend observed against duckweed in this strain also occurred in the larval model. These experiments demonstrated greater activation of C5274 virulence at low oxygen at both timepoints (Figure 29), although the difference in LD<sub>50</sub> between the two conditions was only ~10-fold at 24 h and ~1.5-fold at 48 h. This contrasts the ~2,000,000-fold difference in LD<sub>50</sub> observed under the same two conditions during duckweed infection, and could be the result of similar oxygen concentrations being maintained within the larval hemolymph in different external oxygen concentrations.

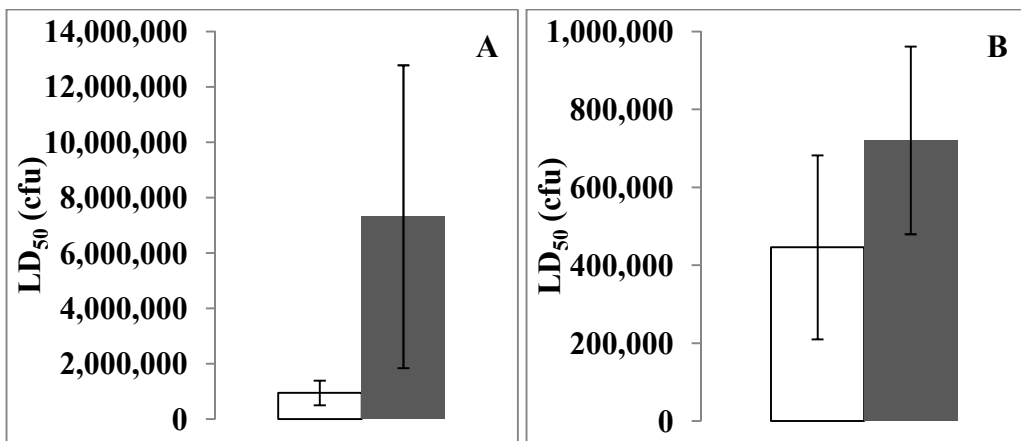


**Figure 29. Low oxygen increases the virulence of *B. multivorans* C5274**

**during *G. mellonella* infection.** Bacteria were grown for 20 h on ½ LB agar at 5% O<sub>2</sub> (white) or 20% O<sub>2</sub> (grey) and inoculated into larvae, which were then incubated under the same conditions in which the bacteria were grown. Results

shown are the average LD<sub>50</sub> +/- SE at 24 h (A) and 48 h (B) obtained from 3 (20% O<sub>2</sub>) or 4 (5% O<sub>2</sub>) biological replicates performed during 2 independent trials.

## Discussion

### Microaerophilic virulence activation (MVA)

The CF lung is characterized in part by microaerophilic conditions near the mucosal surfaces and inside phagocytes. In addition, the mammalian alveolar temperature is very close to the core body temperature (9), suggesting that 37°C is an accurate representation of the CF lower lung. The results shown in this study point to phenotypic switches that occur in certain members of the Bcc during growth in microaerophilic and physiological temperature conditions. Higher temperature appeared to act synergistically with MVA in some cases; however, MVA was not tested at 30°C. Despite this, MVA clearly occurs in the absence of temperature effects, since some strains showed MVA without an associated temperature effect. MVA appears to be common in *Bm*, with four of five tested clinical isolates demonstrating microaerophilic virulence activation (MVA) against duckweed to varying degrees, while the single environmental isolate tested, *Bm* ATCC 17616, did not exhibit virulence under any condition. MVA also occurs in *B. anthina* and *B. stabilis*, though *B. stabilis* virulence remained relatively low even at its maximum. While *B. anthina* is rarely isolated from CF patients, *B. stabilis* is more common and *B. multivorans* has emerged as one of the two most prevalent Bcc species in the CF community in most countries (11). *Bm* C5274 virulence against wax moth larvae was also investigated, and it appears

that MVA may occur in this model host as well, although the difference was not nearly as large as that observed in the plants. One factor that may explain the difference between the two systems is that while duckweed infections are carried out in liquid media exposed to the conditions of the surrounding environment, bacteria inoculated into larvae enter an environment characterized by homeostasis in which the animal likely strives to maintain a congenial oxygen balance within its hemolymph. During these experiments, care was taken to maintain a low oxygen environment around cells to be inoculated into low oxygen-incubated larvae, though all larvae were maintained in ambient oxygen prior to injections to avoid repeated stress to the animals. In addition, survival of blank buffer-injected control larvae was similar at both oxygen levels, demonstrating that the difference observed in *Bm* pathogenicity was not due to larval sensitivity.

Meanwhile, *B. pyrrocinia*, which also rarely infects CF patients (19), showed an enormous decrease in virulence as a result of oxygen limitation that is not linked to a growth defect, although growth was not quantified. The loss of virulence at low oxygen in this otherwise hypervirulent strain remains to be explained, but could be examined in the context of the production of the antifungal compound pyrrolnitrin, which is synthesized by this strain (41). If antifungal activity was also lost at low oxygen, it might demonstrate another case of a compound responsible for multihost pathogenesis, similar to the hemolytic toxin discussed in Chapter 2.

An appropriate surrogate model for the CF lung has recently been developed using CFTR-deficient pigs (26), described in the General Introduction.

While this model will no doubt prove highly useful for research into all aspects of CF, including bacterial infection, the cost of such a model limits its use to high-level studies that will be initialized with simpler models. We adapted the duckweed model to mimic physical conditions of the CF lung. Worlitzsch *et al.* (43) made use of fiberoptic bronchoscopy to insert oxygen probes into mucopurulent regions of the lung lumen of chronically infected CF patients, demonstrating that *P. aeruginosa* resides within hypoxic mucus in the lung lumen. Electron microscopy of lung sections of several patients revealed that the bacteria typically reside between 5 and 17  $\mu\text{m}$  from the epithelial surface, with some bacteria inhabiting the zone 2-5  $\mu\text{m}$  from the epithelial surface and no bacteria directly associated with the epithelium. A model was therefore proposed for chronic *P. aeruginosa* in which epithelial cells consume oxygen from static mucus prior to the colonization of bacteria, which results in further oxygen depletion and the generation of a steep oxygen gradient from the lumen to the epithelial surface. Within this environment, it is now known that *P. aeruginosa* continues to respire aerobically, rather than switching to alternative terminal electron acceptors such as nitrate (1). Likewise, *Bc* does not use nitrate during hypoxic growth, and Bcc species are generally considered to be obligate aerobes (29). Bcc bacteria have not been localized within the CF lung oxygen gradient, but they are known to interact with lung epithelial cells and an array of surface proteins, mucins and glycolipids *in vitro* (21), suggesting that Bcc bacteria likely also persist within the microaerophilic or hypoxic mucus during chronic infection.

To identify MVA-associated genes, a screening of *Bm* C5274 random plasposon mutants is currently underway. The method will be identical to that used to identify *Bc* K56-2 virulence factors, except the screening will be carried out at 5% oxygen and 37°C. Genes expected to appear in the screening include those up-regulated in a recent study examining growth of *Bc* at 6% oxygen (29). A large cluster of genes comprising *bcam0275a* through *bcam0323* was found to be up-regulated 2 to 240-fold at low oxygen and was thus designated the low-oxygen-activated (*lxa*) locus. Sequence analysis suggests that it is not a genomic island, based on a similar GC% to the chromosome on which it is housed. However, the *lxa* locus is chromosomally encoded between two other islands implicated in virulence, the T4SS and *cci* pathogenicity island. Knocking out the *lxa* locus in two *Bc* strains caused growth defects in minimal medium under aerobic growth, the affect was not crippling to the cells and in strain J2315 was only slight. However, the mutants showing decreased viability following placement at low oxygen. The authors point out the induction of the *cepI* AHL synthase independently of cell density, as well as the consequent upregulation of flagellar, exotoxin, adhesin, and type I secretion system biosynthesis.

Several other genetic loci showed upregulation at low oxygen and carried the same upstream consensus motif identified at several positions within the *lxa* locus. These loci included genes involved with stress response, resource turnover, and regulation. One potential candidate for a virulence switch is a putative regulator encoded by *bcam1351*, which has an ortholog in *Bm*. This gene was among the most up-regulated during low oxygen incubation at 210-fold.

Regulators activated at low oxygen both from *lxa* and non-*lxa* loci include two-component signal transduction systems (*bcam0288*, *bcam0289*, *bcam0322*, *bcam0323*, *bcam1484*, *bcam1493*, *bcam1494*), CRP-family regulators (*bcam0049*, *bcams0287*, *bcam1483*), and LysR-like regulators (*bcam0048*, *bcam1114*), all of which have homologs in *Bm*, except *bcam0322*, *bcam0323*, and *bcam1114*.

Since *Bc* J2315 showed similar, low virulence levels among the different oxygen and temperature conditions (Table 15), it seems unlikely that the genes within these J2315 low oxygen-activated operons have roles in virulence that would be detectable in duckweed. However, the dramatic switch observed in *Bm* suggest that MVA is occurring in 4 out of 6 of these strains. Therefore, as implied by the results of this study, there are likely significant regulatory differences both among and within *Bcc* species in response to low oxygen exposure.

The *lxa* locus shows high synteny with a locus in the only sequenced *Bm* strain, ATCC 17616, with the exception of several genes at the 3' region of the cluster that includes *bcam0322* and *bcam0323*. In the present study, 17616 did not exhibit MVA. However, the lack of virulence displayed by 17616 may be due to the absence of one or more specific virulence loci, and the potential remains for a role of the *lxa* locus and the other low oxygen-affected loci in the MVA of other *Bm* species. Other bacterial pathogens that colonize regions of low oxygen within their hosts also appear to have oxygen switches, including *Campylobacter jejuni* (42), *Mycobacterium tuberculosis* (14), and *P. aeruginosa* (1). Low oxygen-linked virulence genes have also been identified, such as the *orgA* cellular

invasion gene of *Salmonella* Typhimurium (17), the *lasI* quorum sensing system of *P. aeruginosa* (1), and the type III secretion systems of *Shigella flexneri* (20) and *P. aeruginosa* (25). Low oxygen-mediated T3SS activation in *P. aeruginosa* was shown to occur through an oxygen sensing regulator Anr (25), which has several possible homologs in *Bc*, including *bcam0049*, *bcam0287* and *bcam1483*. All three genes occur in most sequenced Bcc strains, including *Bm* ATCC 17616. Furthermore, the regulatory motif associated with the *lxa* locus is identical to the Anr-binding motif in *P. aeruginosa* (29). These findings suggest that a similar oxygen sensor acts upon the *lxa* locus in *Bc* and possibly *Bm*.

It seems likely that *Bm* MVA is tied to low oxygen responses of host cells. A recent review has summarized some of the effects of hypoxia on the innate immune system (10). These include several deficiencies important in CF that were discussed in the General Introduction. Increased chemotaxis of neutrophils to the site of hypoxia likely results in higher elastase activity at the epithelial surface, and yet the reduced phagosomal killing of microbes as a result of decreased reactive oxygen species production would render the increased neutrophil numbers ineffectual. Meanwhile, increased transepithelial migration of monocytes would exacerbate the microbleeds that leak iron and other resources into the lung. Exacerbating these effects is the up-regulated production of proinflammatory cytokines by macrophages exposed to LPS during hypoxic incubation. Therefore, the consequences of hypoxia transcend bacterial virulence, producing disruptive miscues in the host's innate defence machinery and promoting bacterial persistence by increasing availability of limiting nutrients.

Ultimately, the results of this study may reflect a change in gene expression that more closely relates to the intracellular lifestyle than to growth in hypoxic CF mucus. The study by Worlitzsch *et al.* (43) identified a steep oxygen gradient within CF mucus, and showed oxygen levels within the mucus as low as 0.3%. Meanwhile, the oxygen concentration within macrophages is approximately 2.6% (14). The present study is investigating changes at 5% oxygen, which more closely approximates intracellular oxygen levels than levels likely encountered by the Bcc deep in lung mucus, though oxygen levels within the mucus presumably vary between ambient ~21% and the minimum 0.3%. Therefore, the MVA in *Bm* and other Bcc species could represent a sensor that activates virulence near the hypoxic epithelium of the CF lung. In addition, MVA could be utilized for persistence within and destruction of phagocytes and epithelial cells; while *Bm* maintains similar resilience to the harsh environment of the CF lung, it may adopt a more insidious strategy than *Bc* by delaying virulence factor activation until the time of cellular uptake. Studies using multicellular infection models have yet to demonstrate *Bm* invasion of host cells *in vivo*, although invasion by *Bm* is commonly observed *in vitro* (12, 23, 24, 31), and one study found that more invasive *Bm* strains in A549 epithelial cell lines also demonstrated greater systemic dissemination during mouse infection (6).

To characterize the MVA phenotype, an appropriate parallel study in addition to a high-throughput *Bm* virulence screening at low oxygen would be to produce genetic deletions of the oxygen-responsive loci identified by Sass *et al.* (29) in *Bm* and compare the virulence of these mutants to the parent strain at 5%

oxygen. However, this approach will likely produce some mutants with growth defects or sensitivity to hypoxia as seen in the above study; such mutants would be expected to demonstrate virulence attenuation simply on account of reduced fitness.

### **Temperature-linked virulence activation**

In addition to MVA, this study produced evidence that some *Bcc* strains activate virulence pathways during growth at the physiologically relevant temperature of 37°C. While in some cases this effect is likely due to a faster bacterial growth rate, this explanation largely does not account for the observed effect because several *Bm* strains that demonstrated avirulence or low virulence at 30°C became moderately or highly virulent at 37°C. Growth alone could not account for such a switch, considering that this effect was observed in some strains but not in others. Previous studies have demonstrated greater plant morbidity by *Bc* as a result of higher temperature incubation (2, 27), but these studies did not isolate the observation of greater morbidity from greater bacterial growth.

If physiological temperature virulence activation (PTVA) is occurring in these *Bm* strains, it could parallel previously described phenotypic changes that occur from 30°C to 37°C, including lipid profile variations and decreased flagellar production (37). The study described at length in the preceding section that examined transcriptional differences in *Bc* during growth at ambient and low oxygen also examined transcriptional differences at 20°C and 37°C (29). Although the lower temperature in the present study was 30°C, it is nonetheless

worth noting that, similar to low oxygen, the expression of several virulence factors was up-regulated at the higher temperature in the microarray. Some of these include *cepI*, type VI secretion, *zmpA*, and adhesins.

PTVA is thought to occur through most cellular molecules, since subtle structural changes in DNA, RNA, proteins, or lipids could conceivably resonate throughout the cell (34). Bacterial virulence pathways activated by physiologically relevant temperature include type III and type VI secretion in *Edwardsiella tarda*, which occurs through a two-component system (5), adhesins in *Yersinia pestis* (36) and *Listeria monocytogenes* (16), which occurs through permissive RNA conformations, and type III secretion in *Salmonella* Typhimurium (13), which occurs through the H-NS DNA stabilizing protein.

With further experimentation, the results of this study could prompt a working model by which pathogenic *Bm* strains surreptitiously engage their virulence pathways: as the bacteria enter the CF lung, they first sense increased temperature, which gives rise to the up-regulation of a first set of virulence-linked genes. Upon entry into the steep oxygen gradient of the mucus, the bacteria up-regulate a second set of virulence genes as they are met with a large population of defective neutrophils, which are unable to process the invaders because of hypoxia-induced NADPH oxidase attenuation. Freely-available iron released through the effects of abundant neutrophil elastase and the transepithelial migration of monocytes could promote bacterial growth and persistence within this environment. The present results further substantiate the possibility that upon entry into host cells, *Bm* cells sense decreased oxygen pressure and up-regulate

this second set of virulence-linked genes that help the bacteria persist within the new environment.

## References

1. Alvarez-Ortega C, Harwood CS. Responses of *Pseudomonas aeruginosa* to low oxygen indicate that growth in the cystic fibrosis lung is by aerobic respiration. *Mol Microbiol*. 2007;65(1):153-65.
2. Bernier SP, Silo-Suh L, Woods DE, Ohman DE, Sokol PA. Comparative analysis of plant and animal models for characterization of *Burkholderia cepacia* virulence. *Infect Immun*. 2003;71(9):5306-13.
3. Cardona ST, Wopperer J, Eberl L, Valvano MA. Diverse pathogenicity of *Burkholderia cepacia* complex strains in the *Caenorhabditis elegans* host model. *FEMS Microbiol Lett*. 2005;250(1):97-104.
4. Castonguay-Vanier J, Vial L, Tremblay J, Deziel E. *Drosophila melanogaster* as a model host for the *Burkholderia cepacia* complex. *PLOS One*. 2010;5(7):e11467.
5. Chakraborty S, Li M, Chatterjee C, Sivaraman J, Leung KY, Mok YK. Temperature and Mg<sup>2+</sup> sensing by a novel PhoP-PhoQ two-component system for regulation of virulence in *Edwardsiella tarda*. *J Biol Chem*. 2010;285(50):38876-88.
6. Cieri MV, Mayer-Hamblett N, Griffith A, Burns JL. Correlation between an *in vitro* invasion assay and a murine model of *Burkholderia cepacia* lung infection. *Infect Immun*. 2002;70(3):1081-6.
7. Cooper VS, Carlson WA, Lipuma JJ. Susceptibility of *Caenorhabditis elegans* to *Burkholderia* infection depends on prior diet and secreted bacterial attractants. *PLOS One*. 2009;4(11):e7961.
8. De Soyza A, Meachery G, Hester KL, Nicholson A, Parry G, Tocewicz K, et al. Lung transplantation for patients with cystic fibrosis and *Burkholderia cepacia* complex infection: a single-center experience. *J Heart Lung Transplant*. 2010;29(12):1395-404.
9. Dery R. Humidity in anaesthesiology. IV. Determination of the alveolar humidity and temperature in the dog. *Canadian Anaesthetists' Society journal*. 1971;18(2):145-51.
10. Dietz I, Jerchel S, Szaszak M, Shima K, Rupp J. When oxygen runs short: the microenvironment drives host-pathogen interactions. *Microbes Infect*. 2012;14(4):311-6.
11. Drevinek P, Mahenthiralingam E. *Burkholderia cenocepacia* in cystic fibrosis: epidemiology and molecular mechanisms of virulence. *Clin Microbiol Infect*. 2010;16(7):821-30.
12. Duff C, Murphy PG, Callaghan M, McClean S. Differences in invasion and translocation of *Burkholderia cepacia* complex species in polarised lung epithelial cells *in vitro*. *Microb Pathog*. 2006;41(4-5):183-92.
13. Duong N, Osborne S, Bustamante VH, Tomljenovic AM, Puente JL, Coombes BK. Thermosensing coordinates a cis-regulatory module for transcriptional activation of the intracellular virulence system in *Salmonella enterica* serovar Typhimurium. *J Biol Chem*. 2007;282(47):34077-84.

14. Gazdik MA, McDonough KA. Identification of cyclic AMP-regulated genes in *Mycobacterium tuberculosis* complex bacteria under low-oxygen conditions. *J Bacteriol.* 2005;187(8):2681-92.
15. Ibrahim M, Tang Q, Shi Y, Almoneafy A, Fang Y, Xu L, et al. Diversity of potential pathogenicity and biofilm formation among *Burkholderia cepacia* complex water, clinical, and agricultural isolates in China. *World J Microbiol Biotechnol.* 2012;28(5):2113-23.
16. Johansson J, Mandin P, Renzoni A, Chiaruttini C, Springer M, Cossart P. An RNA thermosensor controls expression of virulence genes in *Listeria monocytogenes*. *Cell.* 2002;110(5):551-61.
17. Jones BD, Falkow S. Identification and characterization of a *Salmonella typhimurium* oxygen-regulated gene required for bacterial internalization. *Infect Immun.* 1994;62(9):3745-52.
18. Kaza SK, McClean S, Callaghan M. IL-8 released from human lung epithelial cells induced by cystic fibrosis pathogens *Burkholderia cepacia* complex affects the growth and intracellular survival of bacteria. *Int J Med Microbiol.* 2011;301(1):26-33.
19. Lipuma JJ. The changing microbial epidemiology in cystic fibrosis. *Clin Microbiol Rev.* 2010;23(2):299-323.
20. Marteyn B, West NP, Browning DF, Cole JA, Shaw JG, Palm F, et al. Modulation of *Shigella* virulence in response to available oxygen *in vivo*. *Nature.* 2010;465(7296):355-8.
21. McClean S, Callaghan M. *Burkholderia cepacia* complex: epithelial cell-pathogen confrontations and potential for therapeutic intervention. *J Med Microbiol.* 2009;58(Pt 1):1-12.
22. Moura JA, Cristina de Assis M, Ventura GC, Saliba AM, Gonzaga L, Jr., Si-Tahar M, et al. Differential interaction of bacterial species from the *Burkholderia cepacia* complex with human airway epithelial cells. *Microbes Infect.* 2008;10(1):52-9.
23. Mullen T, Callaghan M, McClean S. Invasion of *Burkholderia cepacia* complex isolates into lung epithelial cells involves glycolipid receptors. *Microb Pathog.* 2010;49(6):381-7.
24. Mullen T, Markey K, Murphy P, McClean S, Callaghan M. Role of lipase in *Burkholderia cepacia* complex (Bcc) invasion of lung epithelial cells. *Eur J Clin Microbiol Infect Dis.* 2007;26(12):869-77.
25. O'Callaghan J, Reen FJ, Adams C, Casey PG, Gahan CG, O'Gara F. A novel host-responsive sensor mediates virulence and type III secretion during *Pseudomonas aeruginosa*-host cell interactions. *Microbiology.* 2012;158(Pt 4):1057-70.
26. Ostedgaard LS, Meyerholz DK, Chen JH, Pezzulo AA, Karp PH, Rokhlina T, et al. The DeltaF508 mutation causes CFTR misprocessing and cystic fibrosis-like disease in pigs. *Sci Transl Med.* 2011;3(74):74ra24.
27. Parke JL, Gurian-Sherman D. Diversity of the *Burkholderia cepacia* complex and implications for risk assessment of biological control strains. *Annu Rev Phytopathol.* 2001;39:225-58.

28. Saldias MS, Ortega X, Valvano MA. *Burkholderia cenocepacia* O antigen lipopolysaccharide prevents phagocytosis by macrophages and adhesion to epithelial cells. *J Med Microbiol.* 2009;58(Pt 12):1542-8.
29. Sass AM, Schmerk C, Agnoli K, Norville PJ, Eberl L, Valvano MA, et al. The unexpected discovery of a novel low-oxygen-activated locus for the anoxic persistence of *Burkholderia cenocepacia*. *ISME J.* 2013;7(8):1568-81.
30. Schmerk CL, Valvano MA. *Burkholderia multivorans* survival and trafficking within macrophages. *J Med Microbiol.* 2013;62(Pt 2):173-84.
31. Schwab U, Leigh M, Ribeiro C, Yankaskas J, Burns K, Gilligan P, et al. Patterns of epithelial cell invasion by different species of the *Burkholderia cepacia* complex in well-differentiated human airway epithelia. *Infect Immun.* 2002;70(8):4547-55.
32. Schwab UE, Ribeiro CM, Neubauer H, Boucher RC. Role of actin filament network in *Burkholderia multivorans* invasion in well-differentiated human airway epithelia. *Infect Immun.* 2003;71(11):6607-9.
33. Seed KD, Dennis JJ. Development of *Galleria mellonella* as an alternative infection model for the *Burkholderia cepacia* complex. *Infect Immun.* 2008;76(3):1267-75.
34. Shapiro RS, Cowen LE. Thermal control of microbial development and virulence: molecular mechanisms of microbial temperature sensing. *mBio.* 2012;3(5).
35. Silva IN, Ferreira AS, Becker JD, Zlosnik JE, Speert DP, He J, et al. Mucoid morphotype variation of *Burkholderia multivorans* during chronic cystic fibrosis lung infection is correlated with changes in metabolism, motility, biofilm formation and virulence. *Microbiology.* 2011;157(Pt 11):3124-37.
36. Skurnik M, Toivanen P. LcrF is the temperature-regulated activator of the *yadA* gene of *Yersinia enterocolitica* and *Yersinia pseudotuberculosis*. *J Bacteriol.* 1992;174(6):2047-51.
37. Taylor CJ, Anderson AJ, Wilkinson SG. Phenotypic variation of lipid composition in *Burkholderia cepacia*: a response to increased growth temperature is a greater content of 2-hydroxy acids in phosphatidylethanolamine and ornithine amide lipid. *Microbiology.* 1998;144 ( Pt 7):1737-45.
38. Tomich M, Herfst CA, Golden JW, Mohr CD. Role of flagella in host cell invasion by *Burkholderia cepacia*. *Infect Immun.* 2002;70(4):1799-806.
39. Turton JF, Kaufmann ME, Mustafa N, Kawa S, Clode FE, Pitt TL. Molecular comparison of isolates of *Burkholderia multivorans* from patients with cystic fibrosis in the United Kingdom. *J Clin Microbiol.* 2003;41(12):5750-4.
40. Uehlinger S, Schwager S, Bernier SP, Riedel K, Nguyen DT, Sokol PA, et al. Identification of specific and universal virulence factors in *Burkholderia cenocepacia* strains by using multiple infection hosts. *Infect Immun.* 2009;77(9):4102-10.
41. Wiesner W, van Pee KH, Lingens F. Detection of a new chloroperoxidase in *Pseudomonas pyrrocinia*. *FEBS Lett.* 1986;209(2):321-4.
42. Woodall CA, Jones MA, Barrow PA, Hinds J, Marsden GL, Kelly DJ, et al. *Campylobacter jejuni* gene expression in the chick cecum: evidence for adaptation to a low-oxygen environment. *Infect Immun.* 2005;73(8):5278-85.

43. Worlitzsch D, Tarran R, Ulrich M, Schwab U, Cekici A, Meyer KC, et al. Effects of reduced mucus oxygen concentration in airway *Pseudomonas* infections of cystic fibrosis patients. *J Clin Invest.* 2002;109(3):317-25.
44. Zlosnik JE, Speert DP. The role of mucoidy in virulence of bacteria from the *Burkholderia cepacia* complex: a systematic proteomic and transcriptomic analysis. *J Infect Dis.* 2010;202(5):770-81.

# Conclusion

---

## Research question

While some pathogens adapt to a narrow range of hosts, others maintain a generalized strategy and the large genomic investment that accompanies it. Bcc relative *Burkholderia pseudomallei* and its evolutionary descendant, *Burkholderia mallei*, are a prime example of this process: while *B. mallei* descended to become a strict mammalian pathogen following insertion sequence proliferation and consequent genome-reductive evolution, the former maintained a relatively stable genome and the lifestyle of an opportunistic pathogen (16). At the root of this lifestyle is a repertoire of core genetic traits that enable the success of the organism in diverse and variable environments. Diverse *B. pseudomallei* strains maintain nearly identical core genome elements unperturbed by functionally-disruptive mutations that include traits relevant to the pathogen's ability to infect its hosts and to the soil dweller's ability to resist predation and harsh environmental conditions. Such positively-selected elements encode traditional virulence factors such as adhesins for host cell binding, in addition to host metabolite-utilization proteins (10). Research into atypical virulence factors such as metabolism proteins represents an emerging paradigm in the field of microbial pathogenesis that integrates both host and pathogen factors.

However, neither the host nor the bacterial factors that contribute to the often devastating disease state accompanying Bcc infection of CF are well understood. Since a financially viable model system has yet to be developed that imitates the CF disease state, there are numerous possible approaches to gaining insight into Bcc pathogenesis. If research into Bcc pathogenesis seeks to reveal

the process by which Bcc bacteria infect CF patients, then it is appropriate given the multihost pathogenicity demonstrated by these organisms to determine instead how Bcc bacteria infect vastly different eukaryotic hosts. Approaching a complex human system such as the CF lung with infection data yielded from alternative model hosts such as plants and insects is bound to produce false positives, and while conserved mechanisms may be responsible for pathogenesis against multiple hosts, the biological differences of these host models makes it unlikely that the infection process as a whole could be the same within such disparate environments. Rather, it is likely the culmination of environmental cues prompting differential gene regulation that prompt the pathogen to select from a large repertoire of virulence traits, some of which may be effective against multiple hosts. In the case of the Bcc, their repertoire of virulence traits likely reflects their sizeable genomes, and, like *B. pseudomallei*, their ecological origins. For example, the adaptation of Bcc bacteria to an intracellular lifestyle (7) (9) (12), which is characterized by low oxygen levels (4), likely emerged as a response to amoebal predation in their soil habitats (8); this adaptation may have important implications when the bacteria enter the low oxygen CF lung or the cells therein. By using a model system that is adaptable enough to begin to imitate some of the important features of the target host such as low oxygen, the reductionist approach of studying “virulence” gains more context, potentially allowing the identification of virulence traits that may be turned on in response to CF lung-specific cues.

In a similar way, a pathogen's natural ecology can take on pathological meaning. For example, a soil microbe with invasive capacity into plant roots or persistence within predator cells that emerges as a human pathogen may have adapted these traits to suit its new niche. The characteristics of Bcc infection that have so far been identified, including the unfailing susceptibility of model hosts to a subset of Bcc strains (1) seems to suggest that a similar process has occurred during the evolution of the Bcc as human pathogens. The present set of studies has applied alternative model systems to identify and characterize genetic traits within the three most prevalent species of the Bcc that may have contributed to the emergence of these soil bacteria as human pathogens.

## **Project goals**

To accomplish this overarching objective of advancing the current knowledge on Bcc virulence pathways, both reductionist and more elaborate alternative models were introduced. First, hemolysis production in the Bcc was investigated using both sheep and human erythrocytes. This investigation yielded a novel secondary metabolism gene cluster that gives rise to toxic effects in both cellular (erythrocytes) and multicellular (wax moth larval) animal systems. The results helped to prompt the question of whether the toxin was also effective against plants, and subsequently gave rise to the development of a new model host with the capacity for both high-throughput data collection and exposure to CF-relevant environmental conditions. The realization of the advantages provided by the duckweed model motivated a screen for virulence traits in *B. cenocepacia* as

well as an analysis of physical conditions relevant to the CF lung on the different species of the Bcc. Finally, the realization among researchers that the T6SS provided the capacity for interbacterial killing in both *P. aeruginosa* and *V. cholerae* unveiled a potential avenue for research in Bcc infection of CF lungs, since commensal microflora is considered a major component of innate immunity. Therefore, an additional component of this research project examined the role of the *B. cenocepacia* T6SS in interbacterial competition and the potential effector proteins that *B. cenocepacia* applies to this end.

## Findings

The major underlying themes to these studies include the linking of Bcc virulence in plant and animal hosts, identifying virulence factors likely relevant to acute infection, and applying current knowledge about the CF lung to identify Bcc paths to infection. These investigations centred on the three most prevalent CF-infecting species, *B. cenocepacia*, *B. multivorans* and *B. vietnamiensis*.

Concerning the first topic, a large quantitative analysis of a panel of Bcc strains indicates that there are conserved virulence mechanisms promoting Bcc infection of both duckweed and wax moth larvae. This finding both validated the duckweed model and prompted its high-throughput application to the identification of *B. cenocepacia* virulence factors, the study of potential Bcc therapeutic agents such as bacteriophage, and the screening of collections of Bcc isolates under CF-relevant environmental conditions. The present study includes only the second mutant screen of a Bcc strain in an acute model of infection in an

intact, unwounded organism, while two other virulence screens have sought the basis for persistence during chronic rat lung infection (5) and watersoaking in onion (3). In total, these screens have examined less than 20,000 mutants in four dissimilar contexts. Otherwise, Bcc virulence factors have been identified by their homology with known virulence genes in other organisms and through observation of specific phenotypes such as the hemolysis described at present. Therefore, additional whole-organism virulence studies may discover entirely new pathways that would remain obscured by the singular use of reductionist approaches.

One of the most striking findings emerging from a comparison of the findings in Chapters 2 and 3 is the multifactorial nature of pathogenesis in *B. cenocepacia* and *B. vietnamiensis*. While highly divergent factors were found to confer virulence in these two organisms (a nonribosomally-synthesized peptide in *B. vietnamiensis* and a range of gene products in *B. cenocepacia*), with two exceptions (*shvR* and *bcas0210*), the virulence factors identified contributed only partially to the overall virulence profiles of these organisms. Furthermore, the mechanism of plant killing builds on previous data from the wounded onion model that showed the involvement of both type II secretion (15) and type IV secretion (3) that confer two distinct modes of pathogenesis.

## **Study limitations**

The obvious limitation of all of these studies is the lack of clarity in regard to the functionality of the identified genes of interests in the context of

human hosts, even though the *B. vietnamiensis* NRPS cluster, various genes identified in the *B. cenocepacia* duckweed screen, and the *B. cenocepacia* T6SS were all shown to exhibit relevance against model hosts (or other bacteria, in the case the the T6SS). Although we attempted to expose Bcc bacteria to imitations of CF lung environmental conditions, there are likely additional factors at play that contribute heavily to the pathogenesis mechanisms, not the least of which is the formidable host response and ensuing self-damage that is inflicted. Further understanding of this environment will no doubt potentiate a better understanding of Bcc pathogenesis and new methods to study it.

While the bacteria were exposed to some CF-relevant conditions, the medium used throughout the study was a minimal plant growth medium supplemented with sucrose. Given the regulatory modulations to which growth in minimal media gives rise in *B. cenocepacia* (13), it is likely both that some attenuating mutations from the virulence screen were artifacts of the infection medium selected and that many more attenuating mutations could be identified by modifying this medium.

The determination that *B. cenocepacia* adapts its T6SS for interbacterial competition was carried out using *E. coli* as a model prey species. While the first objective in studying this phenomenon is to identify what role, if any, T6S might play in the broader context of Bcc pathogenesis, the detailed description emerging of the CF lung microbiome suggests substantial microbial diversity (11). Therefore, even considering that *E. coli* is not a CF colonizer, the finding that *B. cenocepacia* is able to interact with *E. coli* in such a way surely indicates that at

least a subset of the CF microbial population would be sensitive to attack by *B. cenocepacia*. Further characterization of the airway microbiome, particularly with respect to the localization of different species within the variably oxygenated mucus layer, may reveal the likely targets of T6SS-mediated killing by *B. cenocepacia*.

An ideal approach to virulence factor characterization using available tools would combine multihost virulence assessment with *in vivo* transcriptomic analysis during both chronic (rat/mouse agar bead models) and acute (plant, insect and zebrafish models) infection, which would provide the added benefit of determining if the genes disrupted in attenuated mutants are induced or repressed in the CF lung during these phases of infection. While the rodent agar bead models are useful tools for studying chronic respiratory infection by the Bcc (17), most current models are based on acute infection. One exception to this is the nematode model, which allows for the investigation of slow, fast or paralytic killing by bacteria depending on the medium in which the infection is carried out (6). By similarly adjusting the duckweed model, additional virulence characteristics could probably be identified among the Bcc or other pathogens. Consider the difference in killing time between virulent Bcc strains and EPEC, for example. Within two days, most plants show signs of morbidity during Bcc infection, whereas EPEC infection manifests similarly only after five days. Zhang *et al.* observed the formation of *P. aeruginosa* biofilms on duckweed surfaces (18). Perhaps bacteria such as EPEC induce morbidity only following the

establishment of a mature biofilm, similar to the cellular invasion phenotype exhibited by a *B. cenocepacia* strain (14).

## **Future directions**

While multihost approaches were taken in the characterization of the NRPS toxin and the *B. cenocepacia* T6SS to determine their contributions to virulence, a major drawback of the duckweed screen was that most mutants were not tested in additional models such as wax moth larvae. The demonstration that these mutations do or do not cause attenuation in additional model hosts would have several benefits. First, it would further challenge duckweed as an appropriate model for the study of Bcc virulence factors. It is now clear that virulence-linked genes can be identified using this plant, but the question remains as to relevance of the identified genes in human pathogenesis. Second, in separating pathologically-relevant from less relevant or host-specific genes, stronger direction would be provided for further investigation in more complex systems such as chronic infection in rat lungs, or eventually CF pig lung infection. Finally, the correlation observed between the virulence of Bcc strains in duckweed and wax moth larvae would be provided some explanatory support. Therefore, a primary direction from this research should be the testing of the duckweed-relevant virulence factors in simple models such as wax moth larvae, nematodes or cell lines.

Also left undetermined is whether or not the T6SS is effective in helping Bcc bacteria to secure niche space within the lung. To this end, a larger panel of

known Gram negative CF colonizers should be tested for susceptibility to *B. cenocepacia* T6SS-mediated killing. If additional species are found to be susceptible, a model system could be developed to test competitive indices of these species against *B. cenocepacia* and the T6SS knockout strain. One ideal system in which to test this would be within chronic rat lung infection, since the microaerophilic conditions under which the *B. cenocepacia* T6SS has been shown to be down-regulated (13) are represented in this system (2).

In addition to modelling the *in vivo* relevance of the *B. cenocepacia* T6SS, there are abundant data concerning the possibility that *vgrG* clusters encode T6SS effector proteins with diverse putative functions. The identification of their functions would provide mechanistic insight into the *in vivo* relevance of the T6SS, if that is first established by means described above.

Finally, there is an urgent need to determine both the mechanism and pathological relevance of the microaerophilic and temperature-linked virulence activation (MVA and PTVA) phenotypes outlined in Chapter 5. If some Bcc bacteria employ this strategy to sense their environment and respond with virulence up-regulation, then this almost certainly has pathological implications in CF lungs. Furthermore, this would help to solve the long-standing discrepancy between *B. multivorans* virulence in model hosts (which are typically incubated at 30°C and ambient oxygen levels) and this species' propensity to establish infection and cause morbidity in CF patients.

## References

1. Bernier SP, Silo-Suh L, Woods DE, Ohman DE, Sokol PA. Comparative analysis of plant and animal models for characterization of *Burkholderia cepacia* virulence. *Infect Immun*. 2003;71(9):5306-13.
2. Bragonzi A. Murine models of acute and chronic lung infection with cystic fibrosis pathogens. *Int J Med Microbiol*. 2010;300(8):584-93.
3. Engledow AS, Medrano EG, Mahenthiralingam E, LiPuma JJ, Gonzalez CF. Involvement of a plasmid-encoded type IV secretion system in the plant tissue watersoaking phenotype of *Burkholderia cenocepacia*. *J Bacteriol*. 2004;186(18):6015-24.
4. Gazdik MA, McDonough KA. Identification of cyclic AMP-regulated genes in *Mycobacterium tuberculosis* complex bacteria under low-oxygen conditions. *J Bacteriol*. 2005;187(8):2681-92.
5. Hunt TA, Kooi C, Sokol PA, Valvano MA. Identification of *Burkholderia cenocepacia* genes required for bacterial survival *in vivo*. *Infect Immun*. 2004;72(7):4010-22.
6. Kothe M, Antl M, Huber B, Stoecker K, Ebrecht D, Steinmetz I, et al. Killing of *Caenorhabditis elegans* by *Burkholderia cepacia* is controlled by the cep quorum-sensing system. *Cell Microbiol*. 2003;5(5):343-51.
7. Lamothe J, Huynh KK, Grinstein S, Valvano MA. Intracellular survival of *Burkholderia cenocepacia* in macrophages is associated with a delay in the maturation of bacteria-containing vacuoles. *Cell Microbiol*. 2007;9(1):40-53.
8. Lamothe J, Thyssen S, Valvano MA. *Burkholderia cepacia* complex isolates survive intracellularly without replication within acidic vacuoles of *Acanthamoeba polyphaga*. *Cell Microbiol*. 2004;6(12):1127-38.
9. Martin DW, Mohr CD. Invasion and intracellular survival of *Burkholderia cepacia*. *Infect Immun*. 2000;68(1):24-9.
10. Nandi T, Ong C, Singh AP, Boddey J, Atkins T, Sarkar-Tyson M, et al. A genomic survey of positive selection in *Burkholderia pseudomallei* provides insights into the evolution of accidental virulence. *PLoS Pathog*. 2010;6(4):e1000845.
11. Rabin HR, Surette MG. The cystic fibrosis airway microbiome. *Current opinion in pulmonary medicine*. 2012;18(6):622-7.
12. Sajjan US, Yang JH, Hershenson MB, LiPuma JJ. Intracellular trafficking and replication of *Burkholderia cenocepacia* in human cystic fibrosis airway epithelial cells. *Cell Microbiol*. 2006;8(9):1456-66.
13. Sass AM, Schmerk C, Agnoli K, Norville PJ, Eberl L, Valvano MA, et al. The unexpected discovery of a novel low-oxygen-activated locus for the anoxic persistence of *Burkholderia cenocepacia*. *ISME J*. 2013;7(8):1568-81.
14. Schwab U, Leigh M, Ribeiro C, Yankaskas J, Burns K, Gilligan P, et al. Patterns of epithelial cell invasion by different species of the *Burkholderia cepacia* complex in well-differentiated human airway epithelia. *Infect Immun*. 2002;70(8):4547-55.
15. Somvanshi VS, Viswanathan P, Jacobs JL, Mulks MH, Sundin GW, Ciche TA. The type 2 secretion pseudopilin, gspJ, is required for multihost

pathogenicity of *Burkholderia cenocepacia* AU1054. *Infect Immun*. 2010;78(10):4110-21.

16. Song H, Hwang J, Yi H, Ulrich RL, Yu Y, Nierman WC, et al. The early stage of bacterial genome-reductive evolution in the host. *PLoS Pathog*. 2010;6(5):e1000922.

17. Starke JR, Edwards MS, Langston C, Baker CJ. A mouse model of chronic pulmonary infection with *Pseudomonas aeruginosa* and *Pseudomonas cepacia*. *Paed Res*. 1987;22(6):698-702.

18. Zhang Y, Hu Y, Yang B, Ma F, Lu P, Li L, et al. Duckweed (*Lemna minor*) as a model plant system for the study of human microbial pathogenesis. *PLOS One*. 2010;5(10):e13527.